CARBOHYDRATE FUNCTIONALIZED SYNTHETIC ELASTOMERS: SYNTHESIS, CHARACTERIZATION AND APPLICATIONS

A thesis submitted to the

UNIVERISITY OF PUNE

For the degree of

DOCTOR OF PHILOSOPHY

In

(CHEMISTRY)

By

Mr. RAKESH SINGH

Research guide

Dr. A. J. VARMA

POLYMER SCIENCE AND ENGINEERING DIVISON

NATIONAL CHEMICAL LABORATORY

PUNE- 411 008, INDIA

AUGUST-2010

CERTIFICATE

Certified that the work incorporated in this thesis entitled **"Carbohydrate functionalized synthetic elastomers: synthesis, characterization and applications"** submitted by Mr. Rakesh Singh was carried out by him under my supervision/guidance. Such material as has been obtained from other sources has been duly acknowledged in the thesis.

August, 2010   Dr. A. J. Varma

(Research Guide)

Declaration by the Candidate

I declare that the thesis entitled **"Carbohydrate functionalized synthetic elastomers: synthesis, characterization and applications"** submitted for the degree of Doctor of Philosophy to the University of Pune, has been carried out by me at the National Chemical Laboratory, Pune, under the supervision of Dr. A. J. Varma. The work is original and has not been submitted as a part or full by me for any degree or diploma to this or any other university.

August, 2010   Rakesh Singh

Dedicated to my beloved Parents and my Wife

Acknowledgments

I would like to take this opportunity to first thank my research supervisor and mentor Dr. A. J. Varma, for giving new lease of life to my aspirations of completing my doctoral degree and whose inspiration, encouragement and constant guidance led to bringing my dream to reality. I am deeply indebted to him for his guidance, support, teachings and moral advice, which not only helped me in solving scientific problems but also helped me in my personal life. My sincere regards and reverence are for him, forever.

I express my sincere thanks to, Dr. D. V. Gokhale for biodegradation studies, Dr. D. Sarkar for biocompatibility studies and Dr. R.C. Kuhad for antimicrobial studies. I am also greatly indebted to Mr. K. V. Pandare, Dr. (Mrs.) K. D. Trimukhe, Mr. B. Y. Shaikh, Dr. (Mrs.) Padmaja Galgali, Mukund, Anil, Chandrashekhar, Jyotsna and Sanjeev for their constant help and maintaining a cheerful and cordial atmosphere in the laboratory, and finally Hamid my colleague and friend who is always there for me whenever I needed him.

I would like to express my deep felt gratitude to my colleagues and friends Alok, Shefali, Mahesh, Swati, Ganesh, Maduri, Girish, Ravi, Sonali, Sandeep, Yogesh, Janmejay, Nagraj, Naman, Jiten, Shailesh, Suresh, Hemanth, Ashish, Elan, Sameer, Noor, Arvind, Dilip, Pratheep, Mukesh, Sarika, Santosh, Vivek, Pankaj, Rishi and many in NCL and outside who are not named in person, for their valuable friendship and helping hand.

I find no words to express my gratitude for my parents, whose moral support, love and constant encouragements have helped me to complete this long journey.

I would like to thank my Uncle, sister Bandana, Jija and little Chirag; my brothers Kaushik, Amit, Abhishek, Vivek, and sisters Preeti, Swati and Tripti, Father and Mother-in-law, Sister-in- law Dr. pankaja and Shloka, Brother in law Indu Prakash, Arunendra and Sandeep and new born Ishika, for their

List of contents

Chapter 2: Synthesis of carbohydrate functionalized SBS from epoxidized SBS by glycosidation reaction

Chapter 3: Synthesis of carbohydrate functionalized SBS by click chemistry from epoxidized SBS

Chapter 4: Evaluation of carbohydrate functionalized SBS as fluorescent and

biocompatible material for biomedical applications

Chapter 6: A morphological study of carbohydrate functionalized SBS

Chapter 7:   Isolation and characterization of natural polymer Lignin containing residual carbohydrates as a model for synthetic cross linked polystyrene with anchored carbohydrate moieties

Chapter 8: Conclusion and suggestion for future work

List of Figures and tables

List of Figures

Chapter 1

Chapter 2

Chapter 3

Chapter 4

Chapter 5

Chapter 6

Chapter 7

List of tables

Chapter 2

Chapter 5

Chapter 7

Abbreviations

SBS: Polystyrene-block-polybutadiene-block-polystyrene

PS: Polystyrene

DMAP: 4- Dimethyl Amino Pyridine

mCPBA: meta Chloro Peroxy Benzoic Acid

HEMA: Hydroxy Ethyl Methacrylate

GMA: Glycidyl Methacrylate

UV: Ultra Violet

XPS: X-ray Photoelectron Spectroscopy

NCIM: National collection of industrial microorganism

CLSM: Confocal laser scanning microscopy

NMR: Nuclear Magnetic Resonance Spectroscopy

TGA: Thermogravimetric Analysis

FTIR: Fourier Transform Infra Red Spectroscopy

DTG: Differential Thermogravimetry

TG: Thermogravimetry

SEM: Scanning Electron Microscopy

OECD: Organisation for Economic Co-operation and Development

ASTM: American Society for Testing and Materials

OD: Optical Density

Abstract of the thesis

Introduction

Synthesis and incorporation of functional moieties on polymers continues to generate significant research interest both in academia and industry. A functional group when incorporated into a polymer can deliver enhanced properties, such as biocompatibility, fluorescence behavior, antimicrobial property, biodegradation etc., as evidenced by numerous reports in scientific literature. The utility of these new materials have been demonstrated as commodity polymers as well as specialty polymers in biodegradable plastics, coatings, membranes, compatibilizer, drug delivery systems, polymeric microbicides, tissue engineering, implants and many other applications.

Two approaches exist for functionalization of synthetic polymers and accordingly, the desired moiety can be attached to the polymer either during polymerization or after polymerization (post polymerization). The available polymerization techniques like anionic or cationic polymerization restricts the choice of monomers that could be polymerized to produce specialized polymers, thus restricting the end use of these polymers. "Styrene-butadiene-styrene (SBS)" a commodity elastomer and the subject of investigation of this research work is an example of such a polymer having narrow applications. The anionic polymerization technique used for the synthesis of this block copolymer hinders the incorporation of polar monomers during polymerization. This in turn limits the usefulness range of this polymer for diverse applications.

Here, post polymerization modification techniques comes to our rescue, enabling us to synthesize tailor-made polymers with a wide range of functional groups, based on the intended function and end use of these polymers.

SBS is an important class of synthetic thermoplastic elastomers (TPE) which derives its strength and elasticity from physical cross linking of the molecules into a three-dimensional network. The polystyrene end blocks impart the strength to the polymer while the polybutadiene rubbery matrix blocks give the material its high viscosity and elasticity. SBS is used in for disposable medical products, food packaging, tubing, sheet, belting, mallet heads, and shoe soles. Another major bulk application of SBS is as bitumen modifier. These materials are also used as sealants, hot-melt adhesives, coatings, and for wire and cable insulation. Automotive applications includes airbag covers, hoses, ducts, and dust boots. These also find application in power, communication, data and flexible cords; injection molded plugs and connectors. However, with suitable chemical modification, several new high value niche applications can also be developed.

Polystyrene-polybutadiene-polystyrene (SBS) is an important triblock copolymer having unsaturation, which can be utilized for introducing suitable functional groups, thus altering its physical and chemical properties. Although functionalization of polybutadiene have been studied in detail, including functionalization with sugar, only few examples of functionalized SBS can be found, with no report for functionalization of SBS with sugars. Synthesis of synthetic polymers having sugar branches (synthetic glycopolymers) has become an interesting area of work because of importance of these materials for numerous biological and biomedical applications. This is because these synthetic glycopolymers are expected to have functions similar to natural glycoconjugates and so can mimic their performance in

specific applications. Many studies have been published on the use of glycopoly-mers as drug delivery systems, artificial tissues, biocompatible devices, hydrogels and surface modifiers. Synthetic glycopolymers have also been synthesized, for use as biological recognition molecules, as cell-specific culture substrata, in human vaccines, for tumor diagnosis, as probes for receptors, and in targeted drug delivery systems. Expansive research efforts have been devoted on developing new strate-gies for the immobilization of biomolecules like proteins and carbohydrates. How-ever, the field still is in its infancy. There are numerous reports on epoxidation of SBS by different methods, but further opening of the epoxide to introduce func-tional groups on the SBS polymeric backbone has not been much explored besides synthesis of SBS ionomers. Taking advantage of rich literature on epoxidation and epoxide ring opening in general, we explored the further functionalization of SBS by epoxide ring opening. This was done with the aim of introducing polar mole-cules such as sugars and quaternary nitrogen pendants on the SBS backbone.

Thus, the main goal of this thesis work is to develop an understanding of the effect of incorporation of carbohydrates and quaternary nitrogen moieties onto a syn-thetic elastomer like SBS in terms of enhancement of properties like biocompati-bility, biodegradation, fluorescence and antimicrobial properties along with the physical and morphological changes. The present work is directed towards func-tionalization of Styrene-Butadiene-Styrene (SBS) with carbohydrates (monosacha-rides, disaccharides and pentose sugars) and evaluation of the functionalized SBS for potential biomedical applications.

The thesis has been divided into the following eight chapters.

Chapter 1: Introduction and literature survey:

This chapter gives a detailed review of literature on functionalization and modifications of elastomers and their applications in general, with focus on SBS elastomer. It meticulously delivers a comprehensive literature incorporating the significant work done in this area. It also elaborates on the functionalization of styrene butadiene copolymers with sugars and common methods of synthesizing synthetic glycopolymers. The existing and emerging applications of this work are also presented.

Chapter 2: Synthesis of carbohydrate functionalized SBS by glycosidation from epoxidized SBS

This chapter describes the synthesis of epoxidized SBS, followed by the synthesis of glucose, mannose, galactose, xylose, fructose, maltose, sucrose and methyl glucoside linked SBS by epoxide ring opening. XPS analysis was performed to gain insight into the mechanism of the reaction leading to sugar linked SBS. The functional groups generated after functionalization were evaluated by ^{1}H NMR, ^{13}C NMR, XPS and FTIR spectroscopy. We were successful in synthesizing carbohydrate functionalized SBS containing quaternary nitrogen pendants and also established the reaction mechanism leading to sugar linked SBS.

Chapter 3: Synthesis of carbohydrate functionalized SBS by click chemistry from epoxidized SBS

This chapter describes synthesis of carbohydrate functionalized SBS from epoxidized SBS using propargyl sugars (acetyl protected and unprotected) by click chemistry approach. SBS azide was synthesized from epoxidized SBS which was

reacted with propargyl sugars to yield sugar linked SBS. The products were characterized by FTIR and TGA. The morphologies of functionalized SBS were studied using scanning electron microscopy (SEM) and wide angle x-ray diffraction (WAXRD). Click chemistry approach was successfully utilized for the synthesis of carbohydrates functionalized SBS.

Chapter 4: Evaluation of carbohydrate functionalized SBS as fluorescent and biocompatible material for biomedical applications

This chapter describes the fluorescence study of synthesized carbohydrate functionalized SBS, by measuring the fluorescence by fluorimeter and Confocal scanning laser microscopy (CSLM) at three different wavelengths along with the UV-Vis absorption characterization. The sugar linked SBS polymers were found to fluorescent and UV active. The biocompatibility of these elastomers was evaluated using HL-60 cell line and THP-1 cell lines by MTT assay. The antimicrobial property was investigated using bacterial and yeast cultures. The carbohydrates functionalized SBS were found to be fluorescent besides showing enhanced biocompatibility and antimicrobial properties.

Chapter 5: Biodegradation and thermal studies of carbohydrate functionalized SBS

This chapter describes the biodegradation and thermal studies of carbohydrate functionalized SBS. Biodegradation studies were conducted for a period of 30 days using fungal and bacterial culture. The fungal culture used in this study was Pseudomonas sp. (NCIM 2220) and the bacterial culture was Aspergillus Niger (NCIM 1025). Biodegradation was monitored by weight loss in case fungal culture and by optical density (OD) in case of bacterial culture. The transition temperatures (Tg)

of these elastomers were determined by differential scanning calorimetry (DSC). Thermal stability of the polymers was studied by thermogravimetry (TGA). The synthesized elastomers were biodegradable and showed good thermal stability along with well characterized Tg.

Chapter 6: A morphological study of carbohydrate functionalized SBS

This chapter describes the morphological study of the synthesized elastomers using different techniques. The morphologies of carbohydrate functionalized SBS were studied using scanning electron microscopy (SEM), atomic force microscopy (AFM), transmission electron microscopy (TEM) and wide angle x-ray diffraction (WAXRD). SEM, AFM, TEM in conjunction with WAXRD, provided the complete morphological picture of the carbohydrates functionalized SBS.

Chapter 7: Isolation and characterization of natural polymer Lignin containing residual carbohydrates as a model for synthetic cross linked polystyrene with anchored carbohydrate moieties

This chapter deals with the study towards lignin containing residual sugars as synthetic cross linked polystyrene polymer. Lignins from different sources were characterized and their sugar content was determined by xylanase treatment. The effect of sugar content on thermal stability and lignin biodegradation by laccase enzyme was also studied.

Chapter 8: Summary and conclusions

This chapter summarizes the results and describes salient conclusions of the investigations reported in the thesis with the suggestion for future work

Chapter 1

Introduction and literature survey

Introduction and literature survey

1.1. Thermoplastic elastomers

Elastomers can be classified in three main broad groups as natural rubber, synthetic rubber and thermoplastic elastomers (TPE). TPE can be further classified into six classes namely, styrenic block copolymers, polyolefin blends, elastomeric alloys, thermoplastic polyurethane, thermoplastic copolyester and thermoplastic polyamides. Styrene–butadiene–styrene (SBS) is an important class of thermoplastic elastomers (TPE). TPE sometimes referred to as thermoplastic rubbers, are a class of copolymers which consist of materials with both thermoplastic and elastomeric properties. TPE derive their strength and elasticity from physical cross linking of the molecules into a three-dimensional network. TPEs possess many of the physical properties of cross linked or vulcanized elastomers at room temperature like softness, flexibility, and elasticity; but in contrast to conventional rubbers, they can be processed as thermoplastic materials [1]

Natural rubbers are covalently (irreversibly) crosslinked and, therefore, they cannot be processed once the material is shaped and vulcanized. In contrast, the crosslinks in thermoplastic elastomers are reversible in nature, allowing a processing applying conventional technique for thermoplastics, e.g. injection molding and extrusion. Another important properties of TPE is that they are phase separated system consisting of a hard thermoplastic phase having a T_g or if semi-crystalline, a melting transition temperature T_m above room temperature and a soft elastomeric phase with T_g below room temperature.

Upon heating the TPE above hard phase T_g or T_m the TPE flows and can be processed. When cooled again below this temperature, the TPE solidifies regaining its elastomeric properties and becomes phase separated. The same phenomenon also occurs when the hard phase is dissolved in a solvent. Upon dissolution, the TPE solution will flow and it will reset once the solvent evaporates. In contrast, a chemical crosslink will not allow flow upon heating or dissolution in a solvent with breaking the covalent bond, nor will the covalent bond reforms after cooling or evaporation of the solvent. For this reason the strength imparted by the hard phase in TPE is referred as 'physical cross-links' rather than a chemical cross-links [2-3]. The thermoreversible nature of the crosslinks in TPEs can be of various type *e.g.* phase separation, reversible chemical bonding, hydrogen bonding, metal complexation, or electrostatic interactions.

This characteristic of mimicking the properties of vulcanized rubber without undergoing a crosslinking reaction has enabled TPE to take over market previously held by thermoset rubber. Another advantage is the possibility to recycle the TPE scraps and thus reducing environmental pollution.

1.2. Background of TPE

During world war II there was high demand for natural rubber and supply was limited, this led to search for materials that can be used as an alternative for natural rubber. Soon TPE were discovered as a substitute for natural rubber and it was first commercialized in the late 1950 to mid 1960. The initial commercial TPE to enter the market were thermoplastic polyurethanes and styrenic block copolymers and since that time their commercial significance has continued to grow.

The methods of synthesizing a wide variety of thermoplastic elastomers and their characteristics have been described in the patent literature, scientific journals and books [4–21]. Global demand for TPE was forcasted by freedonia group to be 301 million metric ton in 2009 with a growth rate of 6.4 %. Thus, it was no surprise when Plastics Technology magazine pronounced thermoplatic elastomers (TPE) as one of the 50 most important innovations that changed the plastic industry over the past 50 years.

ABA-type thermoplastic elastomers like poly(styrene-b-butadiene-b-styrene) which became commercially available in 1965, exhibit unique properties of high tensile strength and high elongation without curing or reinforcement by fillers owing to their heterophase morphology [22-25]. The styrene-butadiene block copolymers possess a two-phase microstructure due to incompatibility between the polystyrene and polybutadiene blocks, the former separating into spheres, rods or lamella depending on the exact composition. With low polystyrene content, the material is elastomeric with the properties of the polybutadiene predominating. The incompatibility of the polystyrene A blocks—a minority component—and the polydiene B blocks produces a dispersion of very small polystyrene domains within the polydiene matrix. These polystyrene domains, which are glassy at room temperature, function as both fillers and thermally reversible crosslinks for the rubbery polydiene matrix, and thus account for the thermoplastic elastomer (TPE) properties of these amorphous triblock copolymers.

Polybutadiene blocks, joined together by polystyrene clusters acting as cross links

Clusters of polystyrene block
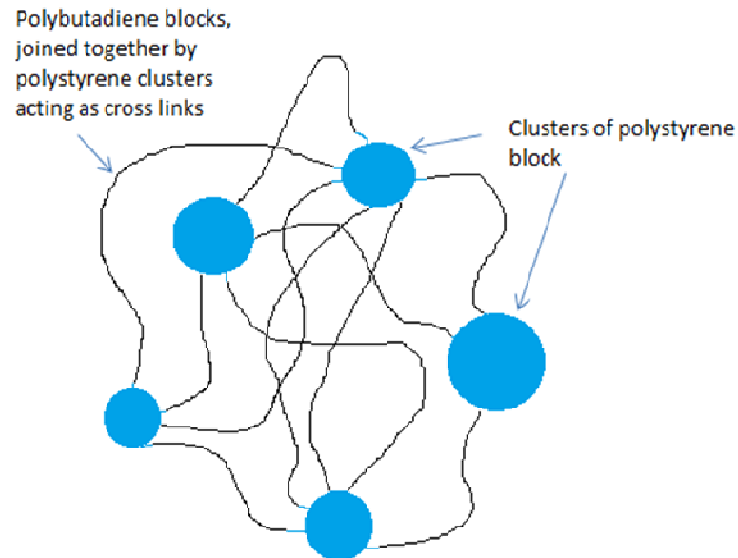
Figure 1.1 Schematic representation of SBS

1.3. Styrenic block copolymers (SBCs)

SBCs are the most commercially significant elastomers among the thermoplastic elastomer (TPE) class. Styrenic block copolymers (SBCs) are the largest-volume TPE which are mainly used in the foot wear industry. In 2007 the Americas accounted for around 30%, Europe 21% and Asia almost half of the total world market. The global market is forecast to grow around 4% per year during 2007–2012 [26]. They have four different structures: triblock, diblock, diblock/triblock mixtures and branched copolymers.

The polymerization technique used to synthesize SES is called anionic polymerization [27-28] and is limited to the use of three different monomer building blocks: styrene as the hard segment (S) and either isoprene or butadiene as the soft segment, or elastomer segment (E). Therefore, only styrene-isoprene-styrene (S-I-S) and styrene butadiene styrene (S-B-S) copolymers can be formed from this process.

This polymerization method is started by the addition of an alkyl lithium initiator to styrene (S) monomer which polymerizes to form an S block. Then S block initiates the polymerization with the E monomer forming the E block, which in turn initiates further polymerization with S. The end of the reactive polymer blocks will remain active or "living" to initiate continued polymerization until special terminating agents is added. Once the desired SBCs block copolymer structure is achieved, the reaction is complete.

1.4. Synthesis of SBS

Styrene-Butadiene (SB) copolymers are synthesized through anionic polymerization via either sequential or coupling methods [27-28]. For synthesizing SBS triblock copolymers, in both methods, the synthesis comprises of initiation of styrene polymerization using a mono-anionic organolithium compound to form living polystyryl anion, followed by addition of a butadiene monomer to form living SB di-block. In the sequential method, a second quantity of styrene is added to the living SB di-block in order to complete the formation of SBS tri-block copolymer.

The coupling process differs from the sequential one in that the tri-block copolymer is terminated by coupling two living SB di-blocks using difunctional compounds such as dicarboxylic acid esters, phosgene, etc. The efficiency of each method depends on the temperature, polarity of the solvent, and presence of impurities (water, alcohol, etc). Generally coupling process produces more symmetrical end blocks and highly monodisperse block copolymers compared to the sequential one [29].

1.5. Microstructure of SBS

SBS triblock copolymer consists of immiscible, but covalently bonded, linear blocks of polystyrene and polybutadiene. Polybutadiene microstructure consists of two type of linkages 1,4 linked butadiene and 1,2 linked butadiene; 1,4 butadiene consists of cis and trans butadiene configuration. Generally, SBS copolymer contain higher amount of 1,4 trans content followed by 1,4 cis and the remaining is 1,2 linked butadiene . These structures are shown in figure 1.2
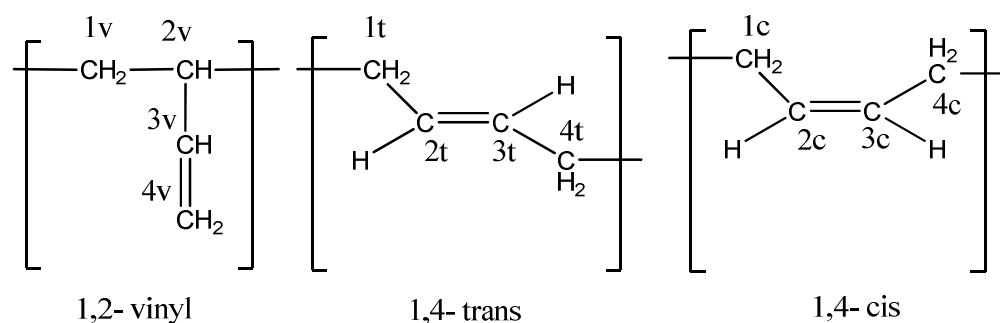
Figure 1.2 1, 2 and 1, 4 structural units (microstructures) of butadiene in SBS **v:** vinyl, **t:** trans, **c:** cis

1.6. Modification of SBS

Studies on modification of SBS has itself become an exciting playfield for polymer chemists, due to wide ranging changes in the structure, microstructure, and physical properties that can be incorporated on the original SBS elastomer. SBS is a hydrophobic block copolymer prepared by anionic polymerization technique which makes incorporation of polar monomer during polymerization a difficult task. The only possibility of incorporating polar monomers is through post polymerization modification of this copolymer. Since it contains reactive double bonds in the form

of 1,4 and 1,2 linked polybutadiene units, it could be functionalized with polar molecules leading to formation of amphiphilic SBS from a hydrophobic SBS. This approach has attracted interest and had been utilized to widen the end applications of SBS.

Among the different strategies used for modifying polymers, the most important are grafting, blending and curing as illustrated schematically below [30].
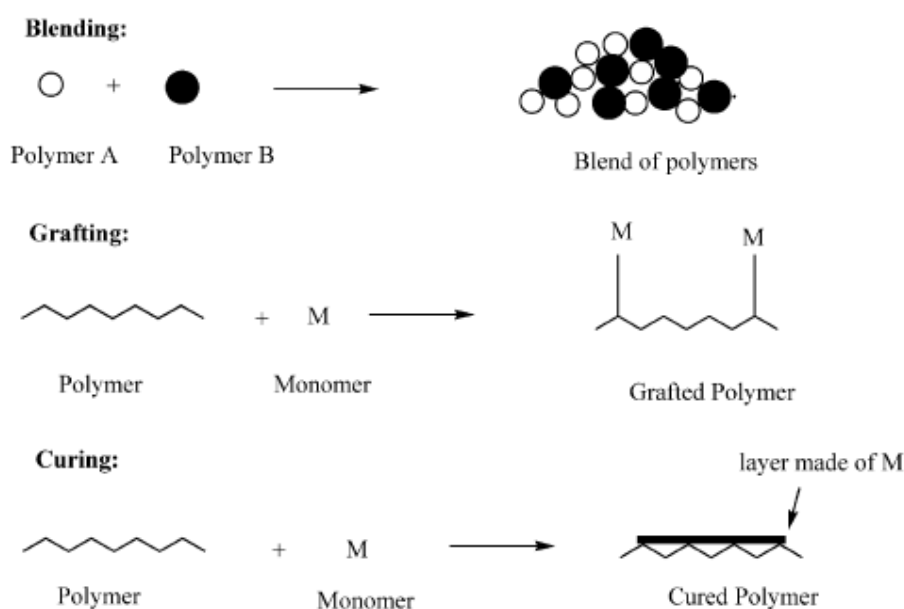
Figure1.3 Schematic representation of the methods of polymer modification [30]

The common methodologies used for SBS modification utilizing the butadiene reactivity are hydrogenation, epoxidation, free radical addition, UV and gamma ray irradiation induced graft copolymerization, Alder ene functionalization, melt functionalization, composites and blending. Amongst these epoxidation has been the most widely used technique for SBS modifications.

1.6.1 Epoxidation of Styrene butadiene copolymer

The epoxidation of unsaturated polymers is an important reaction because epoxide groups can be used as reactive intermediates for further reactions such as crosslinking, the attachment of bioactive substances, and the introduction of ionisable groups. Epoxidation reactions have been applied to natural rubber and polybutadiene elastomers [31]. Many types of peracids, such as performic acid, peracetic acid, and *m*-chloroperbenzoic acid (MCPBA) [32], dioxirane [33], hydrogen peroxide [34-35], monoperoxyphthalic acid [36] and in situ generated peracetic acid [37] have been used for the epoxidation of unsaturated polymers [38-40]. Epoxidation of olefinic polymers with hydrogen peroxide as the oxidant and methyltrioctylammonium tetrakis (diperoxotungsto) phosphate has also been reported [41].

The reactivity of double bonds in polybutadiene units toward epoxidation has been studied by many authors [42-43] using peracids, and it has been found that 1,4-unit is more reactive than 1,2-unit.

Hsiue et al. epoxidized SBS in toluene solution with in situ generated peroxyformic acid [44] and studied the gas permeability and gas selectivity with the epoxidized SBS membranes. They found that gas permeability decreased with increasing epoxide content, while it increased with increasing the operating temperature in the range of 273-303 K. Udipi studied the epoxidation of Styrene butadiene copolymer in toluene and cyclohexane solutions, with in situ generated peroxyformic acid using formic acid and hydrogen peroxide and evaluated its resistance to ASTM oils.

The epoxidation by peracids depends on the source of the peracid (performed or *in situ* generated), its chemical nature, and the presence of a catalyst. The *in situ*

method is usually acid-catalyzed. However, the presence of an acid as a catalyst leads to side reactions such as hydroxylation or ester formation [45].

The in situ epoxidation takes place according to the following mechanism [46].
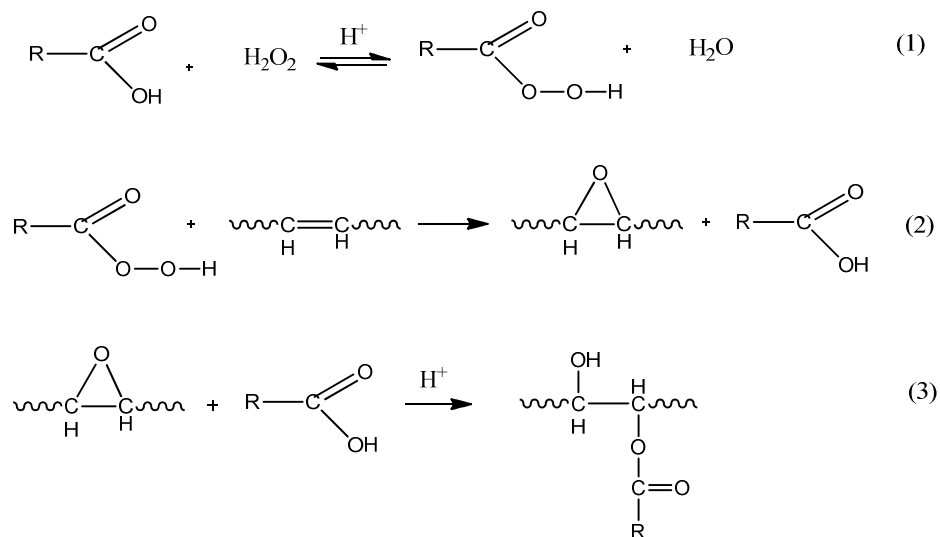
Figure 1.4 Mechanism of in situ epoxidation with formic acid and hydrogen peroxide

It can be seen from the above mechanism that in situ generated peroxyacetic acid in step (1), attacks the alkene leading to epoxidation in step (2). The epoxide can further react with the acid forming ester as side product as shown in step (3).

Jiang et al. [47] performed the epoxidation of styrene butadiene triblock copolymer upto 70 % conversion with hydrogen peroxide as the oxidant and methyltrioc-tylammonium tetrakis (diperoxotungsto) phosphate (3-) as the catalyst in 1,2 di-chloethane solvent. Huang et al. performed homogeneous epoxidation [48] of SBS using monoperoxyphthalic acid at different temperatures in dioxane and in mixed solvents containing chloroform.

Recently Ocando et al. studied the epoxidation of SBS with hydrogen peroxide in water/dichloroethane biphasic system and evaluated the minimum degree of epoxidation required to develop nanostructured epoxy systems.

1.6.2 Hydrogenation of SBS

SBS block copolymers do not have good long term heat, weather, ozone and UV stability because of the presence of unsaturated double bonds in its polybutadiene blocks [49]. One way to circumvent this drawback is through selective hydrogenation of polybutadiene segments keeping the aromatic polystyrene microstructure intact so as to maintain its elastic property. The hydrogenation is an important modification process used for improving the chemical and mechanical properties of variety of thermoplastic polymers including SBS [50]. Hydrogenation of adhesives based on styrene butadiene copolymers have found to lead to significant improvement in their stability. Hydrogenation of an SBS triblock copolymer with a moderate amount of 1,2 units in the centre block yields a copolymer with a poly(ethylene-co-butylene) centre segment. This modified polymer has greatly improved thermal and oxidative stability, by virtue of its poly(ethylene-co-butylene) centre block.

There are two types of catalysts which are normally used for the hydrogenation of SBS; (**1**) homogeneous catalyst, such as a bis(cyclopentadienyl) titanium catalyst or aluminum alkyl with a group VIII metal containing catalyst and (**2**) heterogeneous catalyst, such as a refractory oxide-supported metal catalyst[51-52]. Heterogeneous and homogeneous hydrogenation, both has been reported for unsaturated polymers. Heterogeneous hydrogenation needs drastic conditions, which leads to side

reactions like crosslinking or chain scission [53]. However, homogeneous catalytic hydrogenation requires mild conditions and has high activity and selectivity.

The SBS rubber hydrogenation process using a homogeneous catalyst requires removal of group VIII metal from the hydrogenated polymer because the group VIII metal remaining in the polymer will catalytically degrade the hydrogenated polymer. Removing the residue metal is complicated due to the fine size of the colloidal catalyst suspension [54]. Moreover, the equipment and the wastewater treatment for the residue metal removal are expensive because of the utilization of phosphoric acid or sulphuric acid for dissolving the residue metal. On the other hand, SBS hydrogenation by heterogeneous catalyst does not have the problem of residue-metal removal. However, the activity of the catalyst is low and the process requires high catalyst concentration and long reaction time to obtain high levels of hydrogenation.

The catalyst recovery and its separation from the product and residual metal residue are major drawbacks of both these catalytic processes. A patent from Shell Oil Company reported metallic residue of 300-400 ppm [55] after hydrogenation and before a post treatment. However, even after post treatment 25 ppm of metal residue still remains in the polymers, making complete metal removal a costly affair. There have been concerted efforts towards development of process for effective metal residue removal [56-57] besides avoiding crosslinking [58].

Metals known to be useful for hydrogenation reaction include Ni, Pt, Pd, and Ru. Hydrogenation of SBS block copolymers is typically done in cyclohexane solution using nickel octoate and triethylaluminum catalysts at high temperatures and pressures [59-60]. Use of homogeneous metallocene catalysts [61] and noble metal complex catalysts [62-66] has also been reported for unsaturated polymer hydro-

genation. Considerable studies have been found in the patent literatures on hydrogenating conjugated diolefin polymers using metallocenes as the hydrogenation catalyst. Kishimoto et al. found that bis-(cyclopentadienyl)titanium(IV) compounds, in the presence of an alkyl lithium compound, were effective hydrogenation catalysts [58], and Chamberlain et al. claimed that a bis-(cyclopentadienyl)titanium(III) compound would also be effective as well [67].

Ionic liquids have been demonstrated to be ideal immobilizing agents for organometallic catalysts in hydrogenation reactions. However, only few papers have been reported about polymer hydrogenation in ionic liquids. The first report for hydrogenation of SBS in ionic liquid was by Wei et al., catalyzed by Ru/TPPTS complex in polyether modified ammonium salt ionic liquid biphasic system [68].

1.6.3 Free radical grafting onto SBS

Among the methods of modification of polymers, grafting is one the most important and commonly used method. The grafting polymerization is a well known method for anchoring functional groups on polymer and to modify the chemical and physical structure of polymers to be suitable for specific applications. Several studies have appeared in literature dealing with grafting vinyl monomers onto polymers such as styrene-butadiene block copolymers [69] styrene-isoprene copolymers [70], styrene-(ethylene -co- butadiene)-styrene triblock copolymers [71] polycis- butadiene rubber (PcBR) [72] and acrylonitrile-butadiene- styrene (ABS) terpolymer [73] .

Graft copolymerization is used to modify the properties of polymers such as wetability, dyeability, adhesion or enhancing the hydrophilic character of polymer. The common method of graft copolymerization is a radical polymerization of vari-

ous monomers that is initiated by a chemical initiator including grafting polymerization both in solution and in melt using benzoyl peroxide [74], hydrogen peroxide [75], azobisisobutyronitrile [76] and ceric ions [77], plasma [78], high energy irradiation (electromagnetism, gamma ray) [79],and ultraviolet light (UV) photografting [80].

Hsiue et al. reported grafting of 2-Hydroxyethyl methacrylate (HEMA) onto a membrane of SBS by ^{60}Co gamma-ray irradiation method [81]. The mechanical properties of SBS-*g*-HEMA were found to be superior to those of poly(HEMA) and were identical with those of SBS, and the wetting and nonthrombogenic properties of SBS-*g*-HEMA were found to be better than those of unmodified SBS.

Yang et al. extended the work of Hsiue et al. and reported synthesis of dimethylaminoethyl methacrylate (DMAEMA) grafted SBS copolymer membrane by the UV irradiation method [82]. They also measured protein absorption of fibrinogen and albumin to evaluate the blood compatibility of the modified SBS. From the contact angle, surface energy and protein absorption measurements, it was concluded that SBS-g- DMAEMA copolymer membranes showed better wetting and blood compatibility properties than SBS. In a subsequent report by these authors [83] they quaternized the amino group present in SBS-g- DMAEMA copolymer with idomethane and subsequently synthesized heparin containing SBS-g-DMAEMA (SBS-g-DMAEMA-HEP) by treatment with heparin. The reaction scheme for this reaction is shown in figure 1.5 below.
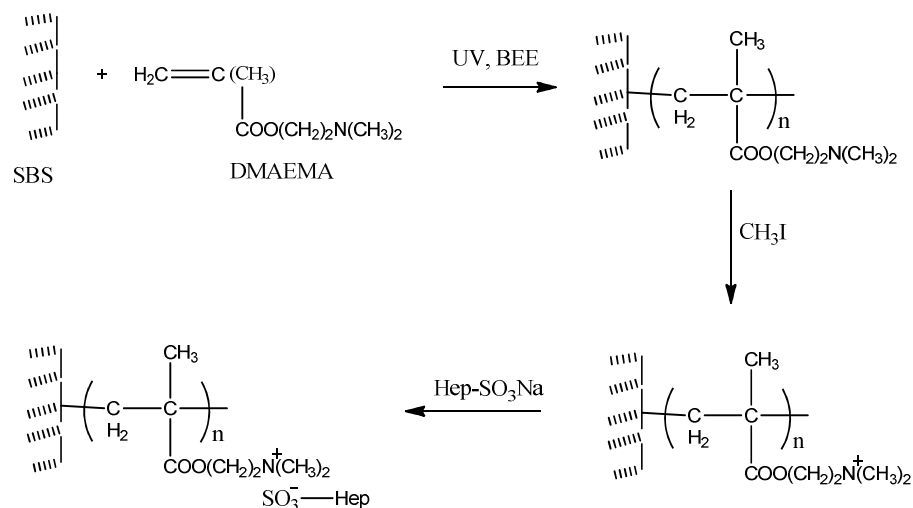
Figure 1.5 Synthetic procedure for the heparin-containing SBS-g-DMAEMA graft

copolymer [83]

In yet another report by Yang et al. on SBS-g- DMAEMA [84], they studied the gas

permeability, gas selectivity and mechanical strength of the modified SBS. The

changes of properties of SBS-g-DMAEMA copolymer membrane reduced the gas

permeability and diffusivity of oxygen and nitrogen through the membrane, but

increased the gas solubility of oxygen through the membrane and the gas selectivity

between oxygen and nitrogen. When the operating temperature is between 288 K

and 308 K the solubility of oxygen in the SBS-g- DMAEMA copolymer membrane

increases with increasing DMAEMA grafting but the solubility of nitrogen in the

SBS-g-DMAEMA copolymer membrane reduces.

Recently, Kennedy et al. [85] explored grafting of SBS with acrylic acid (AA) via UV

polymerisation technique using benzophenone as the photoinitiator for use as a

potential biomedical material. They proposed that allylic hydrogen associated with

butadiene in SBS copolymer reacted with acrylic acid monomer, as illustrated in figure 1.6 below.
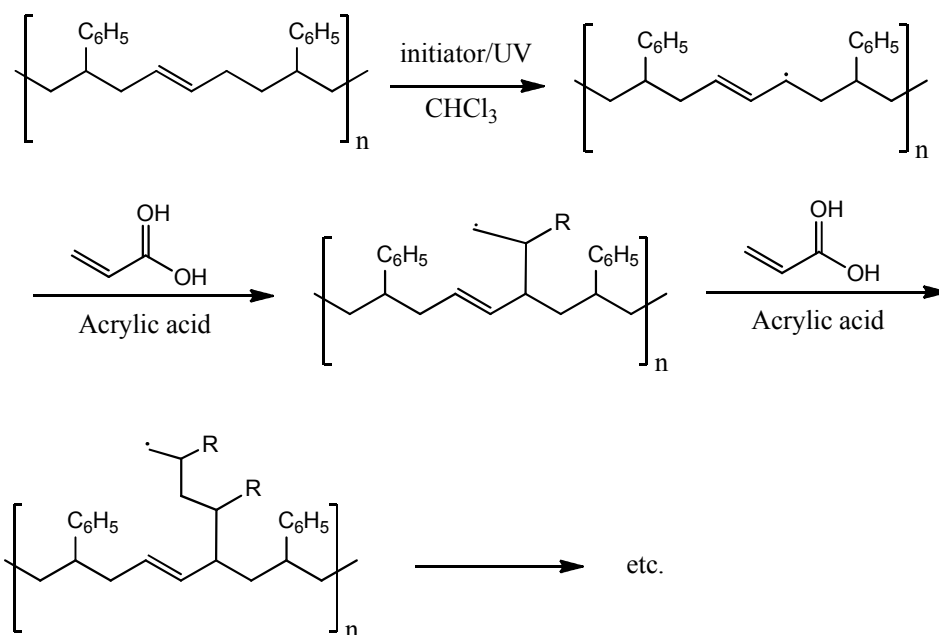
Figure 1.6 Proposed reaction scheme illustrating the reaction of SBS and AA to

yield SBS-g-AA copolymers [85]

They showed that the glass transition values for each of the grafted copolymers increased in the butadiene domain, thus proving that grafting had occurred. They further evaluated the mechanical properties of acrylic acid modified SBS by DSC, DMTA and tensile studies and found these properties suitable for use in biomedical applications. This work was further extended by these authors, and in the subsequent publication they reported the grafting of N isopropylacrylamide (NI-PAAm) on SBS by UV polymerization using benzophenone as the photoinitiator [86] for potential use as biomaterials, by improving the water absorption and thermosensitivity of SBS.

Functionalization of polymers with maleic anhydride (MAH) has been extensively used due to the high reactivity of anhydride ring for subsequent reactions. The MAH grafting reaction can be conducted in solution or in melt state. Wilhelm et al. reported the bulk modification of SBS with MAH in a mixing chamber of a Haake rheomixer with benzoyl peroxide initiator in melt [87]. They evaluated the effect of temperature, MAH and benzoyl peroxide concentration on the grafting efficiency. They found low grafting efficiency along with crosslinking of the product under their reaction conditions. They also studied the effect of addition of a diamine, 4,4'-diaminediphenylmethane towards inhibition of the crosslinking reaction and reported that at low concentration this diamine effectively reduces the crosslining reaction, but at high concentration it increases the crosslinking by acting as a cross linker.
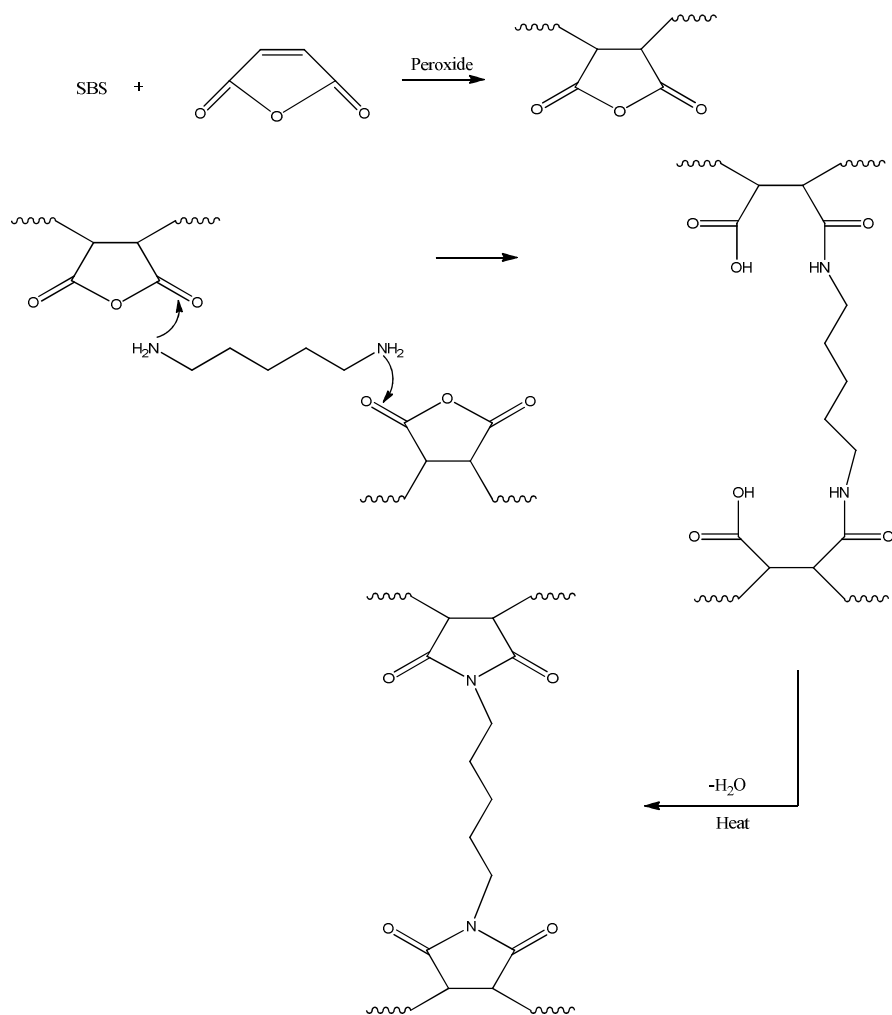
Figure 1. 7 Schematic representation of the crosslinking of the modified SBS with

diamine [87]

MAH has also been grafted on polymers using 2,2'-azo-bis-isobutyronitrile (AIBN) and benzoyl peroxide (BPO) are used as radical initiators, this grafting takes place either by addition to C=C or by removal of an allylic hydrogen atom. Rao et al. [88] showed that MAH is grafted onto the ABS by adding on the double bond with BPO as initiator, whereas Kang et al. [89] reported that BPO functioned by removal of allylic hydrogen atom whereas AIBN functioned by addition to the double bond. Brydon et al. [90-91] studied the grafting reaction styrene polybutadiene system and found that no grafting occurs when AIBN is used as initiator. Gasperowicz et

al. [92] studied the grafting of styrene on polybutadiene and they found that graft reaction occurs by the abstraction of a hydrogen atom from a methylene group and supported this by claiming no change in double bond content after grafting. The reaction of methyl methacrylate with SBS in the presence of either BPO or AIBN as initiators in two different solvents, chloroform and tetrahydrofuran (THF) was reported by Jiang and Wilkie [93]. They found that the combination of benzoyl peroxide in chloroform gave the highest graft yield and the reaction proceeds by removal of allylic hydrogen from SBS by the initiator radical followed by addition of monomer units to that site. They also found that both AIBN and BPO function by removal of allylic hydrogen atom from SBS and the efficiency of BPO was higher than AIBN.

To clear the doubt regarding the site of grafting when AIBN and BPO are used as initiators, Aimin et al. explored the grafting of maleic anhydride (MAH) on SBS with benzoyl peroxide (BPO) and 2, 2'-azo-bis-isobutyronitrile (AIBN) as initiators [94]. They showed that grafting reaction initiated by AIBN radical occurs by addition to the double bond, while with BPO radical it occurs both by removal of allylic hydrogen atom from SBS as well as addition to C=C of SBS. The mechanism for both of these processes is shown in the figure 1.8.

(a) Abstraction of α-hydrogen (allylic hydrogen) from the Polybutadiene (PB) main chain by the initiator radical:
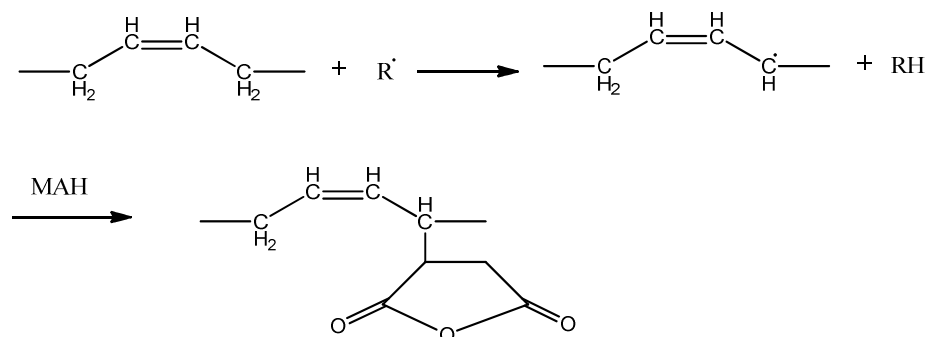
(b) Addition of the radical to the double bond of PB chain:
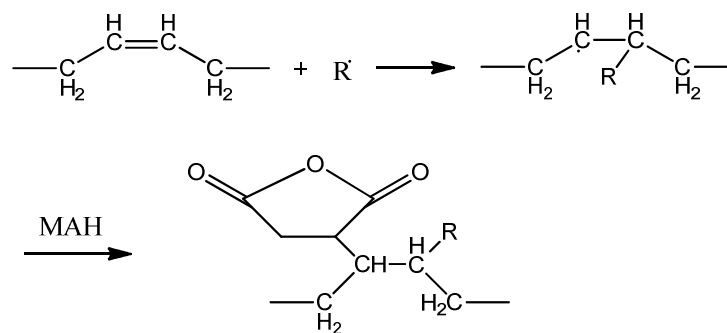
Figure 1.8 Mechanism for radical grafting of maleic anhydride (MAH) on SBS [94]

Cordella et al. studied the melt functionalization of SBS with glycidyl methacrylate (GMA) and dicumyl peroxide as initiator [95]. They used factorial design to evaluate the influence of GMA and peroxide content on the grafting degree, conversion and cross linking. Taha et al. [96] reported the condensation of succinic anhydride functionalized polystyrene-hydrogenated polybutadiene-polystyrene triblock co-polymers with polymethyl methacrylate, polyoxyethylene and polyoxyethylene-

oxypropylene oligomers having hydroxy or amine end group and various chain length.

In a series of publications, Huang et al. have studied grafting reaction of vinyl monomers styrene, benzyl methacrylate, and benzyl acrylate on cis polybutadiene (PBD) [97-100] . They showed that benzoyl peroxide BPO is a more effective initiator for graft copolymerization than is AIBN for styrene and benzyl methacrylate but that both initiators are about equally efficient for benzyl acrylate. Several reports are also there for modification of acrylonitrile-butadiene-styrene (ABS) by grafting with methacrylic acid [101], acrylamide [101] and acrylic acid [102].

1.6.4 Grafting via epoxide ring opening

Epoxide ring opening of epoxidized polymers with various nucleophilic reagents such as acid, amine, thiol and alcohol has been a useful strategy to synthesize amphiphilic polymers from hydrophobic polymers. Soutif et al. [103] reported the addition of napthylacetic acid on epoxidized 1, 4 polyisoprene using tetramethyl-ammonium salt of the acid as catalyst. . Derouet et al. [104] modified epoxidized 1,4- polyisoprene via ring-opening reaction with alcohol using cerium ammonium nitrate as catalyst.

Epoxide ring opening have been employed for synthesis of SBS ionomer from epoxidized SBS. Ionomers are polymers containing less than 10 mol % ionic group and shows useful properties and applications due to presence of ionic domains. They have applications in packagings, as elastomers, adhesives, polymer additives and rheology modifiers. Nandi et al [105] synthesized sulphonated cis-1, 4 polybutadiene ionomer using tetrabutylammonium bromide as a catalyst. Recently Xie et al. [106] synthesized quaternary ammonium ionomer of SBS via ring-opening reac-

tion of epoxidized SBS with triethylamine hydrochloride with 100% conversion. Xie et al. [107] reported the synthesis of maleated Styrene butadiene rubber iono- mer by ring opening of epoxidized SBS with potassium hydrogen maleate in the presence of a phase transfer catalyst without nitrogen atmosphere. They found that with increasing ionic groups, the water absorbency of the ionomer increases whereas their oil absorbency decreases. They further showed that this ionomer can find use as a compatibilizer for the blends of SBS and chlorosulphonated polyethyl- ene (CSPE).
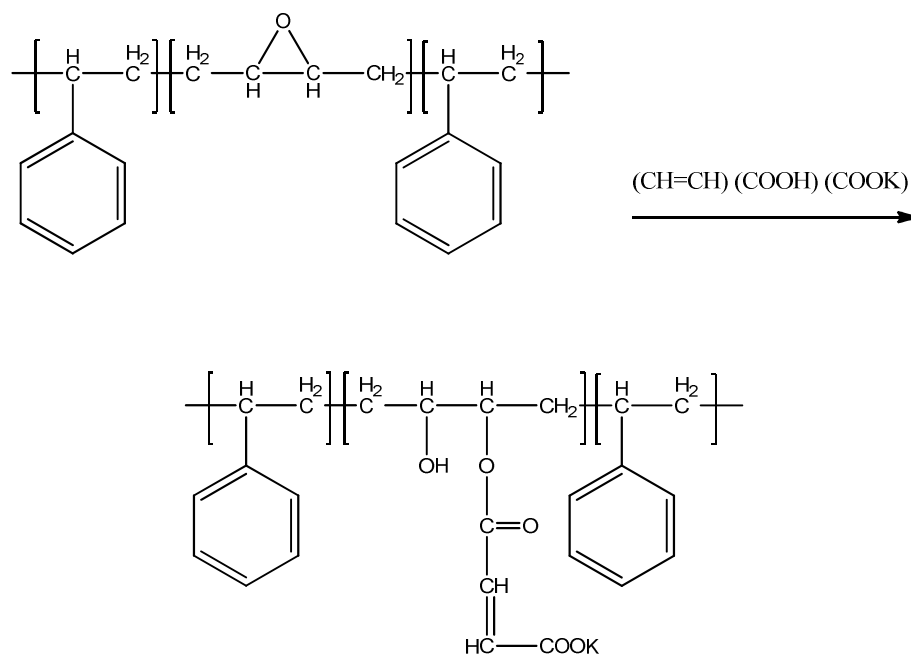
Figure 1.9 Schematic representation for synthesis of potassium maleate ionomer

of SBR [107]

Xie et al. [108] reported the synthesis of maleated SBS ionomer from epoxidized SBS following a similar experimental protocol previously used for synthesis of SBR ionomer [107]. They showed that this SBS ionomer can be used as a compatibilizer for the blends of SBS and oil resistant chlorohydrin rubber. Styrene butadiene ionomers were also synthesized by grafting of maleic anhydride on Styrene butadiene copolymer and subsequent opening of the anhydride ring with potassium hydroxide.

A. Molnar performed the first study in 1992 of sulfonated hydrogenated styrene-butadiene random copolymers [109]. Later, Nishida et al. reported the synthesis of Sodium sulfonated poly(styrene-ethylene-butylene) random ionomers [P(SEB-co-SSNa)] by hydrogenation, sulfonation, and neutralization of styrene-butadiene copolymers containing 45 wt % styrene [110] and carried out detailed study of mechanical studies of this ionomer.

Samuel et al. [111] reported the sulfonation of styrene-butadiene rubber (SBR) with higher styrene content to obtain ionomers, which act as thermoplastic elastomer. Xie et al. [112] reported that in the presence of small amount of ketone, both common SBR with 23% styrene content and SBS can be sulfonated in petroleum ether or cyclohexane without gelation. Xie et al. reported the synthesis of sulfonated ionomer of (styrene-butadiene-styrene) triblock copolymer (SBS) [113]. SBS was first epoxidized by performic acid formed in situ, followed by ring-opening reaction with an aqueous solution of $NaHSO_3$. They studied the optimum conditions for ring-opening reaction of the epoxidized SBS with aqueous solution of $NaHSO_3$ and properties of the ionomer. It has been found that during the ring-opening reaction phase transfer catalyst, ring-opening catalyst, and a pH regulator are necessary to raise the conversion of epoxy groups to ionic groups. This iono-

mer have potential application as a compatibilizer for blending equal amount of SBS and oil-resistant chlorohydrin rubber via polar-ionic interaction. Xie et al. [114] had also studied the dynamic mechanical properties of sulfonated butyl rubber ionomers neutralized with different amine or metallic ion (zinc or barium) and their blends with polypropylene (PP), high-density polyethylene (HDPE), or styrene-butadiene-styrene (SBS) triblock copolymer using viscoelastometry. Xie et al. [115] also reported the synthesis of phosphated ionomer of (styrene-butadiene-styrene) triblock polymer (SBS) by ring opening of epoxidized SBS with aqueous solution of disodium hydrogen phosphate. It is important to note that epoxidized SBS has not been used so far for incorporating sugar moieties onto SBS to render it hydrophilic, biocompatible and possibly biodegradable. These aspects are dealt with in this thesis.

1.6.5 Hydrosilylation of SBS

The addition of the Si-H bond to carbon-carbon double bonds of polymers offers a useful method of preparing silane-modified polymers [116]. Hydrosilylation of unsaturated polymers have been used to prepare polymers with special properties such as.....[117]. In addition, a considerable number of patents have been granted on the hydrosilylation of polymers.

Sol-gel process has been used to prepare hybrid materials by reaction of polymers with ceramics like silica. Hsu et al. [118] used this approach for the synthesis of triethoxysilyl functionalized poly (styrene-butadiene-styrene) triblock copolymer, SBS. This was prepared by hydrosilylation of double bonds in SBS using triethoxysilane catalyzed by cis-bis (diethyl sulphide) platinum (II) dichloride (CPD). The triethoxysilyl functionalized (TS-SBS) then underwent an in-situ sol-gel process with TEOS to give TS-SBS /SiO$_2$ hybrids. Platinum and rhodium-catalyzed hy-

drosilylation reaction [119] with various polybutadiene and copolymers of polybutadiene has also been reported.

1.6.6 Blends / Composites of SBS

'Blending' is the physical mixture of two (or more) polymers to obtain new properties. SBS is commonly use for blending with asphalt to improve its rheological properties. Adedeji et al. [120] studied the miscibility of asphalt with SBS by varying the composition of asphalt from 0-96 weight %, with aim of improving the load bearing properties of asphalt. They also evaluated the microstructural transformation of this blended system.

Crystalline polypropylene (PP) and amorphous polystyrene (PS) have been investigated to modify SBS with the aim of improving the performance of SBS. Saroop et al. [121] investigated the mechanical and rheological properties, and the crystalline structure of PP in vulcanized SBS/PP blends that contained up to 40 wt % of SBS. Halavata et al. [122] examined the crystalline structure of PP in blends with several thermoplastic elastomers. Gallego et al. [123] analyzed the morphology of SBS blends with various PP contents and the improvement in their mechanical properties. Perera et al. [124] investigated the effects of gamma radiation on PP, SBS, and PP/SBS blends. Ichazo et al. [125] compared the rheological and mechanical behaviors of dynamically and statically vulcanized PP/SBS blends. Sanchez et al. [126] examined the reinforcing effect of a dispersed phase of PS on the mechanical properties of an SBS triblock copolymer. Jelcic et al. [127] analyzed the mechanical properties and fractal morphology of SBS/ PS blends that contained up to 85 wt % SBS elastomer. Boyanova et al. [128] evaluated the phase boundary in PS/SBS blends by microindentation analysis.

1.7. Modification by utilizing 1, 2 linked butadiene units of SBS

Since ABA linear triblock polymer like SBS butadiene has two types of unit 1, 4 linked and 1,2 linked, so there is possibility of modifying SBS by utilizing the 1,2 unsaturation besides 1,4 unsaturation. Modification on the 1, 4 linked butadiene units effects changes on the SBS main polymer chain. On the other hand, modification on the 1, 2 linked butadiene units leads to new pendants on the polymer chain of SBS. There are only few reports for modification of SBS utilizing 1,2 unit. B.X. Fu et al. [129] reported the grafting of polyhedral oligomeric silsesquioxanes on SBS using the 1,2 unit of the polybutadiene segment. They first synthesized the POSS hydride (c-C5H9)7[Si8O12]((CH2)$_3$ SiMe$_2$(C $_6$ H$_4$)SiMe$_2$H), derived from commercially available POSS trisilanol, and grafted this hydride to 1,2 butadiene unit of SBS triblock copolymer by hydrosilylation reaction using Pt catalyst.
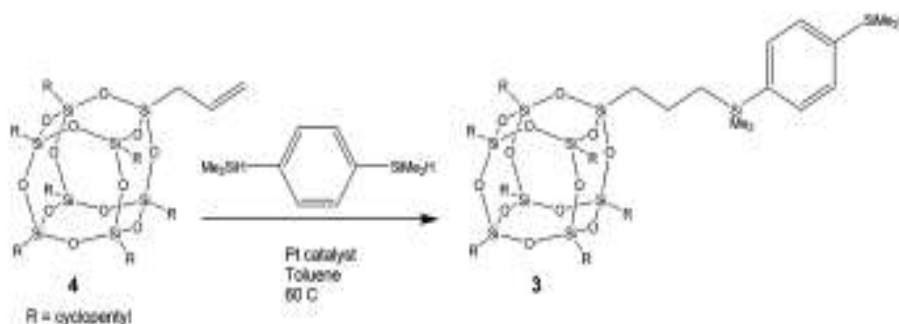
Figure 1.10 Synthesis of reactive cylopentyl POSS hydride [129]

They observed that the incorporation of POSS did not cause significant changes to the morphology of SBS and they confirmed this by SAXS study of the POSS grafted SBS. They concluded that incorporation of POSS to the butadiene block enhanced the T$_g$ value for the polybutadiene block and even improved the load carrying capability of the POSS modified SBS triblock copolymer.
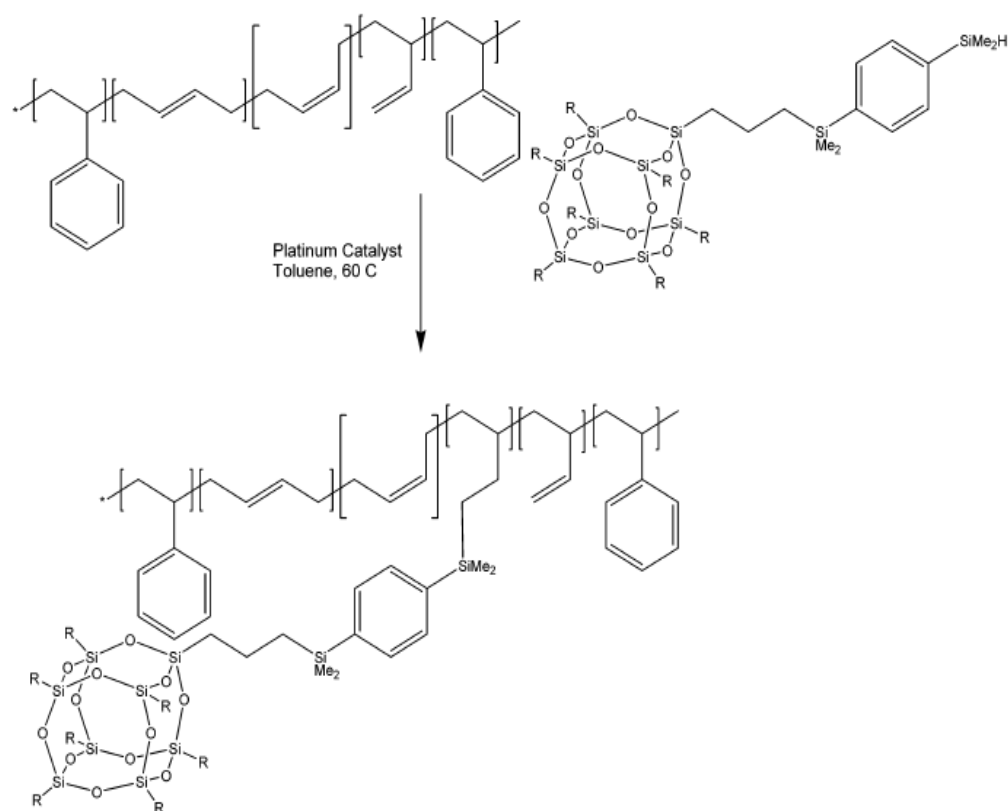
Figure 1.11 Grafting of cyclopentyl POSS hydride to SBS [129]

Alder ene reactive modification of vinylidene terminated polyolefins has been in-vestigated [130]. This type of modification cannot be carried out on the 1,4 linked butadiene. 1, 2 butadiene unit of SBS also contains such a functionality there is a possibility of modifying SBS with a suitable enophile employing the Alder ene re-action. Alder ene reaction involves the interaction between an alkene, having an allylic hydrogen (an ene), and a compound containing an insaturation (enophile), to form a new bond with migration of the ene bond and 1, 5 hydrogen shift [131].

A. Pucci et al. [132] reported the Alder ene functionalization of polyisobutene oli-gomer (PIB) and styrene-butadiene- styrene triblock copolymer (SBS) with maleic anhydride (MAH) or diethyl maleate (DEM) as enophiles.

1.8. Modification of styrene butadiene copolymers with sugars (synthesis of synthetic glycopolymers)

There are limited reports for the modification of polybutadiene with sugars, while we across with one report for glucose grafting onto styrene butadiene rubber, whereas there is no report for functionalization of SBS with sugars (protected or unprotected) till date. A 1981 Japanese patent describes emulsion grafting of glucose onto styrene butadiene rubber but they obtained a crosslinked product [133].

In recent years, carbohydrate science has become a fast developing field [134] because carbohydrates have various functions as structural materials, energy storage and recognition markers at cell membranes. Carbohydrate plays a very important role in living organisms as a highly specific recognition tool through carbohydrate - protein interactions [135]. Carbohydrate –protein interactions occur through glycoprotein, glycolipids or polysaccharides displayed on the cell surface with lectins. The binding between lectin and monovalent carbohydrate is typically weak. This limitation posed by the weak bonding has been overcome by multivalent interactions i.e simultaneous contact by the clustered carbohydrate and protein receptors that contain multiple carbohydrate recognition domains (CRD).

One of the ways to utilize saccharides in polymer science is to introduce the saccharide units onto natural or synthetic polymers. The resulting hybrid materials known as synthetic glycopolymers have many potential applications as functional materials including biomedical applications.

In 1988 Alvarez et al. [136] reported the synthesis of sucrose polyesters using a carboxylated polybutadiene. Recently, You et al. reported the synthesis of thioglucose attached 1,2-polybutadiene-block-polystyrene block copolymer [137]. They

performed this synthesis using AIBN as the initiator by a free radical addition of thioglucose tetraacetate to 1,2- polybutadiene followed by deacetylation to yield thioglucose linked 1,2-polybutadiene-block-polystyrene copolymer. They observed that the glucose-grafted polybutadiene-block-polystyrene having 17 wt % glucose, self assembled into vesicles in both organic and aqueous media. These types of synthetic glycopolymers have potential applications as model system for bioinspired structure formation and as drug carrier. The reaction scheme for this synthesis is depicted in figure 1.12 below.
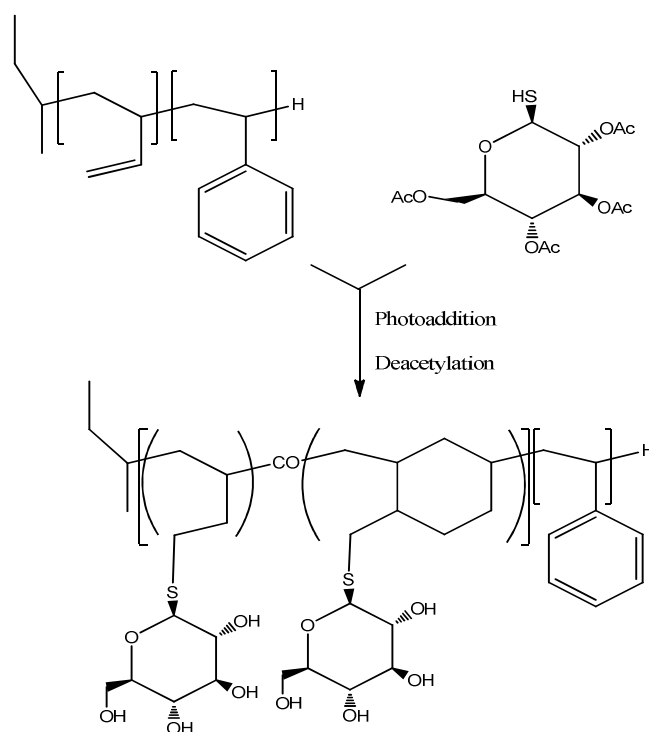
Figure 1.12 Synthesis of a glycopolymers through the radical addition pathway (Ac = acetyl) [137]

Baran et al. [138] reported the free radical addition of mercaptans (including thioglucoside) to 1,2 polybutadienes to produce hydrophobically modified polybutadienes, which self assembled in unilammelar or multilamellar vesicles in aqueous

solution. These vesicles have similarity to liposomes, hence these biohybrid systems can be used as model membranes to study biological recognition processes or for biomedical applications. Ikeda et al. reported the synthesis of a new type of amphiphilic elastomer by the reaction of butyl rubber and D-maltose [139], with butyl rubber constituting the backbone and maltose derivative served as the pendant group. This synthesis was completed in three steps: (1) Hydroxyl groups of D-maltonolactone were protected by a trimethylsilyl group (2) The resulting maltonolactone derivative was subjected to a reaction with chemically modified butyl rubber having amino groups (3) The protecting trimethylsilyl groups on the maltose residues were removed by treating with tetra-n-butylammonium fluoride to yield maltose linked butyl rubber. The physical and structural properties of this amphiphilic elastomer were studied by different methods including viscoelastic measurement and SAXS. The authors also observed aggregation of saccharide modified butyl rubber segments and confirmed this by transmission electron microscopy. They explained this aggregation behaviour as caused due to tendency of the saccharide containing domains to self assemble because of the intermolecular hydrogen bond interactions of the sugar hydroxyl groups which are dispersed in a nonpolar rubber matrix.

1.9. Synthetic glycopolymers synthesis

Sugar containing polymers are known as synthetic glycopolymers. The term glycopolymer is still not clearly defined. In a broad sense, it includes both natural and artificial carbohydrate-containing polymers, as well as synthetically modified natural sugar-based polymers. Research in the area of carbohydrate containing polymers has increased dramatically as witnessed by the increasing number of reviews

and publications in this area. The important methods for synthesis of synthetic glycopolymers are [140]:

(1) Glycopolymer synthesis via free radical polymerisation

(2) Glycopolymer synthesis by ionic polymerisation

(3) Glycopolymer synthesis by ring-opening polymerisation (ROP)

(4) Glycopolymer synthesis by nitroxide-mediated radical polymerisation

(5) Glycopolymer synthesis by click chemistry

Since there is large number of examples for each of the methods mentioned above for the synthesis of synthetic glycopolymers, we have taken only few representative examples for each of the methods described below.

1.9.1 Glycopolymer synthesis via free radical polymerization

Free radical polymerization is a very common synthetic technique used for synthesis of a variety of polymers. The first glycopolymer synthesis was reported by Horejsi et al. in 1978 [141]. They copolymerised acrylamide and allyl glycosides of various sugars **1** (fig. 1.13) in water using ammonium persulfate as initiator and tetramethylethylenediamine (TMEDA) as catalyst. The synthesized O-glycosyl derivatives of polyacrylamides showed lectin binding activities similar to natural polysaccharides. Polyacrylamide derivatives are synthetically important because of their water solubility and their stability towards hydrolysis.
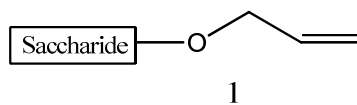
Figure 1.13 Synthesis of allyl glucoside

Kitazawa et al. [142] reported the synthesis of acrylic monomers containing a pendent monosaccharide **2-5** (Fig. 1.14), by glycosidation of methyl glycosides with 2-hydroxyethyl acrylate or methacrylate with a heteropolyacid catalyst and free radical initiator.
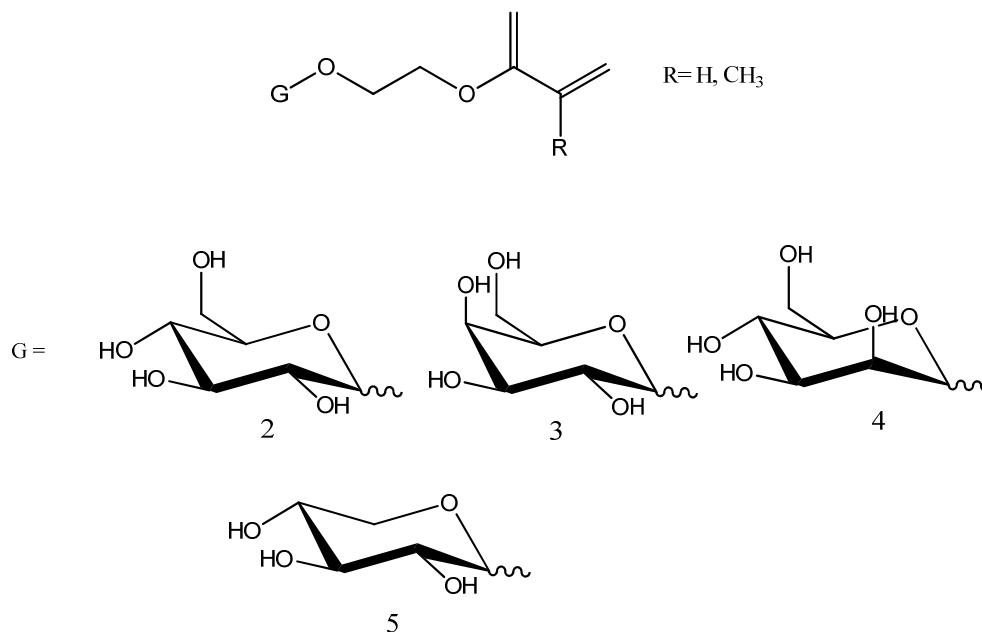
Figure 1.14 (2) glucopyranosyloxyethyl acrylate and methacrylate (3) galactopyranosyloxyethyl acrylate and methacrylate (4) mannopyranosyloxyethyl acrylate and methacrylate (5) xylopyranosyloxyethyl acrylate and methacrylate

Kobayashi et al. [143] synthesised (p-vinylbenzamido)-b-chitobiose and (p-vinylbenzamido)-b-lactose **6-7** (fig. 1.15), and polymerized with acrylamide in DMSO using AIBN as an initiator.
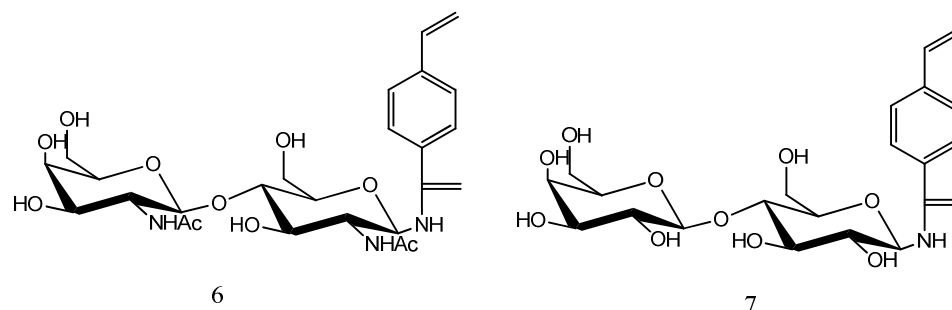
Figure1.15 (6) (p-Vinylbenzamido)-b-chitobiose (7) (p-vinylbenzamido)-b-lactose

Tsuchida et al. synthesized Poly(p-vinylbenzoyl-b-sialyllactosylamine) with ammonium peroxodisulfate and TMEDA in water [144]. This polymer showed a strong inhibition of the hemagglutination of influenza virus, with very high activity. Yoshida et al. reported the synthesis of polymethacrylates bearing sulfated maltoheptaose using AIBN as the initiator, which displays anti-HIV activity.

Akai et al. synthesized monomers with styrene attached to α- mannopyranoside **8** (fig. 1.16) and various C-2 substituted β- mannopyranosides **9** (fig. 1.16) and obtained the corresponding glycopolymer by polymerization with AIBN in DMSO [145]. They then carried Con A binding ELISA study with these glycopolymers and reported that α-mannopyranoside and C-2 fluoro substituted β-mannopyranoside glycopolymer showed 10^3 higher affinity as compared to monomeric α-mannopyranoside and α-glucopyranoside. Klein et al. [146] reported the synthesis of anionic maleicamido saccharide monomers which were copolymerized in water with acrylamides using azo-initiator.
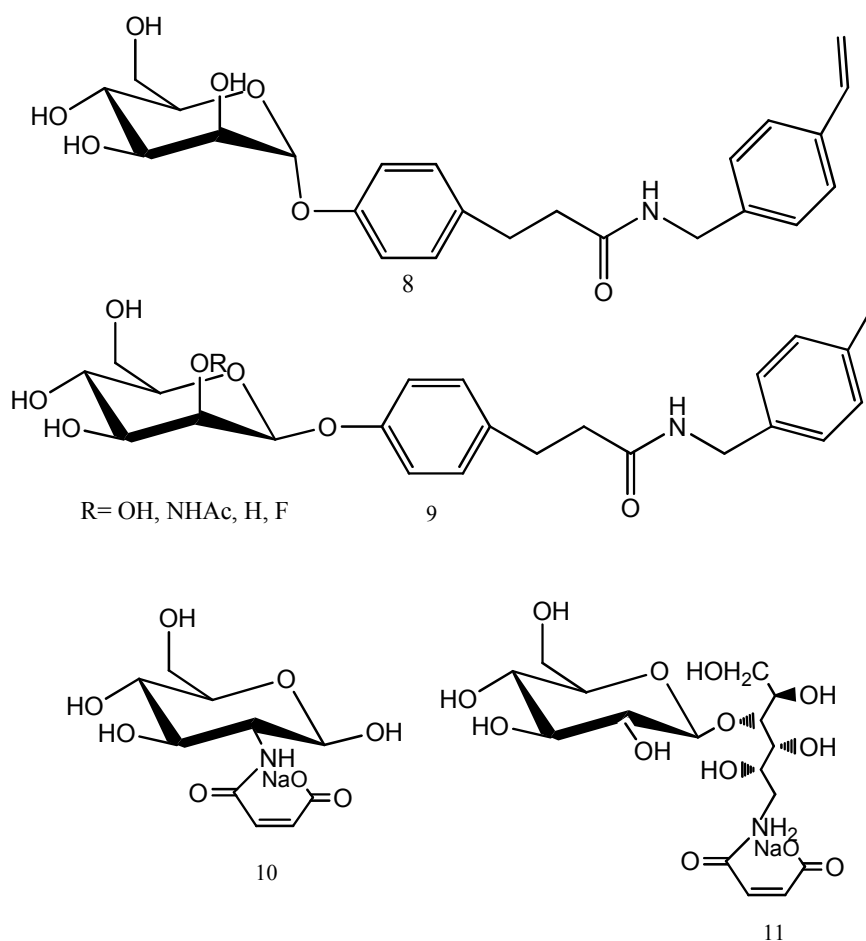
Figure 1.16 (8) p-[2-[N-(p-vinylbenzyl)carbamoyl]ethyl]phenyl α-D manno-

pyranoside (9) p-[2-[N-(p-vinylbenzyl)carbamoyl]ethyl]phenyl β-D manno-

pyranoside; p-[2-[N-(p-vinylbenzyl)carbamoyl]ethyl]phenyl 2-acetamido-2-deoxy-

β-D-mannopyranoside; p-[2-[N-(p-vinylbenzyl) carbamoyl]ethyl]phenyl β-D-

arabino-hexopyranoside; p-[2-[N-(p-vinylbenzyl)carbamoyl]ethyl]phenyl 2-deoxy-

2-fluoro-β-Dmannopyranoside (10) N-maleicamido-2-deoxy-glucose sodium salt

(11) N-maleicamido-1-deoxy-lactitol sodium salt

Glycopolymer synthesis using free radical polymerization is frequently used and

has numerous examples as is evident from the above discussion, but it has some

drawbacks. The most important drawback is that there is no control over the mo-

lecular weight of the polymer, for which toxic initiator and chain transfer agents

have to be used. Moreover, this technique leads to branching in the product which is sometime undesired.

1.9.2 Glycopolymer synthesis by ionic polymerisation

Ionic living polymerisation by both anionic and cationic methods is extremely selective. This technique leads to glycopolymer architecture like graft and block copolymers with very low polydispersities and with control over molecular weights. On the other hand, the main drawback of ionic polymerization technique is that they are very costly; this makes this technique unsuitable for production on industrial scale.

M. P. Labeau et al. employed cationic polymerization for the synthesis of polystyrene-b-polyglucopyranose vinyl ether by deprotection of the moieties with trifluro-caetic acid [147]. Loykulnant et al. synthesized styrene monomers having meta substituted acetal protected monosaccharides via the Williamson reaction of m-(chloromethyl)styrene [148]. They homopolymerized these monomers in THF at -78 ^{0} C using sec-BuLi.

K. Yamada et al. [149] reported the synthesis of amphiphilic block copolymers of vinyl ethers (VES) of the type — $[CH_2CH(OCH_2CH_2OR)]_m$ — $[CH_2CH(OiBu)]_n$ — by living radical cationic polymerization, where R is a D-glucose residue and m and n are degree of polymerization. They synthesized this glycopolymer by sequential living block copolymerization of isobutyl vinyl ether (IBVE) and the vinyl ether carrying 1,2:5,6 -diisopropylidene) D -glucose residue, using the HCl adduct of IBVE, and $CH_3CH(OiBu)Cl$ as initiator along with zinc iodide. The product was deprotected with trifluroacetic acid to yield the target amphiphilic copolymer **12** (fig.

1.17). Thin films of these glycopolymer were found to have various phase separated

surface morphologies depending on the length (m,n) of the two blocks.
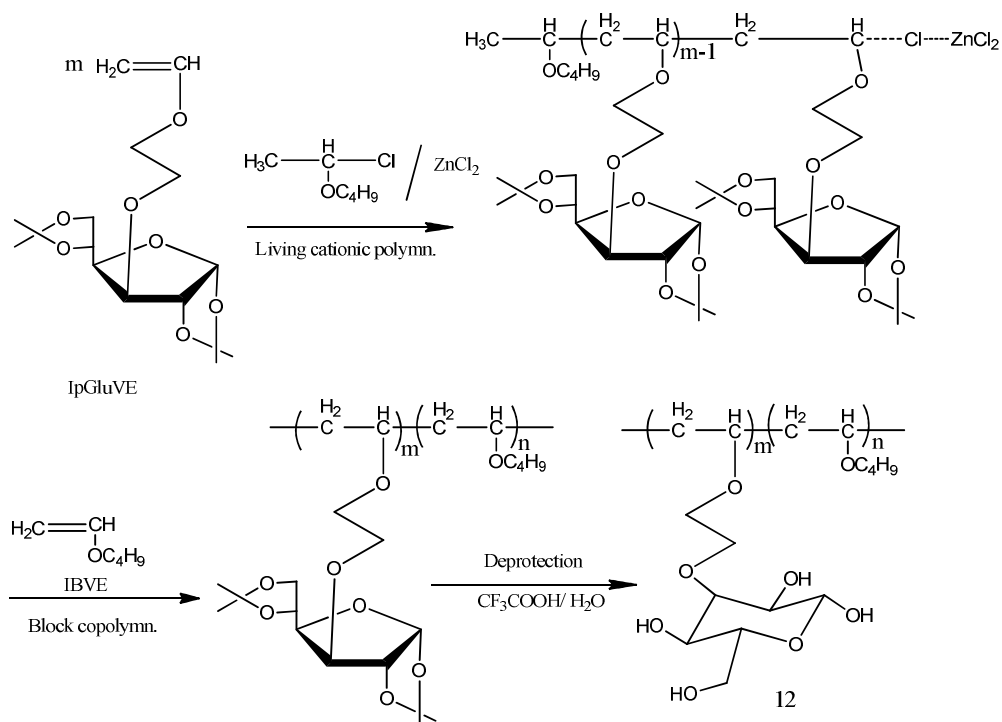
Figure 1.17 Synthesis of amphiphilic block copolymers with pendant glucose residues [149]

1.9.3 Glycopolymer synthesis by ring-opening polymerisation (ROP)

Heterocyclic compounds may undergo cationic (CROP) or anionic (AROP) ring-opening polymerisation, depending on their nature. In both cases there are only a narrow range of highly specific monomers available, which have the desired ring-strain, bond types and reactivity. AROP has the advantage that it may be used to produce polymers and block copolymers of controlled, high molecular weights. CROP is applicable to much broader range of monomers provided there is sufficient ring strain. In the cases of both anionic and cationic the reactions conditions must be precisely defined in order to produce living polymers. Aoi et al. [150] was

the first group to synthesize glycopolymers by AROP. They reported the synthesis of glycopeptides from glycosylated Ncarboxyanhydrides (NCAs). This synthesis was achieved by ROP of O-(tetra-O-acetylb-D-glucopyranosyl)-L-serine N-carboxy-anhydride **13** (fig. 1.18) using using primary and tertiary amine initiators. Initiation by primary amine led to chain growth by the amino end group, whereas initiation by tertiary amine proceeded by "activated monomer mechanism. The resulted product was deprotected with hydrazine monohydrate to yield high molecular weight poly (L-serine) with glucose side chains.
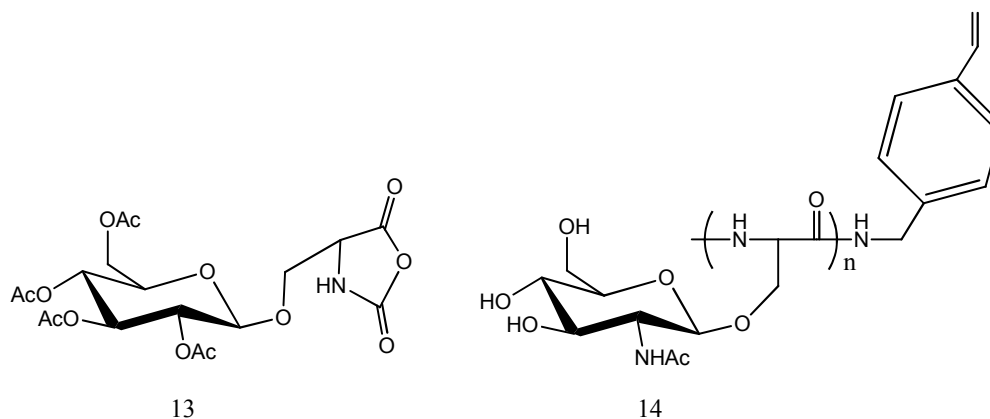
Figure 1.18 (13) O-(tetra-O-acetyl-β-D-glucopyranosyl)-L-serine N-carboxy-anhydride (14) glycopeptide macromonomer carrying N-acetyl-D-glucosamine residue

Glycopolymer synthesis, having pendant N-acetyl glucosamine residues have also been reported [151]. This was achieved by ring opening polymerization of poly-glyco(L-serine) carrying pendant N-acetyl glucosamine residues **14** (fig. 1.18) initiated by p vinylbenzylamine in dichloromethane. The macromonomer thus obtained contain a polymerisable vinyl moiety, which was copolymerised with acrylamide under free radical conditions to yield the target glycopolymer.

1.9.4 Glycopolymer synthesis by nitroxide-mediated radical polymerisation

Very few glycopolymers have been synthesised by nitroxide-controlled polymerisation to date. Ohno et al. [152] in 1998 reported the synthesis of the first glycopolymers by nitroxide- mediated polymerisation. They synthesized the glycopolymer by polymerization of N-(p-vinylbenzyl)-[O-β-D galactopyranosyl- (1 ⟶ 4)]-D-gluconamide (VLA) **15** (fig. 1.18) and acetylated VLA monomer, using BSDBN **16** (fig. 1.18) as a radical initiator and dicumyl peroxide as an accelerator.
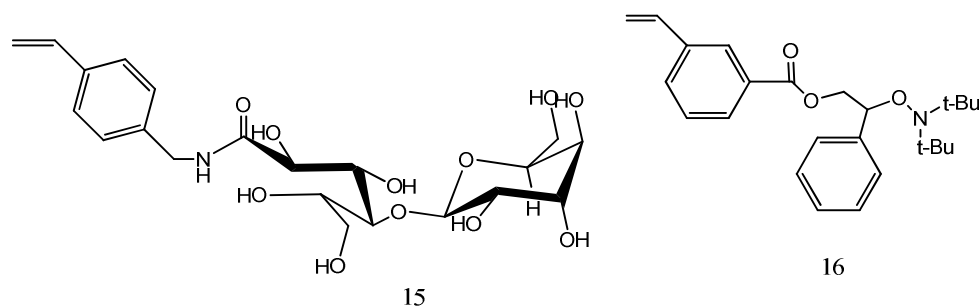
Figure 1.19 (15) N-(p-vinylbenzyl)-[O-β-D-galactopyranosyl-(1 ⟶4)]-D glucona-mide (VLA) (16) 2-(benzoyloxy)-1-(phenylethyl)-di-tertbutyl nitroxide [152]

Narumi et al. [153] synthesized a glycopolymer, polystyrene-poly (4-vinylbenzyl glucoside peracetate)-polystyrene carrying pendants glucose using bis TEMPO-like initiator and (1S)-(+)-10-camphorsulfonic acid anhydride (CSA) as an accelerator. Gotz et al. polymerized 1,2,5,6-di(isopropylidene)-D-Glucose- 2-propenoate using a dioctadecyl-substituted nitroxide initiator to yield a lipoglycopolymer carrying glucose residue.

1.9.5 Glycopolymer synthesis by click chemistry

The copper(I)-catalyzed Huisgen 1,3-dipolar cycloaddition of alkynes and azides has become an attractive route for the preparation of new synthetic glycopolymers featuring well-defined macromolecular architectures. Click chemistry comprising of 1,3-dipolar cycloaddition of azides and terminal alkynes, catalyzed by copper(I) was popularized by sharpless et al. in 2001 [154]. These reactions have a very high thermodynamic driving force which makes them one of the most efficient reactions available. Such reactions were found to be very practical because they can tolerate many functional groups giving high yield. The reactions can be performed in multiple solvents including water. Moreover, the 1,2,3-triazole product is chemically very stable. Because of their efficiency and simplicity, these cycloadditions were named "click" Reactions. In the click chemistry strategy, reactive molecular building blocks consisting of azide and alkyne blocks are designed to click together selectively, covalently and stereo specifically.

Although this strategy was initially developed for use in organic synthesis but within a very short span of time, because of its wide range of applications, it percolated to carbohydrate chemistry, polymer chemistry, chemical biology, drug discovery and other fields. For the synthesis of glycopolymers through click coupling, alkyne polymers have been used more extensively than azide polymers, as this reduces the number of azide groups in the same molecule [155].

Many applications involve the conjugation of clickable sugar moieties onto appropriately functionalized macromolecular materials such as dendrimers and polymers. Following this approach, the construction of a series of precisely defined multivalent 1,4-disubsituted 1,2,3-triazole neoglycoconjugates, was reported by the group of Santoyo- Gonzalez using cycloaddition reactions either in the absence of a

metal catalyst[156] or catalyzed by organic soluble copper complexes such as $(Ph_3P)_3$. CuBr and $(EtO)3P$ .Cu(I) [157]. During the later study, it was found that microwave irradiation shortens the reactions' times considerably.

Recently O. Otman et al. reported the synthesis of glycopolymers with mannose units prepared by click chemistry of an azido mannopyranoside derivative and a poly (propargyl acrylate-co-*N*-vinyl pyrrolidone) [158]. Chen et al. used click chemistry for the synthesis of two classes of supports bearing covalently linked carbohydrates **17, 18** [159]. In the first one mannose containing azides were 'clicked' on alkyne modified Wang resin; in the second case, Wang resin beads were first converted into immobilized living radical polymerization initiators with subsequent polymerization of trimethylsilanyl- protected propargyl methacrylate followed by deprotection with TBAF to yield the desired polyalkyne clickable scaffold. The mannose azide was subsequently reacted with this alkyne containing macromolecular scaffold to yield the glycopolymer-bead hybrid material. They further studied the lectin binding abilities of these mannose modified Wang resins using fluorescein labelled Con A, a mannose binding lectin. There studies revealed that the synthesized glycol-hybrid material indeed recognized Con A and showed binding with it. They proposed that this material could have many potential applications in affinity chromatography, sensors and protein recognition fields.
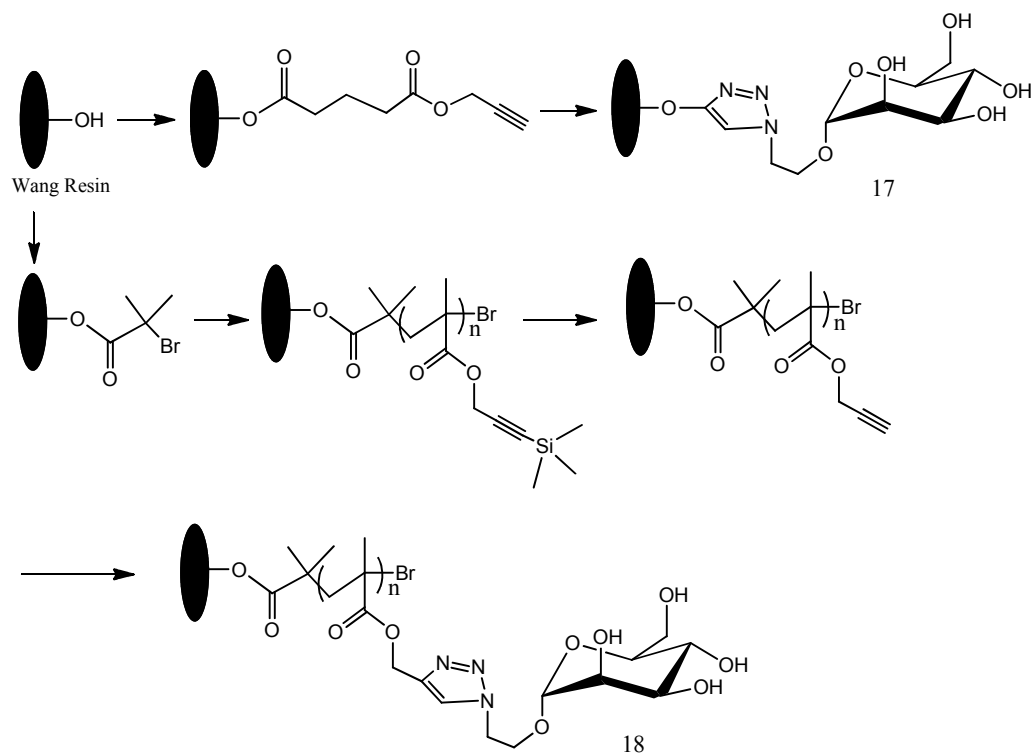
Figure 1.20 Synthesis of mannose modified Wang resin by click reaction [159]

Fazio et al. [160] used the Cu (I) catalyzed click chemistry approach for the synthesis and attachments of in situ of sugars arrays to the microtiter plate at room temperature in high yield. They attached azide functionalized sachharides to a C_{14} hydrocarbon chain which was covalently attached to microtiter well surfaces as shown schematically in figure 1.21.
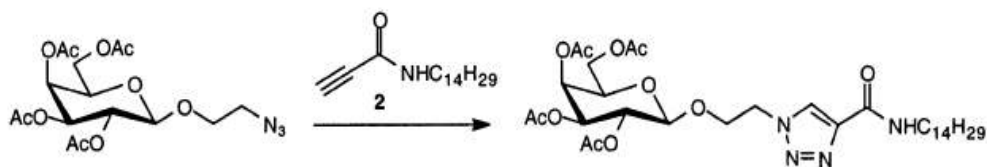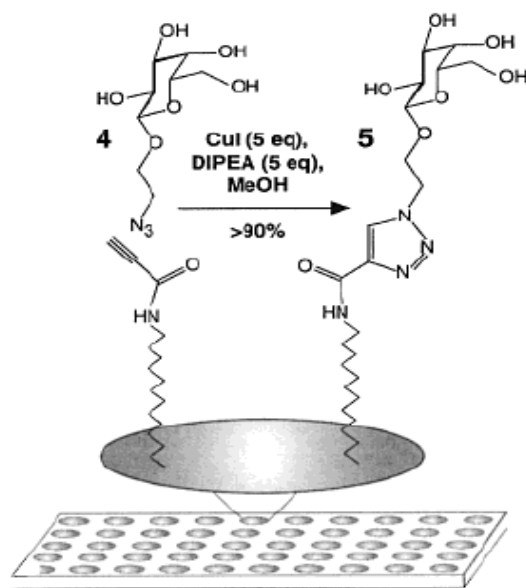
Figure 1.21 Click approach for sugar microarrays [160]

The microarray fabrication of carbohydrates was achieved by the cycloaddition of the azido sugars with a suitable alkyne immobilized on the microtiter plate as shown above. This copper (I) catalyzed triazole formation by click approach was applied to a series of oligosaccharides. The corresponding triazole derivatives were synthesized in the mocrotiter plates from the corresponding azides.
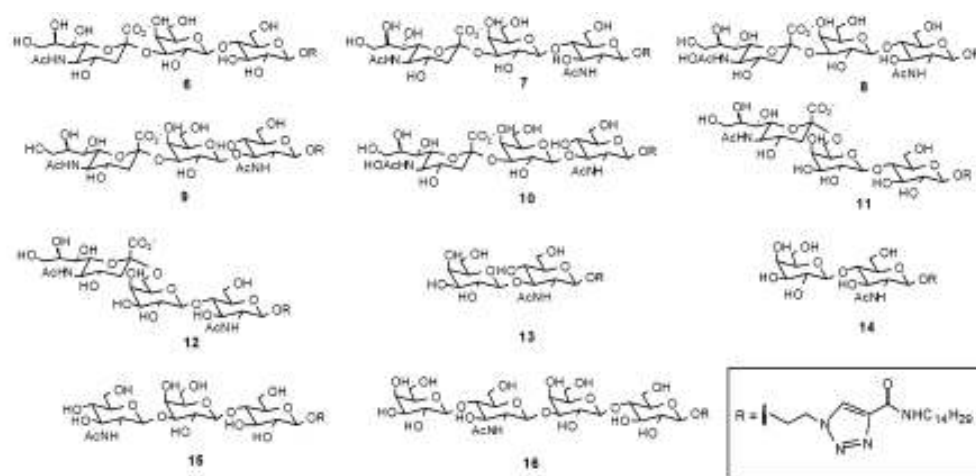
Figure 1.22 Oligosaccharides displayed in the microtiter plate via Cu (I) catalyzed

1, 3-dipolar cycloaddition reaction

These saccharide arrays acts as substrates for glycosyltransferases and are suitable for high throughput specificity studies of sugar – protein interaction studies besides enzyme inhibitor screening and diversity oriented synthesis.

Similarly, Wang et al. [161] used the Huisgen`s dipolar cycloaddition to immobilize azide functionalized sugars (mannose, lactose, and α-galactose) onto alkyne – terminated self assembled monolayers (SAM) on gold (fig. 1.23). The clicked mannose, lactose, α-galactose tri-saccharide SAMs are used in the analysis of specific carbohydrate -protein interactions.
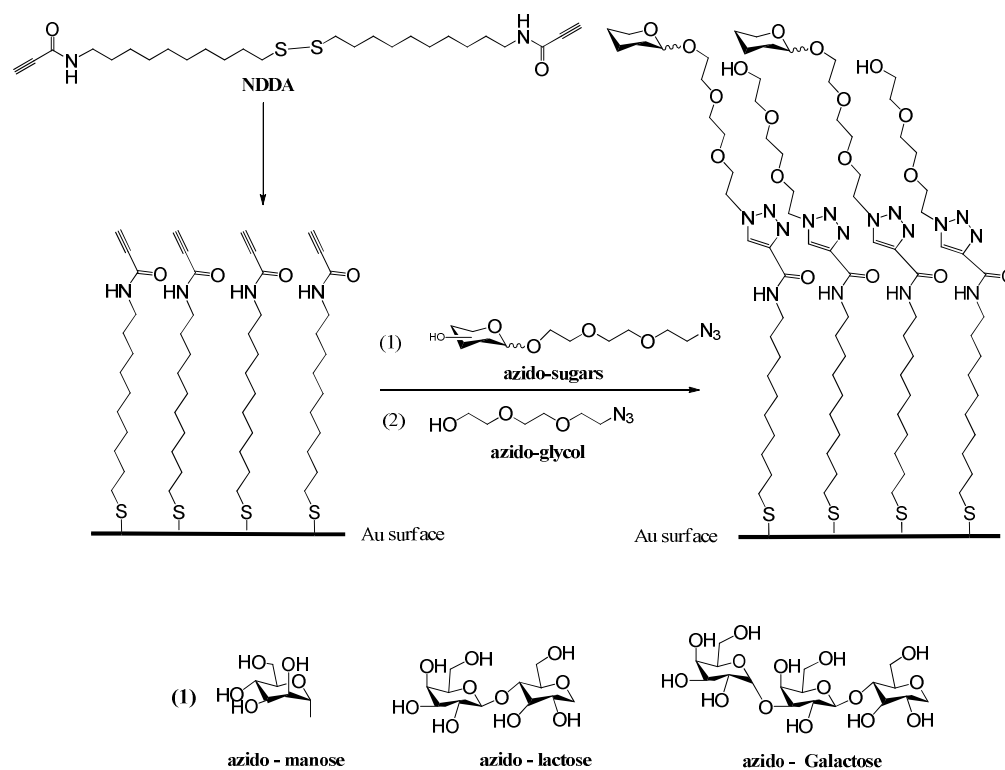
Figure 1.23 Carbohydrate SAM strategy using click chemistry [161]

Chevolot et al. [162] reported, surface immobilization of oligosaccharides using glycoconjugate molecules in which click chemistry was a key step. They designed a glycoconjugate consisting of carbohydrate residue(s) for interacting with a lectin (which decreases the limitation imposed by the weak carbohydrate-lectin interaction), an oligonucleotide sequence for anchoring on the surface and a fluorescent tag for determining relative surface densities of the glycoconjugate. The authors claimed that this approach was the first of its kind in the field of glycoarrays.
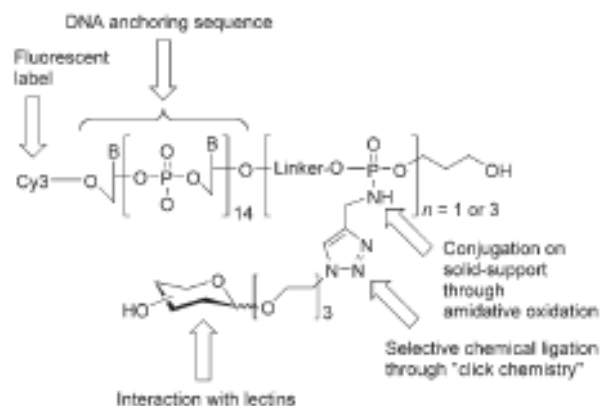
Fig 1.**24** Schematic structure of the glycoconjugate [162]

It is clear from the literature that click chemistry offers a simple method of modifying polymers, and can be applied to the modification of SBS with various sugars.

1.10. Conclusion

In this chapter on literature review pertaining to the work done in the thesis, we have elaborated known methods of synthesis of SBS and their chemical modifications by various techniques. We have also highlighted the fact that sugar linked SBS has not been investigated so far. Since sugar linked SBS offers a new series of modified SBS polymers with several potential applications in biodegradable polymers and polymers having biomedical applications, we have carried out research to synthesize sugar linked SBS followed by investigation on their potential as biomaterial.

1.11. References

1. R. J. Spontak, N. P. Patel, *Current Opinion in Colloid & Interface Science* **2000**, 5, 333-340

2. C. S. Schollenberger, H. Scott, G. R. Moore, *Rubber world* **1958**, 137, 549;

3. C. S. Schollenberger, *U.S. Patent* **1955**, 287 12 18

4. G. Holden, R. Milkovich, *US Patent 3 265 765*, **1966**

5. R. Milkovich, G. Holden, E. T. Bishop, W. R. Hendericks, *British Patent 1 035 873*, **1966**; *US Patent 3 231 635*, **1966**

6. R. P. Zelinski, *US Patent 3 287 333*, **1966**

7. *British Patent 895 980,* **1962** (to Phillips Petroleum Co.).

8. G. Kraus, C. W. Childers, J. T. Gruver, *J. Appl. Polym. Sci.* **1967**, 11, 1581

9. G. Holden, E. T. Bishop, N. R. Legge, *J. Polym Sci. C*, **1969**, 26, 37.

10. B. M. Walker, C. P. Rader, *Handbook of Thermoplastic Elastomers* **1988**, 2nd edn. Van Nostrand Reinhold, New York

11. N. R. Legge, *Rubber Chemistry and Technology*, **1989**, 60, G79; *Rubber and Plastics News* (15 May 1989) p. 23.

12. J. E. McGrath, *Anionic Polymerization, Kinetics, Mechanisms and Synthesis*, *ACS Symposium Series* **1981,** No. 166. American Chemical Society, Washington, DC

13. E. N. Kresge, *J. Appl. Polym. Sci., Appl. Polym. Symp.*, **1984**, 39, 37.

14. J. Lal, J. E. Mark, *Advances in Elastomers and Rubber Elasticity* **1987,** Plenum, New York,.

15. N. R. Legge, G. Holden, J. E. Schroeder, *Thermoplastic Elastomers—A Comprehensive Review* **1987,** Hanser, New York,.

16. A. Y. Coran, *Rubber Chemistry and Technology*, **1995**, 68, 351.

17. A. Y. Coran, R. P. Patel, *Rubber Chemistry and Technology*, **1980**, 53, 141.

18. A. M. Gessler, *US Patent 3 037, 954*, **1962**

19. W. K. Fishcer, *US Patents 3 758 643*, **1973**; *3 835 201*, **1974**; and *3 862 106* **1975**

20. A. Sabet, M. A. Fath, *US Patent 4 311 628*, **1982**

21. O'Connor, G. E. and Fath, M. A., *Rubber World* **1982**, 185(4), 49.

22. R. Zelinski, C. W. Childers, *Rubber Chem. Technol.*, **1968**, 41, 161.

23. A. Noshay, J. E. McGrath, *Block Copolymers—Overview and Critical Survey* **1977,** Academic Press, New York

24. L. J. Fetters, *Block and Graft Copolymerizations* **1973**, Vol. 1, Chap. 5, ed. R. J. Ceresa. Wiley, New York

25. G. Holden, R. Milkovich, *US Patent 3 265 765*, **1966**

26. *SRIC*, sriconsulting.com; March **2008**

27. M. Morton, *Anionic Polymerization." Principles and Practice* **1983**, Academic Press

28. R. N. Young, R. P. Quirk, L. J. Fetters, *Advances in Polymer Science* **1984**, 56, Anionic Polymerization, Springer-Verlag

29. D. C. Huang, Y. C. Lin, R. C. Tsiang, *Journal of Polymer Research* **1995**, 2, 91-98

30. A. Bhattacharya, B.N. Misra, *Prog. Polym. Sci.* **2004**, 29, 767–814

31. **31** D. D. Sotiropoulou, K. G. Gravalos, and N. K. Kalfoglou, *J. Appl. Polym. Sci.* **1992,** 45, 273

32. M. Antonietti, S. Forster, J. Hartman, S. Oestreich, *Macromolecules* **1996**, 29, 3800–3806

33. R. B. Grubbs, M. E. Broz, J. M. Dean, F. S. Bates, *Macromolecules* **2000**, 33, 2308–2310

34. J. R. Gregorio, A. E. Gerbase, A. N. F. Mendes, P. D. Marcico, A. Rigo, *React. Funct. Polym.* **2005**, 64, 83–91

35. X. Jian, A.S. Hay, *J. Polym. Sci. Part A: Polym. Chem* **1991**, 29, 1183–1189

36. W-K. Huang, G-H. Hsuie, and W-H. Hou, *J. Polym. Sci. Part A: Poly. Chem.* **1988**, 26, 1867

37. S. M. Wang, R. C. Tsiang, *J. Polym. Sci. Part A: Polym. Chem* **1996**, 34, 1483–1492

38. J. Rebek, Jr., L. Marshall, J. McManis, and R. Wolak, *J. Org. Chem.* **1985,** 51, 1649

39. A. M. Al-Ajlouni and J. H. Espenson, *J. Am. Chem. Soc.* **1995**, **117,** 9243 ().

40. N. N. Schwartz and J. H. Blumbers, *J. Org. Chem.* **1964**, 29, 1976

41. D. Zuchowska, *Polymer,* **1980**, 21, 514

42. H. *S.* Makowski, M. Lynn, and D. H. Rotenberg, *J. Macromol. Sci. Chem.A4* **1970**, 7, 1563

43. V. W. Dittman and K. Hamann, *Chem. Ztg.,* **1971**, 95, 684

44. J. H. Hsiue, J. M. Yang, *Journal of Polymer Science Part A: Polym. Chem.* **1990,** 28, 3761-3773

45. D. Swern, ***Org. React.,*** **1953**, 7, 378

46. K. Udipi, *Journal of Applied Polymer Science* **1979,** 23, 3301-3309

47. X. Jian, A. S. Hay, *Journal of Polymer Science Part A: Polym. Chem.* **1991,** 29, 1183-1189

48. W. K. Huang, G. H. Hsiue, W. Hou, *Journal of Polymer Science Part **A:** Polym. Chem.* **1988,** 26, 1867-1883

49. Q. Pan, G. L. Rempel, *Macromol. Rapid Commun.* **2004**, 25, 843–847

50. S. M. Wang, R. C. Tsiang, *Journal of Polymer Science Part **A:** Polym. Chem.* **1996,** 34, 1483-1491

51. Y. S. Shyr, R. L. Bobsein, M. M. Jhonson, *US Patent* **1986**, 4 629 767

52. C. J. Gibler, S. E. Wilson, *US Patent* **1993**, 5 244 980

53. L. Wei, J. Y. Jiang, Y. H. Wang, Z. L. Jin, *Chinese Chemical Letters* **2005,** 16, 338-340

54. S. N. Massie, *US Patent* **1995**, 5 378 767

55. H. V. D. Heijden, H. V. D. Weg, *US Patent* **2002**, 6 461 993

56. J. D. Wilkey, *US Patent* **2001**, 6 207 795

57. D. K. Schisla, M. J. Modic, E. M. De Groot, *US Patent* **2001**, H1956

58. R. C. Bening, C. L.Willis, J. D. Wilkey, Z. Diaz, *US Patent* **2001**, 6 242 538

59. R.J. Hoxmeier, *US Patent* **1989**, 4 879 349

60. D.S. Bresolw, A.S. Matlack, *US Patent* **1963**, 3 113 986

61. R.C. Tsiang, W.S. Yang, M.D. Tsai, *Polymer* **1999**, 40, 6351

62. K. Kato, K. Kishimoto, J. Kameda, *Japan Patent* JP 01,289,805 **1989**

63. X. Guo, P.J. Scott, G.L. Rempel, *J. Mol. Catal.* **1992**, 72, 193

64. J.W. Yang, L. Bao, R.Q. Xue, *China Synth. Rubber Indus.* **2000**, 23, 31

65. N.K. Singha, S. Sivaram, *Polym. Bull.* **1995**, 121, 35

66. Y. Kishimoto, H. Morita, *US Patent 4 501 857*, **1985**

67. L. Chamberlain, C. Gibler, *US Patent 5 141 997*, **1993**

68. L. Wei, J. Jiang, Y. Wang, Z. Jin, *Journal of Molecular Catalysis A: Chemical* **2004**, 221, 47–50

69. D. D. Jiang, C. A. Wilkie, *J. Polym. Sci., Part A: Polym. Chem.* **1997**, 35, 965

70. Z. Morrov, R. Velichkova, *Eur. Polym. J.* **1993**, 29, 597-601

71. E. Passaglia, S. Ghetti, F. Picchioni, G. Ruggeri, *Polymer* **2000**, 41, 4389

72. S. Jing, L. Xiao, D. Y. Kang, *J. Macromol. Sci-Chem* **1990**, 27, 167-176

73. B. M. Rao, P. R. Rao, *Polym. Plast. Technol. Eng.* **1999**, 38, 967-977

74. M. Saqak and E. Pulat, *J. Appl. Polym. Sci.* **1989 ,** 38, 539

75. A. Hebeish, S. E. Shalaby, and A. M. Bayazeed, *J. Appl. Polym. Sci.* **1981,** 26, 32523

76. R. Tsuzuki and S. Maeta, *Jpn. Pat. 71,29 918*, **1971**

77. A. K. Pradhan, N. C. Pati, and P. L. Nayak, *J. Appl. Polym. Sci.* **1982** , 27,1973

78. M. Suzuki, A. Kishida, H. Iwata, Y. Ikada, *Macromolecules* **1986**, 19, 1804

79. G. H. Hsiue, J. M. Yang, *Makromol. Chem.* **1991,** 192, 2687

80. J. M. Yang, Y. J. Jong, Y. G. Hsu, C. H. Chang, *J. Biomed. Mater. Res.* **1998**, 39, 86

81. G. H. Hsiue, J. M. Yang, R. L. Hu, *Journal of Biomedical Materials Research* **1988**, 22, 405-415

82. J. M. Yang, Y. J. Jong, K. Y. Hsu, *J. Biomed. Mater. Res. Part A* **1997**, 35, 175

83. J. M. Yang, Y. J. Jong, Y. G. Hsu, C. H. Chang, *J. Biomed. Mater. Res.* **1998**, 39, 86

84. J. M. Yang, C. P. C. Chian, K. Y. Hsu, *Journal of Membrane Science* **1999**, 153, 175

85. J. E. Kennedy, J. G. Lyons, L. M. Geever, C. L. Higginbotham, *Material Science and Engineering C 29* **2009**, 1665-1661

86. J. E. Kennedy, C. L. Higginbotham, *J. Mater. Sci.* **2010**, 45, 599–606

87. H. M. Wilhelm, M. I. Felisberti, *Journal of Applied Polymer Science* **2002**, 83, 2953-2960

88. M. Rao, R. Rao, *Polym. Plast. Technol. Eng.* **1999**, 38, 967-977

89. J. Sheng, X. L. Lu, K.D. Yao, *J. Macromol. Sci-Chem.* **1990**, 27, 167-176

90. A. Brydon, G. M. Burnett, G. G. Cameron, *J. Polym. Sci. Polym. Chem. Ed.* **1973**, 11, 3255

91. A. Brydon, G. M. Burnett, G. G. Cameron, *J. Polym. Sci. Polym. Chem. Ed.* **1974**, 12, 1011

92. A. Gasperowicz, W. Laskawski, *J. Polym. Sci. Polym. Chem. Ed.* **1976**, 14, 2875

93. D. D. Jiang, C. A. Wilkie, *J. Polym. Sci. A: Polym. Chem.* **1997**, 35, 965-973

94. Z. Aimin, L. Chao, *European polymer Journal* **2003**, 39, 1291-1295

95. C. D. Cordella, N. S. M. Cardozo, R. B. Neto, R. S. Mauler, *Journal of Applied Polymer Science* **2003**, 87, 2074-2079

96. M. Taha, V. Frerejean, *Eur. Polym. J.* **1997**, 33, 1073-1079

97. N. J. Huang, D. C. Sundberg, *J. Polym. Sci. Part A: Polym. Chem.* **1995**, 33, 2533

98. N. J. Huang, D. C. Sundberg, *J. Polym. Sci. Part A: Polym. Chem.* **1995**, 33, 2551

99. N. J. Huang, D. C. Sundberg, *J. Polym. Sci. Part A: Polym. Chem.* **1995**, 33, 2571

100. N. J. Huang, D. C. Sundberg, *J. Polym. Sci. Part A: Polym. Chem.* **1995**, 33, 2587

101. M. Suzuki, C. A. Wilkie, *J. Polym. Sci., Part A: Polym. Chem.* **1995**, 33, 1025

102. C. Deacon, C. A. Wilkie, *Eur. Polym. J.* **1996**, 32, 451

103. J. C. Soutif, P. Klinpituksa, J. C. Brosse, *Makromol. Chem.* **1992**, 193, 315

104. D. Derouet, J. C. Brosse, A. Challioui, *Eur. Polym. J.* **2001**, 37, 1315

105. A. Nandi, M. D. Gupta, A. K. Banthia, *Macromol. Rapid Commun.* **1999**, 20**,** 582–585

106. H.Q. Xie, Y. Chen, J.G. Guan, D. Xie, *J. Appl. Polym. Sci.* **2006**, 99, 1975

107. H. Q. Xie, Y. Chen, W. Wei, D. Xie, *J. Appl. Polym. Sci.* **2006**, 101, 792

108. H. Q. Xie, W. G. Yu, D. Xie, D. T. Tian, *Journal of Macromolecular Science Part A: Pure and Applied Chemistry* **2007**, 44, 849–855

109. A. Molnar, *Ph.D. Thesis*, Department of Chemistry, McGill University, Montreal, Canada, **1992**

110. M. Nishida, A. Eisenberg, *Macromolecules* **1996**, *29,* 1507-1515

111. J. Samuel, T. Xavier, T. Kubian, *J. Appl. Polym. Sci.* **2002**, 85, 2294

112. H. Q. Xie, D. G. Liu, D. Xie, *J. Appl. Polym. Sci.* **2005**, 96, 1398

113. H. Q. Xie, W. Gang, G. Y. Liao, D. Xie, *Journal of Elastomers and Plastics* **2007**, 39, 317

114. H. Q. Xie, J. G. Xu, *J. Macromol. Sci. Phys. B39* **2000**, 4, 569-581

115. H. Q. Xie, W. Zhao, D. T. Tian, D. Xie, *Journal of Macromolecular Science Part A: Pure and Applied Chemistry* **2008**,45, 151-158

116. B. Marciniec, *Comprehensive Handbook on Hydrosilylation* **1992**, Pergamon Press, Oxford, Chapter 6, pp 215-217.

117. G. G. Cameron, M. Y. Qureshi, *Makroml. Chem. Rapid Commun.* **1982**, 2, 287

118. Y. G. Hsu, G. R. Wang, K. H. Lin, *Journal of Polymer Research* **2001**, 8, 133-141

119. X. Guo. R. Farwaha, G. L. Rempel, *Macromolecules* **1990**, 23, 5047-5054

120. A. Adedeji, T. Grunfelder, F. S. Bates, C. W. Macosko, *Polymer Engineering and Science* **1996**, 36, 1707

121. M. Saroop, G. N. Mathur, *J. Appl. Polym. Sci.* **1997**, 65, 2691.

122. D. Halavata, J. Plestil, D. Zuchowska, R. Steller, *Polymer* **1991**, 32, 3313.

123. G. Gallego Ferrer, A. Alba Perez, J. L. Gomez Ribelles, M. Monleon Pradas, E. Verdu Sanchez, *J. Macromol. Sci. Phys.* **2001**, 40, 443

124. R. Perera, C. Albano, J. Gonzalez, P. Silva, M. Ichazo, *Polym. Degrad. Stab.* **2004**, 85, 741.

125. M. Ichazo, M. Hernandez, J. Gonzalez, C. Albano, N. Dominguez, *Polym. Bull.* **2004**, 51, 419

126. E. Verdu Sanchez, J. L. Gomez Ribelles, M. Monleon Pradas, M. Rodrguez Figueroa, F. Romero Colomer, *Eur. Polym. J.* **2000**, 36, 1893

127. Z. Jelcic, T. Holjevac Grguric, V. Rek, *Polym. Degrad. Stab.* **2005**, 90, 295

128. M. Boyanova, F. J. Balta Calleja, S. Fakirov, *J. Mater. Sci. Lett.* **2003**, 22, 1741

129. B. X. Fu, A. Lee, T. S. Haddad, *Macromolecules* **2004**, 37, 5211-5218

130. G. Moad, *Prog. Polym. Sci.* **1999**, 24, 81-142

131. F. R. Benn, J. Dwyer, I. J: Chappel, *Chem. Soc. Perkin Trans. II* **1977**, 5, 533

132. A. Pucci, C. Barsocchi, R. Rausa, L. D. Elia, F. Ciardelli, *Polymer* **2005**, 46, 1497-1505

133. Showa, *Japan Patent JP 5 604 7415*, **1981**

134. A. Lutzen, *Encyclopedia of supramolecular chemistry* **2004**, Taylor & Francis

135. C. R. Bertozzi, L. L. Kiesling, *Science* **2001**,291,2357)

136. C. Alvarez, M. Strumia, H. Bertello, ***Polymer Bulletin*** **1988**, 19, 521

137. L.You, H. Schlaad, *J. Am. Chem. Soc.* **2006**, 128, 13336-13337

138. Z. H. Baran, L. You, *Macromolecules* **2007**, 40, 3901-3903

139. Y. Ikeda, Y. Nakamura, K. Kanjiwara, S. Kohjiya, *J. Polym. Sci. Part A: Polym. Chem.* **1995**, 33, 2657-2665

140. V. Ladmiral, E. Melia, D. M. Haddleton, *Eur. Polym. J.* **2004**, 40, 431-449

141. V. Horejsi, P. Smolek, J. Kocourek, *Biochim Biophys Acta* **1978**, 538, 293

142. S. Kitazawa, M. Okumura, K. Kinomura, T. Sakakibara, *Chem Lett* **1990**, 19, 1733–1736

143. K. Kobayashi, A. Tsuchida, T. Usui, T. Akaike, *Macromolecules* **1997**, 30, 2016

144. A. Tsuchida, K. Kobayashi, N. Matsubara, T. Muramatsu, T. Suzuki, Y. Suzuki, *Glycoconjugate J.* **1998**, 15, 1047

145. S. Akai, Y. Kajihara, Y. Nagashima, M. Kamei, J. Arai, M. Bito, *J. Carbohydr. Chem.* **2001**, 20, 121–43.

146. J. Klein, C.F. Huttermann, B. Skeries, *J. Macromol. Sci.-Pure Appl. Chem.* **2003**, A40, 21–35

147. M.P. Labeau, H. Cramail, A. Deffieux , *Macromol. Chem. Phys.* **1998**, 199, 335-342

148. S. Loykulnant, M. Hayashi, A. Hirao, *Macromolecules* **1998**, 31, 9121

149. K. Yamada, K. Yamaoka, M. Minoda, T. Miyamoto, *J. Polym. Sci. Part A: Polym. Chem.* **1997**, 35, 255; K. Yamada, M. Minoda, T. Fukuda, T. Miyamoto *J. Polym. Sci. Part A: Polym. Chem.* **2001**, 39, 459

150. K. Aoi, K. Tsutsumiuchi, M. Okada *Macromolecules* **1994**, 27, 875

151. K. Aoi, K. Tsutsumiuchi, E. Aoki, M. Okada, *Macromolecules* **1996**, 29, 4456–8.

152. K. Ohno, Y. Tsujii, T. Miyamoto, T. Fukuda, M. Goto, K. Kobayashi, *Macromolecules* **1998**, 31, 1064

153. A. Narumi, T. Matsuda, H. Kaga, T. Satoh, T. Kakuchi, *Polymer* **2002**, 43, 4835

154. H. C. Kolb, M. G. Finn, K. B. Sharpless, *Angew. Chem., Int. Ed.* **2001**, *40*, 2004-2021

155. F. S. González, F. H. Mateo, *Top. Heterocycl. Chem.* **2007,** 7, 133–177

156. F. G. C. Flores, J. I. Garcia, F. H. Mateo, F. P. Balderas, J. A. C. Asin, E. S. Vaquero, F. S. Gonzalez, *Org. Lett.* **2000**, 2, 2499

157. F. P. Balderas, M. O. Munoz, J. M. Sanfrutos, F. H. Mateo, F. G. C. Flores, J. A. Calvo-Asin, J. I. Garcia, F. S. Gonzalez, *Org. Lett.* **2003**, 5, 1951

158. O. Otman, P. Boullanger, E. Drockenmuller,T. Hamaide, *Beilstein J. Org. Chem.* **2010,** 6, No. 58, 1-7

159. G. Chen, L. Tao, G. Mantovani, J. Chen, D. Nystrom, D. M. Haddelton, *Macromolecules* **2007**, 7513-7520

160. F. Fazio, M. C. Bryan,O. Blixt, J. C. Paulson, C. H. Wong, *J. Am. Chem. Soc.* **2002**, 124 , 14397–14402

161. Y. Zhang, S. Luo, Y. Tang, L. Yu, K. Hou, J. Cheng, X. Zeng, P. Wang *Anal. Chem.* **2006**, 78, 2001

162. *Angew. Chem. Int. ed* **46**, 14, 2398-2402

Chapter 2

Synthesis of carbohydrate functionalized SBS by glycosidation reaction from epoxidized SBS

2.1. Introduction

Elastomers can be classified in three broad groups as natural rubber, synthetic rubber and thermoplastic elastomers. Styrene–butadiene–styrene (SBS) is an important class of thermoplastic elastomers (TPE) and is considered a two-phase thermoplastic block copolymer in which spherical polystyrene (PS) domains are dispersed in a polybutadiene (PB) matrix [1-2]. SBS derives its strength and elasticity from physical cross linking of the molecules into a three-dimensional network. The polystyrene end blocks impart strength to the polymer while the polybutadiene rubbery matrix blocks give the material its high viscosity and elasticity.

As a result of its properties SBS find considerable use in industry, but the anionic polymerization technique [3] used for the synthesis of this block polymer hinders the incorporation of polar monomers during polymerization. This in turn limits the usefulness range of this polymer for diverse applications.

Specialized applications for the styrene-butadiene block copolymers include disposable medical products, food packaging, tubing, sheet, belting, mallet heads, and shoe soles. These materials are also used as sealants, hot-melt adhesives, coatings, and for wire and cable insulation. Automotive applications includes airbag covers, hoses, ducts, and dust boots. These also find application in power, communication, data and flexible cords, injection molded plugs and connectors. Currently, for bulk applications SBS is the most commonly used polymer for bitumen modification followed by other polymers such as styrene butadiene rubber (SBR), ethylene vinyl acetate (EVA) and polyethylene. Thus, SBS is generally used

for low technology applications and this could change to high end applications with suitable chemical modifications of this polymer.

Under these circumstances chemical modification is the only solution available to increase the useful spectrum of this important block polymer. Presently, unsaturated polymers have attracted the fancy of chemists to produce new materials with desired and specific properties. An ABA linear triblock polymer such as polystyrene-polybutadiene-polystyrene (SBS) is an important block copolymer having unsaturation and usefulness ranging from thermoplastic elastomers to impact modified plastics. As discussed in the above paragraph chemical modification is the basic tool used to access the properties of both block and graft copolymers.

Although, functionalization of polybutadiene has been studied in detail [4-10], including functionalization with sugar [11-12], while there is no report for functionalization of SBS with sugars. Synthesis of Synthetic polymers having sugar branches (synthetic glycopolymers) has become an interesting area of work because of importance of these materials for numerous biological and biomedical applications [13]. This is because these synthetic glycopolymers are expected to have functions similar to natural glycoconjugates and so can mimic their performance in specific applications. These applications are based on biological recognition phenomena, that is, specific interactions between carbohydrates on the polymers and proteins [14-15]. Many studies have been published on the use of glycopolymers as drug delivery systems, artificial tissues, biocompatible device, hydrogels and surface modifiers [16-17]. Synthetic glycopolymers has also been synthesized, for use as biological recognition signaling molecules [18], as cell-specific culture substrata, in human vaccines, for tumor diagnosis, as probes for

receptors, and in targeted drug delivery systems [19-20]. Expansive research efforts have been devoted on developing new strategies for the immobilization of biomolecules like proteins and carbohydrates. However, the field still is in infancy.

There have been lot of activity on the copolymerization approach such as copolymerization of synthetic monomer and natural monomers such as sugars [21-33], peptides [34-36], nucleic acids [37-41] or by grafting these biomolecules as pendants on synthetic polymers [42], but the grafting approach has comparatively limited literature, due complications of unwanted side reactions and cross linking.

There are numerous reports on epoxidation [43-44] of SBS by different methods, but further opening of the epoxide to introduce functional groups on the SBS polymeric backbone has not been much explored besides synthesis of ionomers including sulfonated [45], maleated [46] phosphated [47] and quaternary ammonium ionomer [48]. The chemistry of polymeric epoxide opening with alcohol has been reported, but opening of epoxide with carbohydrate has not been reported yet.

Ring opening of epoxides with an appropriate alcohol under acidic and basic conditions leads to the formation of β-hydroxy ether. Robinson et al. have reported alcoholysis of epoxides in the presence of catalytic amount of mesoporous aluminosilicate [49]. Challioui et al. has also reported alkoxylation of epoxidized polyisoprene by opening of oxirane rings with alcohols by free radical mechanism [50].

We decided to explore this strategy of epoxide ring opening with sugars to obtain sugar functionalized elastomers by grafting glucose, mannose, galactose, xylose, fructose, methyl glucoside, sucrose and maltose on SBS. Using this methodology

we can control the amount of sugar grafted by controlling the extent of epoxide formation on SBS. This can enable one to obtain SBS with varying hydrophilicity caused by anchor sugar molecules.

Taking the advantage of rich literature on epoxidation and epoxide ring opening in general, we explored the further functionalization with the aim of introducing polar monomers such as sugars as pendants on the SBS backbone so as to introduce hydrophilicity and biocompatibility and further usefulness as a biomaterial.

Herein, we report an efficient and easy approach for attaching sugars to unsaturated synthetic polymers, without protection-deprotection of sugar hydroxyl groups and without using cytotoxic catalysts.

In the present work, we have developed a new and highly efficient chemical modification protocol for the addition of monosacharides, disaccharides and pentose onto the partially epoxidized 1, 4 polybutadiene unit of polystyrene-block-polybutadiene-block-polystyrene (SBS). SBS was first partially epoxidized in toluene solution using 3-chloroperoxybenzoic acid (mCPBA). Taking the advantage of reactivity of epoxide ring in general, SBS epoxide was opened with carbohydrates (sugars) in presence of 4-DMAP and NH_4Cl using a mixture of pyridine and DMF as solvent to yield functionalized SBS with ether linked sugar moiety.

2.2. Experimental

2.2.1 Materials

Polystyrene-block-polybutadiene-block-polystyrene (Aldrich, M_w 140,000, 30% polystyrene, 70% polybutadiene,) was used as a starting material. 3-chloroperoxybenzoic acid (77% max.) was procured from Aldrich Chemicals, USA, ammonium chloride (AR) and methanol (LR) were obtained from Ranbaxy, India. Toluene (GR), Pyridine (GR), N, N-dimethyl formamide (GR) were obtained from Merck and distilled and dried before use. 4-dimethyl amino pyridine (DMAP) was also purchased from Merck and used as such without further purification. Dextrose anhydrous (GR) was obtained from Merck. D-mannose (AR) was obtained from SRL, D(+) galactose (LR), D(+) xylose (LR), D(-) fructose (AR), sucrose (AR) and maltose (AR) were obtained from S.D fine chemicals, India. Methyl -α-D-glucopyranoside 99% was purchased from Aldrich. All the sugars were used as received.

2.2.2 Analytical methods

2.2.2.1 ^{1}H and ^{13}C NMR analysis

^{1}H and ^{13}C spectra of all the samples were recorded on a bruker 200 MHz with CDCl$_3$ as the solvent and tetramethylsilane as external reference. The solid state ^{13}C spectra were recorded at 300 MHZ. All the spectrum is referenced at δ=77ppm for ^{13}C and δ=7.25ppm for ^{1}H with respect to deuterated chloroform which was used as the NMR solvent.

2.2.2.2 FTIR analysis

Spectra were recorded with a Perkin Elmer 1 FTIR instrument with a resolution of 4 cm^{-1} in transmission mode, in which the samples were cast onto a KBr disk from a solution of the polymer dissolved in chloroform.

2.2.2.3 GPC (gel permeation chromatography)

GPC of SBS and epoxidized SBS (data presented in appendix 2.5) were carried out using a Dionex GPC with RI detector, at room temperature. Shodex KF 803, 804 and 805 columns were used with HPLC grade chloroform as an eluent. The flow rate was 1 mL/min. A polystyrene calibration curve (20 samples of weight average molecular weights from 164 to 1.5 million) was used to estimate the molecular weights and polydispersity of CA samples. Sample preparation: 15-20 mg of CA was dissolved in 5 mL of Chloroform and 20 uL was injected. The sugar linked SBS samples due to partial insolubility in chloroform could not be analyzed.

2.2.2.4 Quantification of epoxidation percentage by ^{1}H NMR

The mole percentage of epoxidation was calculated from ^{1}H NMR spectra by comparison of the area of signal at 2.68 δ ppm and 2.92 δ ppm corresponding to the trans and cis proton respectively on oxirane ring of the epoxidized units of SBS with that of the 1,4 and 1,2 butadiene units at 5.4 ppm and 4.99 ppm respectively [44].

2.3. Synthesis of carbohydrate functionalized SBS

2.3.1 Synthesis of partially epoxidized SBS: Epoxidation is one of the most important addition reactions of alkenes. This can be carried out either by using

homogenous catalyst or heterogenous catalyst. We performed the epoxidation of SBS with a peracid as a homogenous catalyst. Partial epoxidation of Polystyrene-block-polybutadiene-block-polystyrene (SBS) was performed using 3-chloroperoxybenzoic acid, MCPBA (amount used appropriate for the desired percentage of epoxidation) in toluene at room temperature. The synthesis is outlined in reaction scheme 2.1

In a 250 ml. round-bottomed flask, 10g SBS, Aldrich (13 mmol) was dissolved in 100 ml toluene at room temperature. 6.25g of MCPBA (75% Aldrich) dissolved in 40ml of toluene was added drop wise with a dropping funnel over a time of 20 min. The reaction mixture was maintained at RT and the reaction was continued for 3.5 hr after which it was precipitated in 1L methanol. The precipitated polymer was washed many times with methanol. The polymer was then dried in desiccator under vacuum at room temperature.

 Thus, various degree of epoxidized SBS (7, 13, 22 and 46 mole % epoxidized) were synthesized using the appropriate amount of MCPBA with (SBS: toluene) ratio of 1:10 (w/v) using the above procedure.

^{1}H NMR [200 MHz, CDCl$_3$, δ ppm] showed signals of different protons at δ values of 7.05 -6.57 (10H), 5.40 (2H), 4.99 (3H), 2.92 (2H), 2.68 (2H), 2.03(1H), 1.61, 1.58 and 1.55

^{13}C NMR [400 MHz, CDCl$_3$,δ, ppm] showed values at 145.26, 142.6, 131.22-127.61, 114.20, 58.42, 56.73, 43.54, 40.28, 38.13, 33.90, 32.66, 27.35 and 24.34

FTIR: (KBr, cm^{-1}): 3080, 3060, 3025, 3004, 2920, 2846, 1639, 1601, 1493, 1452, 1404, 1386, 1352, 1312, 1260, 1071, 1028, 967, 910, 841 and 804
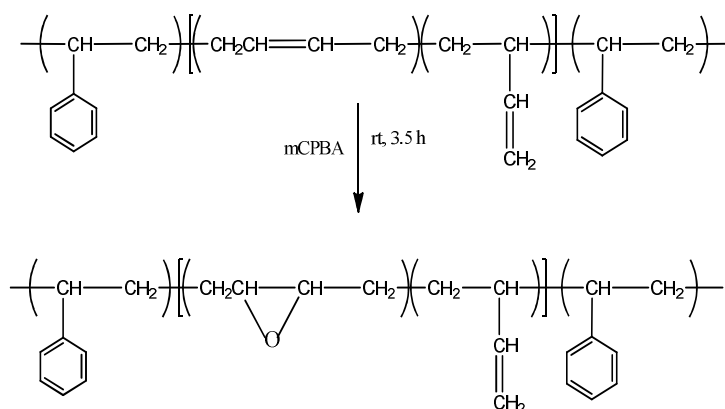
Reaction scheme 2.1 Synthesis of partially epoxidized SBS

2.3.2 General procedure for synthesis of carbohydrate functionalized SBS from partially epoxidized SBS

In a 250 ml. round-bottomed flask, 5g of partially epoxidized SBS (16.25 mmol epoxide functionality) was dissolved in 50 mL Pyridine (GR, Merck) with constant stirring until completely dissolved. Sugar (glucose, mannose, galactose, xylose, methyl glucoside, xylose, sucrose and maltose) 3 eq. (48.75 mmol) was completely dissolved in 100 mL DMF (GR, Merck). The ratio of pyridine All the sugars were heated on a hot plate at 50-60 ^{0}C for 5 min, except galactose which was heated at 90 ^{0}C for 15 min to make it completely soluble in DMF. The sugar solution was cooled to RT and then 500 mg of DMAP was added to it with constant stirring until fully soluble. This solution was then added drop wise to SBS epoxide solution maintained at 60 ^{0}C under nitrogen. This was followed by addition of NH_4Cl (48.75 mmol). The temperature of the reaction mixture was raised to 80^{0}C and the reaction was done at 4-16 h depending on the sugar used. The colour of the reaction mixture changed from white to dark chocolate colour with the progress of

the reaction in case of glucose, mannose, galactose, maltose, fructose and xylose. While the colour changed to light orange in case of sucrose and methyl glucoside.

The reaction mixture was cooled to RT after the reaction was over and it was ppt. in brine, followed by repeated washing with water to remove sodium chloride and pyridine. When the product became salt free as indicated by aq. Silver nitrate solution, the product was filtered on nylon cloth and dried overnight under vacuum at RT. The colour of the product was brown, whereas the starting SBS and SBS epoxide both were white in colour.
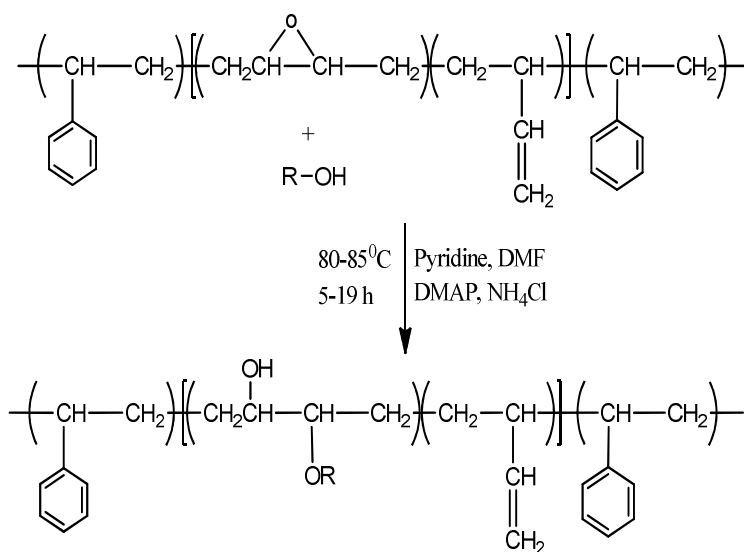
R−OH = glucose, mannose, galactose, xylose, fructose, methyl glucoside, sucrose and maltose

Reaction scheme 2.2 Synthesis of carbohydrate functionalized SBS from partially epoxidized SBS

2.4. Results and discussion

2.4.1 Synthesis and characterization of partially epoxidized SBS

A detailed procedure for the synthesis is described in experimental part. This partially epoxidized SBS (SBS EP 24) was synthesized from SBS by reaction with 3-chloroperoxybenzoic acid in one step. The product was purified by dissolving in chloroform and re-precipitation in methanol. The chemical structure of the product was confirmed by FT-IR, ^{1}H NMR and ^{13}C NMR spectroscopy.

2.4.1.1 FTIR spectral analysis of SBS and partially epoxidized SBS

Figure 2.1 shows overlapped FT-IR spectrum of SBS and SBS EP 24 which clearly shows the observed changes in absorption bands before and after epoxidation.
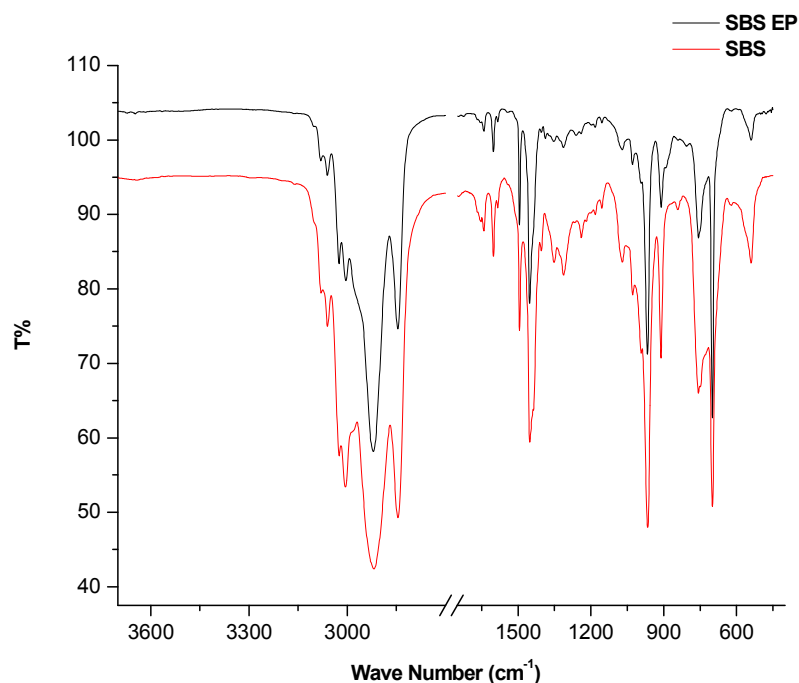
Figure 2.1 FTIR spectrum of SBS and partially epoxidized SBS

In both the FTIR spectra of SBS and epoxidized SBS (EP24), there exists peak in the region of 3006-3080 cm^{-1} for olefinic (C=**C-H**) and phenyl C-H stretching and those at 1600, 1493, 1452, 1311 and 699 cm^{-1} are for phenyl groups of the polystyrene block in SBS. There are also peaks at 1639 cm^{-1} for C=C stretching and 842 cm^{-1} which is due to out of plane bending of =C-H of the 1, 4 unsaturation of polybutadiene segment.

Since polybutadiene segment of SBS has 1,4- and 1,2-isomeric unsaturation, the epoxidized polybutadiene segments comprise two isomeric structures, 1,4- epoxide and 1,2-epoxide, as shown in Figure 2.6 . For the 1,4-isomers there exist cis and trans forms. In the FTIR spectra, the cis- 1, 4-polybutadiene appears typically at 756 cm^{-1}, trans-1,4-polybutadiene at 967 cm^{-1}, and the 1,2- polybutadiene at 910 cm^{-1} [44] . It is noteworthy that 1,2-polybutadiene has a characteristic IR peak at 910 cm^{-1} and so has the polystyrene at 907 cm^{-1}. Both peaks are too close to the epoxide characteristic peak at 906 cm-', and it is therefore hard to distinguish these peaks. Therefore, the increasing peak at 910 cm-' after the epoxidation is essentially a combination of the polystyrene peak, the 1, 2-polybutadiene peak, and the increasing epoxide peak.

The epoxide functional groups can be identified at several different places, such as 804, 1260, and 1386 cm^{-1}[51]. These peaks in the spectrum of the epoxidized polymer appear to be stronger than that in the unmodified SBS. The epoxidation reaction of polybutadiene segment therefore could be monitored through the decrease of unsaturation and the appearance of the epoxide.

Furthermore there is no absorption band in 3400-3600 cm^{-1} region indicating that there was no side reaction such as opening of epoxide ring commonly observed

during the epoxidation. The epoxidized SBS was completely soluble in chloroform and toluene indicating that there was no cross linking of the product epoxide.
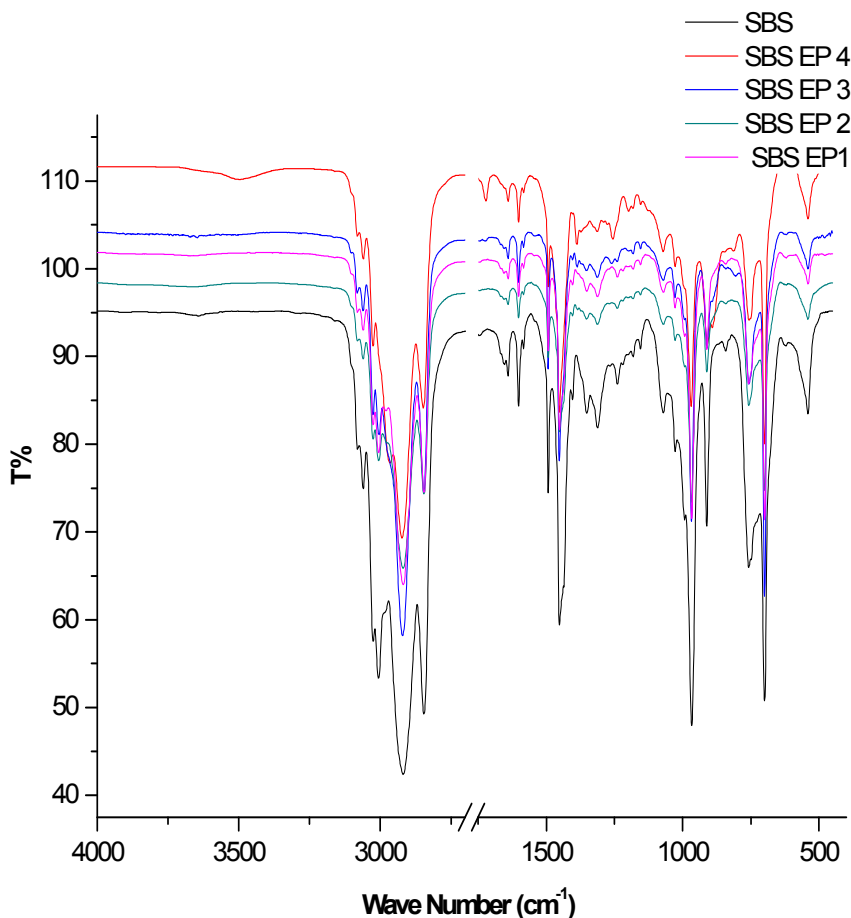
Figure 2.2 FTIR spectrum of SBS and epoxidized SBS with different degree of epoxidation

Figure 2.2 shows FTIR spectrum of epoxidized SBS with gradually increasing degree of epoxidation viz. SBS EP1 7%, SBS EP2 13 %. SBS EP3 22% and SBS EP4 46 % epoxidation (mol %). The epoxide functional group shows peaks at 804 cm^{-1}(weak symmetry in plane ring deformation), 1255-1260 cm^{-1}(epoxide ring stretching), and at 1385-1387 cm^{-1} with the simultaneous decrease in intensity of C=C peaks at 1639 and 842 cm^{-1}. The peak at 804 cm^{-1} gradually increases in intensity with the increase in degree of epoxidation from SBS EP1-SBS EP4 (7-46

mol %). The peaks in 1255-1260 cm^{-1} and 1385-1387 cm^{-1} region also follow the same pattern as expected. With increase in epoxidation, broadening of 911 cm^{-1} peak occurs. As the epoxidation reaches 46 mol% as in SBS EP4, a shoulder at 891 cm^{-1} clearly appears which was not visible at lower degree of epoxidation which is due to the epoxide functionality. The epoxies from SBS EP1- EP3 does not show absorption in the –OH region whereas SBS EP4 with a 46 mol% epoxidation shows peak at 3497 cm^{-1} indicating slight opening of the epoxide ring during epoxidation. All these facts points to the successful epoxidation of SBS with desired degree of epoxidation.

To avoid epoxide opening and cross linking of the product we choose to use 22 mol% epoxidized SBS EP 3 for our further modification studies with carbohydrates during the course of this work.

2.4.1.2 ^{1}H, ^{13}C and ^{13}C DEPT NMR spectral analysis of SBS and partially epoxidized SBS

The ^{1}H NMR, ^{13}C and ^{13}C DEPT NMR spectrums of SBS are showed in figure 2.4 - 2.6. Signals in the region of 7.05-6.59 δ ppm corresponding to aromatic hydrogen of styrene unit. The absorption at 5.42 δ ppm was due to tertiary hydrogen of double bond (3v, 2t, 3t, 2c and 3c in figure 2.3) in both 1,2 and 1,4 structures of the butadiene units besides the signal at 5.00 δ ppm is due to methylene hydrogen's of double bond (4v in figure 2.3) of the 1,2 structure. The signal at 2.04 δ ppm is due methine proton (2v in figure 2.3) in the main chain of 1,2 structure. The signal at 1.42-1.25 δ ppm is due to the cis and trans double bond protons of the 1, 4 structure.
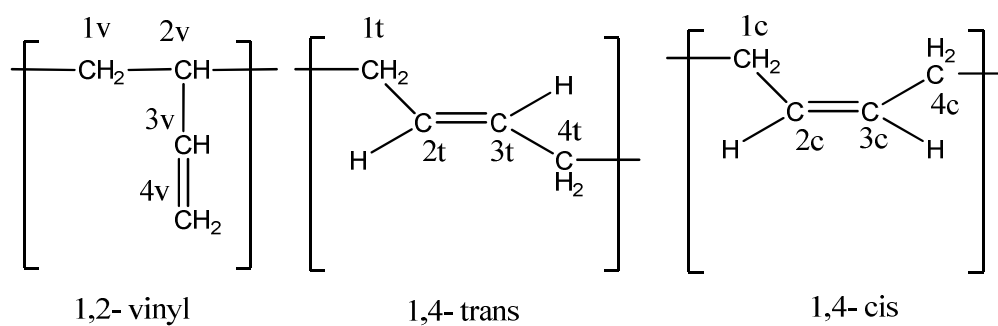
Figure 2.3 1,2 and 1,4 structural units (microstructures) of butadiene in SBS
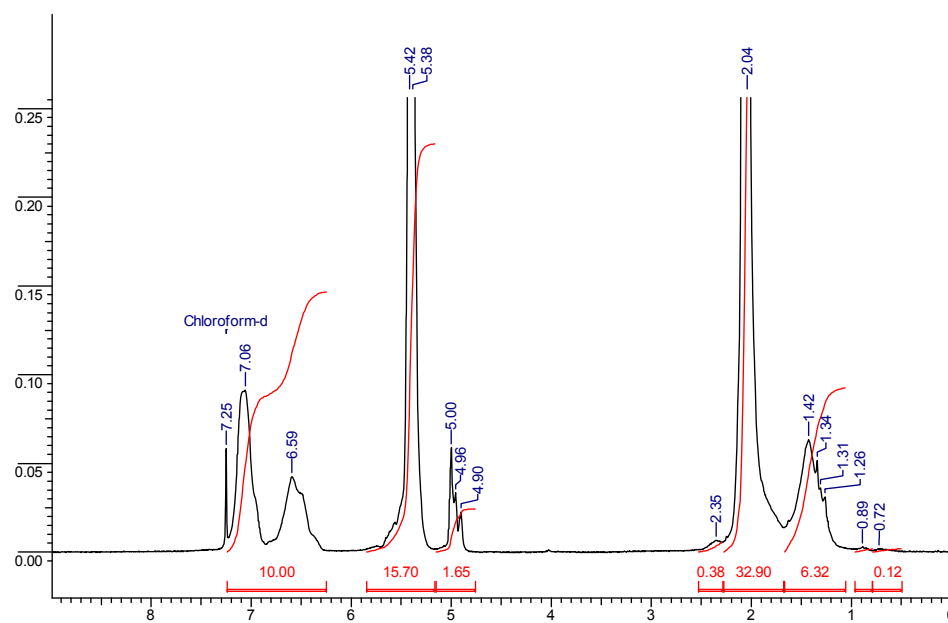
Figure 2.4 ^{1}H NMR of SBS
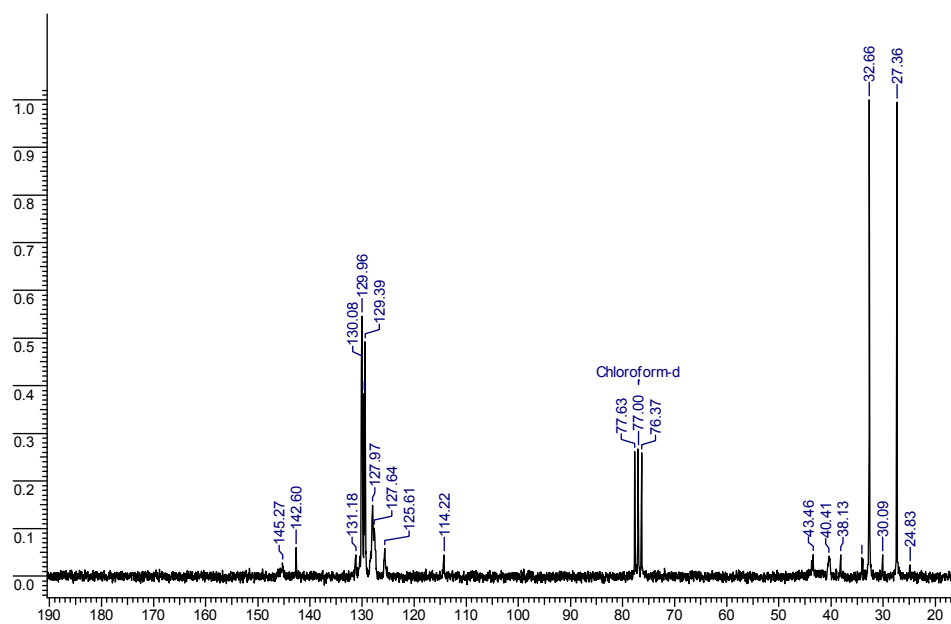
Figure 2.5 ^{13}C NMR of SBS
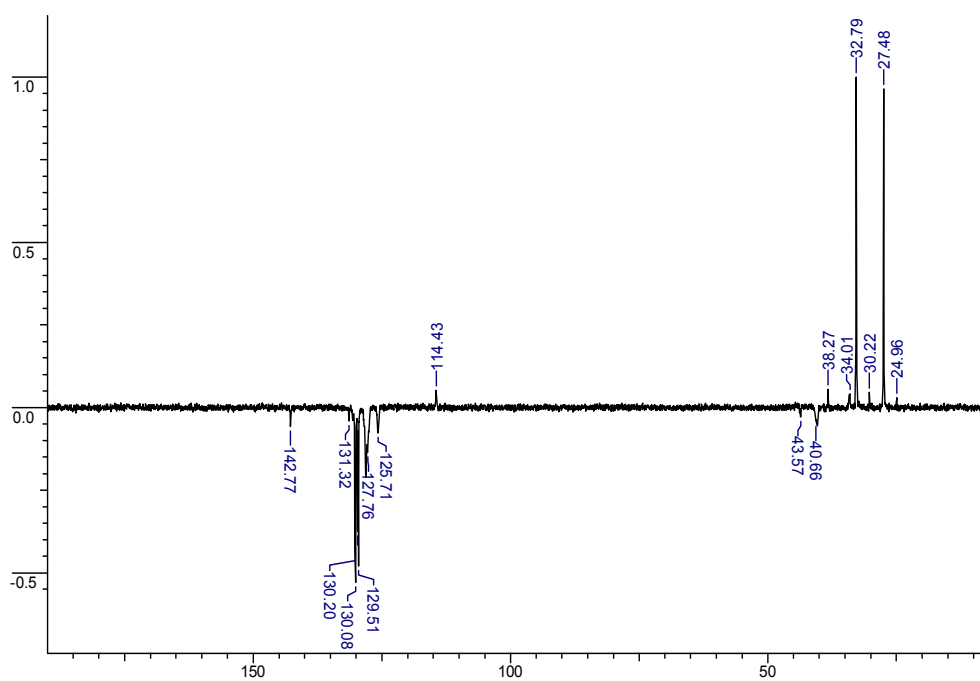
Figure 2.6 ^{13}C DEPT NMR of SBS

In the ^{13}C spectrum of SBS , olefinic carbons (H**C**=) from trans 1,4 unit showed

peak at 130.08 and 131.18 δ ppm, whereas cis 1,4 unit exhibited peaks at 129.39

and 129.96 δ ppm [52]. The 1,2 unit signal was seen at 43.46 and 114.42 δ ppm. The signal from 125.61-127.97 are assigned to the (H**C**=) aromatic carbons. The signal between 27.36-40.29 δ ppm corresponds to methylenic carbons (-**C**H$_2$-) from cis trans-1,4 and 1,2 units [52]. A signal at 43.45 δ ppm is assigned to the methine group (-**C**H-) from the 1,2 units [52].
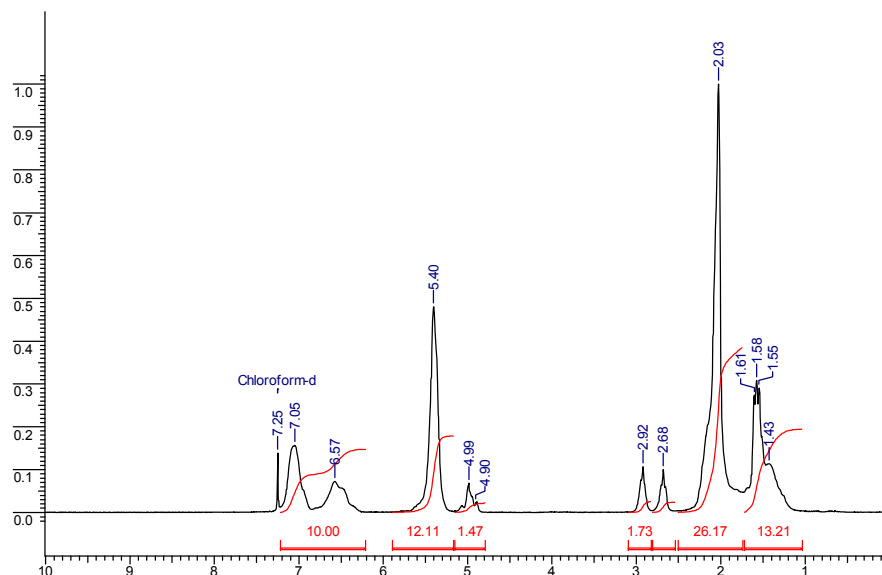
Figure 2.7 ^{1}H NMR of epoxidized SBS (22 %)

Epoxidation of SBS (figure 2.7) results in formation of epoxide ring and gives new signals at 2.92 δ ppm which is due to the epoxide from cis-1,4 structure and the signal at 2.68 δ ppm is due to the epoxide from trans-1,4 structure of the butadiene unit of SBS [44]. It was observed from the NMR spectrum that the 1,4 structure double bonds reacted preferentially to those of the vinyl double bonds of 1,2 structure. Further the reactivity of cis-1,4 structure double bond was more than the trans-1,4 structure.

The mole percentage of epoxidation was calculated from ^{1}H NMR spectra by comparison of the area of signal at 2.68 δ ppm and 2.92 δ ppm corresponding to

the trans and cis proton respectively on oxirane ring of the epoxidized units of SBS with that of the 1,4 and 1,2 butadiene units at 5.4 ppm and 4.99 ppm respectively [44].
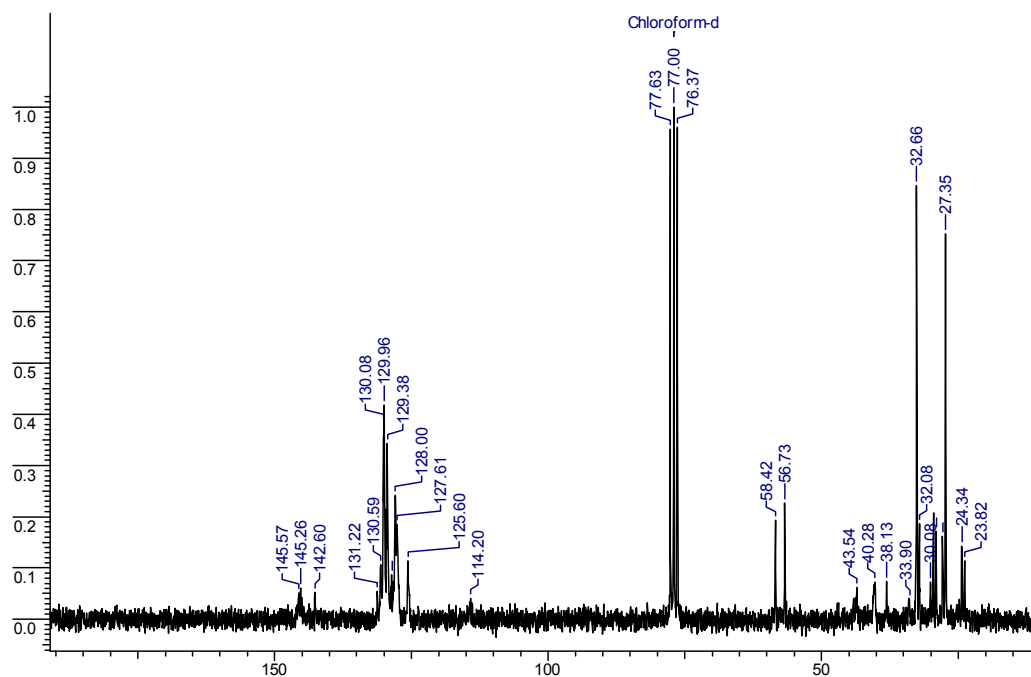
Figure 2.8 ^{13}C NMR of epoxidized SBS (22 %)

The ^{13}C NMR spectrum of SBS epoxide (figure 2.8) shows signal at 58.42 δ ppm and 56.73 δ ppm which are due to the epoxide ring formed from 1,4-trans & cis structure double bonds of butadiene segments of the SBS respectively [51]. This is absent in the unmodified ^{13}C NMR spectrum of SBS which further confirms the epoxidation. Moreover the 1,2 unit signal was also present at 43.46 and 114.42 δ ppm, which proves that 1,2 units were not attacked much during epoxidation.

2.4.2 Synthesis of hydro-chlorinated SBS from partially epoxidized SBS

In a 100 ml. round-bottomed flask, 2g of partially epoxidized SBS was dissolved in 20 mL toluene with constant stirring until completely dissolved at room temperature (RT). Then 0.5 mL HCl (35%) dissolved in 10 mL toluene was added to the reaction mixture drop wise with constant stirring (rapid addition of HCl resulted in gel like product). The reaction was continued at room temperature for 5 h. The product was precipitated and washed many time in methanol and dried overnight in vacuum oven at RT. The product was characterized by ^{1}H NMR.
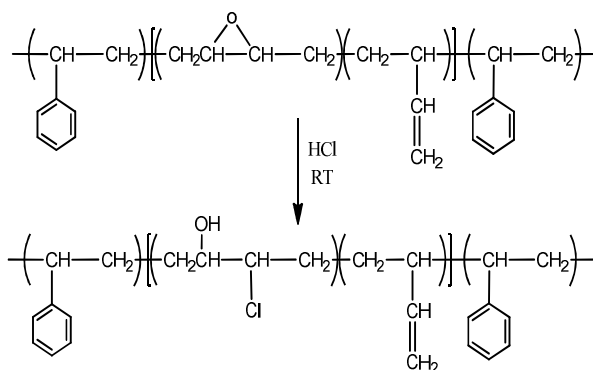
Reaction Scheme 2.3 Hydro-chlorination of SBS

Charaterization of hydro-chlorinated SBS by ¹H NMR
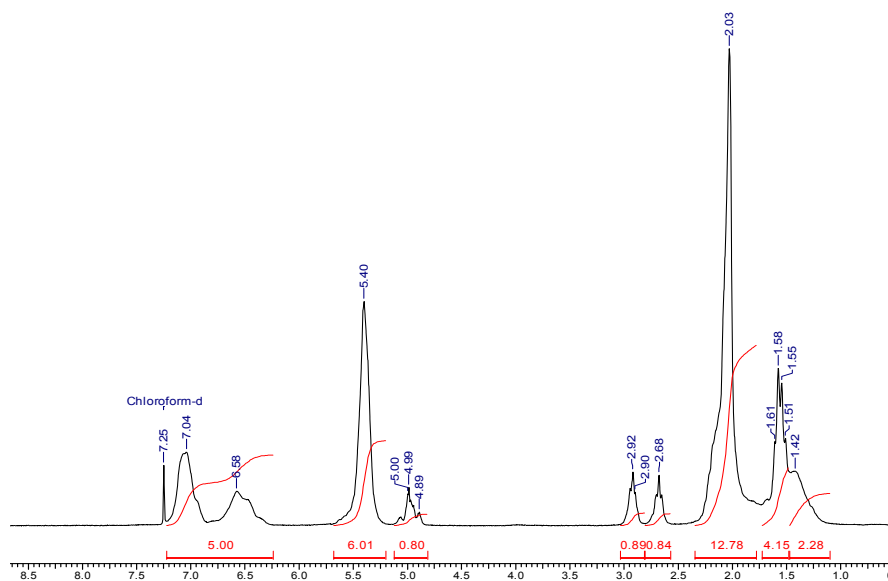
Figure 2.9 ¹H NMR of epoxidized SBS
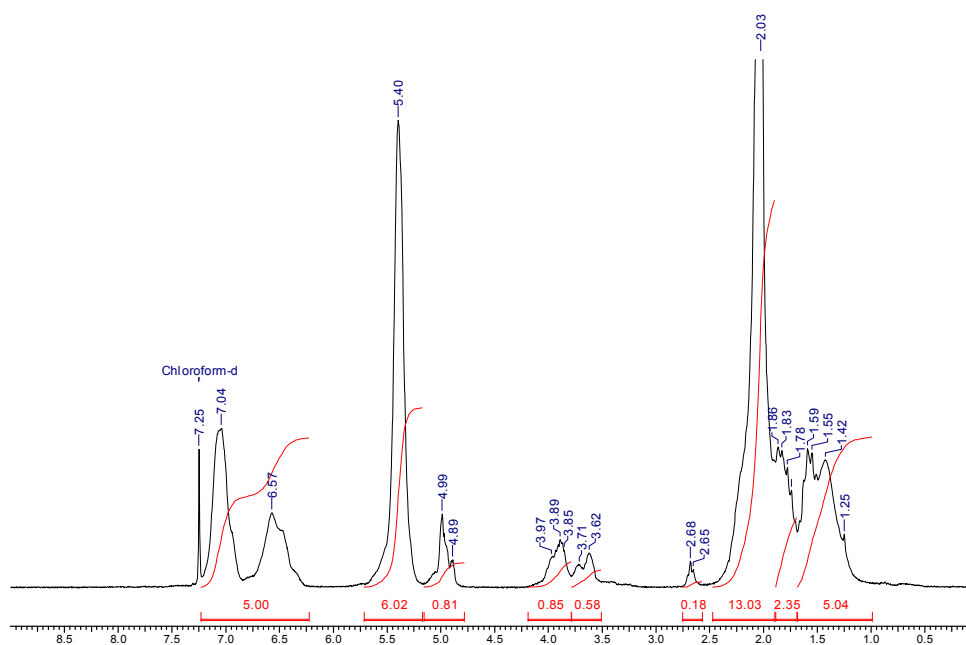
Figure 2.10 ¹H NMR of hydro chlorinated SBS

Epoxide ring in partially epoxidized SBS is protonated by H^+ form HCl and then Cl^- attacks the protonated ring in SN^2 fashion to give the hydro-chlorinated SBS. ^{1}H NMR of hydro-chlorinated SBS clearly shows the quantitative disappearance of epoxide peaks at 2.92 δ ppm (-C**H**-proton, cis) and 2.68 δ ppm (-C**H**- proton, trans), with the simultaneous appearance of additional signals at 3.62 & 3.71 δ ppm assigned to C**H**-OH and the signal at 3.89 δ ppm is assigned to–C**H**-Cl [53].

 Thus, ^{1}H NMR clearly establishes the formation of hydro chlorinated SBS as depicted in reaction scheme 2.4.

2.4.3 Synthesis and characterization of carbohydrate functionalized SBS from partially epoxidized SBS

A detailed procedure for the synthesis is described in experimental part of this chapter. Carbohydrate functionalized SBS were synthesized from partially epoxidized SBS by reaction with sugars (glucose, mannose, galactose, xylose, methyl glucoside, xylose, sucrose and maltose) and ammonium chloride using 4-DMAP as a catalyst in N, N-DMF and pyridine [2:1 (v/v)] solvent.

A blank reaction of partially epoxidized SBS was also performed under the same reaction conditions in the absence of sugar in order to check whether the epoxide ring opens under these experimental conditions. We found out that epoxide ring does opens under these conditions.

The chemical structure of the products was confirmed by XPS, FTIR, ^{1}H NMR, and ^{13}C NMR spectroscopy for the carbohydrate linked SBS.

The primary evidence of successful accomplishment of functionalization of SBS elastomer with different sugars was obtained by quantification of sugar content by phenol sulphuric acid method.

2.4.3.1 Characterization of blank reaction (without sugar)

The blank reaction product was characterized by ^{1}H NMR shown in figure below
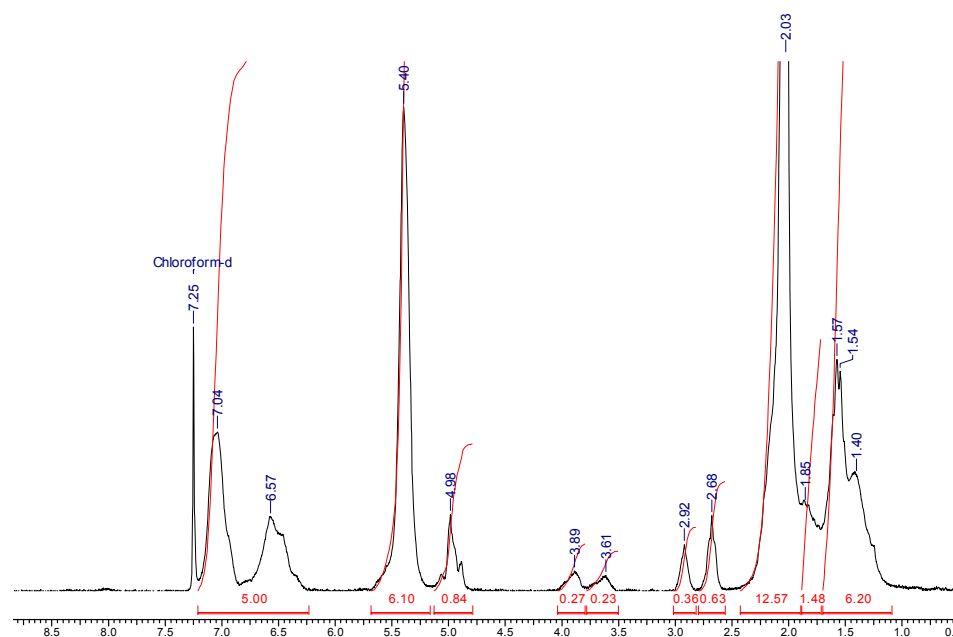
Figure 2.11 ^{1}H NMR of blank reaction of partially epoxidized SBS

A partial epoxide opening for blank reaction is seen from ^{1}H NMR in figure 2.11. This is evident from the decrease in proton integration of epoxide peak at 2.68 & 2.92 δ ppm with simultaneous appearance of additional signals at 3.61 & 3.89 δ ppm, similar to hydro-chlorinated SBS. 43 % epoxide ring opening was observed under the blank reaction condition as calculated from the ^{1}H NMR integration of residual epoxide protons.

Hydro-chlorination of SBS leads to appearance of signal at 3.62 & 3.89 δ ppm as discussed earlier and blank reaction also shows new signals at the same peak position. These two observations in conjugation, points to the formation of same product under their respective reaction conditions. This shows that hydro chlorination of SBS takes place in the blank reaction conditions.

Quaternary ammonium salts (Q^+X^-) were used by White et al. for the polymerization of bisepoxides with bisphenols to give poly(hydroxyl ethers) [54-55]. Our reaction system also has ammonium chloride and unprotected sugar having free hydroxyls which can react with epoxidized SBS leading to the observed hydro-chlorination of SBS. Moreover, since sugar hydroxyl is weak nucleophile by themselves, 4 DMAP has been used in the reaction mixture as a catalyst to activate the free hydroxyl groups. Van Dijik- Wolthuis et al. [56] also reported coupling of glycidyl methacrylate (GMA) epoxide functionality with dextran hydroxyl using 4-DMAP as catalyst.

The reaction mechanism for this reaction is depicted below:

R-OH = sugar
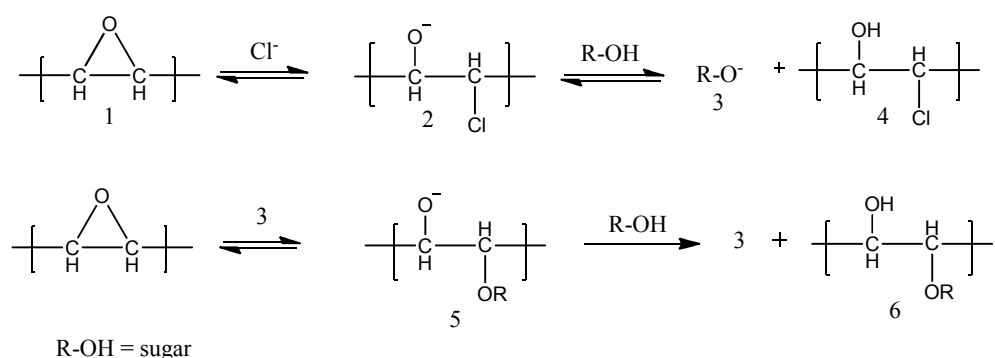
Reaction Scheme 2. 4 Reaction mechanism for hydro-chlorination and β- hydroxy ether formation from epoxidized SBS

The anionic component $X^-(Cl^-)$ of the quaternary salt attacks an SBS epoxide functionality to yield alkoxide 2, which deprotonates activated primary sugar hydroxyl to generate 3 and halohydrin 4. Reaction of 3 with an unreacted epoxide group gives intermediate 5; neutralization of 5 leads to hydroxyl ether 6.

This explains the observed formation of hydro-chlorinated SBS under blank reaction conditions.

Besides hydro-chlorination, blank reaction product ^{1}H NMR also shows peaks of very low intensity at 8.02 & 8.34 δ ppm in pyridine region.

It is known in literature that reaction of polymeric epoxides with pyridine and vinyl pyridines leads to the formation of pyridinium intermediate 1 [57] which immediately attacks the α-position of the pyridine ring, forming a conjugated 3, 5-diene in the 6-membered ring. Since in our reaction condition chloride is already available, being generated from the ammonium chloride in the reaction mixture it can trap the pyridinium intermediate forming a pyridinium chloride containing product 2 instead of rearranging to conjugated 3, 5-diene in the 6-membered ring.

The reaction of pyridine with epoxidized SBS and formation of pyridinium chloride can take place according to the following reaction mechanism:
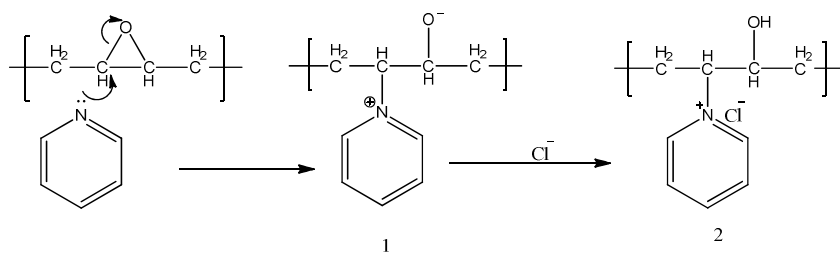
Reaction scheme 2.5 Mechanism for formation of pyridinium chloride pendant on

SBS

The formation of 2 explains the observed peak at 8.02 and 8.34 δ ppm in the blank

reaction. Thus from the above discussion we can say that the reaction of

epoxidized SBS with our reaction system leads to hydro-chlorination as well as

formation of pyridinium chloride pendants on SBS.

2.4.3.2 Synthesis and Characterization of D-glucose functionalized SBS

D-Glucose functionalized SBS was synthesized as shown in the reaction scheme 2.6 below according to the procedure described in section
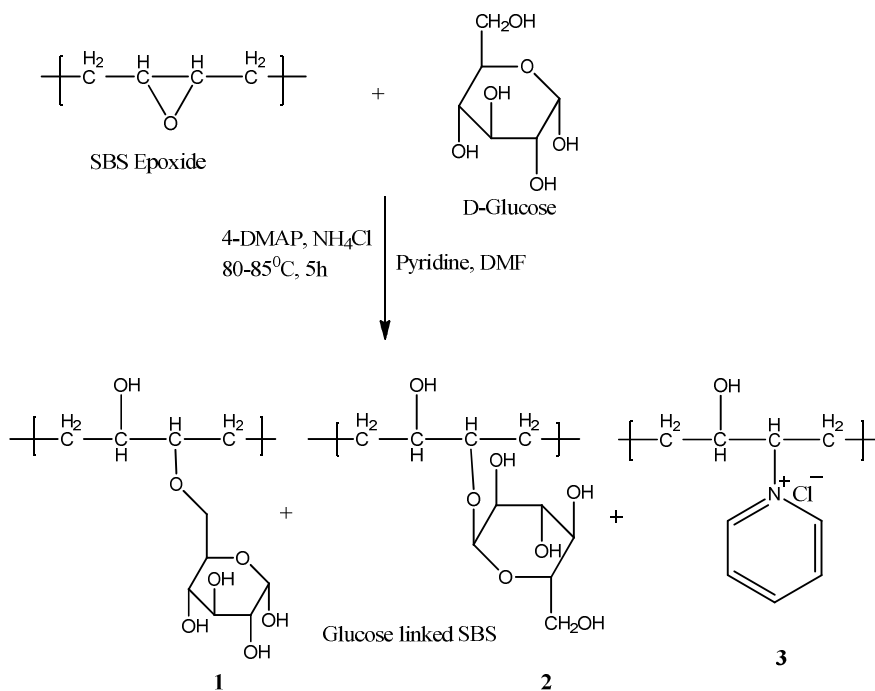
Reaction scheme 2.6 Glucose functionalized SBS
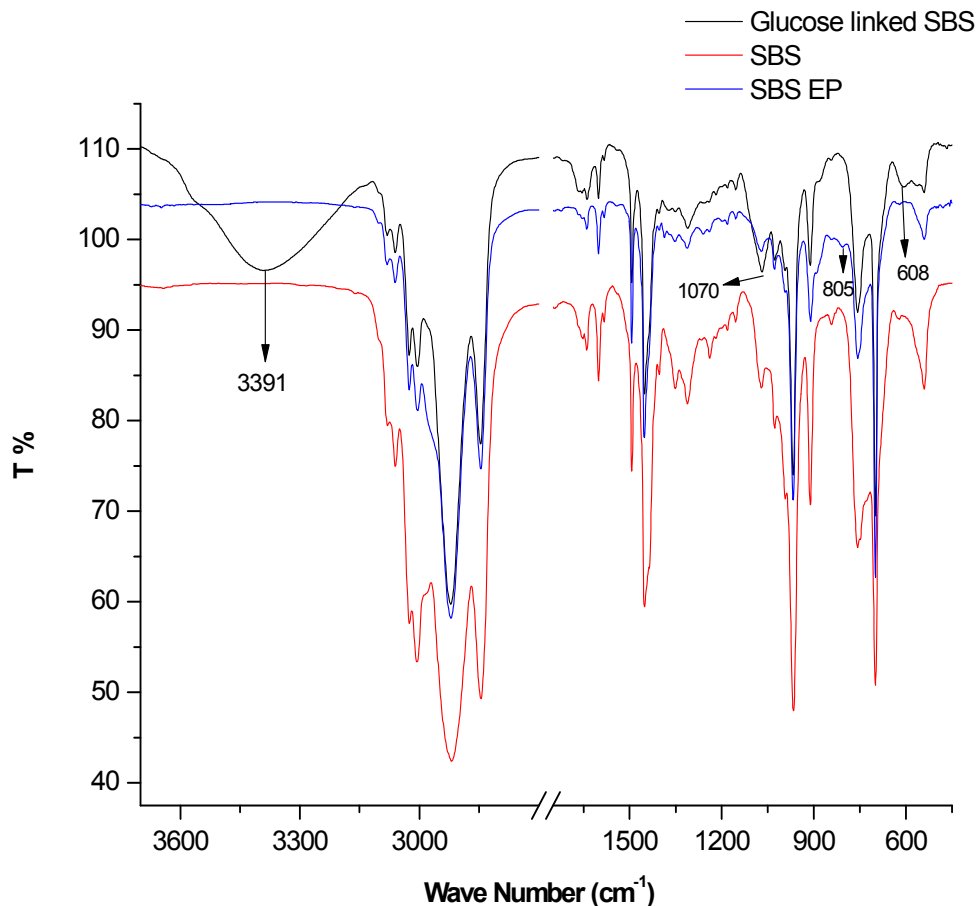
Figure 2.12 Overlapped FTIR spectrum of glucose linked SBS, epoxidized SBS and

SBS

Figure 2.12 shows the overlapped FTIR spectrum of glucose linked SBS, epoxidized SBS (SBS EP, 22 mol% epoxidized) and SBS. On reaction of SBS epoxide with an alcohol (in this case glucose), the epoxide rings cleaves to give hydroxy ether linked glucose unit as shown in reaction scheme 2.6. The progress of the reaction was monitored using FTIR and completion of reaction was confirmed by the total disappearance of the epoxide peak at 805 cm^{-1}.

FTIR shows the epoxy absorption band which was present in SBS EP 24, no longer exists in final product. The epoxide peaks at 805 cm^{-1}, 1260 cm^{-1} and 1387 cm^{-1}

disappeared, while a broad peak at 3391 cm⁻¹ appeared which was absent in the SBS EP 24. This peak is assigned to the H- bonded O-H stretching vibrations, which is due to –OH groups generated on SBS backbone from epoxide ring opening by glucose, pyridine and ammonium chloride, besides sugar hydroxyl are also contribute to this peak.

A peak at 608 cm⁻¹ also appeared which was neither present in SBS nor in epoxidized SBS and is attributed to CH-Cl stretching vibrations [58] due to the hydro chlorinated butadiene segments. There was also visible increase in the 1070 cm⁻¹ peak intensity as compared to both unmodified SBS and epoxidized SBS, this can be attributed to the hydroxyl groups. All these facts points to the successful functionalization of SBS.

This was further analyzed and confirmed by ¹H and ¹³C NMR of the glucose linked SBS.
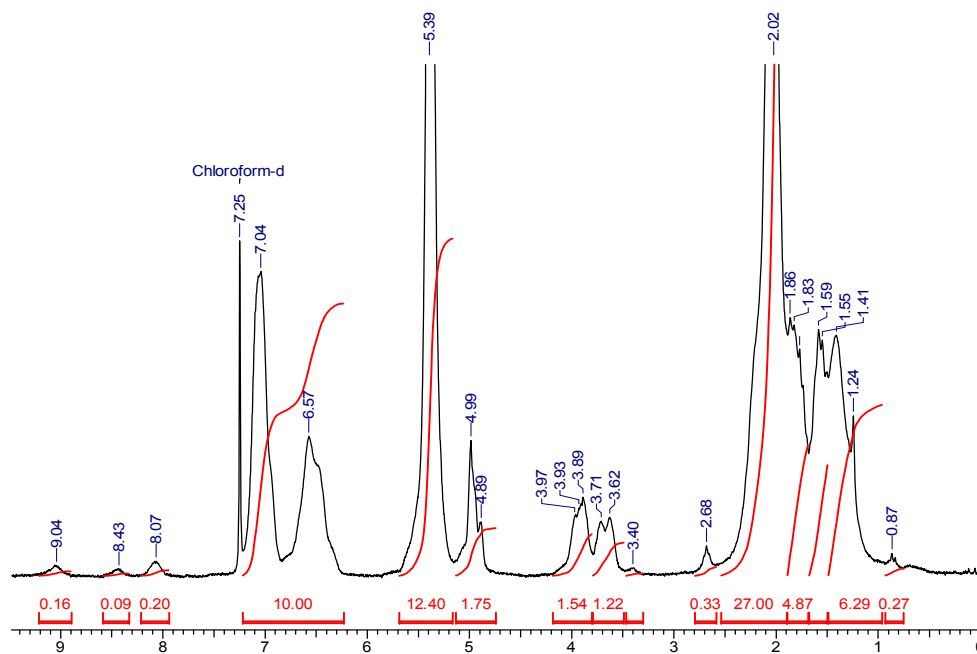
Figure 2.13 ¹H NMR of glucose linked SBS

Figures 2.13- 2.15 shows the ^{1}H, ^{13}C and ^{13}C DEPT NMR spectra of glucose linked SBS. The functionalization of SBS is confirmed by ^{1}H NMR spectra (Fig.2.13) which clearly shows the quantitative disappearance of epoxide peaks at 2.92 (-CH-proton, cis) and 2.68 δ ppm(-CH- proton, trans), with the simultaneous appearance of additional signals at 3.62, 3.71, 3.89- 3.97 δ ppm. The attack of glucose on both the 1, 4-cis and trans epoxide leads to formation of β –hydroxy ethers (glucose linked to the SBS backbone with an ether linkage) along with hydro chlorination as shown in reaction scheme 2.4, resulting from the opening of SBS epoxides.

Peaks at 8.07, 8.34 and 9.04 δ ppm are also observed which is due to side reaction of epoxidized SBS with pyridine resulting in the formation of pyridinium chloride pendants on SBS, as explained in the reaction scheme 2.5. The intensity of these peaks is much higher as compared to the blank reaction.

Since 1, 4 cis epoxide is more reactive as compared to the trans epoxides, there is complete disappearance of the 1, 4 cis signal at 2.92 δ ppm, whereas some residual 1, 4-trans still remains unreacted as shown by presence of the signal at 2.68 δ ppm. The amount of unreacted epoxide is less (10.5%) as shown by the integrated peak areas.

The signal at 3.89-3.97 δ ppm in glucose linked SBS is assigned to proton attached to carbon of –**CH**-Cl and the signal at 3.61 and 3.62 δ ppm is assigned to protons attached to the carbon of –**CH**-OH (reaction scheme 2.3), while the signal at 3.4 δ ppm may be due to the sugar hydroxyls.
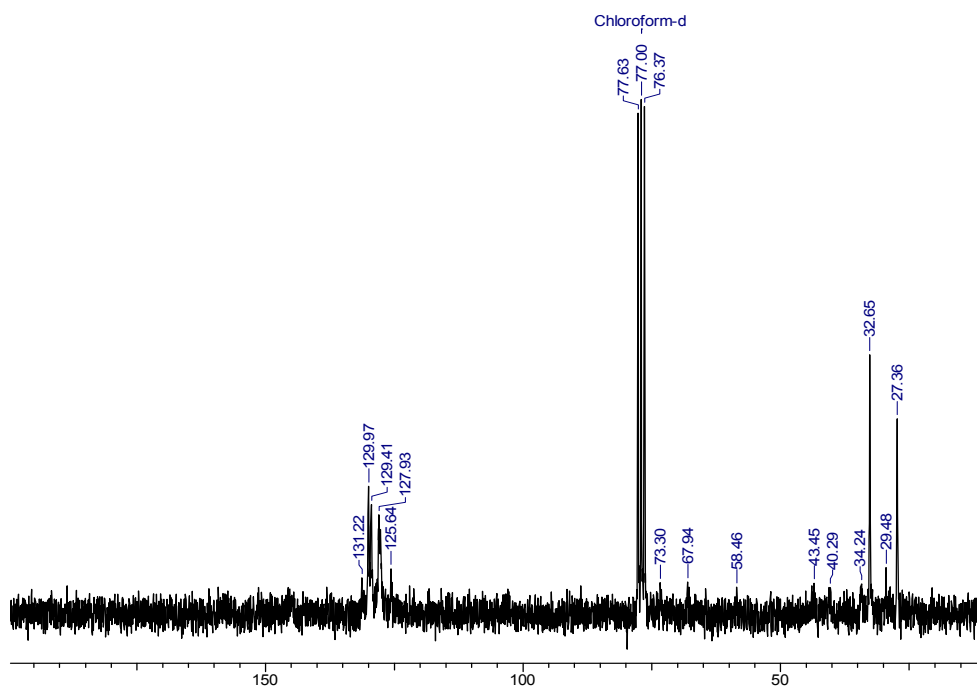
Figure 2.14 ^{13}C NMR of Glucose linked SBS
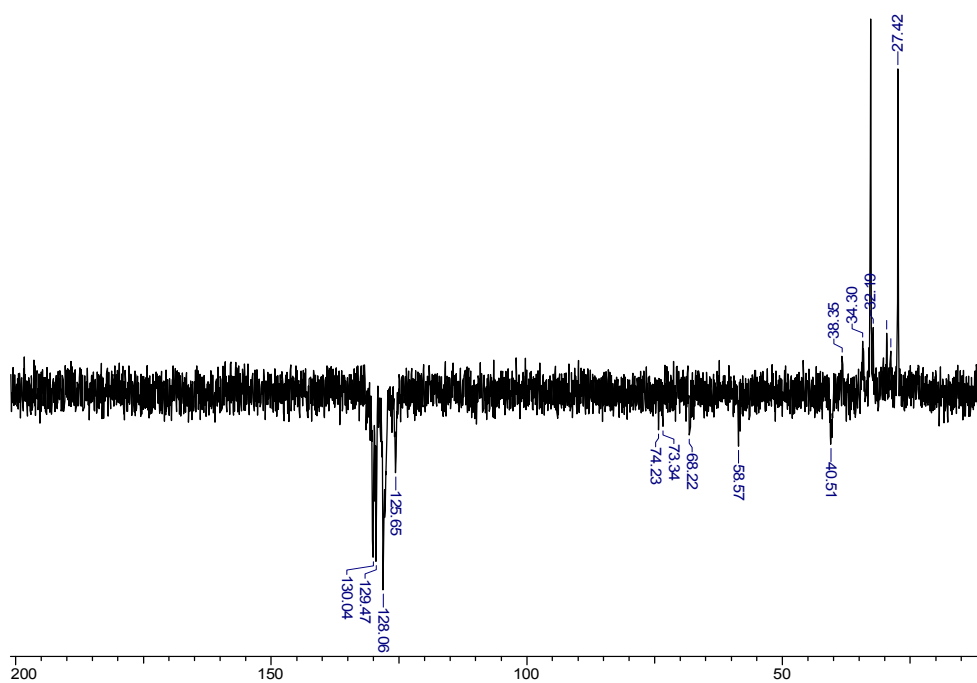
Figure 2.15 ^{13}C DEPT NMR of Glucose linked SBS

Similar to ^{1}H NMR, disappearance of epoxy carbon peaks was also observed in ^{13}C NMR spectra at 56.73 and 58.42 δ ppm due to the epoxide ring opening. Appearance of new peaks in the range of 67-74 δ ppm corresponding to –**C**H-OH and –**C**H-Cl was also observed (figure 2.14 and figure 2.15). Residual epoxide signal at 2.92 δ ppm is seen in ^{1}H NMR spectra and a corresponding reduced peak at 58.57 δ ppm is also observed in ^{13}C spectra.

The olefinic carbons (H**C**=) from trans 1,4 unit showed diminished peak at 131.22 δ ppm compared to unmodified SBS, whereas cis 1,4 unit exhibited peaks at 129.41 and 129.97 δ ppm. However the 1, 2 unit signal at 114 δ ppm is not visible. The signal between 27.36-40.29 δ ppm corresponds to methylenic carbons (-**C**H$_2$-) from cis trans-1, 4 and 1, 2 units. A signal at 43.45 δ ppm is assigned to the methine group (-**C**H-) from the 1, 2 units.

Although hydro chlorination and formation of pyridinium chloride pendants on SBS was detected by combination of NMR and FTIR, anchoring of glucose units on SBS could not be proved conclusively by these techniques because of overlapping signals of hydroxyl groups generated on the SBS back bone and sugar hydroxyl groups.

Hence to remove this ambiguity, sugar content was determined by phenol sulphuric acid method [59] and glucose content in the functionalized SBS was found to 0.9 weight % (sugar content determination presented in appendix of Chapter 5). Since the amount of anchored sugar was very less it could not be effectively detected in NMR.

Here it is interesting to note that in the blank reaction with absence of sugar only 57% epoxide opening takes place, whereas when glucose is present in the reaction

mixture >90% epoxide opening is observed. This shows that presence of glucose increases overall epoxide opening by 1.5 fold. Further investigation on effect of sugar on epoxide opening is under progress in our lab.

Thus, apart from the new signals due to the functionalization of the SBS, its back bone structure signals are mostly intact. In all the previous studies reported in literature for opening of epoxy with alcohols, the reaction proceeded with considerable rearrangements, but our strategy gave no such rearrangement or cross linked products, besides keeping the back bone structure (microstructures) of SBS intact.

2.4.3.3 Synthesis and Characterization of D-Mannose functionalized SBS

D-Mannose functionalized SBS was synthesized as shown in the reaction scheme 2.4 below.
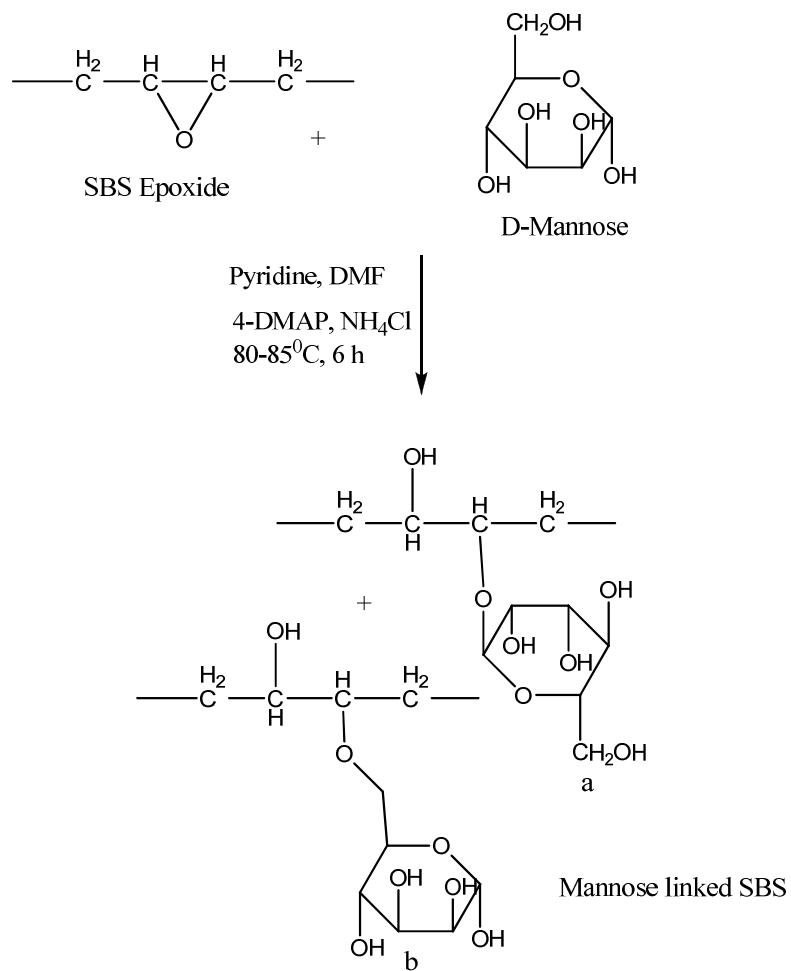
Reaction scheme 2.7 Mannose functionalized SBS (a) anomeric linkage (b) primary linkage
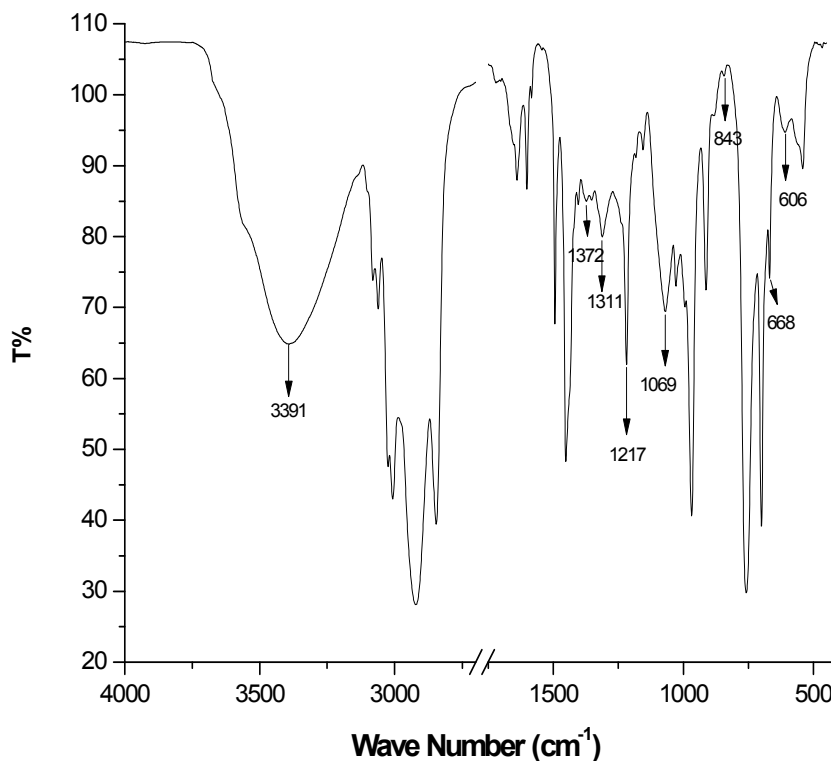
Figure 2.16 FTIR spectrum of mannose linked SBS

Figure 2.16 shows the FTIR spectrum of D-Mannose linked SBS. The spectrum shows similar peaks like the D- glucose functionalized SBS. The appearance of a new broad peak at 3391 cm^{-1} due to the H- bonded O-H stretching vibrations, which is a combination of –OH group from epoxide opening and -OH groups of ether linked mannose. There is complete loss of 804 cm^{-1} epoxide showing the quantitative epoxide ring opening, under the reaction conditions employed. Peaks at 806 and 668 cm^{-1}are also observed due to the CH-Cl stretching vibrations. A sharp peak at 1217 cm^{-1} was also observed, compared to a small peak in glucose. This can due to C-O-C stretching of the ether linked mannose or CH-Cl stretching (from hydro-chlorination). The absorption at 1372 and 1069 cm^{-1} are more pronounced as compared to glucose linked SBS. These facts points to the quantitative functionalization of SBS.
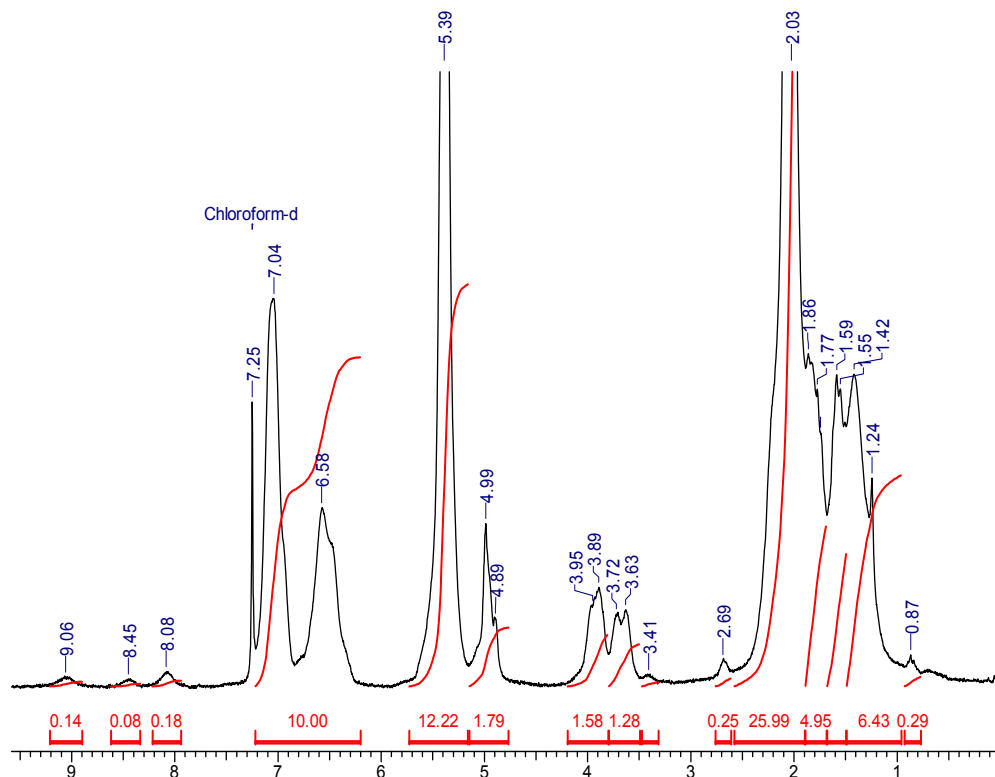
Figure 2.17 ^{1}H NMR of Mannose linked SBS

Figures 2.17- 2.19 shows the ^{1}H, ^{13}C and ^{13}C DEPT NMR spectra of mannose linked SBS. The spectra is similar to glucose linked SBS. Mannose content in the mannose functionalized SBS was found to 0.12 weight % by the phenol sulphuric acid method. The residual epoxide of the mannose linked SBS was found to 8%, which was less than glucose functionalized SBS. All these facts show the quantitative functionalization of SBS in presence of mannose.
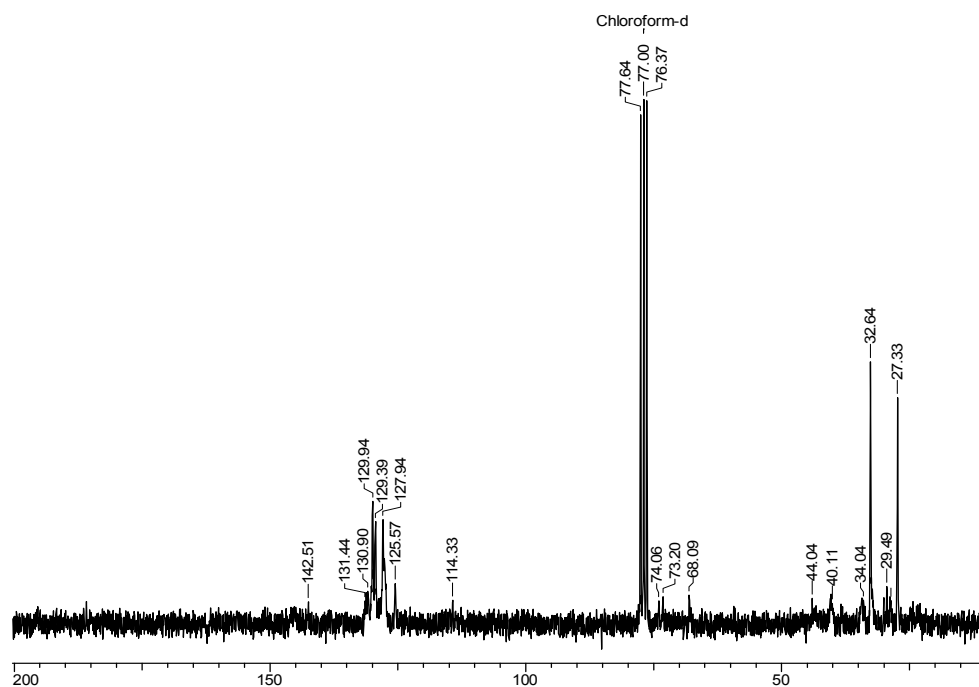
Figure 2.18 ^{13}C NMR DEPT of Mannose linked SBS
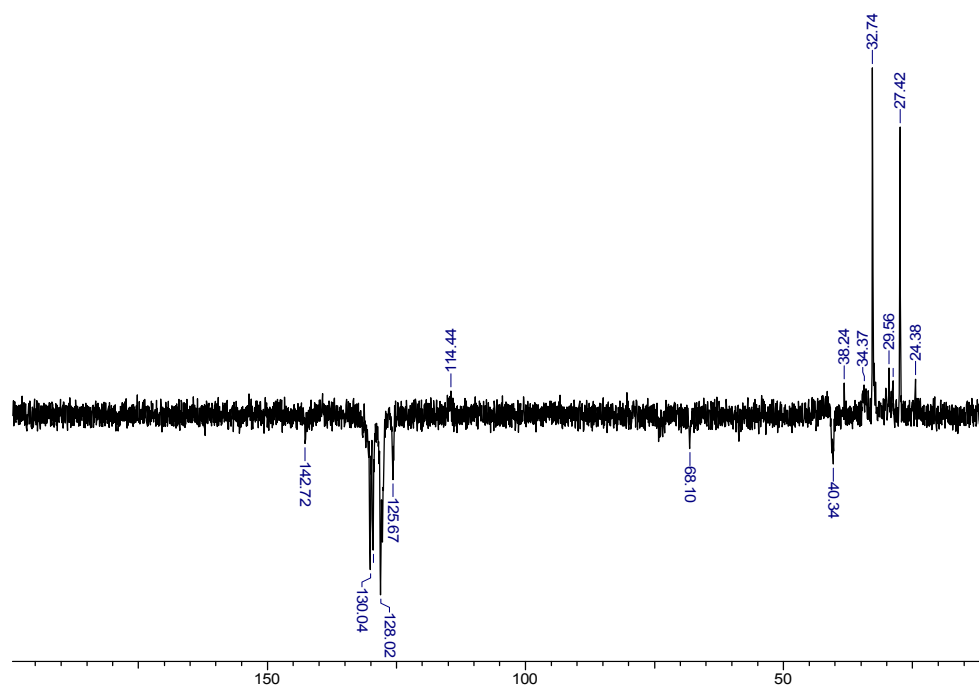
Figure 2.19 ^{13}C NMR DEPT of Mannose linked SBS

Similar results were obtained for SBS epoxide opening with galactose, maltose and xylose (FTIR and NMR data presented in appendix) Galactose linked SBS showed a 4.5% residual epoxide and the galactose content was 0.12 weight %. Similarly, maltose linked SBS had 8 % residual epoxide with maltose content of 0.37 weight%, while xylose linked SBS did not show any residual epoxide with xylose content of 0.16 weight%. This shows that among these sugar linked SBS samples, maltose linked SBS showed the highest sugar content.

Sucrose, Methyl glucoside and fructose reactions with epoxidized SBS under same reaction conditions lead to partial opening of epoxide ring, as observed from the NMR and FTIR spectra of these samples (FTIR and NMR spectra presented in appendix) which showed very high epoxide content. One reason for this may be the precipitation of the epoxidized SBS in the reaction mixture which was observed during the course of reaction. This may have lead to incomplete reaction even after continuing the reaction for 20 h, while glucose, mannose, galactose, maltose and xylose took only 5h for quantitative epoxide opening.

Our aim was to modify SBS with minute amount of sugar so as not to alter it physical and mechanical properties. Thus, with our present strategy we were successful in anchoring minute quantities of sugar ranging from 0.9-0.37 weight % as pendants on SBS along with the controlled introduction of chlorine and hydroxyl groups on the SBS back bone.

2.4.4 X-ray photoelectron spectroscopy study of the carbohydrate functionalized SBS containing sugar, quaternary nitrogen, chlorine and hydroxyl pendants

Absolute quantification of functional groups in a functionalized polymer is limited by the available diagnostic means. The typically employed detection techniques include photoelectron spectroscopy (XPS), secondary-ion mass spectrometry (SIMS) usually with time of flight (TOF) detection systems. By means of XPS measurements all chemical elements except hydrogen can be detected. XPS is of particular importance, since shifts in the electron binding energy caused by electronegative or positive bond partners permit to characterize the chemical neighborhood of an element.

Atomic composition of functionalized SBS

Atomic composition of the surfaces of sugar linked SBS films were examined by X-ray photoelectron spectroscopy (XPS).Analysis of the sugar functionalized SBS, confirmed the presence of nitrogen and chlorine along with carbon and oxygen. All binding energy (BE) were referenced to the C 1s hydrocarbon peak at 284.6 eV. However, since the product is homogeneous the surface and the bulk composition of the polymer film are same.

Table 2.1 provides the atomic composition of some representative samples examined by XPS.

Table 2.1 Surface composition (at %) of sugar linked SBS films by XPS

Sample	C	N	Cl	O
Galactose linked SBS	81.73	1.53	2.3	14.45
Galactose linked SB	81.03	1.68	1.86	15.43
Blank reaction (without sugar)	78.62	2.13	0.82	18.44

Figure 2.20- 2.31 shows comparison high resolution (HR) spectra of N1s, Cl (2p), O1s and C1s from the surfaces of sugar linked SBS consisting of hydro-chlorinated and quaternary nitrogen pendants.

2.4.4.1 XPS analysis of nitrogen in sugar linked SBS

Figure 2.20- 2.22 shows comparison high resolution (HR) spectra of N1s core level spectra of galactose and maltose linked SBS along with blank reaction product (without sugar).

Figure 2.20 N 1s HR spectrum of Galactose linked SBS

Table 2.2 N 1s peak parameters for Galactose linked SBS

Peak	Position (eV)	Area	FWHM (eV)	GL (%)
0	401.4	1275.87	2.500	32
1	399.9	3374.91	2.300	9
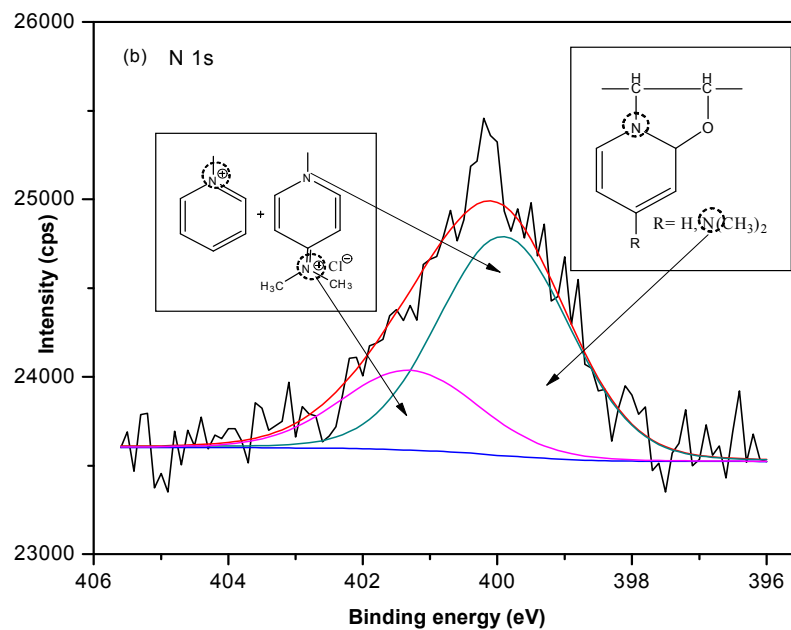
Figure 2.21 N 1s HR spectrum of Maltose linked SBS

Table 2.3 N 1s peak parameters for Maltose linked SBS

Peak	Position (eV)	Area	FWHM (eV)	GL (%)
0	401.3	1203.786	2.400	10
1	399.9	3167.398	2.300	10
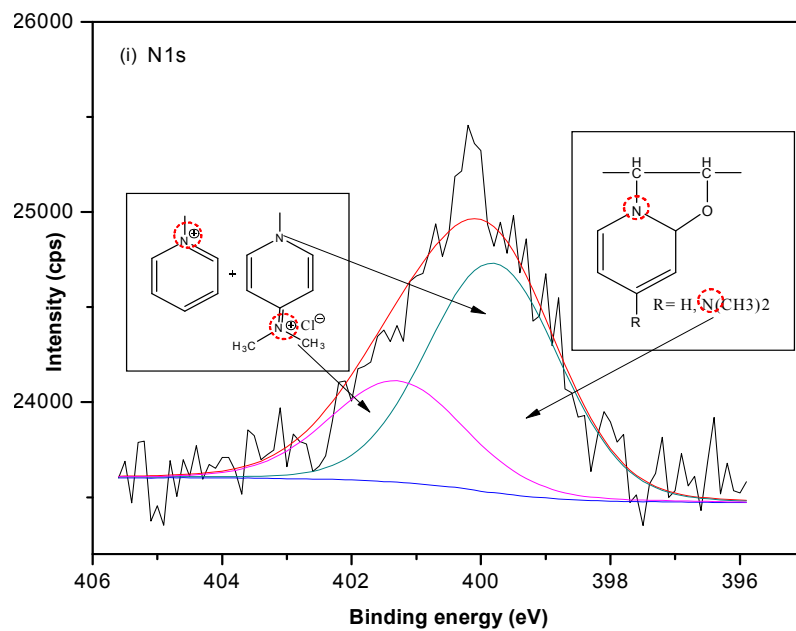
Figure 2.22 N 1s HR spectrum of blank reaction (without sugar)

Table 2.4 N 1s peak parameters for blank reaction

Peak	Position (eV)	Area	FWHM (eV)	GL (%)
0	401.3	1490.92	2.45	10
1	399.8	3200.90	2.40	10

N1s spectra for galactose and maltose linked SBS samples shows two component peaks at BEs 401.3 eV and 399.9 eV. The peak at 401.3 eV is assigned to the

quaternary nitrogen arising from the pyridinium [60] and peak at lower binding energy at 399.9 eV is attributable to amines and in this case a tertiary amine [60] whose structure is shown as insets in figures 2.20-2.22. N 1s spectrum for the blank reaction (reaction with all components except sugar) is shown in Figure 3. It also showed two component peaks at 401.3 eV and 399.8 eV corresponding to quaternary nitrogen and neutral nitrogen from amine.

XPS analysis throws light on the mechanism of reaction which leads to the formation of N- cation and neutral N pendants on SBS, under the reaction condition employed for the functionalization of SBS with sugars. It is known in literature that reaction of polymeric epoxides with pyridine and vinyl pyridines leads to the formation of a polymer having a pyridinium intermediate 2 [57]; the ring opened epoxide ion immediately attacks the α-position of the pyridine ring, forming a bicyclic 5 and 6 membered ring, **4**. In our case we get an additional side reaction; the chloride generated from the ammonium chloride present in the reaction mixture traps the pyridinium intermediate forming SBS linked pyridinium chloride. The presence of ionic chloride is proved by the Cl (2p) peak at 198.1 and 199.7 eV as detailed in the chlorine Cl 2p analysis section.
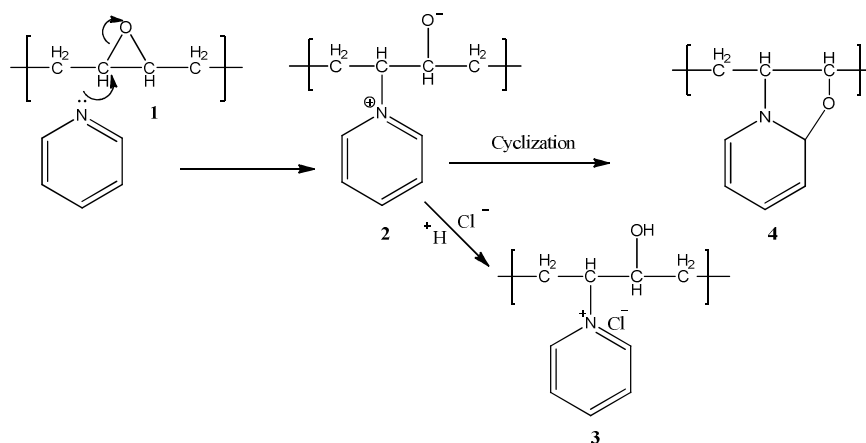
Reaction scheme 2.8. Mechanism of pyridine nucleophilic attack on SBS epoxide yielding pyridinium chloride and conjugated 3, 5 diene pendants on SBS

Presence of 3 in SBS polymer chain is proved by ^{1}H NMR (see discussion in the preceding sections of this chapter). This is only possible when some proportion of pyridinium intermediate 2 is trapped by chloride before the formation of bicyclic structure 4. Moreover, the conjugated 3, 5-diene can undergo rearrangement to a carbonyl containing pyridone, but here this possibility is ruled out since the pyridone peak which appears at about 400.6 eV is absent in the spectrum.

The HR N1s spectrum confirms this mechanism which indeed shows two peaks, one corresponding to quaternary-N and other corresponding to tertiary amine as discussed in the preceding paragraph. These observations are consistent with the formation of quaternary pyridinium salt, as schematically shown in reaction scheme 2.9. All these facts taken together establish the existence of pyridinium ionomer pendant in the carbohydrate functionalized SBS.
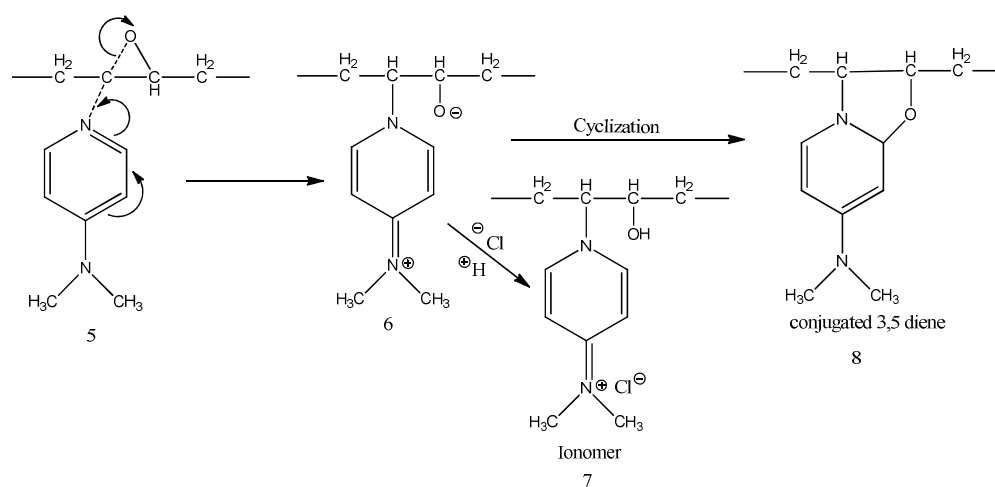
Reaction Scheme 2.9 Mechanism of DMAP nucleophilic attack on SBS epoxide

Further, N, N-DMAP is a known initiator for homo-polymerization of polymeric epoxides to polyether [61]. It seems that DMAP present in our reaction system initiates the SBS epoxide opening, since one important visible characteristic for this reaction is the appearance brown colour as soon as the reaction start and this becomes intense brown with progress of reaction. This fact was also observed by William et al. for epoxy homo-polymerization of PGE and DGEBA using DMAP.

 The effectiveness of DMAP in epoxide ring opening is due to the presence of resonance structure with a negative charge placed on the N of the pyridine ring and a positive charge placed on the tertiary amine nitrogen. This structure is responsible for the fast nucleophilic attack on the epoxide ring; a brown colour develops within 10 min of addition of DMAP. Again, the quaternary-N intermediate 6 formed by the reaction of DMAP with SBS epoxide is trapped by chloride forming quaternary chloride **7** or the intermediate undergoes cyclization to bicyclic 5 and 6 membered ring, **8** as shown in reaction scheme 2.9. XPS analysis show that both the processes takes place simultaneously; this is proved by two component peak at 401.3 eV in the HR N 1s XPS spectrum.

Thus the peak at 401.3 eV assigned to quaternary N can originate from pyridinium (structure 2 in reaction scheme 2.8) or quaternary nitrogen (structure 7 in reaction scheme 2.9) and in fact both these species co-exist in the product as discussed above and contribute to this peak. The other peak at 399.9 eV assigned to amine, originates from the tertiary nitrogen of bicyclic 5 and 6 membered ring 4, 8 as shown in reaction scheme 2.8 and 2.9.

Taking all the above facts into consideration, we propose that formation of SBS ionomer proceeds with the formation of a quaternary N followed by cyclization to

a bicyclic conjugated diene 4 & 8. When halide source is present in the reaction mixture, few percent of quaternization occur leading to quaternary halide 3 & 7.

The nitrogen content on the surface (given in atomic percent, at. %) and the contribution of different nitrogen species to the N 1s peak (given as percentage) is presented in Table 5.

Table 2.5 Surface Nitrogen content in sugar linked SBS and the contribution of the nitrogen species to the N 1s peak

Sample	Nitrogen Content (at. %)	Contribution of nitrogen species to the N 1s peak (%)	
		Quaternary N$^+$	Neutral N
Galactose linked SBS	1.53	27.4	72.6
Maltose Linked SBS	1.68	27.5	72.5
Blank reaction (without sugar)	2.13	31.8	67.2
Reaction without DMAP	Only 5% epoxide opening; nitrogen species undetectable		

The data presented in Table 2.5 shows that nitrogen content of Maltose linked SBS is slightly higher than Galactose linked SBS. Relative quantities of surface nitrogen contributing groups as relative percentage of N 1s peak is presented in Table 1 for the sugar linked SBS. Analysis of the N 1s peak confirms the presence of two types of nitrogen groups. Nitrogen is present mainly in the form of bicyclic 5 and 6 membered ring and quaternary N is just around 27.5 % of the total nitrogen content.

 Nitrogen content of the blank reaction done with all the reagents (epoxidized SBS, pyridine, DMAP and ammonium chloride) except sugars is around 30% higher as compared to the reaction where all reagents including sugar are present leading to sugar linked SBS. This may be due the fact that DMAP is known activator of sugar hydroxyl towards nucleophilic addition reaction (as discussed in NMR section). Thus when sugar is also present in the reaction mixture it offers some competition to nitrogen group generating species from the epoxide opening, hence giving less nitrogen content in the final product. Whereas, in the absence of sugar; there is no such competition resulting in higher nitrogen content.

Its noteworthy that in the absence of DMAP around 5% epoxide opening (confirmed from NMR) takes place without any change in colour of reaction mixture, whereas 10 mol% (relative to epoxide functionality) of DMAP induces colour change to dark brown within few minutes of reaction and leads to a quantitative epoxide ring opening.

In summary, all these facts suggest that indeed DMAP initiates the epoxide ring opening and being a stronger nucleophile than both pyridine and sugar hydroxyl; few DMAP molecules gets added to SBS main chain.

2.4.4.2 XPS analysis of chlorine in sugar linked SBS

Figure 2.23-2.25 shows comparison of high resolution (HR) spectra of Cl 2p core level spectra of galactose and maltose linked SBS along with blank reaction product (without sugar).
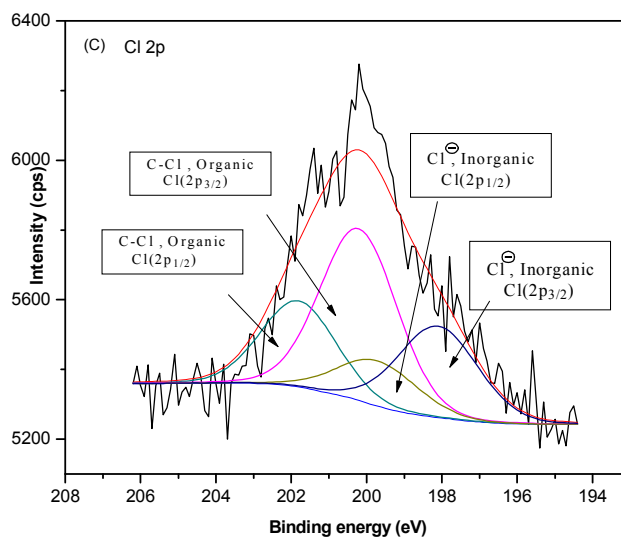
Figure 2.23 Cl (2p) HR spectrum of Galactose linked SBS

Table2.6 Cl 2p peak parameters for Galactose linked SBS

Peak	Position (eV)	Area	FWHM (eV)	GL (%)
0	201.8	652.6	2.35	12
1	200.2	1312.6	2.4	9
2	199.7	361.5	2.5	10
3	198.1	728.5	2.5	9

For chlorine atoms, it has been shown that Cl (2p) spectra can be used to differentiate between organically bound chlorine and inorganic chloride. The high

resolution XPS spectrum of Cl (2p) core level consists of two pairs of spin-orbit split doublets, Cl ($2p_{3/2}$) and Cl ($2p_{1/2}$). Normally, the Cl ($2p_{3/2}$) peak from organo-chlorine is slightly above 200eV while the Cl ($2p_{3/2}$) from inorganic chloride is below 200 eV, usually between 198 eV to 199 eV [62-63]. The Cl ($2p_{1/2}$) peak is also present and is also useful in distinguishing between organically bound chlorine from inorganic chloride.
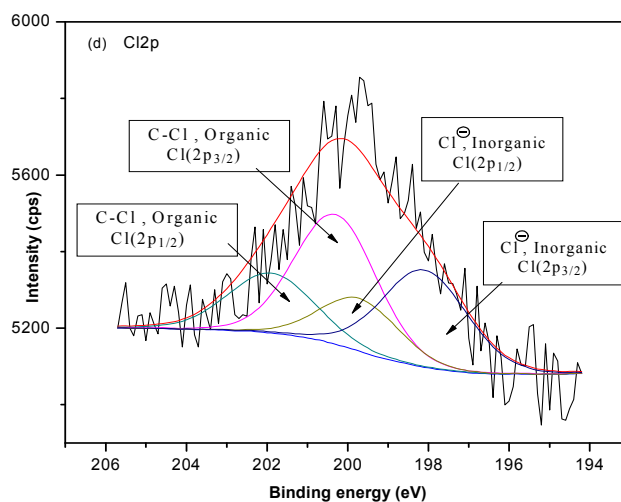
Figure 2.24 Cl (2p) HR spectrum of Maltose linked SBS

Table 2.7 Cl 2p peak parameters for Maltose linked SBS

Peak	Position (eV)	Area	FWHM (eV)	GL (%)
0	201.9	446.5	2.5	15
1	200.3	903.5	2.4	9
2	199.7	352.944	2.30	10
3	198.1	705.600	2.48	11
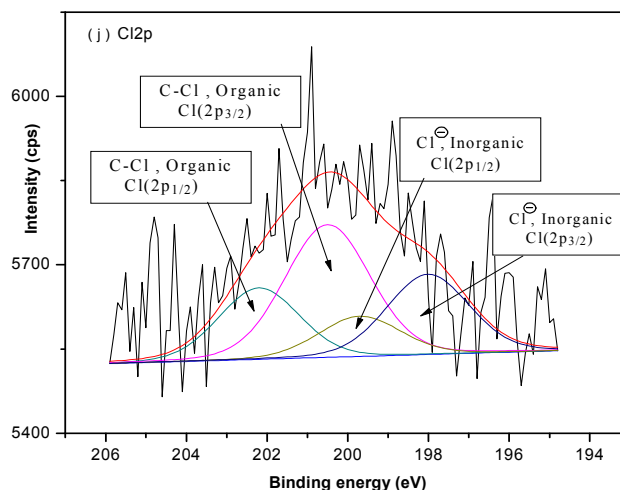
Figure 2.25 Cl (2p) HR spectrum of blank reaction (without sugar)

Table 2.8 Cl 2p peak parameters for blank reaction (without sugar)

Peak	Position (eV)	Area	FWHM (eV)	GL (%)
0	202.2	336.071	2.35	12
1	200.5	673.904	2.50	15
2	199.7	195.604	2.40	15
3	198.0	390.200	2.40	15

A high resolution spectrum of the Cl (2p) shown in figure 2.23-2.25 is deconvoluted into Cl ($2p_{1/2}$) and Cl ($2p_{3/2}$) peaks by a curve fit routine. The Cl ($2p_{3/2}$) located at BE 200.2 eV and Cl ($2p_{1/2}$) at BE 201.8 eV, indicates the presence of C-Cl bond which comes from the covalently linked chlorine in the hydro-chlorinated segment of SBS. The Cl ($2p_{3/2}$) at BE 198.1 eV and Cl ($2p_{1/2}$) at BE 199.7 eV confirm the presence of ionic chloride. This originates from the ionic chloride bound to quaternary nitrogen pendants on SBS. Calculating the integration areas

of these two Cl (2p) doublets using XPS peak software, it can be estimated that ratio of Cl/Cl$^-$ is about 1.8 in the case of Galactose linked SBS.

Table 2.9 Surface Chlorine content in sugar linked SBS and the contribution of the chlorine species to the Cl (2p) peak

Sample	Chlorine Content (at. %)	Contribution of chlorine species to the Cl (2p) peak (%)	
		Cl$^-$	Cl
Galactose linked SBS	2.3	35.7	64.3
Maltose Linked SBS	1.86	44.0	56.0
Blank reaction (without sugar)	0.86	36.7	63.3
Reaction without DMAP	Only 5% epoxide opening; nitrogen species undetectable		

 In summary, the sugar functionalized SBS contains clearly distinguishable, both organic chlorine and inorganic chloride. The HR spectrum of Cl (2p) and N(1s) peaks clearly establish and proves the formation of ionomer segments in SBS consisting of quaternary nitrogen pendants attached to the butadiene segment of the SBS main chain, during the course of functionalization of SBS with sugars.

2.4.4.3 XPS analysis of oxygen in sugar linked SBS

Figure 2.26- 2.28 shows comparison of high resolution (HR) spectra of O1s core level spectra of galactose and maltose linked SBS along with blank reaction product (without sugar).
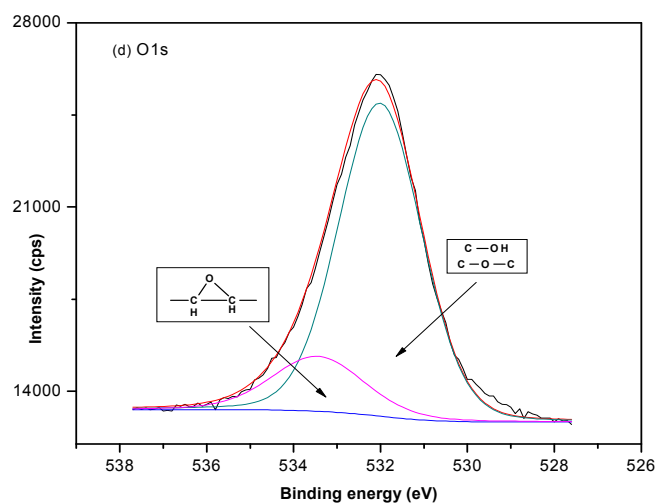
Figure 2.26 O 1s HR spectrum of Galactose linked SBS

Table 2.10 O 1s peak parameters for Galactose linked SBS

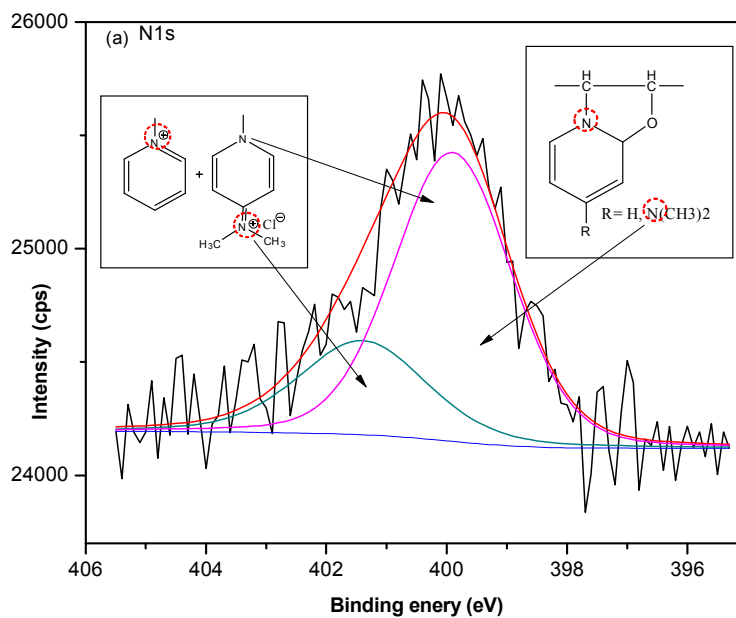| Peak	Position (eV)	Area	FWHM (eV)	GL (%)
0	532	29985.340	2.250	11
1	533.45	6129.890	2.500	22
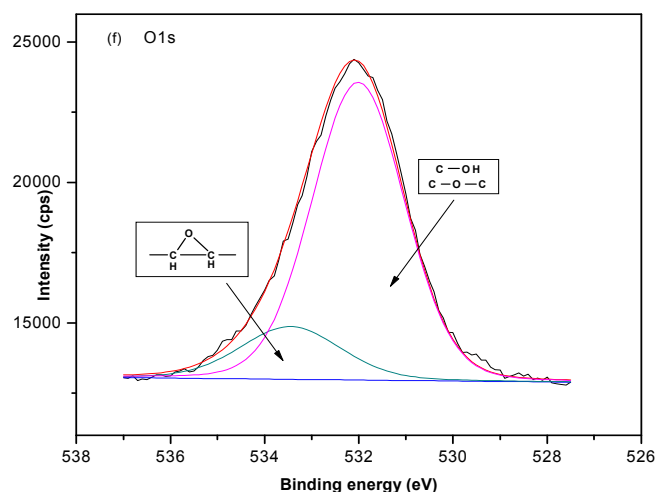
Figure 2.27 O 1s HR spectrum of Maltose linked SBS

Table 2.11 O 1s peak parameters for Maltose linked SBS

Peak	Position (eV)	Area	FWHM (eV)	GL (%)
0	532	27315.880	2.3	10
1	533.45	5433.000	2.5	18

The high resolution O 1s spectrum shown in figures 2.26-2.28 was deconvoluted to give two peaks centered on 532 eV and 533.45 eV. The 532 eV peak can be assigned to C-$\underline{O}$H and C-**O**-C [64]. C-OH originates from hydroxyl groups generated by the epoxide ring opening as well contribution from the sugar hydroxyl groups linked to SBS backbone, while C-O-C ether linkage originates from the sugar linked SBS and also from cyclization of the quaternary nitrogen as shown in reaction scheme1. The 533.45 eV peak is assigned to the residual epoxide-oxygen remaining unreacted. In the case of blank reaction binding energies are shifted slightly to the lower side which may be due a change in chemical environment due to the absence of attached sugar on SBS.
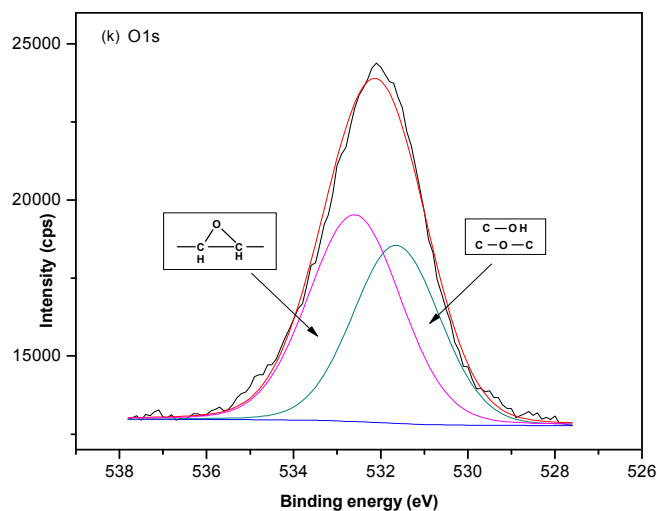
Figure 2.28 O 1s HR spectrum of blank reaction (without sugar)

Table 2.12 O 1s peak parameters for blank reaction (without sugar)

Peak	Position (eV)	Area	FWHM (eV)	GL (%)
0	531.85	22806.120	2.17	9
1	533.15	11003.500	2.50	17

Table 2.13 Surface Oxygen content in sugar linked SBS and the contribution of oxygen species to the O 1s peak

Sample	Oxygen Content (at. %)	Contribution of Oxygen species to the O 1s peak (%)	
		Epoxide	*C-OH, C-O-C*
Galactose linked SBS	14.45	17.0	83.0
Maltose Linked SBS	15.43	16.5	83.5
Blank reaction	18.44	32.5	67.5

(without sugar)			
Reaction without DMAP	Only 5% epoxide opening; nitrogen species undetectable		

The data presented in Table 2.13 shows that both the Galactose and Maltose linked SBS have similar residual epoxide content, while in the blank reaction the residual epoxide content is almost double. This is also reflected in ^{1}H NMR analysis of these polymers discussed in the NMR analysis section of this chapter which supports these observations. Partial epoxide opening (50%) in the absence of sugar suggests that presence of sugar speeds up the reaction and this is possible only when it itself is involved in the nucleophilic attack on the epoxide ring. DMAP is known to activate sugar hydroxyl as discussed earlier in the nitrogen section of this XPS analysis, so it can be safely concluded that sugar is also participating in the epoxide ring opening thereby getting linked to the SBS main chain, as evidenced by quantitative (<90%) epoxide opening (as calculated by ^{1}H NMR integration), as compared to 57 % epoxide ring opening when sugar is absent.

2.4.4.4 XPS analysis of carbon in sugar linked SBS

The high resolution C 1s spectrums of sugar linked SBS and a blank reaction (without sugar) are shown in figures 2.29-2.31.

The C 1s peaks are centered at 284.6 eV and these peaks were not deconvoluted as the functionalized SBS has many carbon linked groups making curve fitting complicated. The binding energies are also very close and overlaps, hence it will not provide precise information about the chemical environment. Moreover the

samples are exposed to air prior to XPS analysis it may not necessarily reflect the true chemical environment. Hence, we choose not to deconvulate the C 1s peaks.
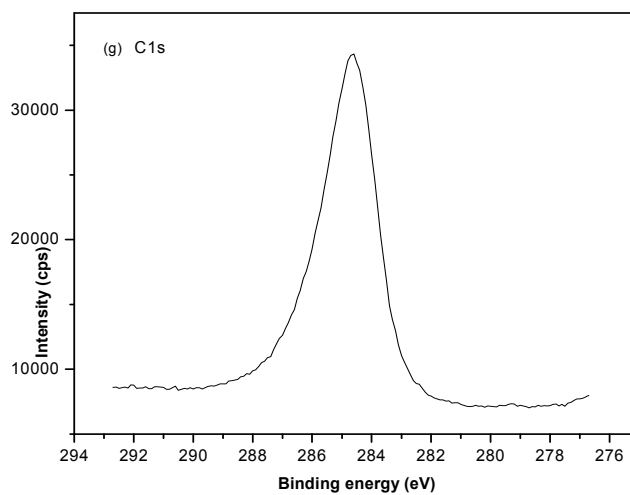
Figure 2.29 C1s HR spectrum of Galactose linked SBS
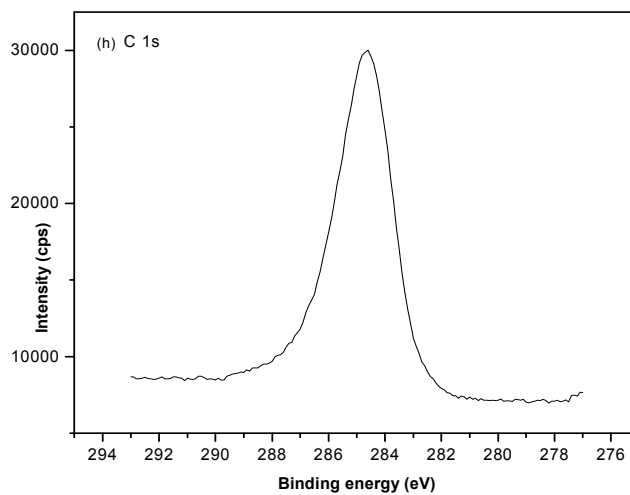
Figure 2.30 C 1s HR spectrum of Maltose linked SBS
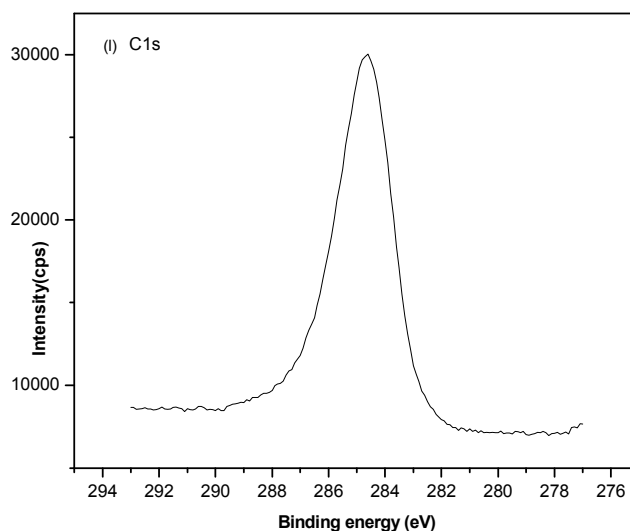
Figure 2.31 C1s HR spectrum of blank reaction (without sugar)

Thus, XPS has provided convincing information regarding the mechanism of formation of quaternary nitrogen and conjugated N-6 3, 5 diene, along with their relative composition which is crucial for explaining the antimicrobial and biocompatibility behavior observed for the functionalized and sugar linked SBS. It has also provided information about the chemical bonding state of chlorine and thus helped in establishing the origin of organic and inorganic chlorine besides the formation of ionomer segments. It also established and supported the finding from ^{1}H NMR analysis of hydro-chlorination of epoxide taking place. This is the first time that quantitative estimates of all possible moieties on an unsaturated olefinic polymer like SBS has been demonstrated using a combination of tools such as FTIR, NMR, XPS and phenol sulphuric acid assay.

 In conclusion we can say that XPS analysis proved to be an invaluable technique which provided a deep insight about the mechanism of the ring opening of partially epoxidized SBS, the intermediates involved and the functional groups thus generated on the SBS chains.

2.5. Conclusion

In conclusion, we can say that we successfully synthesized different sugar linked SBS by epoxide ring opening of partially epoxidized SBS, in the presence of 4-DMAP and ammonium chloride. The sugar content of the functionalized SBS ranged from 0.09-0.37 weight %, fulfilling our objective of modifying SBS with minute quantities of sugar molecules so as to study the effect in enhancement of properties like biocompatibility and biodegradability without compromising the physical properties of the elastomer. We further observed that efficient opening of epoxide ring took place (>90%), only when sugar is present in the reaction mixture. Presence of pyridine in the reaction media caused side reaction leading to quaternary nitrogen pendants on the SBS back bone. The mechanism for formation of sugar, chlorine and quaternary N pendants was established using NMR and XPS analysis. This is perhaps the first report on opening of epoxide ring with unprotected sugar molecules. The sugar linked SBS can have potential biomedical and other niche applications as discussed in later chapters.

2.6. References:

1. R. M Ikeda, M. L Wallach, R. J. Angelo, *Polym. Preprints Am. Chem. Soc.* **1969**, 10, 1445

2. J. F. Masson, S. B. Perc, A. Delgado, *Journal of Polymer Science: Part B: Polymer Physics* 2005, 43, 276–279

3. H. T. Ban, *Macromolecules* **2006**, 39, 171-176

4. J. M. Yang, H. T. Lin, W. C. Lai, *Journal of Membrane Science* **2002**, 208, 105-117

5. M. M. Jacobi, M. V. Braum, T. L. A. C. Rocha, R. H. Schuster, *KGK Kautschuk Gummi Kunststoffe* **2007**, 60, 460-466

6. O. Hayashi, K. Kanda, Y. Matsumoto, *Kobunshi Ronbunshu* **1986**, 43, 385-388

7. V. P. Kirpichev, A. I. Yakubchik, *Polymer Science U.S.S.R.* **1969**, 11, 2610-2617

8. H. N. Nae, *Reactive polymers. Ion exchangers, sorbents* **1986**, 6, 336

9. V. P. Kirpichev, A. I. Yakubchik, G. N Maglysh, *Rubber Chemistry and Technology* **1970**, 43, 1225-1229

10. M. I. Abdullin et al., *Russian Journal of Applied Chemistry* **2006**, 79, 1306-1311

11. Alvarez, H. Bertorello, M. Strumia, *Journal of Applied Polymer Science* **1992**, 45, 25-27

12. C. Alvarez, M. Strumia, H. Bertorello, *Polymer Bulletin* **1988**, 19, 521-526

13. R. A. Gross, A. Kumar, B. Kalra, *Chemical Reviews* **2001**, 101, 2097–2124

14. D. Page, R. Roy, Glycoconj. J. **1997**, 14, 345

15. Y. C. Lee, R. T. Lee, *Acc. Chem. Res.* **1995**, 28, 321

16. Y. Miura, T. Ikeda, K. Kobayashi, *Biomacromolecules* **2003**, 4, 410–415

17. Y. Miura, T. Ikeda, N. Wada, H. Sato, K. Kobayashi, *Green Chemistry* **2003**, 5, 610–614

18. Y. C. Lee, R. T. Lee, *Neoglycoconjugates: Preparation and Applications* **1994**, Academic Press: San Diego, CA

19. N.V. Bovin, *Glycoconj. J.* **1998**, 15, 431

20. S.K. Choi, G. M. Whitesides, *J. Am. Chem. Soc. 1997,* 119, 4103

21. A. Kussrow et al., *Analytical Chemistry* **2009**, 81, 4889-4897

22. D. Appelhans et al., *Biomacromolecules* **2009**, 10, 1114-1124

23. L. Nurmi, J. Lindqvist, R. Randev, J. Syrett, D. M. Haddleton, *Chemical Communications* **2009**, 2727-2729

24. D. Roy, J. N. Cambre, B. S. Sumerlin, *Chemical Communications* **2008**, 2477-2479

25. T. Taniguchi et al., *Colloids and Surfaces B: Biointerfaces* **2009**, 71, 194-199

26. M. T. Barros, K. T. Petrova, *European Polymer Journal* **2009**, 45, 295-301

27. M. Dhayal, D. M. Ratner, *Langmuir* **2009**, 25, 2181-2187

28. H. Abe, D. Murayama, F. Kayamori, M. Inouye, *Macromolecules* **2008**, 41, 6903-6909

29. R. L. Phillips et al., *Macromolecules* **2008**, 41, 7316-7320

30. N. Y. Xiao, A. L. Li, H. Liang, J. A. Lu, *Macromolecules* **2008**, 41, 2374-2380

31. D. Cummins, et al., *Soft Matter* **2009**, 5, 804-811

32. B. Okutucu, A. Telefoncu, *Talanta* **2009**, 78, 1190-1193

33. C. Perrino, S. Lee, N. D. Spencer, *Tribology Letters* **2009**, 33, 83-96

34. R. A. Green, N. H. Lovell, L. A. Poole-Warren, *Biomaterials* **2009**, **30**, 3637-3644

35. B. Li, J. M. Davidson, S. A. Guelcher, *Biomaterials* **2009**, 30, 3486-3494

36. K. T. Wiss, O. D. Krishna, P. J. Roth, K. L. Kiick, P. Theato, *Macromolecules* **2009**, 42, 3860-3863

37. Y. Q. Huang et al., *Biosensors and Bioelectronics* **2009**, 24, 2973-2978

38. Y. Matsumura, K. Kataoka, *Cancer science* **2009,**100, 572-579

39. M. Stevanovia, D. Uskokovia, *Current Nanoscience* **2009**, 5, 1-14

40. X. Gao, et al., *Journal of Controlled Release* **2009**, 137, 38-45

41. B. Lu, et al., *Journal of Controlled Release* **2009**, 137, 54-62

42. P. Galgali, A. J. Varma, U. S. Puntambekar, D. V. Gokhale, *Chem.comm.* **2002**, 2884-2885

43. K. Udipi, *Journal of Applied Polymer Science* **1979**, 23, 3301-3309

44. S. M. Wang, R. C. C. Tsiang, *Journal of Polymer Science Part A: Polymer Chemistry* **1996**, 34, 1483-1491

45. H. Q. Xie, W. G. Yu, G. Y. Liao, W. Yang, D. Xie, *Journal of Elastomer & Plastics* **2007, 3**9, 317

46. H. Q. Xie, W. G. Yu, D. Xie, D. T. Tian, *Journal of Macromolecular Science Part A* **2007**, 44, 849- 855

47. H. Q. Xie, W. Zhao, D. T. Tian, D. Xie, *Journal of Macromolecular Science Part A* **2008,** 45, 2, 151- 158

48. H. Q. Xie, Y. Chen, J. G. Guan, D. Xie, *Journal of Applied Polymer Science* **2006,** 99, 4, 1975-1980

49. M. W. C. Robinson, A. M. Davies, I. Mabbet, D. C. Apperley, S. H. Taylor, A. E. Graham, *Journal of Molecular Catalysis A: Chemical* **2009**, 314, 10

50. D. Derouet, J.C. Brosse, A. Challioui, *Eur. Polym. J.* **2001**, 37, 1327

51. R. V. Gemmer, M. A. Golub, *Journal of Polymer Science : Polymer chemistry edition* **1978,** 16, 2985-2990

52. A. E. Ciolino, O.I. Pieroni, B. M. Vuano, M. A. Villar, E. M. Valles, *Journal of Polymer Science Part A: Polymer Chemistry* **2004**, 42, 2920

53. M. Bruzzone, A. Carbonaro, *Journal of Polymer Science: Polymer Chemistry Edition* **1985**, 23, 139-157

54. J. E White, H.C. Silvis, D. J. Brennan, M. N. Mang, *ACS Symp. Ser.* **2000**, 755, 132

55. J. A. Schomaker, J. E White, A. P. Haag, H. Q. Pham, *US Patent 5401814*, **1995**

56. W. N. E. van Dijik- Wolthuis, O. Franssen, H. Talsma, M.J. van Steenbergen, J. J. Kettenes-van den Bosch, W. E. Hennink, *Macromolecules* **1995**, 28, 6317-6322

57. G. Xue, H. Ishida, J. L. Koenig, *Die Angewandte Makromolekulare Chemie* **1986**, 142, 17-27

58. S. Kar, P.K. Maji, A. K. Bhowmick, *J. Mater. Sci.* **2010,** 45, 64-73

59. M. Dubois, K. A. Gilles, J. K. Hamilton, P. A. Rebers, F. Smith, *Anal. Chem.* **1956**, 28, 350-356

60. R. Pietrzak, H. Wachowska, Piotr Nowicki, *Energy & fuels*, **2006**, 20, 1275-1280

61. I. E. Dell Erba, R. J. J. Williams, *Polym. Eng. Sci.* **2006**, 46,351

62. D. W. Reeve, Z. Tan, *Journal of Wood Chemistry and Technology* **1998**, 18, 417-426

63. S.P. Shi, L. F. Zhang, J. Zhu, W. Zhang, Z. P. Cheng, X. L. Zhu, *eXpress polymer Letters* **2009**, 3, 401-412

64. G. P. Lopez, D. G. Castner, B. D. Ratner, *Surface and Interface analysis* **1991**, 17, 267-272

2.7. Appendix 1.1 *Reaction schemes for carbohydrate functionalized SBS*
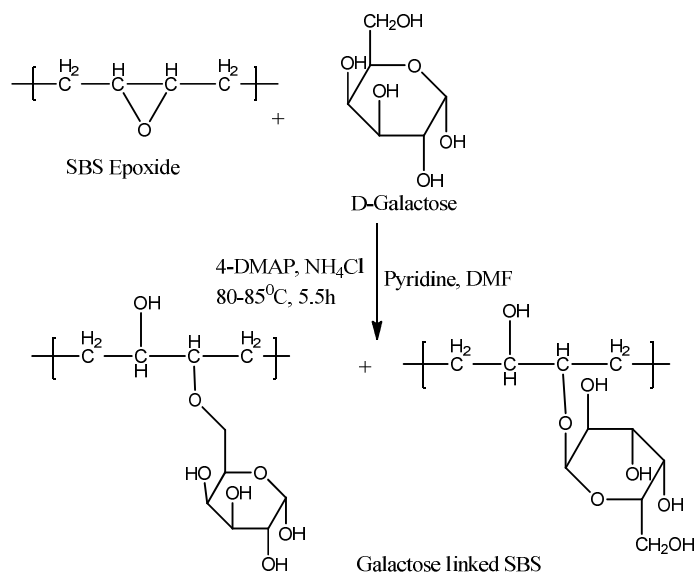
Reaction scheme 2.10 Galactose functionalized SBS
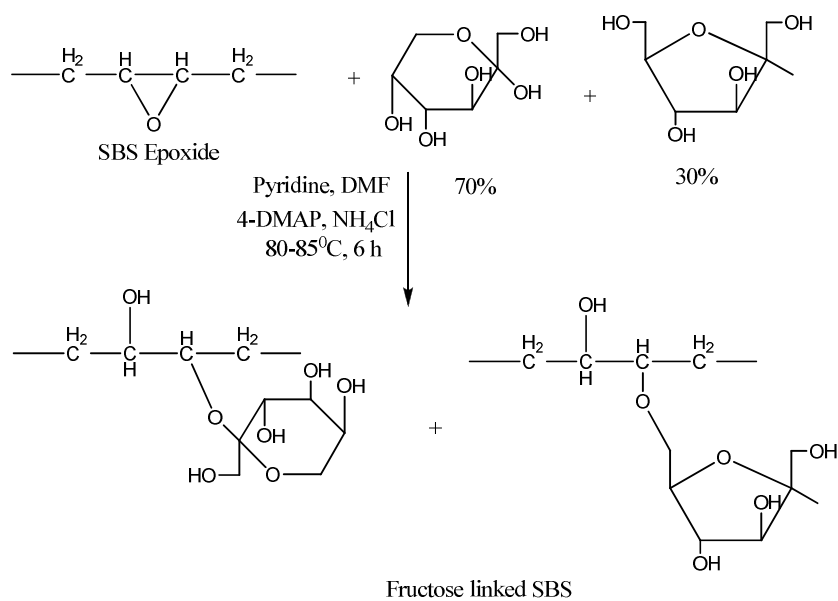
Reaction scheme 2.11 Fructose functionalized SBS
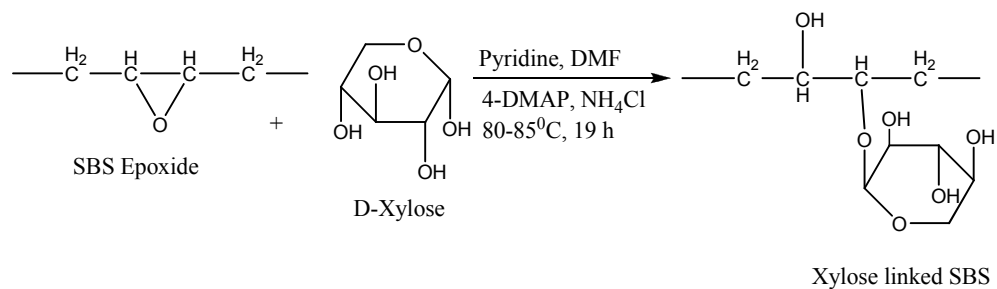
Reaction scheme 2.12 Xylose functionalized SBS
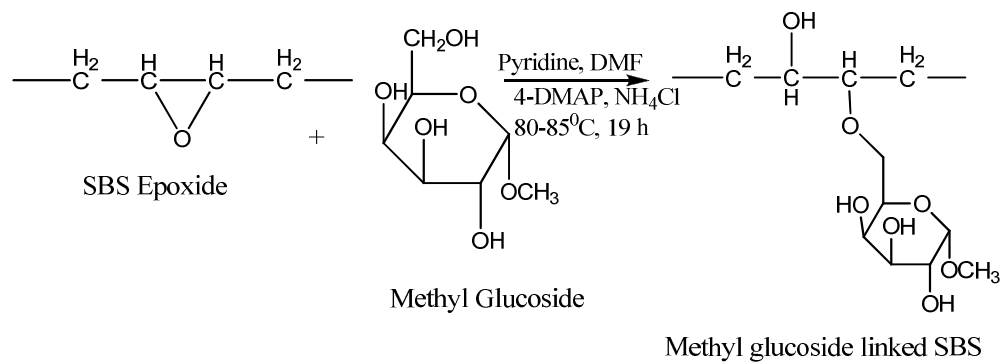
Reaction scheme 2.13 Methyl glucoside functionalized SBS
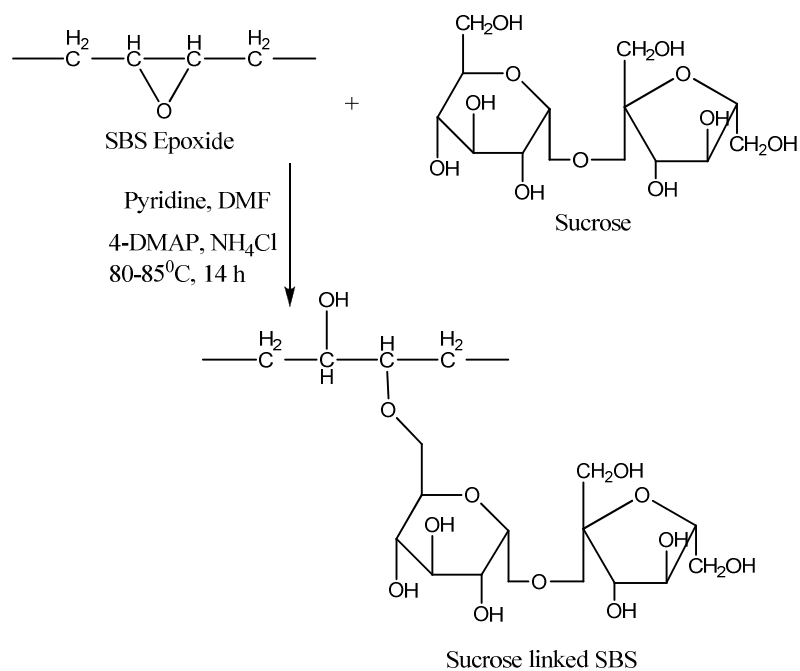
Reaction scheme 2.14 Sucrose functionalized SBS
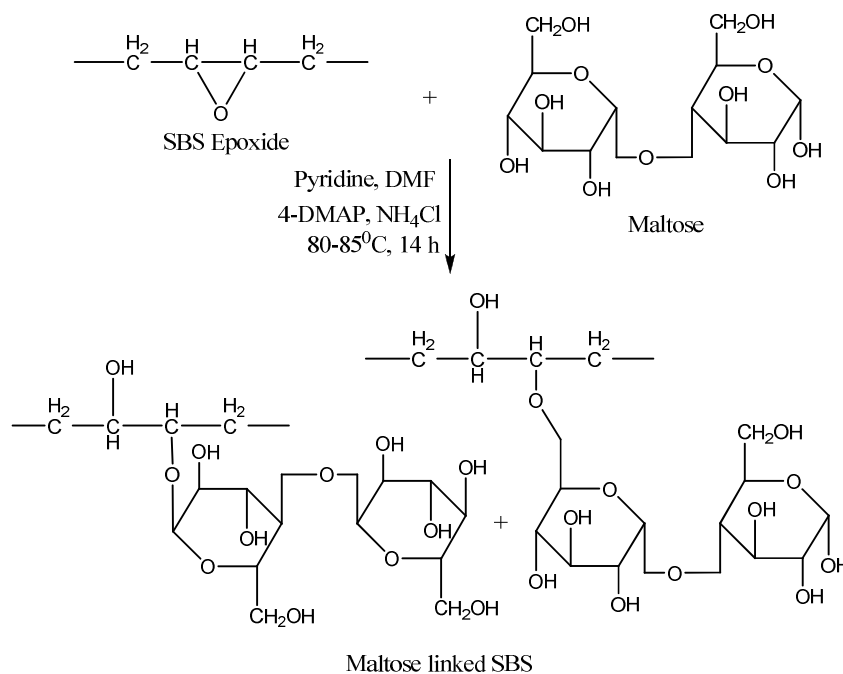
Reaction scheme 2.15 Maltose functionalized SBS

2.8. Appendix 1.2:^{1}H NMR of carbohydrate functionalized SBS
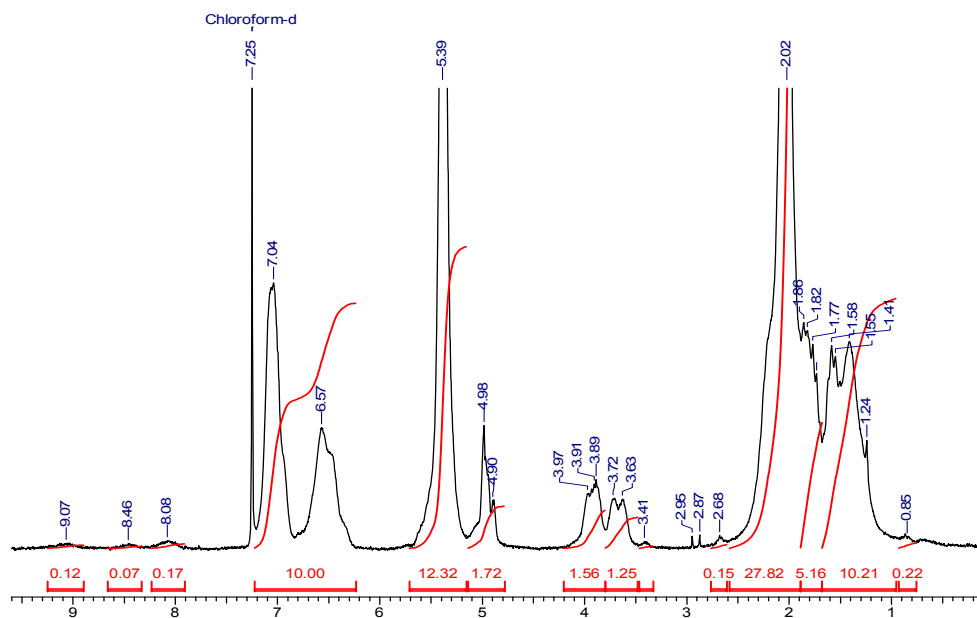
Figure 2.32 ^{1}H NMR of Galactose linked SBS
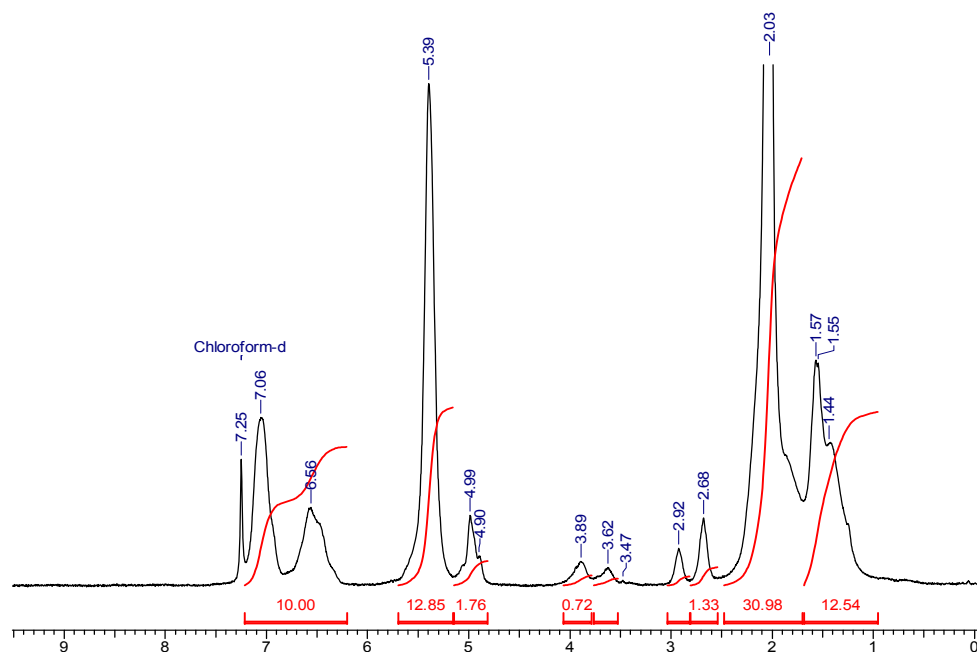
Figure 2.33 ^{1}H NMR of Fructose linked SBS
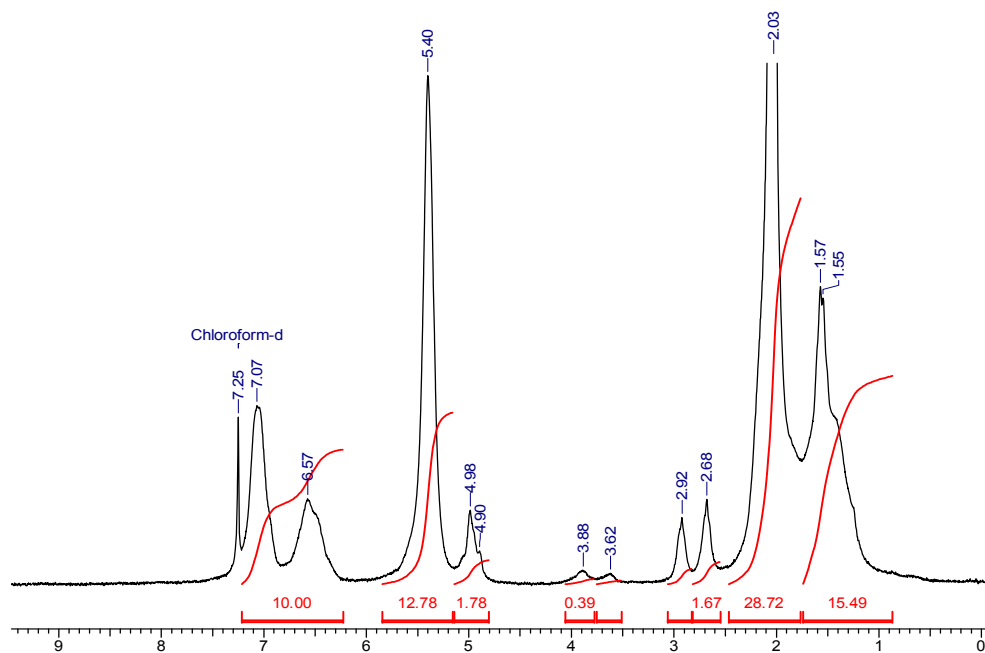
Figure 2.34 ^{1}H NMR of Methyl Glucoside linked SBS
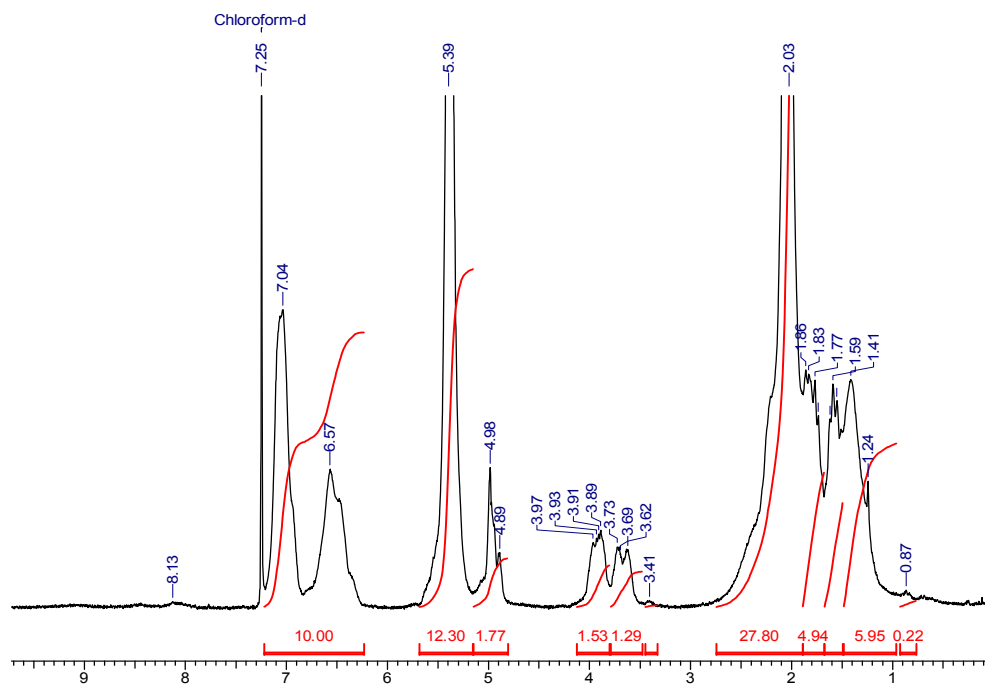
Figure 2.35 ^{1}H NMR of Xylose linked SBS
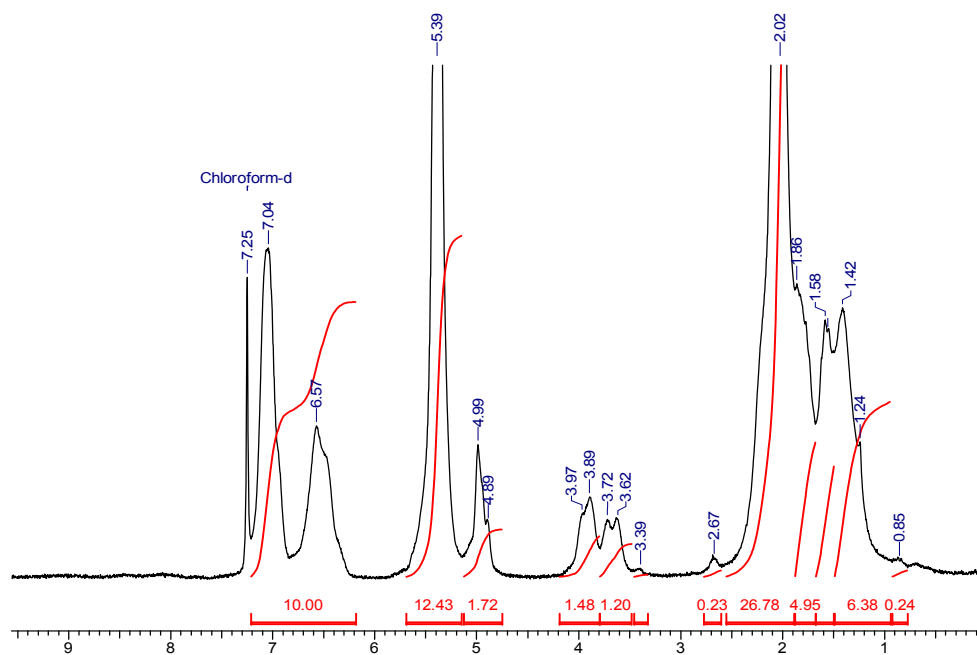
Figure 2.36 ^{1}H NMR of Maltose linked SBS

2.9. Appendix 1.3: FTIR of carbohydrate functionalized SBS
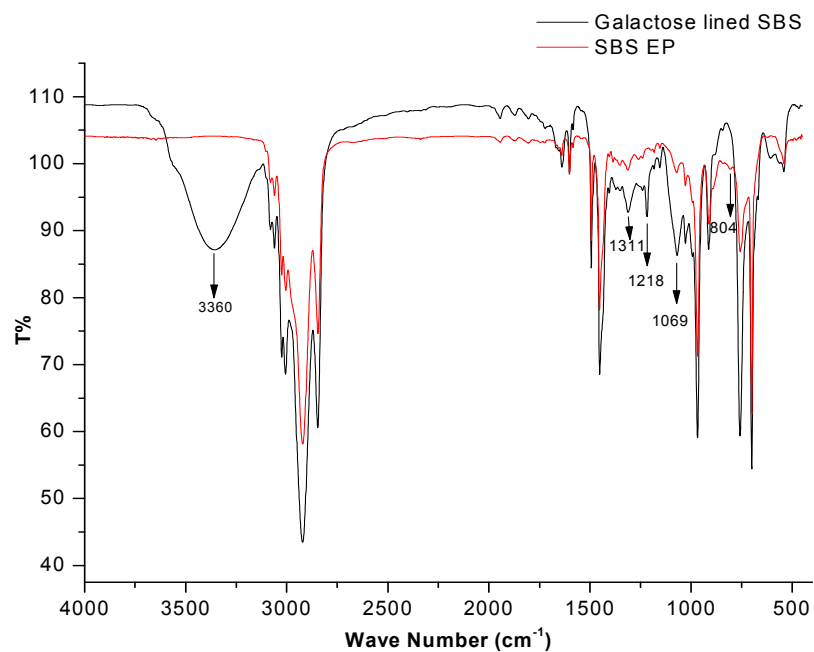
Figure 2.37 FTIR spectra of Galactose linked SBS
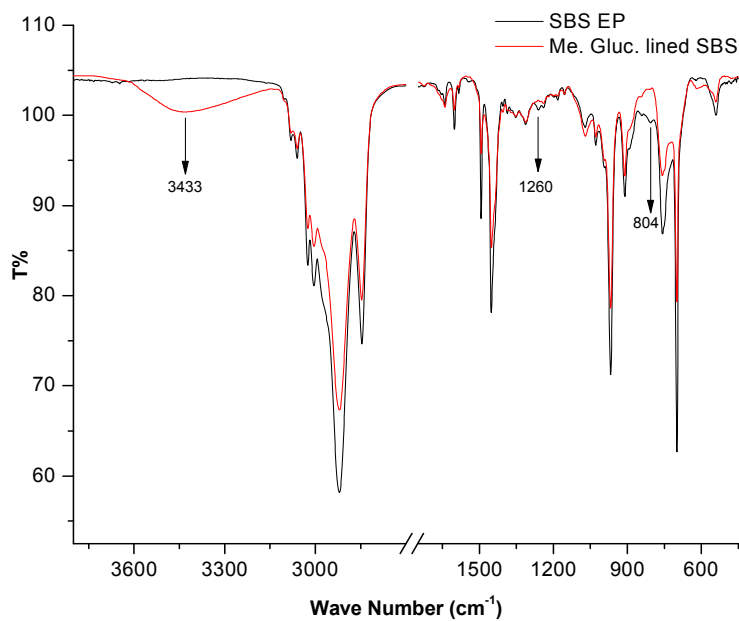
Figure 2.38 FTIR spectra of methyl glycoside linked SBS
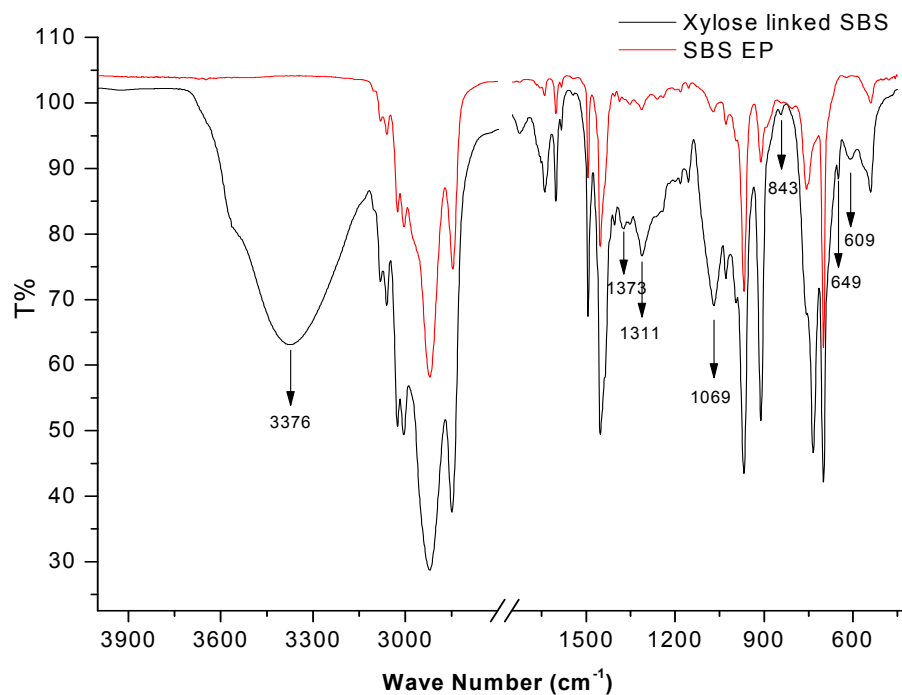
Figure 2.39 FTIR spectra of Xylose linked SBS
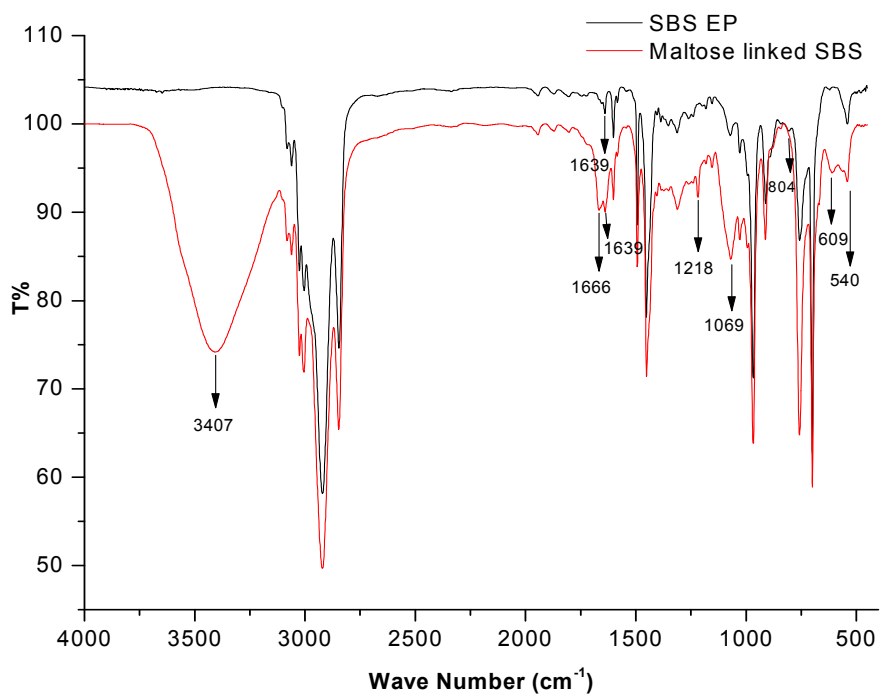
Figure 2.40 FTIR spectra of Maltose linked SBS along with SBS epoxide

2.10. Appendix 1.4: GPC analysis of SBS and epoxidized SBS

Table 2.14 GPC analysis of SBS and epoxidized SBS

Sample	M_w	M_n	M_w/ M_n (PDI)
SBS	148,862	134,906	1.103
Epoxidized SBS	181,427	160,452	1.131

PDI: poly dispersity index

The epoxidized SBS shows comparable PDI to that of SBS with increase of molecular weight, which is expected after epoxidation of SBS. Both the SBS and epoxidized SBS have similar PDI values indicating that there has not been any chain scission or cross linking during epoxidation process.
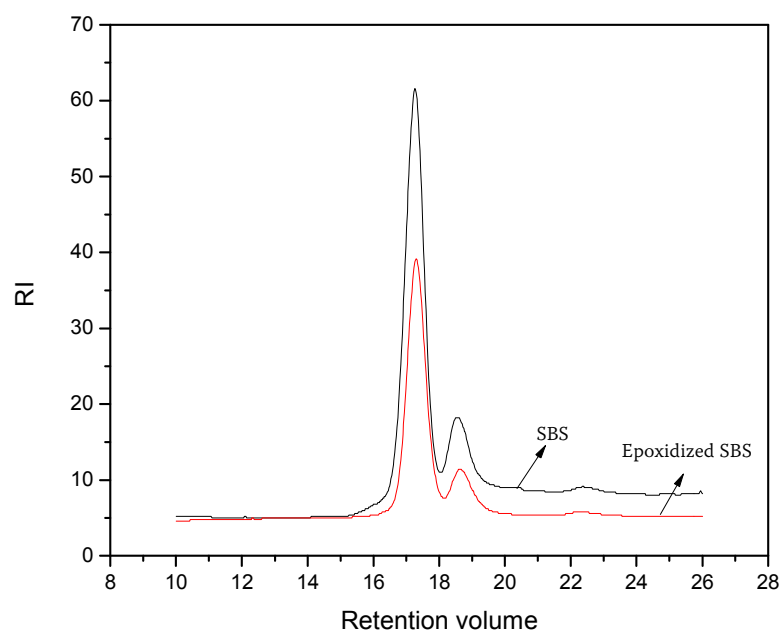
Figure 2.41 GPC traces of SBS and epoxidized SBS

Chapter 3

Synthesis of carbohydrate functionalized SBS by click chemistry from epoxidized SBS

3.1 Introduction

Click reaction, that is Cu (I) catalyzed Huisgen 1,3 dipolar cycloaddition of azides and alkynes, has attracted more and more attention because of its high selectivity, mild reaction conditions, quantitative yields, and almost no by-products. This has led to its application in many processes, including the synthesis of therapeutics [1-2], protein based biohybrids [3-4], sugar arrays [5], dendrimers [6] and functional polymers [7-8] and in nanotube functionalization [9]. In particular "click" process has become an invaluable tool for the synthesis of carbohydrate based polymers. For example, Heinze et al. employed click chemistry in the modification of polysaccharide [10], Cazalis et al. immobilized carbohydrates and proteins onto the solid surfaces [11]. One advantage of the click chemistry is that the azide and alkyne groups can be easily introduced in the polymer backbone, and they are stable in common organic reagents and can coexist with other functional groups, such as hydroxyl, amino and carboxyl. The triazole ring thus formed is stable also, besides the copper (I) catalyst system is easily available and is not sensitive to solvent and pH. Thus, the remarkable functional-group tolerance of click reactions has enabled the facile introduction of reactive groups, such as hydroxyl and carboxyl groups, through conventional pre-[12] or post-polymerization modification[13].

Carbohydrate chains are involved in various recognition phenomena, such as fertilization, cell adhesion, tissue formation, antigen-antibody reaction, cancer metastasis and infection of viruses and bacteria. Cell surface saccharides of

glycolipids, glycoproteins, and glycans participitate in numerous biological pheonomena in which there is mediation by carbohydrate- protein interactions. Carbohydrate-carrying polymers have been used as cell-specific culture substrata, in human vaccines, for tumor diagnosis, as probes for receptors, and in targeted drug delivery systems [14].

Therefore, greater attention has recently been paid towards synthetic polymers with pendant carbohydrate chain moieties.

We decided to use click chemistry approach for the functionalization of SBS with carbohydrates, as it eliminates the need of protecting the sugar hydroxyl groups which otherwise becomes necessary using other methodologies.

3.2 Experimental

3.2.1 Materials

Polystyrene-block-polybutadiene-block-polystyrene (Aldrich, M_w 140,000, 30% polystyrene, 70% polybutadiene,) was used as a starting material. 3-chloroperoxybenzoic acid, 77% max. (Aldrich Chemicals, USA), methanol LR (Ranbaxy, India), toluene GR ,Pyridine GR, N, N-dimethyl formamide GR and 4-dimethyl amino pyridine (DMAP) was purchased from Merck and used as such without further purification. Dextrose anhydrous GR was obtained from Merck. D-mannose AR, (SRL), D(+) galactose LR, D(+) lactose AR were obtained from S.D fine chemicals. Ammonium Chloride AR, sodium ascorbate was obtained from Ranbaxy and sodium azide GR was obtained from Merck. All the sugars were used as received.

3.2.2 Analytical methods

3.2.2.1 ^{1}H and ^{13}C NMR analysis

^{1}H and ^{13}C spectra of all the samples were recorded on a bruker 200 MHz with CDCl$_3$ as the solvent and tetramethylsilane as external reference. The solid state ^{13}C spectra were recorded at 300 MHZ. All the spectrum is referenced at δ=77ppm for ^{13}C and δ=7.25ppm for ^{1}H with respect to deuterated chloroform which was used as the NMR solvent.

3.2.2.2 FTIR analysis:

Spectra were recorded with a Perkin Elmer 1 FTIR instrument with a resolution of 4 cm^{-1} in transmission mode, in which the samples were cast onto a KBr disk from a solution of the elastomer dissolved in chloroform.

3.2.2.3 Thermogravimetric Analysis (TGA and DSC)

The Thermo gravimetric analysis (TGA) was performed on Perkin Elmer TGA-7 in N$_2$ atmosphere at heating rate of 10 °C min^{-1}. Glass transition temperature (T$_g$) was measured using DSC Q-10 (TA) in N$_2$ atmosphere at heating rate of 20 °C min^{-1}

3.2.2.4 Scanning electron microscopy (SEM)

The surface morphology of SBS and functionalized SBS was investigated using Leica SEM stereoscan 440, Cambridge, UK. The polymeric samples in the form of thin films, before analysis were coated with gold in a sputter coater, in order to

achieve conducting surface and were analyzed at an accelerated voltage (potential) of 10 KV.

3.2.2.5 WAXRD

Wide Angle X-Ray Diffraction (WAXRD) analysis was carried by using powder XRD Xpert-1217 diffractometer. The scanning speed was 4°/ min, with a radiation of CuK- α. The samples were scanned from 2 θ values of 3° to 30°.

3.3   Synthesis of carbohydrate functionalized SBS by click chemistry

3.3.1 Synthesis of partially epoxidized SBS

Partially epoxidized SBS (22 %) was synthesized as detailed in chapter 2.

3.3.2 Synthesis of SBS azide from partially epoxidized SBS

In a 250 ml. round-bottomed flask maintained under nitrogen 2g of epoxidized SBS (13mol%) was dissolved in 20 ml pyridine, after the epoxide dissolved completely 40 ml of dry DMF was added slowly at 50 ^{0}C so that the epoxide does not precipitate and the reaction mixture was stirred for some time and the temp was increased to 70^0 C. Sodium azide 1.5 g and ammonium chloride 1.5 g (1:1 mol) was added to the reaction mixture. The reaction mixture was heated at 70 C for 3.5 hr, after which the product was precipitated in 500 ml water and is washed until free from pyridine. The final wash is done with methanol and the product is dried in desiccator under vacuum at room temperature.
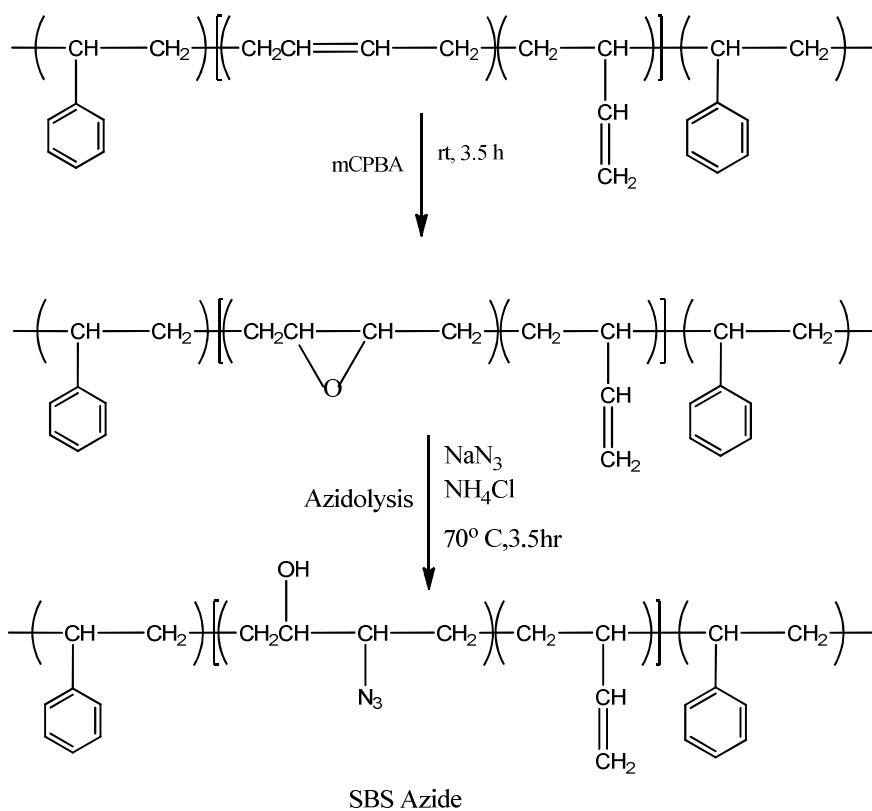
Reaction scheme 3.1 Synthesis of SBS azide from SBS

3.3.3 Synthesis of sugar derivatives for click reaction

3.3.3.1 Synthesis of β-D- Glucopyranose pentaacetate (1)

This derivative was synthesized following the procedure of Wolfrom et al. [17]. In a 2 litre flask containing 350 mL of acetic anhydride, Dextrose (50g) was added and the reaction mixture was heated. Anhydrous sodium acetate (25g) was added and the mixture was stirred until a clear solution was obtained. The temperature was

increased to 90°C and the reaction was continued for 2.5 h at this temperature. It is then cooled and poured with stirring onto 2 litres of ice water. After 3 h the crystalline material is filtered and is crystallized from hot methanol. The product is further purified by recrystallization.

3.3.3.2 Synthesis of 2-proynyl 2, 3, 4, 6-tetra-O-acetyl-β-D-glucopyranoside (2) from β-D- Glucopyranose pentaacetate

2-proynyl 2, 3, 4, 6-tetra-O-acetyl-β-D-glucopyranoside (2) was synthesized following the method reported by Mereyala et al. [12]. To a solution of β-D-Glucopyranose pentaacetate (10g, 25.6 mmol) in chloromethane (200 mL) was added propargyl alcohol (1.8 mL, 30.7 mmol) and BF_3-Et_2O (4.8 mL, 38.4 mmol) at 0° C and the reaction mixture was stirred at room temperature for 2h. After the completion of the reaction anhydrous K_2CO_3 (4.8 g) was added and stirring was continued for an additional 30 min. and the reaction mixture was filtered and washed with dichloromethane. The filtrate was washed with water (2X150 mL) , the aqueous phase was separated and extracted with dichloromethane (2X50 mL) and the combined organic phase were dried over anhydrous sodium sulphate (Na_2SO_4) and concentrated to yield a solid which was crystallized in dichloromethane-hexane to obtain the derivative 2 (9 g , 90 %) as a crystalline compound.
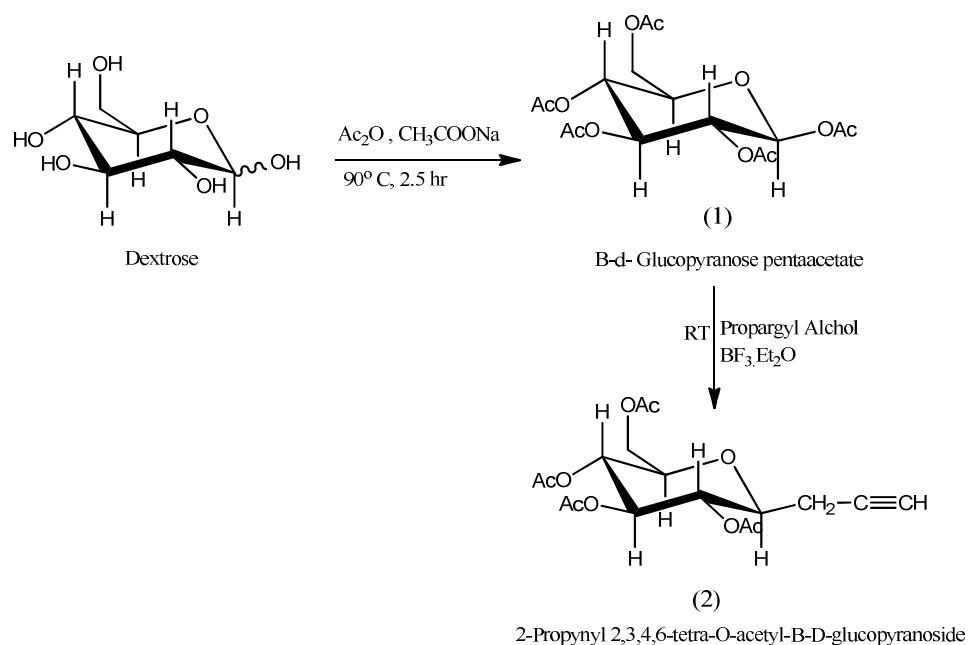
Reaction scheme 3.2 Synthesis of 2-proynyl 2, 3, 4, 6-tetra-β-D glucopyranoside
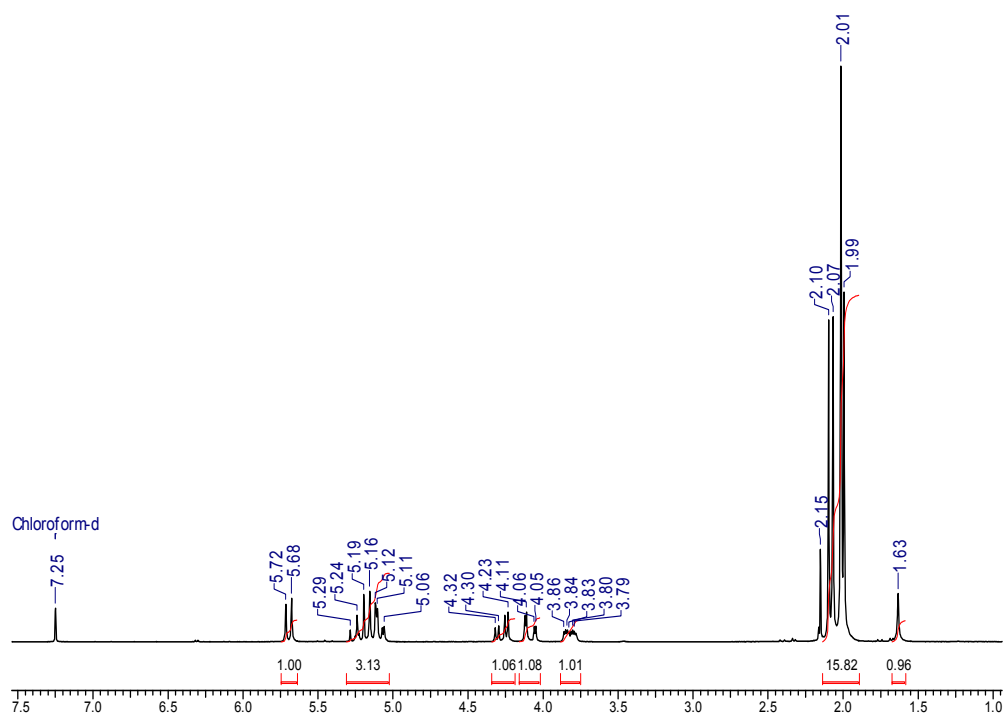
Figure 3.1 ^{1}H NMR of D (+) glucose pentaacetate

NMR: ^{1}H (CDCl$_3$), 5.28-4.9 (m, 3H, H-2, 3, 4), 2.15, 2.10, 2.07, 2.01 and 1.99 (5s, 15 H, OCOCH$_3$)
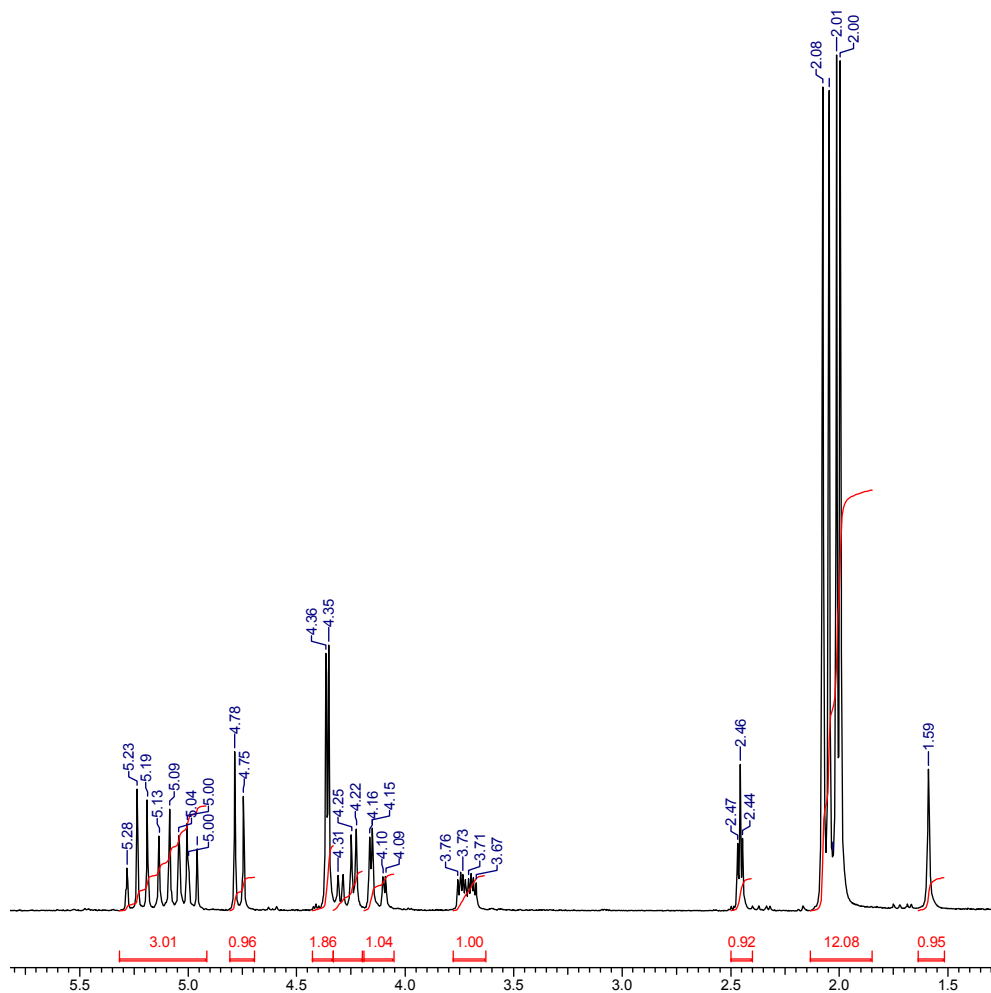
Figure 3.2 ^{1}H NMR of 2-proynyl 2, 3, 4, 6-tetra-β-D glucopyranoside

NMR: ^{1}H (CDCl$_3$), 5.28-4.9 (m, 3H, H-2,3,4), 4.75 (d, 1H, H-1), 4.35 (d, 2H, H-1), 4.4-4.09 (m,4H, H-1,6), 3.76-3.67 (m, 1H, H-5), 2.46 (t, 1H, H-3), 2.09, 2.05, 2.01 and 2.0 (4s, 12 H, OCOCH$_3$) FTIR : 3278 (≡CH), 2118 (C≡C), and 1749cm^{-1} (C═O)

This derivative is characterized by the appearance of anomeric proton at δ 4.66 as doublet and the acetylinic proton at δ 2.45 as a triplet. It is further confirmed by the characteristic FTIR peaks at 3276 cm^{-1} ($\equiv$CH), 2120 cm^{-1} (C$\equiv$C) and 1749 cm^{-1} (C$=$O) due to acetyl groups.

3.3.3.3 Synthesis of unprotected 2- propynyl sugar derivatives

Preparation of H$_2$SO$_4$-Silica

To a slurry of silica gel (10g, 200-400 mesh) in dry ethyl ether (50 mL) was added commercially available conc. H$_2$SO$_4$ (3mL) with shaking for 5 min. The solvent was evaporated under reduced pressure resulting in free flowing H$_2$SO$_4$-silica which was then dried at 110 ^{0}C for 3 h. This was used as a catalyst for the preparation of propargyl sugar derivative

Synthesis of 2-Propynyl-β-D- glucopyranoside and 2-Propynyl-β-D- lactoside

These sugar derivatives were synthesized following the procedure of Roy et al. [18]. D- Glucose (7.2 g, 40 mmol) and lactose (40 mmol) were suspended in propargyl alcohol (11.6 mL, 200 mmol) and stirred at 65^{0}C. H$_2$SO$_4$-Silica (200mg) was added and stirring was continued for 2.5 h until all the solids had dissolved. The reaction mixture was then allowed to stir at room temperature for another 12 h. TLC (CH$_2$Cl$_2$-MeOH; 5:1) and charring with charring solution, showed complete conversion of D-glucose and D lactose. The reaction mixtures were transferred to silica gel column and the excess propargyl alcohol was eluted with CH$_2$Cl$_2$ followed by elution of the product glycoside with CH$_2$Cl$_2$-MeOH (15:1) to afford the propargyl derivative in 80 % yield.
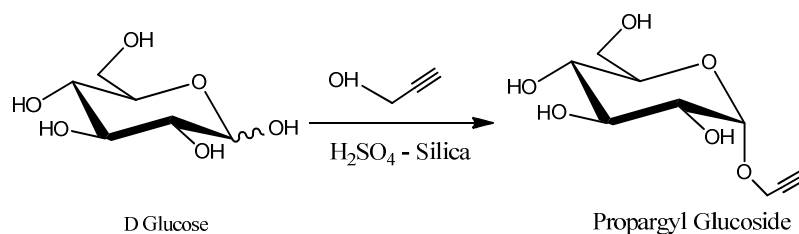
Reaction scheme 3.3 Synthesis of propargyl glucoside from D- Glucose

3.4 General procedure for the synthesis of carbohydrate functionalized SBS from SBS azide by click chemistry

3.4.1 Synthesis of 2-propynyl 2, 3, 4, 6-tetra-O-acetyl-β-D-glucopyranoside (PTAG) functionalized SBS

SBS azide (2g) was dissolved in 30 ml dichloromethane. Propynyl 2, 3, 4, 6-tetra-O-acetyl-β-D-Glucopyranoside (500 mg) dissolved in 20 ml of DMSO is slowly added to the SBS azide polymer solution to avoid precipitation.$CUSO_4.5H_2O$ (8 mg) dissolved in 1mL of water and Sodium ascorbate (13 mg,) dissolved in 1ml of water are added to the reaction mixture at room temperature. The reaction is continued for 3 h at the end of which it is precipitated in methanol. The product is washed with methanol and finally with water.

3.4.2 Synthesis of 2-proynyl lactose and 2- propynyl glucose functionalized SBS

SBS azide (2g) was dissolved in 30 ml dichloromethane. Sugar derivative (2-Propynyl lactose 500 mg and 2-propynyl glucose 230 mg) dissolved in 15 ml of DMSO is slowly added to the SBS azide polymer solution to avoid precipitation.

CUSO$_4$.5H$_2$O (8 mg) dissolved in 1mL of water and sodium ascorbate (13 mg,) dissolved in 1ml of water are added to the reaction mixture at room temperature. The reaction is continued for 3 h at the end of which it is precipitated in methanol. The product is washed with methanol and finally with water.
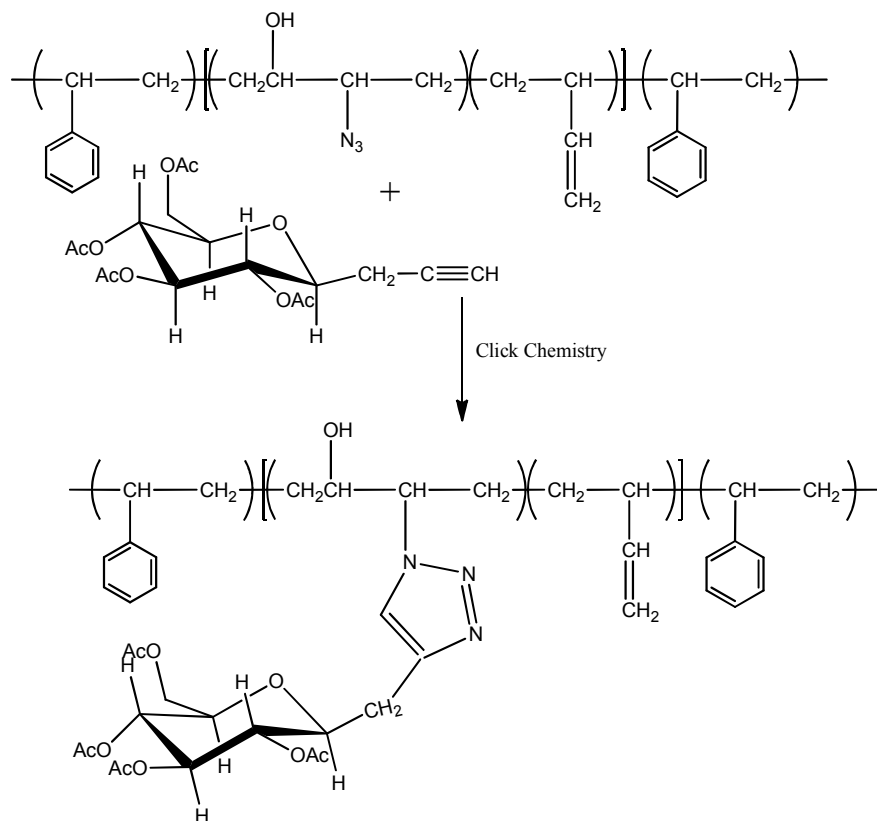
Reaction scheme 3.4 Synthesis of carbohydrate functionalized SBS using click chemistry approach

3.5 Results and discussion

The overall strategy, as presented in reaction scheme 3 above, is based on the azidation of epoxidized SBS followed by coupling with carbohydrate alkyne partner using click chemistry to yield carbohydrate functionalized SBS.

3.5.1 Synthesis and characterization of SBS azide

A detailed procedure for the synthesis is described in the experimental part. The chemical structure of the product was confirmed by FT-IR, ^{1}H NMR and ^{13}C NMR spectroscopy.

3.5.1.1 FTIR spectral analysis of SBS azide:

Figure 2.1 shows overlapped FT-IR spectrum of SBS, partially epoxidized SBS and azidated SBS, which clearly shows the observed changes in absorption bands before and after azidation.
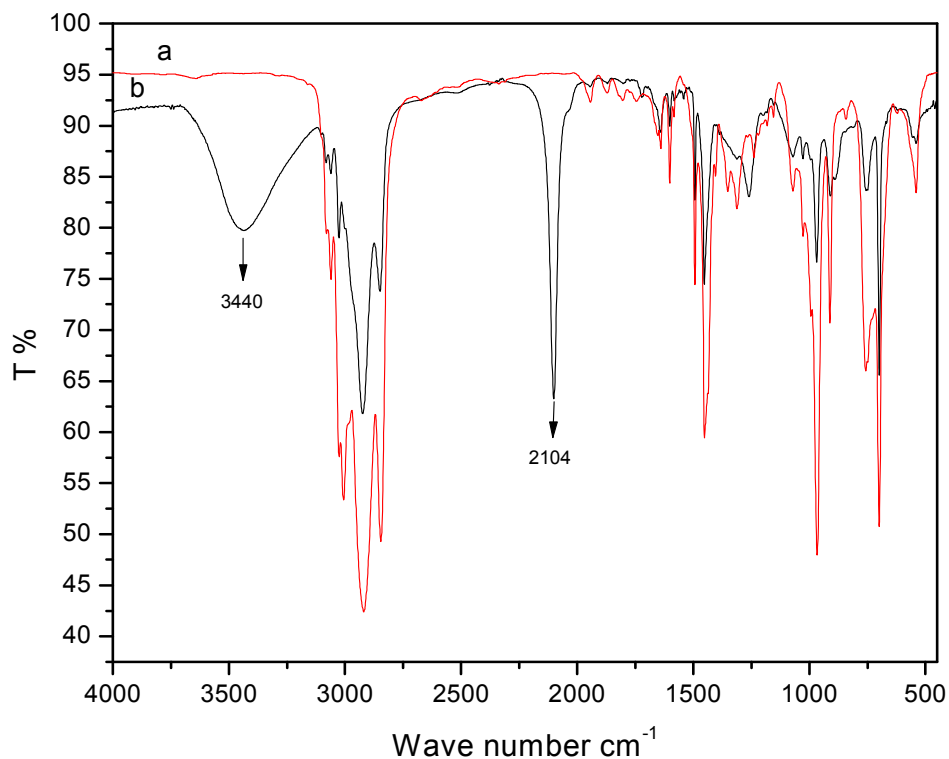
Figure 3.3 Overlapped FTIR spectra of (a) unmodified SBS and(b) SBS azide

Partially epoxidized SBS was ring opened in the presence of ammonium chloride and sodium azide to yield azido alcohol. It can be observed from the above figure that after azidation of epoxidized SBS new peaks appears at 2104 and 3440 cm^{-1}. The presence of the azide group in the product is confirmed by the characteristic peak of azide group at 2104 cm^{-1} and the hydroxy group is confirmed by the 3440 cm^{-1} peak.
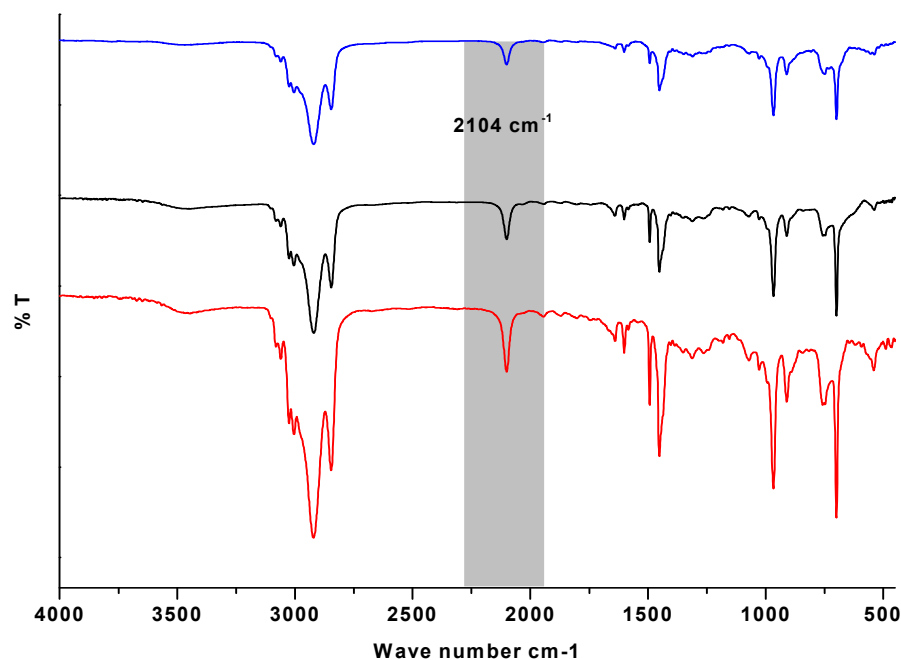
Figure 3.4 SBS azide with different degree of azidation (increasing intensity of - N$_3$ peak at 2104 cm^{-1})

3.5.1.2 Click reaction of SBS azide with propargyl sugar derivative

Click reaction is the Cu (I) catalyzed cycloaddition of azide and alkyne, this reaction can be performed in a number of solvents including water or other polar solvents and is not affected by presence of functional groups. In addition, the copper (I) catalyst system is easily available and insensitive to solvent and pH [11].

In our experiments, the copper (I) catalyst system was introduced to the reaction system by reducing copper (II) sulphate pentahydrate with sodium ascorbate. The reaction was performed in DCM-DMSO solution at room temperature for 3 h.
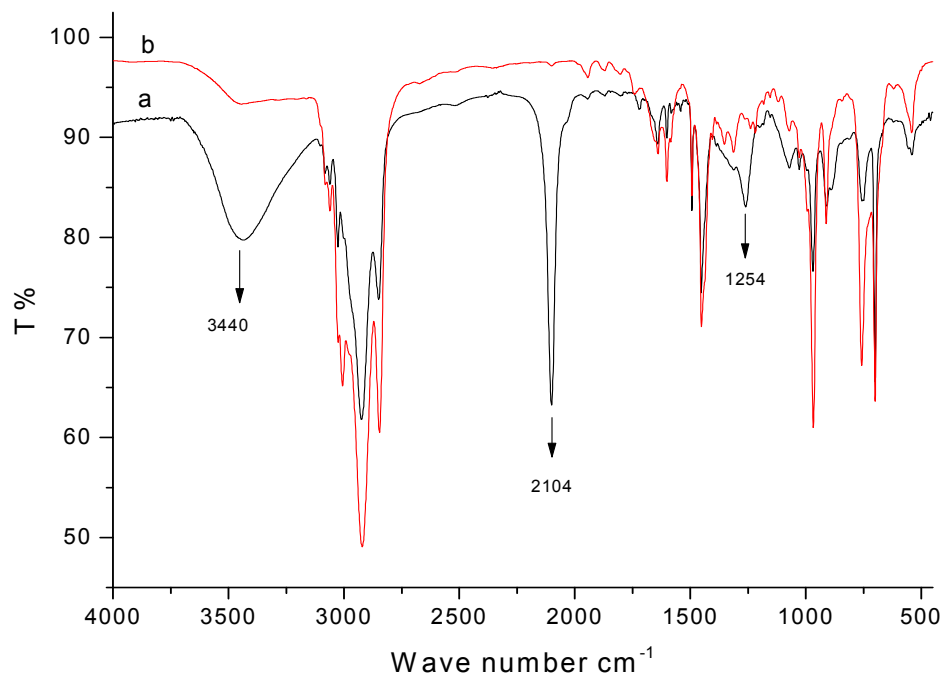
Figure 3. 5 Overlapped FTIR spectra of (a) SBS azide and (b) glucose linked SBS by click chemistry

Figure 3.5 shows the overlapped FTIR spectra of SBS azide and the click reaction product of SBS azide with propargyl glucose. It can be observed from the above spectra that after click reaction the peak at 2104 cm^{-1}, characteristic of azide (N$_3$) disappear completely, due to the cycloaddition of azide and alkyne leading to the formation of 1, 2, 3- triazole linkage. Thus FTIR clearly shows the successful anchoring of glucose units to SBS by click chemistry. In this reaction it is not necessary to protect the hydroxyl groups of the glucose because hydroxyl groups do not interfere with the formation of triazole ring.
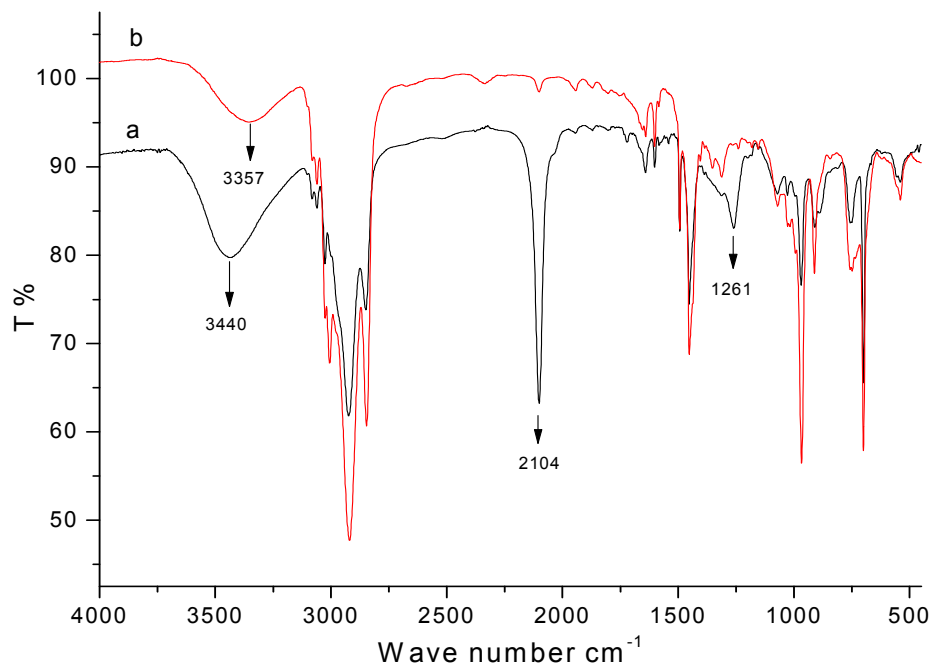
Figure 3.6 Overlapped FTIR spectra of (a) SBS azide and (b) lactose linked SBS by

click chemistry

Figure 3.6 shows the overlapped FTIR spectra of SBS azide and the click reaction product of SBS azide with propargyl lactose. It can be observed from the above spectra that after click reaction the peak at 2104 cm^{-1}, corresponding to azide diminishes significantly. This shows the successful functionalization of SBS with lactose has indeed taken place.
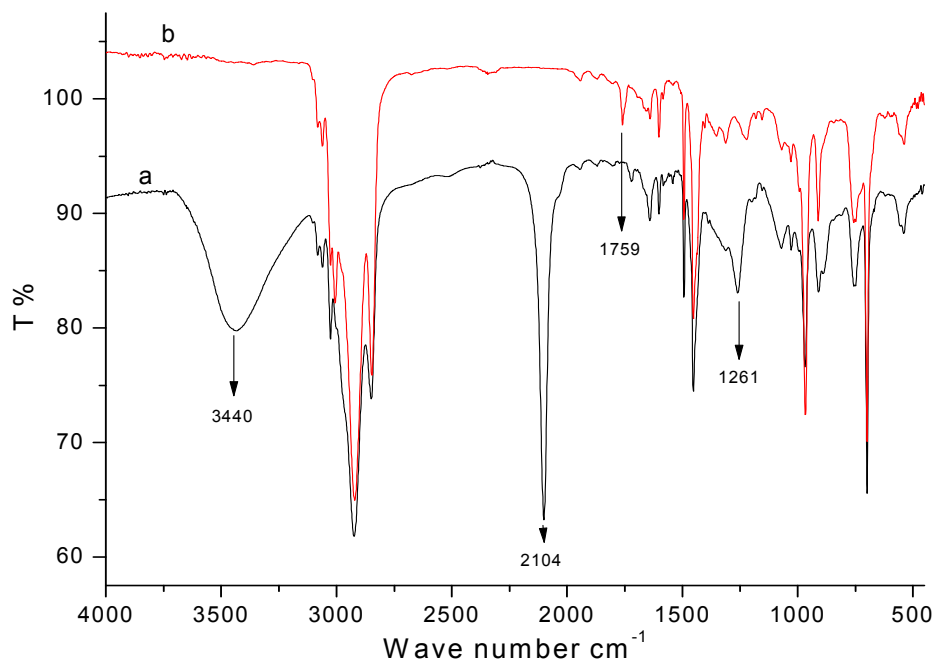
Figure 3.7 Overlapped FTIR spectra of (a) SBS azide and (b) 2, 3, 4, 6-tetra-O-

acetyl-β-D glucopyranoside linked SBS by click chemistry

Figure 3.7 shows the overlapped FTIR spectra of SBS azide and the click reaction product of SBS azide with propargyl acetyl protected glucose. It can be observed from the above spectra that after click reaction the peak at 2104 cm^{-1}, corresponding to azide completely disappears. The acetyl protected glucose shows a new peak at 1759 cm^{-1} due to the carbonyl stretching of acetyl group. The simultaneous disappearance of azide peak and appearance of carbonyl peak in the FTIR spectra of the product clearly proves that functionalization of SBS with protected glucose has been successful.

3.5.1.3 Investigation of morphological structure of sugar linked SBS by click chemistry by Wide angle X-ray diffraction (WAXRD)

SBS is an amorphous [16] thermoplastic elastomer, hence broad peaks corresponding to polybutadiene and polystyrene are observed in the wide-angle X-ray diffraction of unmodified SBS. All the samples were scanned from $2\theta = 3^0$- 30^0 at room temperature.
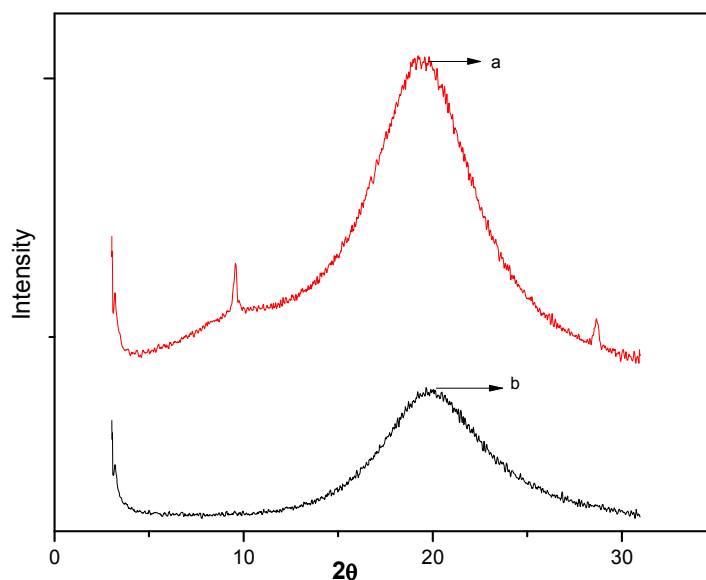
Figure 3.8 WAXRD diffraction plots of (a) unmodified SBS (b) SBS azide

Figure 3.8 shows the wide-angle X-ray diffraction plots of unmodified SBS and azidated SBS. Three broad peaks are observed in the above WAXRD plots centred at 2θ values of 9.5^0, 19.7^0 and 28.7^0. The more intense peak is centered at $2\theta = 19.7^0$ corresponds to amorphous polybutadiene, the weaker one is centred at $2\theta = 9.5^0$ corresponds to polystyrene. It can be observed from the above figure that after azidation of SBS there is significant decrease in intensity of peak at $2\theta = 19.7^0$ associated with polybutadiene domain. The peak at $2\theta = 9.5^0$ and 28.7^0 associated with polystyrene disappears.

Figure 3.9 – 3.11 shows the wide-angle X-ray diffraction plots of lactose, tetraacetyl glucose and glucose linked SBS by click reaction. It can be observed from the above figure that after functionalization of SBS with sugar there is significant decrease in intensity of peak at $2\theta = 19.7^{0}$ associated with polybutadiene domain. This decrease in intensity is more pronounced in tetra acetyl glucose linked SBS.
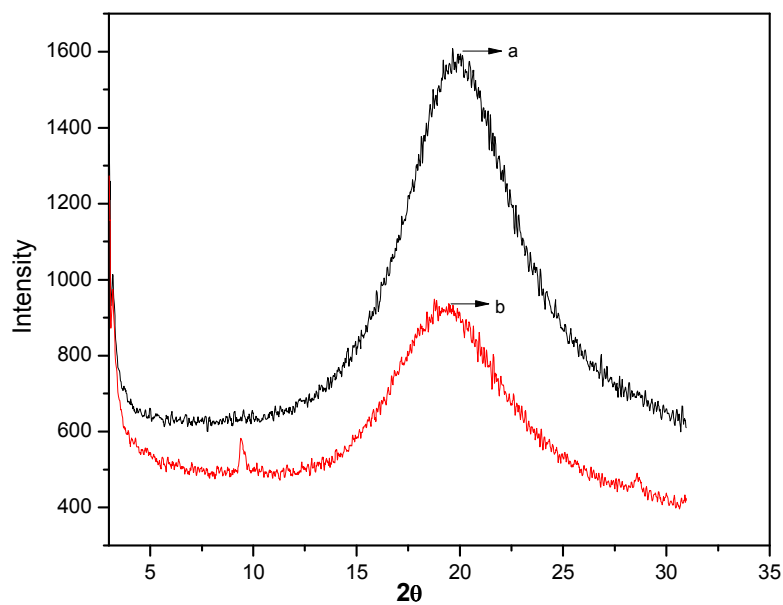
Figure 3.9 WAXRD diffraction plots of (a) SBS azide (b) lactose linked SBS by click reaction
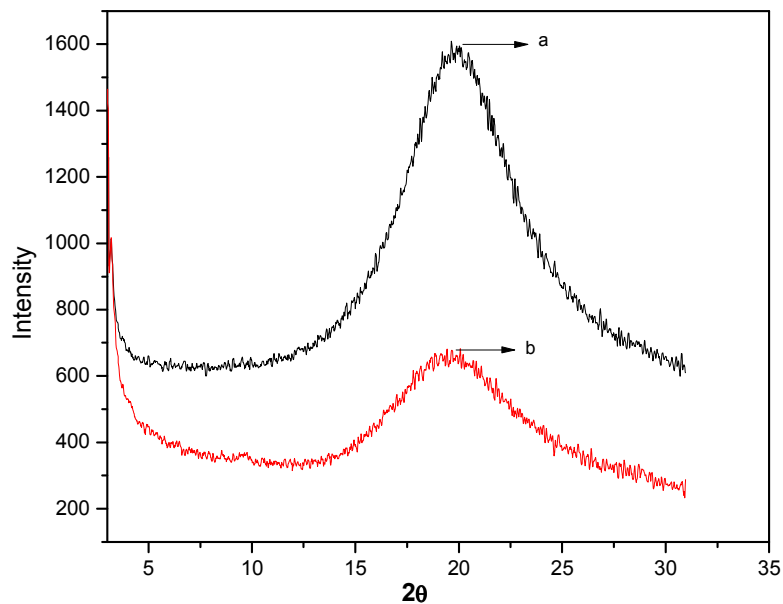
Figure 3.10 WAXRD diffraction plots of (a) SBS azide (b) tetraacetyl glucose

linked SBS by click reaction
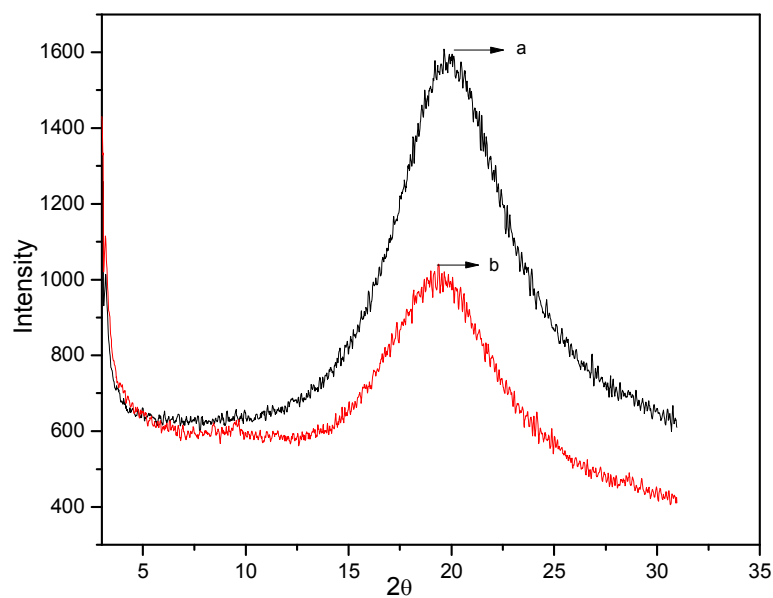
Figure 3.11 WAXRD diffraction plots of (a) SBS azide (b) glucose linked SBS by

click reaction

3.5.1.4 Thermal analysis of sugar linked SBS by click reaction

Thermogravimetric analysis (TGA)

TG curves of various sugar linked SBS were studied under pure nitrogen atmosphere at heating rate of 10^0 C/min from 50-600 ^{0}C. Table 3.1 gives the thermal analysis details such as degradation onset temperature (T_{onset}), residue weight % and maximum degradation temperature (T_{max}) for the thermal degradation of the various sugar linked SBS samples synthesized by click reaction.
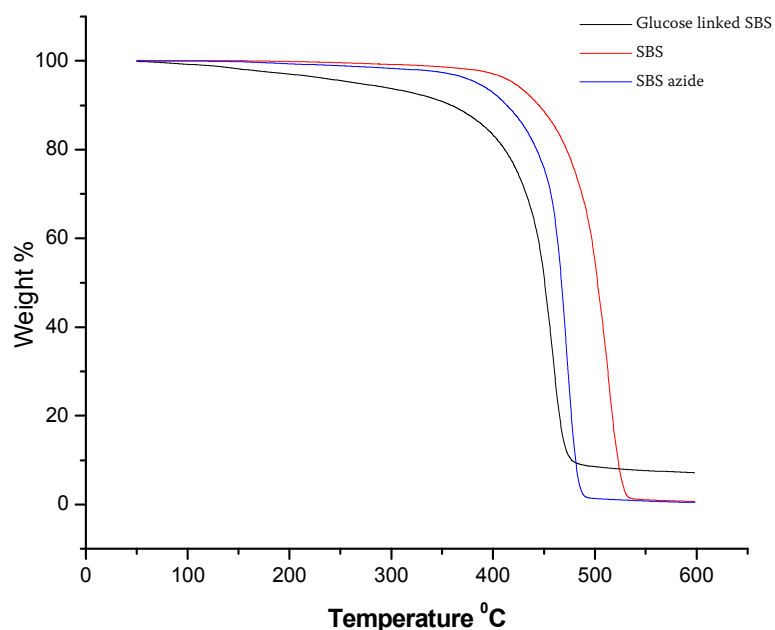
Figure 3.12 Overlapped TGA curves of SBS, SBS azide and glucose linked SBS by

click reaction

Figure 3.12 shows the comparative thermal stabilities of SBS, SBS azide and glucose linked SBS synthesized by click reaction. SBS and SBS azide show single

stage degradation, whereas glucose linked SBS shows two stage degradation. SBS is stable upto 400^{0}C after which it starts degrading rapidly. The rate of degradation reached maximum at 525 ^{0}C and at 600^{0}C it degrades almost completely leaving behind only 0.63 weight% residue. SBS azide thermal stability is less compared to SBS. Thus, azidation seems to reduce the thermal stability of SBS. Further it can be observed from the figure 3.-3. that functionalization with sugar further reduces the thermal stability.
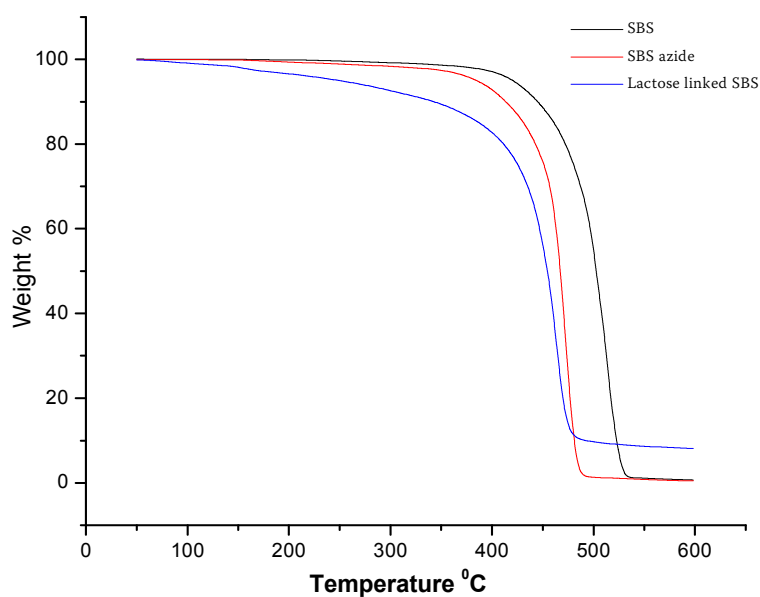
Figure 3.13 Overlapped TGA curves of SBS, SBS azide and lactose linked SBS by click reaction
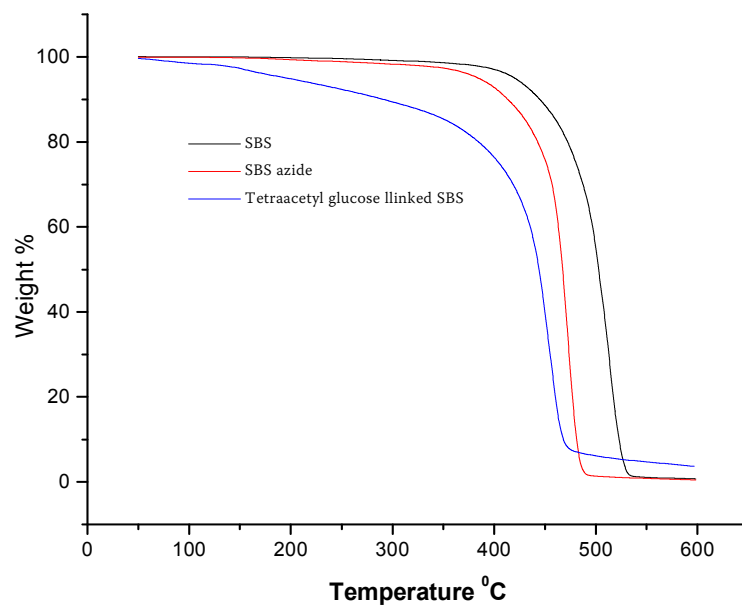
Figure 3.14 Overlapped TGA curves of SBS, SBS azide and tetraacetyl glucose

linked SBS by click reaction
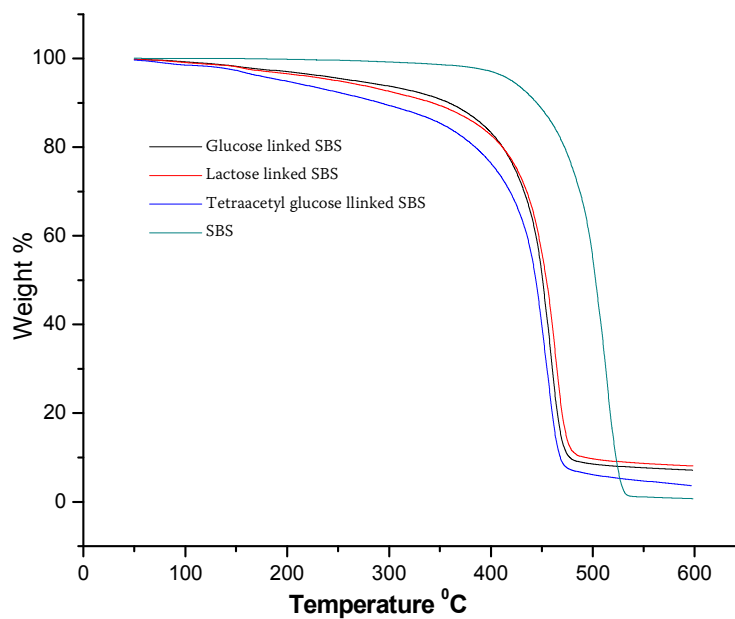
Figure3. 15 Overlapped TGA curves of SBS and different sugar linked SBS by click

reaction

It is seen from the above figure that sugar linked SBS samples shows higher residue at 600 ^{0}C, as compared to unmodified SBS. Among the sugar linked SBS samples the acetyl protected tetraacetyl glucose linked sample shows comparatively less thermal stability, while the unprotected sugars viz. Glucose and galactose linked SBS shows similar thermal stability. Acetyl groups may be the cause of lower thermal stability, since these groups dissociate at low temperatures.
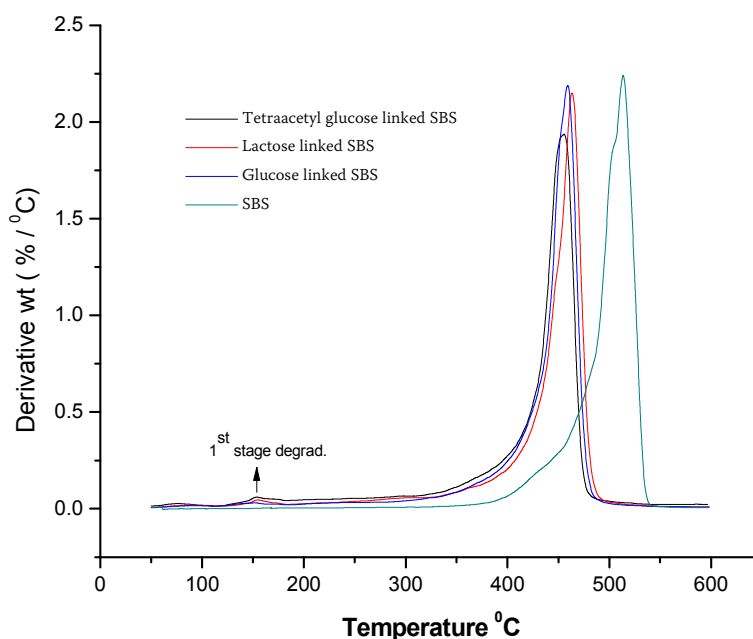
Figure 3. 16 Overlapped DTG curves of SBS and different sugar linked SBS by click reaction

The DTG curves of the sugar linked SBS samples clearly shows a two stage degradation compared to single stage degradation of unmodified SBS. Moreover the shift in T_{max} to lower temperature in sugar linked SBS is also clearly evident.

Table 3.1 Thermal analysis of different sugar linked SBS by click reaction

Sample	$T_{onset}\,^0C$		T_5 (°C)	T_{10} (°C)	T_{max}(°C)	Residue (wt %) 590 °C
	1st Stage	2nd Stage				
SBS	478.3		420	445	525.0	0.6
SBS Azide	449.4		385.6	413.5	483.8	0.45
Glucose linked SBS	--	428.5	264.5	356	474.5	7.2
Lactose linked SBS	139	434.1	245.8	340.8	474.2	0.20
Tetraacetyl glucose linked SBS	141.4	426.4	195.1	288.4	467.0	3.9

T_5, T_{10} and T_{max}: Temperature at which 5%, 10% and maximum weight loss of polymer takes place respectively

From table 3.1, it is observed that 5 % weight loss for SBS takes place at 420 °C, and at 385.6 °C for SBS azide. After functionalization with sugar it further shifts to lower temperature. With acetyl protected glucose linked SBS the 5 % weight loss occurs at much lower temperature of 195 °C. Thus we can say that functionalization of SBS with sugar leads to decrease in thermal stability.

3.5.1.5 Scanning electron microscopy (SEM)

Thin films of the samples were prepared from chloroform solution for examining their surface morphology by SEM. The SEM images are shown below in figure 3.17
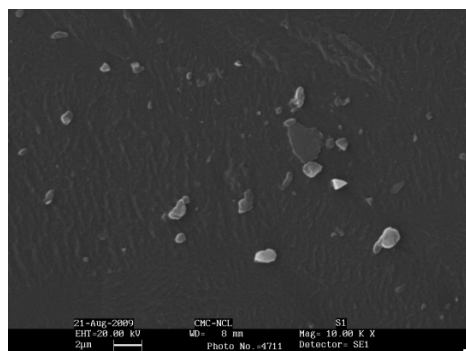
(a)
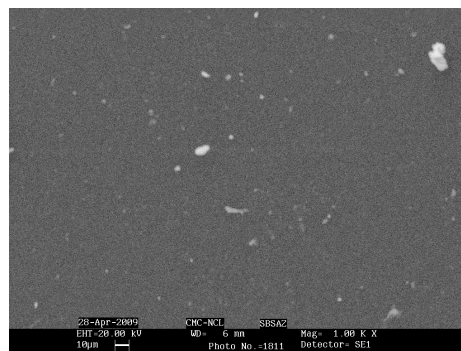
(b)
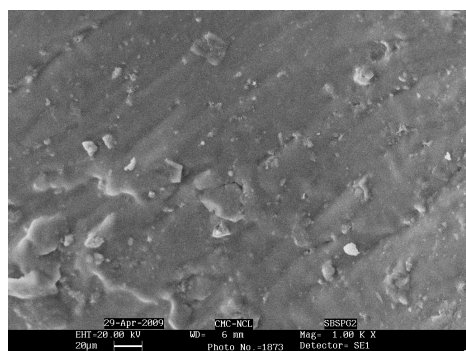
(c)
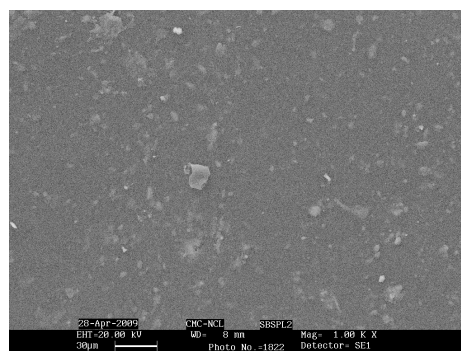
(d)
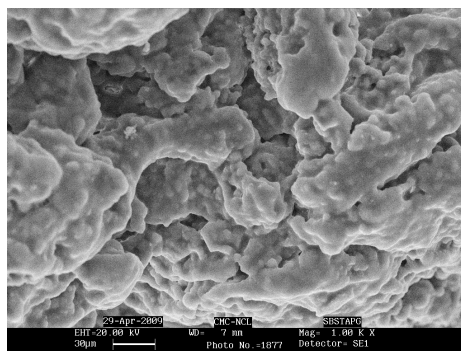
(e)

Figure 3.17 SEM micrographs of (a) SBS (b) SBS azide (c) glucose linked SBS

(d) lactose linked SBS (e) tetra-acetyl glucose linked SBS

Figure 3.17 shows the surface morphology of SBS, SBS azide, lactose, tetraacetyl glucose and glucose linked SBS by click reaction. SBS is considered a two-phase thermoplastic block copolymer in which spherical polystyrene (PS) domains are dispersed in continuous polybutadiene (PB) phase (see chapter 5). It is observed from the above figure that there is not much change in morphology after azidation of SBS, but after functionalizing with sugar by click reaction the morphology changes.

3.6 Conclusions

Thus, in this segment of the work, we have successfully used "click chemistry" to incorporate sugar moieties onto a polymer with double bonds like SBS. These new sugar linked SBS polymers were characterized for chemical structure by FTIR, morphological structures by WAXRD, and thermal properties by TGA/DTG studies. Due to the low amount of sugar incorporated and solubility problem, they could not be characterized further. This synthesis was carried out only to show the applications of click chemistry for such reactions.

3.7References:

1. L. V. Lee, M. L. Mitchell, S. J. Huang, V. V. Fokin, K. B. Sharpless, C. H. Wong, *J. Am. Chem. Soc.* **2003**, 125, 9588–9589

2. R. Manetsch, A. Krasinski, Z. Radic, J. Raushel, P. Taylor, K. B. Sharpless, H. C. Kolb, *J. Am. Chem. Soc.* **2004**, 126), 12809–12818.

3. S. Seo Tae, Z. Li, H. Ruparel, J. Ju, *J. Org. Chem.* **2003**, 68, 609–612

4. X. L. Sun, C. L. Stabler, C. S. Cazalis, E. L. Chaikof, *Bioconjugate Chem.* **2006**, 17, 52–57

5. F. Fazio, M. C. Bryan, O. Blixt, J. C. Paulson and C.-H. Wong, *J. Am. Chem. Soc.* **2002**, 124, 14397–14402

6. P. Wu, A. K. Feldman, A. K. Nugent, C. J. Hawker, A. Scheel, B. Voit, J. Pyun, J. M. J. Frechet, K. B. Sharpless, V. V. Fokin, *Angew. Chem. Int. Ed.* **2004**, 43, 3928–393

7. B. Helms, J. L. Mynar, C. J. Hawker, J. M. J. Frechet, *J. Am.Chem. Soc.* **2004**, 126, 15020–15021

8. J. A. Opsteen, J. C. M. Van Hest, *Chem. Commun.* **2005**, 57–59

9. H. Li, F. Cheng, A. M. Duft, A. Adronov, *J. Am. Chem. Soc.* **2005**, 127, 14518–14524

10. T. Liebert, C. Hansch, T. Heinze, *Macromol. Rapid Commun.* **2006**, 27, 208–213

11. X. L. Sun, C. L. Stabler, C. S. Cazalis, E. L. Chaikof, *Bioconjugate Chem.* **2006**, *17* , 52–57

12. C. Li, M. G. Finn, *J. Polym. Sci., Part A* **2006**, 44, 5513

13. A. D. Thomsen, E. Malmstrom, S. Hvilsted, *J. Polym. Sci., Part A* **2006**, 44, 6360

14.   A. Tsuchida, S. Akimoto, T. Usui, K. Kobayashi, *J. Biochem.* **1998,**123, 715-721

15.   H. B. Mereyala, S. R. Gurrala, *Carbohydrate Research* **1998**, 307, 351-354

16.   E. C. Lopez, D. Mclntyre, L.J. Fetters, *Macromolecules* **1973**, 6, 415-423

17.   M. L. Wolfrom, A. Thompson, *Methods in Carbohydr. Chem.* **1963**, 2, 211

18.   B. Roy, B. Mukhopadhyay, *Tetrahedron Letters* **2007**, 48, 3783

3.8 Appendix 2: CPMAS spectra of sugar linked SBS by click chemistry
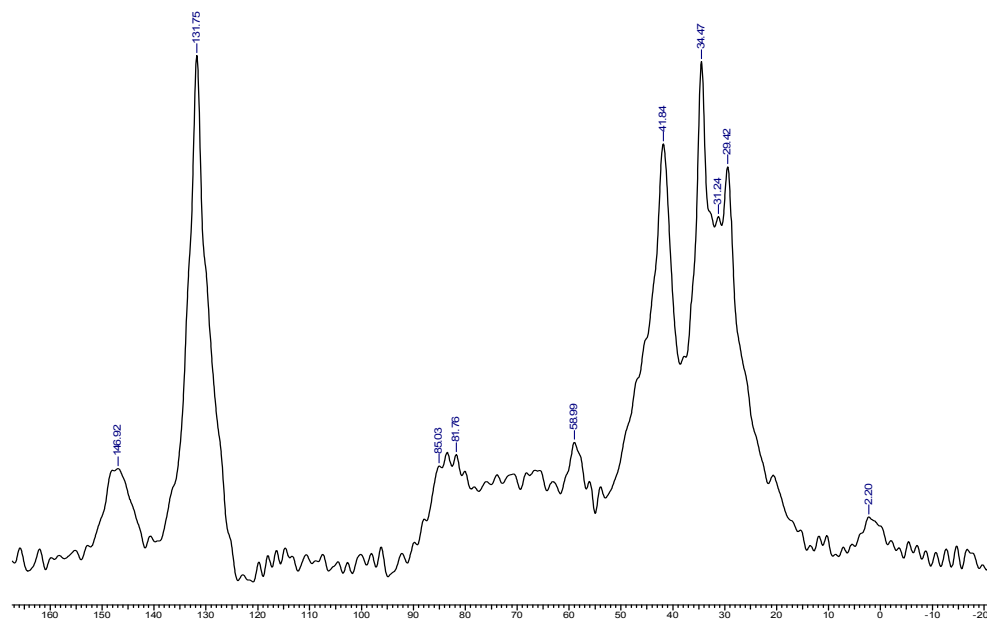
Figure 3.18 CP-MAS ^{13}C NMR spectra of glucose linked SBS by click chemistry
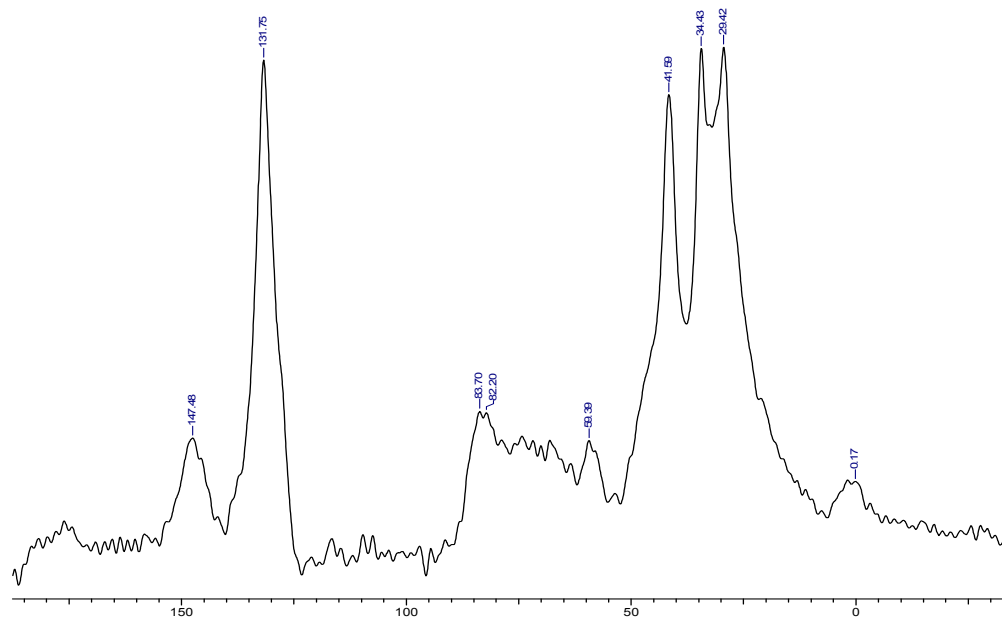
Figure 3.19 CP-MAS ^{13}C NMR spectra of lactose linked SBS by click chemistry

Chapter 4

Evaluation of carbohydrate functionalized SBS as fluorescent and biocompatible material for biomedical applications

4.1. Introduction

Industrial scale production of thermoplastic elastomers (TPE) was soon followed by their use in medical applications [1]. In 1995 only 2-3 % of total TPE production was used for medical applications and its use has seen many folds increase till 2009. This has been a continuously evolving field and has now become an important pillar of the health care industry. This field is known as biomaterial science, which has evolved into an important branch of interdisciplinary science encompassing the trilogy material science, chemistry and biology. The field of biomaterials comprises broadly of tissue engineering, implants, drug delivery, and delivery of bioactive agents.

Biomaterials can be classified in three broad groups; metals, ceramics, semi synthetic polymers and their composites [2]. Among these, polymeric biomaterials are the most extensively used due to the low cost, ease of synthesis and wide range of useful properties besides being amenable to the introduction of an array of specific need based functionality giving rise to versatile shape and structures like gel, films, fibers and solids [3].

Biomaterials find use in numerous medical applications such as artificial heart valves [4], synthetic vascular grafts [5-6], ventricular assist devices, drug-release systems, extracorporeal systems, artificial ligaments and tendons [7], bone plates and cement , contact lenses, breast implants [8] biosensing and a wide range of invasive treatment and diagnostic systems. These biomaterials help to heal, increase function, repair abnormalities, and thus improve the patient's quality of life.

Currently a lot of polymers and modified polymers are being used as biomaterials such as polyurethane, silicone, polyesters and co polyesters, polyolefin, styrene copolymers, hydrogels, polypeptides and collagen elastomers. Polymers with built-in biocompatible and antimicrobial groups can be used as infection preventative coatings [9] in the manufacture of medical devices (e.g., catheters, vascular access devices, peripheral lines, IV sites, drains, gastric feeding and tubes, and other implantable devices). Such materials can also be used as bulk resins, as antimicrobial additives and antimicrobial - antifouling coatings on structures in contact with microorganism in environments that require control of biofilm formation, such as marine products. Efforts are continuously being made on improvement since most of these suffer from some drawbacks. Among these for example polyurethane and polyesters suffers from hydrolytic degradation [10]. Therefore there is need to develop such polymers where their hydrolysis is impeded.

In order to improve the performance of these biomaterials, there is an increased focus on developing novel biomaterials with enhanced biocompatibility, low toxicity, good antimicrobial properties and good mechanical properties along with resistance to nonspecific protein adsorption (antifouling). Among different strategies currently being pursued towards this goal, one is the immobilization by covalent bonding of bioactive molecules like carbohydrates and proteins [11] on synthetic polymers matrices to give amphiphilic polymers which are known to self assemble in versatile structures such as vesicles, micelles, tubules and cylinders. Immobilizations of proteins are well researched but functionalization with unprotected carbohydrate and complex carbohydrates has not been adequately researched as yet.

It is well known that carbohydrates play an important role in cell differentiation, proliferation and adhesion. To date there are few methods for the synthesis of polymers having carbohydrate pendants based on urea [12], amide [13], ester [14-15], and ether [16-17] linkages, due to time consuming synthetic procedures [18] as discussed in the previous chapters.

Bech et al. functionalized poly (ethylene terephthalate) (PET) fibers via aminolysis followed by grafting of maltose, maltotriose and maltohexose [19], Ying et al. attached galactose ligands on an acrylic acid graft- copolymerized PET film for studying heptocytes attachment and cell/substrate interactions [20], Similarly Yoon et al. successfully tethered galactose on poly (D, L- lactic-co-glycolic acid) (PLGA) to study rat heptocytes viability [21]. Recently, Merrett et al. synthesized carbohydrate-functionalized norbornenes, as novel collagen cross linking agents in corneal tissue engineering [22].

Thus, from the above examples it can be inferred that functionalization of polymers, with biomolecules, especially carbohydrates can dramatically increase the biocompatibility of a material.

The most important parameters of biomaterials for being a suitable candidate are their biocompatibility, cytotoxicity and antimicrobial activity. This is necessary to reduce the chances of tissue rejection and infection after implantation in the body. They should also have sufficient physical and mechanical properties combined with processability. Styrene-butadiene-styrene (SBS), the focus of our current study is an important commodity elastomer but does not find much use in biomedical application, except for being used to manufacture catheters, stoppers, surgical gloves etc. Inspite of SBS having great commercial importance, it has not yet been possible to introduce biocompatible and moieties having antimicrobial

activities in a controlled manner so as to preserve its elastomeric property while simultaneously enhancing its biomedical applications. Till date, no report has been published on biocompatibility/cytotoxicity and antimicrobial activity of carbohydrate functionalized SBS or even differently functionalized SBS. Therefore the main objective of this chapter is to gain insight into the potential bio-medical applications of the bio-functionalized SBS elastomer by exploring their fluorescence activity, antimicrobial activity and their in-vitro biocompatibility. With above in view we functionalized SBS with sugars and quaternary nitrogen pendants to improve biocompatibility and antimicrobial properties respectively for evaluating it as potential candidate for various biomedical applications.

4.2. Materials and methods

4.2.1 Materials

Chloroform (HPLC grade) was purchased from Spectrochem, Isopropyl alcohol (HPLC) grade was purchased from SRL, MTT reagent was purchased from Sigma.

4.2.2 Methods

4.2.2.1 Preparation of polymeric film and solution

The carbohydrate functionalized SBS containing quaternary nitrogen pendants (pyridinium and others) were dissolved in $CHCl_3$ with stirring overnight to ensure maximum dissolution. 10 % (w/v) solutions of these polymers were cast into films in Petri dishes by slowly evaporating the chloroform solution at room temperature. These films were used for confocal laser scanning microscopy, antimicrobial activity and biocompatibility studies. UV-Visible absorption was measured in

chloroform solution at 1 mg/mL and fluorescence was measured at 4 mg/mL solutions.

4.2.2.2. UV-visible absorption and fluorescence analysis

UV–visible absorption and fluorescent emission of the functionalized SBS were studied by using a UV–visible spectrophotometer (Chemito, Spectrascan UV 2700 double beam UV VIS spectrophotometer) and a fluoro spectrophotometer (LS 55 Perkin Elmer), respectively. The sample was dissolved in chloroform; the concentration was 1mg/mL for UV-visible absorption and 4mg/mL for fluorescence analysis.

4.2.2.3. Confocal Laser Scanning Microscopy (CSLM)

The Confocal microscopy images were obtained on LSM 510 meta (Carl Zeiss) using a 63X (N.A. = 1.4) oil immersion objective and an excitation wavelength of 405 nm, 488 nm and 543 nm (He-Ne laser) with BP 420-480, BP 505-530, BP 550-690 laser filters. All images were captured after setting their thresholds below saturation. Laser power and other parameters were kept identical for all samples.

4.2.2.4. Antimicrobial Activity

Determination of antimicrobial activity:

The antimicrobial activities were determined against bacterial cultures Escherichia coli k-12, Bacillus sp. and yeast cultures Pichia stipitis NCIM 3499, Pichia stipitis NCIM 3497 using a nutrient agar method. Anti-microbial effect of the polymeric films was studied by adding 25.0 mg of each film separately in 50.0 mL sterilized LB broth for bacterial cultures and YPD for yeasts, in 250.0 mL Erlenmeyer flasks.

Each flask was inoculated with bacterial or yeast culture (0.2 % v/v) grown for 16 and 24 h, respectively. The bacterial cultures were incubated at 37°C and 200 rpm in a rotatory incubator shaker, while the yeasts were grown at 30°C and 150rpm. The samples from each flask were taken after 24 and 48h. The cell growth was analyzed by measuring the absorbance at 600 nm in a UV-Vis spectrophotometer. The flasks without the polymeric films served as control. The percentage of the bacterial growth inhibition was calculated using the difference between the number of colonies from bacteria with samples and that from the bacteria in the control flask.

Micro-organisms and culture conditions:

The micro-organisms included bacterial cultures maintained on nutrient agar slope, Escherichia coli k-12, Bacillus sp. and yeast cultures Pichia stipitis NCIM 3499, Pichia stipitis NCIM 3497.

The bacterial cultures (Escherichia coli and Bacillus sp.) procured from the culture collection of Lignocellulose Biotechnology Laboratory, Department of Microbiology, University of Delhi South Campus, New Delhi, India, were maintained on LB (Luria Bertani) agar plates at 37°C. Pichia stipitis NCIM 3497 and Pichia stipitis NCIM 3499 were procured from National Collection of Industrial Microorganisms, National Chemical Laboratory, Pune, India and were maintained at 30°C on YPD medium containing (g/L): Yeast extract 3.0, Peptone 5.0, Dextrose 20.0, agar 20.0 and pH 5.5. All cultures were subcultured fortnightly and stored at 4°C.

Anti-microbial effect of the polymeric films was studied by adding 25.0 mg of each film separately in 50.0 mL sterilized LB broth for bacterial cultures and YPD for

yeasts, in 250.0 mL Erlenmeyer flasks. Each flask was inoculated with bacterial or yeast culture (0.2 % v/v) grown for 16 and 24 h, respectively. The bacterial cultures were incubated at 37°C and 200 rpm in a rotatory incubator shaker (-40, New Brunswick Scientific, Germany), while the yeasts were grown at 30°C and 150 rpm.

Inoculum preparation for bacterial and yeast culture:

For bacterial culture, a loopful of cell mass from pre-grown agar plates was inoculated into sterile 50mL Nutrient Broth and incubated at 37°C and 200 rpm. Inoculum of yeast cultures was prepared by inoculating a loop-full of cell mass from pre-grown agar plates into 50mL of YPD broth in a 250mL Erlenmeyer flask and incubated at 30°C and 200 rpm.

Procedure

Bacterial culture: 50 mL Nutrient broth + 4% (v/v) inoculum

+ 25 mg   Polymeric film

37°C and 200 rpm

Absorbance at 600 nm was measured

Yeast culture: 50mL Nutrient broth + 4% (v/v) inoculum

+ 25 mg Polymeric film

30°C and 200 rpm

Absorbance at 600 nm was measured

Analytical methods: The samples from each flask were taken after 24h. The biomass present in the culture filtrate was analyzed by measuring the absorbance

at 600 nm in a UV-Vis spectrophotometer (Analytical Jena, Specord 205, Germany). The flasks without the polymeric films served as control.

4.2.2.5. Biocompatibility studies

Cell lines: THP-1 and HL-60 cell line

The monocyte THP-1 and HL-60 Leukemia cell line was obtained from National Centre for Cell Science (NCCS), Pune, India. Cells obtained were at passage numbers 90-93. Cells were cultured at 37°C with 5% CO_2 and 90% humidity in T-75 tissue culture flasks (Corning 430641). Cells were maintained in the culture medium used Minimum essential medium (MEM) without phenol red with 2.5 mM L-glutamine (Sigma, US) and supplemented with 10% fetal bovine serum (FBS; Gibco 10082-139)

Determination of Cell viability (biocompatibility)

To test the in vitro viability/ cytotoxicity of the carbohydrate functionalized SBS polymers we choose two human cell lines THP-1 and HL-60. We examined the effect of the polymer on metabolic function of the cells using a standard MTT assay [23] which is a widely adopted method of measuring cellular proliferation. The MTT assay consists of a yellow tetrazolium 3-(4, 5-dimethylthiazolyl)-2, 5-diphenyltetrazolium bromide) dye that is cleaved by mitochondrial dehydrogenase enzymes to form purple formazan, precipitated by viable cells. The concentration of formazan formed is proportional to the number of viable cells. The molecule created by the cleaving process of the MTT assay, formazan, absorbs light at 490 nm, thus enabling cell viability measurement through ultraviolet-visible (UV-Vis) spectrophotometer. A sample with high cellular viability will absorb a high

percentage of the light at 490 nm, while a sample with low or no viability will allow most light at 490 nm to be transmitted. Cell count method was use for calculating the cell number at the day 5 for THP-1 cell and at the day 2 for HL-60 cell line, for cell proliferation quantification by the MTT cytotoxicity assay. 1 mL of the solution containing 10,000 cells was added to each of the 12 wells tissue culture plate containing the samples. The cells were incubated with the test sample in CO_2 incubator supplied with 5% CO_2, 95% humidity at 37ºc. At the end of the incubation period, the solution containing the unattached cells was discarded and each well containing the test samples was washed thrice with 1 ml of PBS. Next, MTT reagent (5mg/ml) was added and incubated at 37ºC for 1hr. Then 200µl of 100% isopropyl alcohol was added and it was kept at RT for minimum 4hrs. After incubation it was ensured that formazan precipitate is dissolved by pipetting up and down until no precipitate is visible. The absorbance at 490nm was recorded on SPECTRA max PLUS. The MTT assay was completed on both controls and the samples. All experiments were performed in triplicate, and the quantitative value was expressed as the average ± standard deviation.

4.3. Result and Discussions

4.3.1 UV-Visible analysis

We carried out the UV-visible absorption characterization of sugar linked SBS from their dilute solutions in chloroform and the spectra are presented in figure 4.1-4.4.
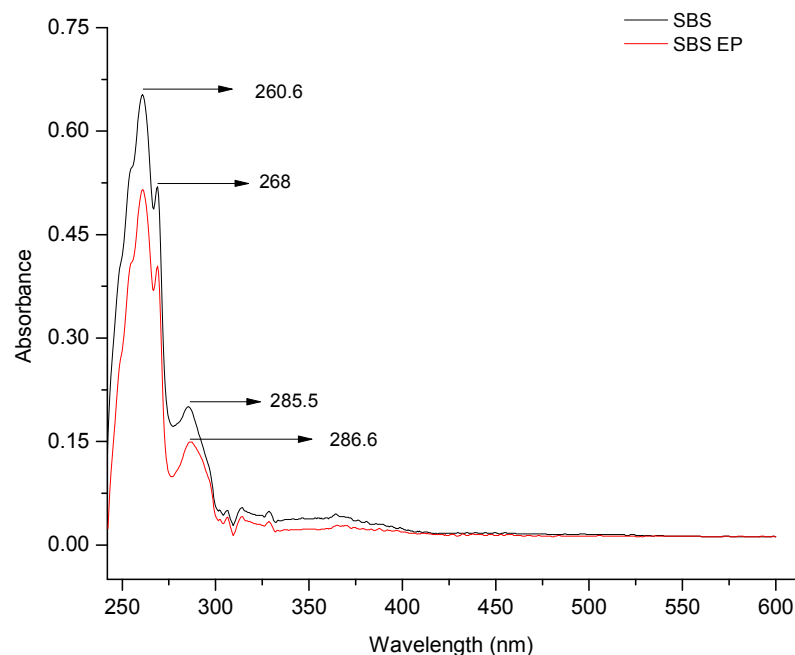
Figure 4.1 Overlapped absorption spectra in the UV-Visible region for chloroform solutions of SBS and SBS epoxide

According to literature reports, UV spectrum of polybutadiene shows absorption peak at 230 nm (cis microstructure) and another peak at 280 nm (trans microstructure) due to π -π^* transition [24] Therefore the peak at 285.5 nm (figure) due to π -π^* transition is assigned to trans microstructure of butadiene component in unmodified SBS. This peak shifts to 286.6 nm and gets broadened in the epoxidized SBS due to the partial conversion of butadiene double bonds to epoxide as shown in figure 4.1. The peak centred at 260.6 nm is due to isolated phenyl group [25] of polystyrene component of SBS which does not undergo any change as the phenyl group is not involved in the functionalization of SBS which takes place exclusively in the butadiene segment of SBS.
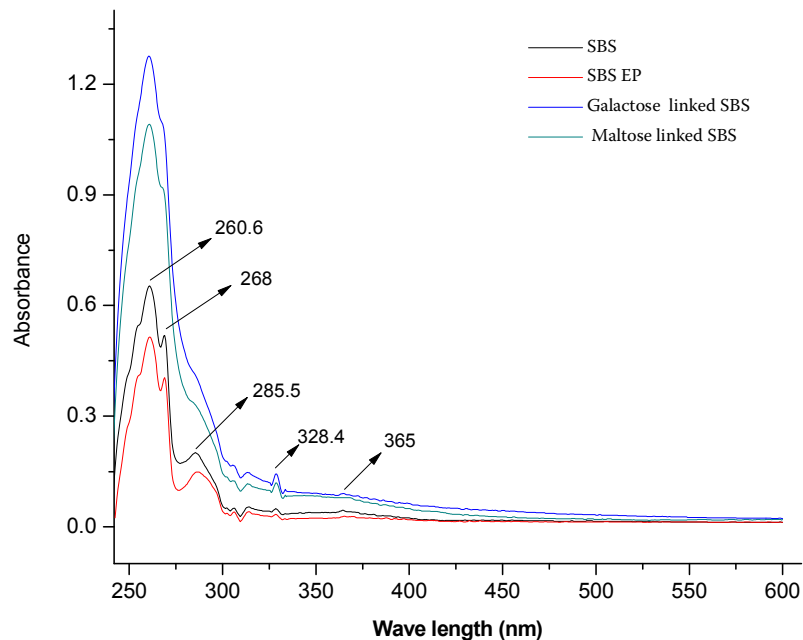
Figure 4. 2 Overlapped absorption spectra in the UV-Visible region for chloroform solutions of SBS, SBS epoxide, Galactose linked SBS and Maltose linked SBS
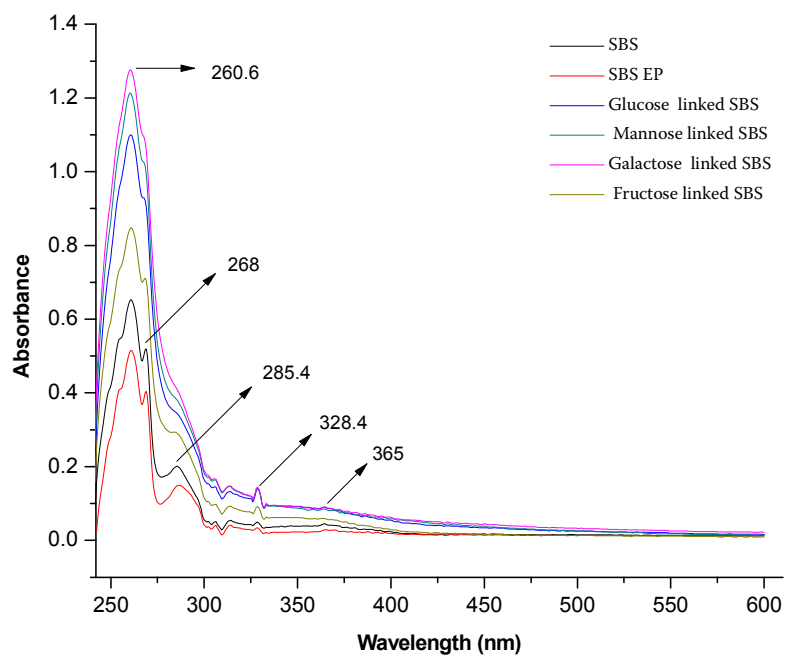
Figure 4.3 Overlapped absorption spectra in the UV-Visible region for chloroform solutions of SBS, SBS epoxide, Glucose, Mannose, Galactose and Fructose linked SBS

Figures 4.2 - 4.3 show the UV-visible absorption of sugar linked SBS samples. Glucose, mannose and galactose linked SBS which had undergone quantitative functionalization (more than 90 % epoxide opening) shows significant broadening of peaks at 268 nm and 286.6 nm. Sucrose linked SBS which is partially functionalized showed less broadening of these peaks. More over in all the sugar linked SBS a broad peak at around 365nm appears which has been reported in literature to be associated with formation of conjugated DMAP intermediate [26] (discussed in chapter 2). Galactose linked SBS shows the highest UV absorption intensity among three monosaccharide viz. glucose mannose and galactose.
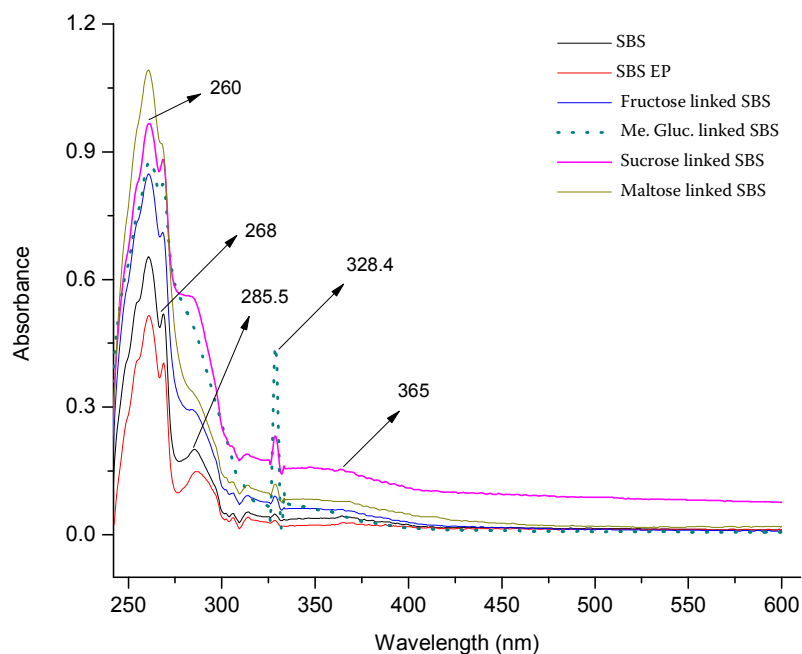
Figure 4.4 Overlapped absorption spectra in the UV-Visible region for chloroform solutions of SBS, SBS epoxide, Fructose, Methyl Glucoside, Sucrose and Maltose linked SBS

A significant change in peak shape and intensity is observed between the partially functionalized sugar linked SBS and fully functionalized sugar linked SBS (figure 4.4). Fructose, methyl glucoside and sucrose linked SBS which are partially

functionalized shows less reduction and less broadening of peak at 268 nm and 286.6 nm, while the maltose linked SBS shows significant broadening of these two peaks with increased intensity.

The UV-visible absorption spectra of the sugar linked and functionalized SBS proves the successful functionalization of SBS has taken place and it can be used to investigate qualitatively the degree of functionalization of SBS.

4.3.2 Fluorescence analysis

The fluorescence emission spectra of sugar linked and functionalized SBS in solvent chloroform are shown in figure 4.19-4.24 in appendix and fluorescence data is shown in table 4.1. All the sugar linked SBS samples shows strong fluorescence emission at 559 nm of varying intensity with the excitation at 549 nm. SBS and partially epoxidized SBS shows very weak fluorescence which increases by 5-10 folds (Table 4.1) in sugar linked SBS containing pyridinium and other quaternary nitrogen pendants.

Table 4.1 Fluorescence analysis of sugar linked SBS containing pyridinium and quaternary nitrogen pendants

S.NO	Sample	Excitation wavelength (nm)	Emission wavelength (nm)	Intensity
1	SBS	549	559	117.74
2	SBS Epoxide	549	559	104.65
3	SBS linked Glucose	549	559	514.52
4	SBS linked Mannose	549	559	491.05
5	SBS linked	549	559	994.61

	Galactose			
6	SBS linked Maltose	549	559	720.68
7	SBS linked Xylose	549	559	565.25
8	SBS linked Fructose	549	559	556.13
9	SBS linked Sucrose	549	559	1010.38
10	SBS linked Me Glucoside	549	559	862.0

We observe a slight decrease in fluorescence intensity in partially epoxidized SBS as compared to unmodified SBS, which could be due to decrease in unsaturation due to epoxidation. A strong relationship is known to exist between fluorescence and saturation or unsaturation character of the main chains and since the double bonds of the butadiene segments in SBS is only partially epoxidized hence there is only slight decrease in fluorescence intensity of the epoxidized SBS.

Fluorescence spectra of polymers is determined both by the chemical structures of the backbone chains themselves and by the physical and chemical nature of their side groups. The fact that strong fluorescence from these sugars linked and functionalized SBS was observed which was very weak in unmodified SBS; indicates the formation of new fluorescent chemical moieties in modified SBS as explained below. During functionalization of SBS with sugar, besides carbohydrates, some quaternary nitrogen pendants 1 and 2 are also generated on the SBS backbone as shown below in figure 4.5 (explained in Chapter 2). The chemical structure of the moiety responsible for fluorescence is under investigation

but we speculate that -OH groups [27] generated on backbone and structures 1 and 2 may be responsible for the observed fluorescence.
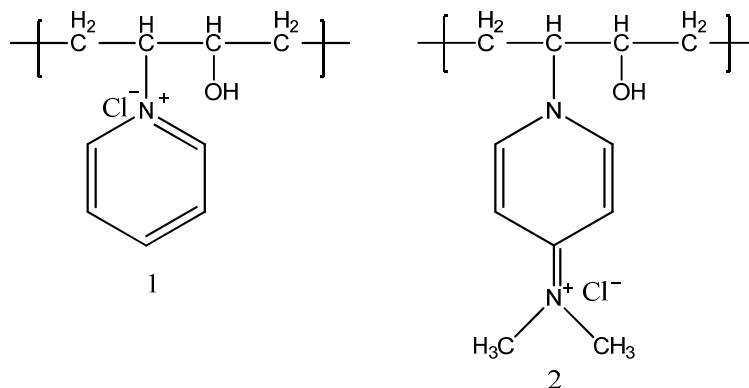
Figure 4.5 Quaternary nitrogen pendants generated on SBS backbone during functionalization of SBS with Sugars

Luminescence behavior of pyridinium halides was firstly reported in 1965, even before the report of fluorescence of pyridine and its derivatives in 1977. The attractive force between a pyridinium ion and an aromatic ring was first studied by Dougherty and coworkers [28] and has been widely used to facilitate reaction catalysis and self-assembly. supramolecular cation–π interactions plays an important role in binding of the pyridinium ring of NAD$^+$ to tryptophan in the active sites of enzymes [29], as well as in the stacking of positively charged alkylated DNA bases in excision repair enzymes [30]. Pyridinium cation–π interactions have also been used as a control element for supramolecular chemistry to form host–guest complexes.

 Fossey et al. studied the pyridinium–π interactions in non restricted pyridiniums and observed many fold enhancement of fluorescence intensity as a result of intramolecular π–π-stacking excimer emission [31]. Yoshida et al. had observed a

similar behavior with poly (4-vinylpyridine) during their study of quaternization of pyridine with alkyl halides [32]. With quaternization, emission band of pyridine around 390 nm disappeared and a new band around 520 nm appeared which increased with degree of quaternization. Thus, these reports support our observation of fluorescence in functionalized SBS containing pyridinium pendants.

Moreover, it is well documented that compounds bearing pyridinium or bipyridinium units, acts as electron acceptors, can form charge-transfer complexes with halide ions acting as electron donors [33-35] and fluorescence is the result of the existence of a charge-transfer complex between the pyridinium cation and its halide counterion [36] There is also possibility of OH-π interactions, which can contribute to fluorescence intensity. Burton et al. [37] and Simmons et al. [38] have reported their study on the interactions OH groups of the sugars with aromatic ring and the effect of different sugar structures on OH-π interactions. In our system SBS does contain aromatic phenyl rings whose interaction with the anchored sugar units may also contribute to fluorescence. Since the studies on sugar-aromatic interactions are in their nascent stage it will take some time to quantify these effects on chemical phenomena.

Thus from all the above facts we can speculate that pendants on SBS having the chemical structure 1 and 2 and the hydroxyl groups from the anchored sugar may be responsible for strong fluorescence in functionalized SBS.

4.3.3 Confocal Laser Scanning Microscopy (CSLM) of sugar linked SBS polymers:

Confocal microscopy was developed by Marvin Minsky [39] in 1955 at Harvard University to visualize 3 D image of specimens. Confocal scanning laser microscopy is widely used in biological and medical fields along with its use in material science for in-depth characterization of the materials and to perform semi-quantitative analysis of the concentration gradients at the phase boundaries. Verhoogt et al. [40] was the first group to report the application of CSLM to a polymeric mixture, in which they presented a 3D image of the structure of the blends. Since then this technique has been widely used to study homogeneity and surface morphology of multicomponent polymer systems. This technique also provides spatial resolution on various length scales within the surface layer and it also shows sufficient depth resolution so that one can observe the transition from surface to bulk structure in the multicomponent material. To study the morphology and to achieve contrast one of the components (usually the minor component) of the multicomponent material is selectively labelled with a fluorescent dye usually (Fluorescein or Rhodamine).

In this section we report the morphological observation of the surface and inner layers of sugar linked SBS containing pyridinium pendants films by CSLM. We believe this is the first study where labelling of one component with fluorescent dyes was not needed inorder to visualize the 3-D image of a complex polymer having a variety of functionality. This is the consequence of selective fluorescence of functionalized butadiene component in SBS eliminating the need of attaching a fluorescent label.

Confocal microscopy images of sugar linked and functionalized SBS are shown in figure 4.6-4.15. Sugars chosen were such that we had pentose (xylose, fructose), hexose (glucose, mannose, galactose) and disaccharides (maltose, sucrose), so that effects of specific sugars, if any, also be noted. Further, we also selected one sugar (methyl glucoside) where the anomeric carbon was blocked. This would help us note any specific effects of anomeric carbon. SBS and partially epoxidized SBS shows weak background fluorescence, whereas all the functionalized SBS having different sugars like glucose, mannose, galactose, maltose, xylose, fructose, sucrose and methyl glucoside shows fluorescence in green, red and blue colour region with varying intensities. The fluorescence occurs selectively in functionalized butadiene component (discussed in fluorescence analysis section of this chapter) and is absent in non functionalized polystyrene component of SBS leading to image contrast needed to view the morphology of the functionalized SBS.

Confocal scanning laser fluorescence microscopy analysis of functionalized SBS serves to compliment our observation of fluorescence as discussed in the fluorescence analysis section of this chapter besides serving as a non destructive technique for visualizing the morphology and heterogeneity/homogeneity of the sugar linked SBS containing pyridinium pendants. Since SBS is considered to be two-phase thermoplastic block copolymer in which polystyrene (PS) domains are dispersed in a polybutadiene (PB) matrix [41] thus the bright areas in CSLM images of sugar linked SBS containing pyridinium pendants corresponds to functionalized butadiene domain and dark region correspond to polystyrene domain.
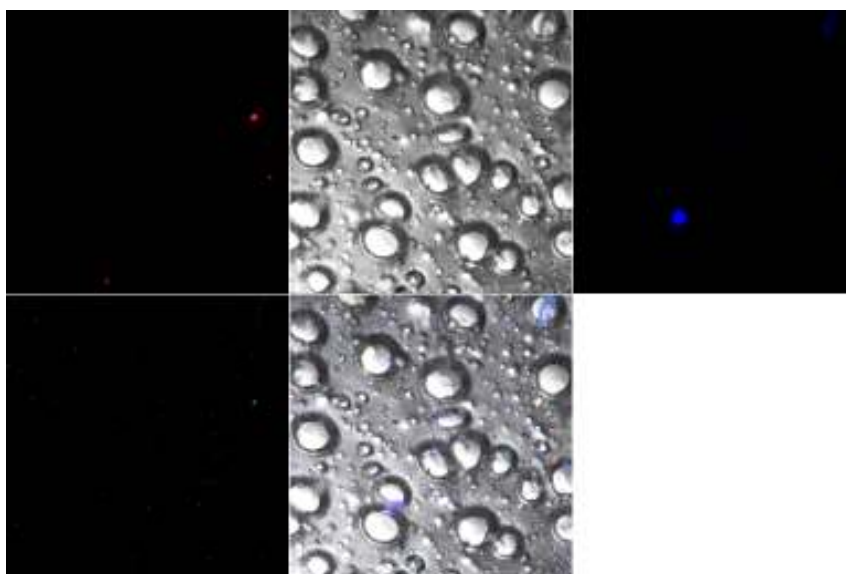
Figure 4. 6 Confocal microscopy images of SBS at 63 X with excitation wavelength (a) 488 nm (b) 543 nm (c) 405 nm
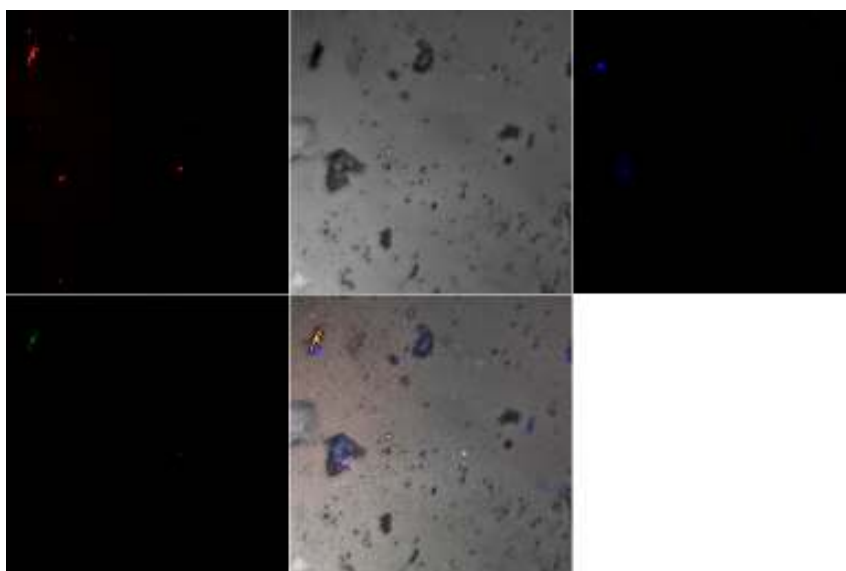
Figure 4. 7 Confocal microscopy images of epoxidized SBS at 63 X with excitation wavelength (a) 488 nm (b) 543 nm (c) 405 nm

SBS and partially epoxidized SBS shows very weak background fluorescence in all three colour region green, red and blue as shown in figure 4.6 and 4.7. The

morphology of the functionalized SBS cannot be visualized due to this weak fluorescence and a dark background is observed.

Figure 4. 8 Confocal microscopy images of glucose linked SBS at 63 X with excitation wavelength (a) 488 nm (b) 543 nm (c) 405 nm

Glucose linked SBS containing pyridinium pendants shows weak fluorescence intensity in red and blue region and comparatively strong intensity in green region as shown in figure 4.8. The morphology is this case is not well resolved and is blurred due to low fluorescence intensity but the resolution is many fold higher than SBS and partially epoxidized SBS which on account of absence of fluorescence shows a featureless dark region. The bright areas in figure 4.8 correspond to functionalized butadiene domain and dark region correspond to polystyrene domain.
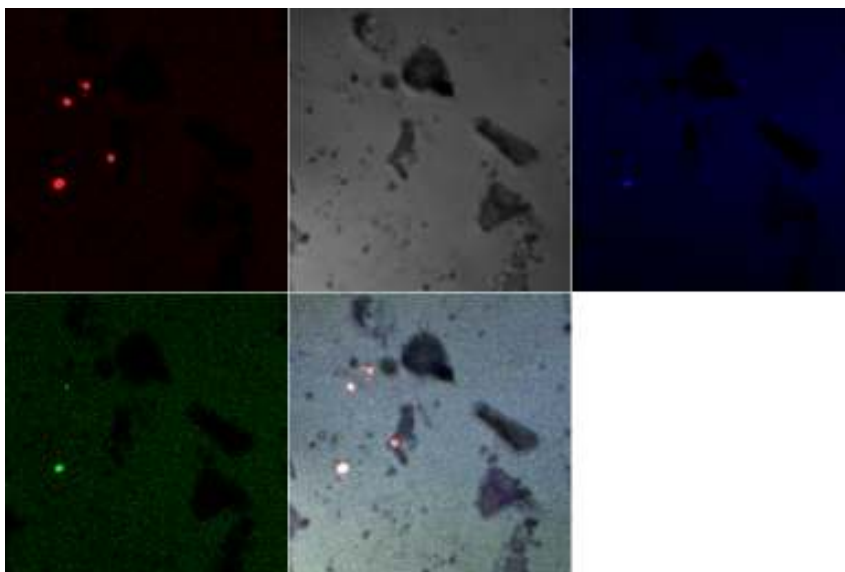
Figure 4.9 Confocal microscopy images of mannose linked SBS at 63 X with excitation wavelength (a) 488 nm (b) 543 nm (c) 405 nm

CSLM images of Mannose linked SBS containing pyridinium pendants are shown in figure 4.9. The fluorescence intensity is of medium intensity but still the morphology is well resolved. The bright and dark region corresponds to functionalized butadiene domains and polystyrene domains respectively. The fluorescence intensity is highest in green region, while it is least in red region. The image in the red region provides a blurred view of the morphology on account of low fluorescence intensity in that region.

Chapter 4
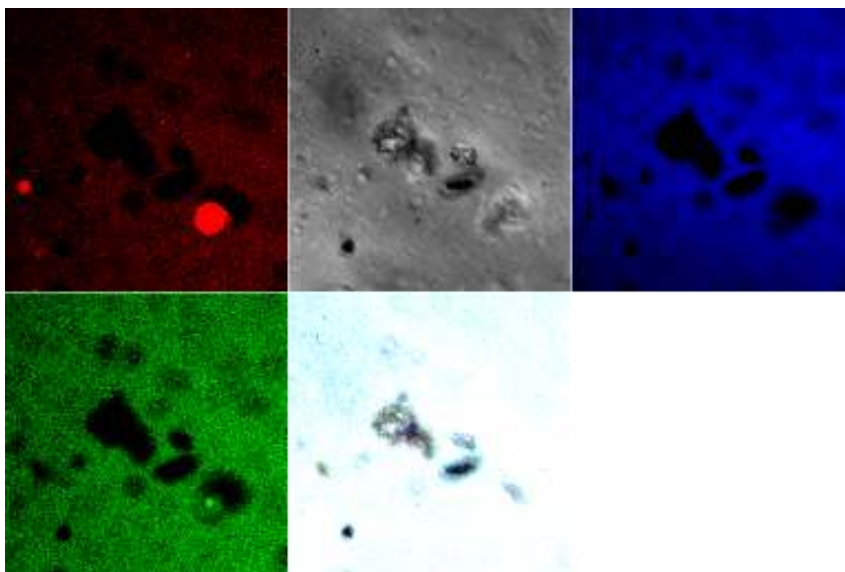
Figure 4.10 Confocal microscopy images of maltose linked SBS at 63 X with excitation wavelength (a) 488 nm (b) 543 nm (c) 405 nm

CSLM images of Maltose linked SBS containing pyridinium pendants are shown in figure 4.10. The fluorescence intensity is high in all three colour region providing to good image contrast. The morphology is well resolved in all three colour regions showing the heterogenous nature of the components in functionalized SBS. The fluorescence intensity as seen in confocal microscopy images of the maltose linked SBS is highest among all the other sugar linked SBS samples. Thus, maltose linked SBS appears to be of interest for studying various applications.
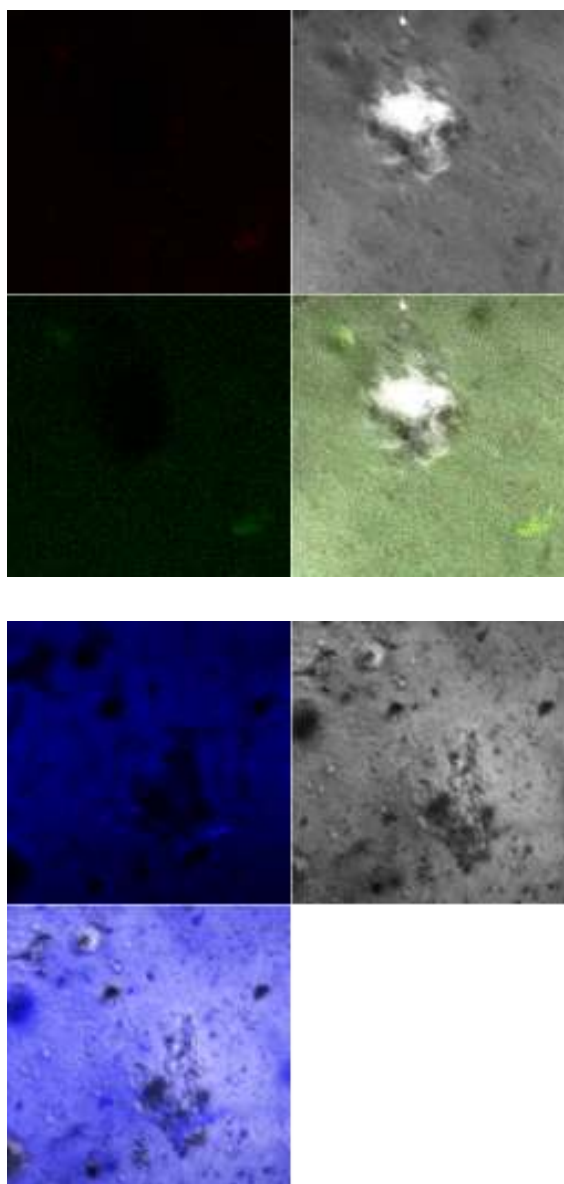
Figure 4.11 Confocal microscopy images of galactose linked SBS at 63 X with excitation wavelength (a) 488 nm (b) 543 nm (c) 405 nm

CSLM images of Galactose linked SBS containing pyridinium pendants are shown in figure 4.11. Fluorescence intensity is high only in blue region and the morphology of the polymer is well resolved in this region. The green region has less intensity with red having the least intensity, thereby providing poorly resolved morphological images in these regions.
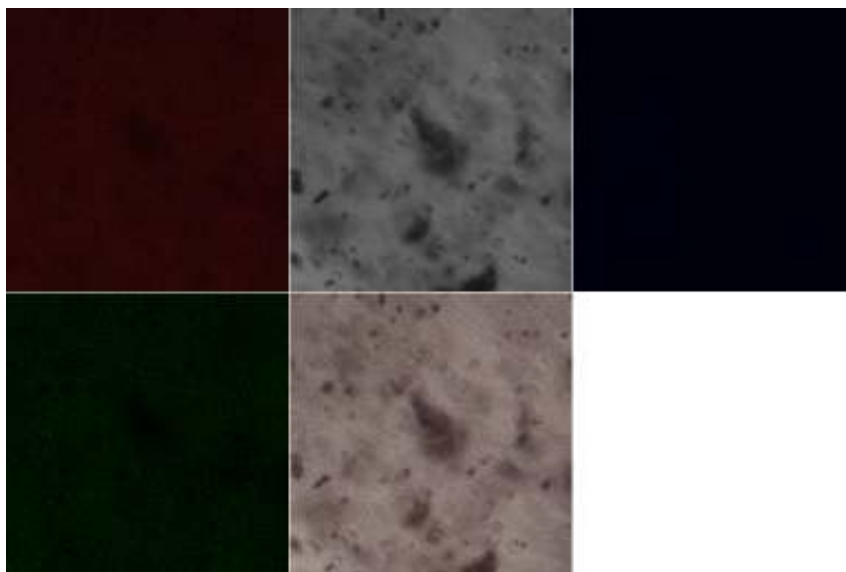
Figure 4.12 Confocal microscopy images of xylose linked SBS at 63 X with excitation wavelength (a) 488 nm (b) 543 nm (c) 405 nm

CSLM images of Xylose linked SBS containing pyridinium pendants are shown in figure 4.12. Fluorescence intensity is low in green and red region and is absent in blue region. The fluorescence images are mostly featureless in terms of morphology and show some faint dark spots corresponding to polystyrene domain.
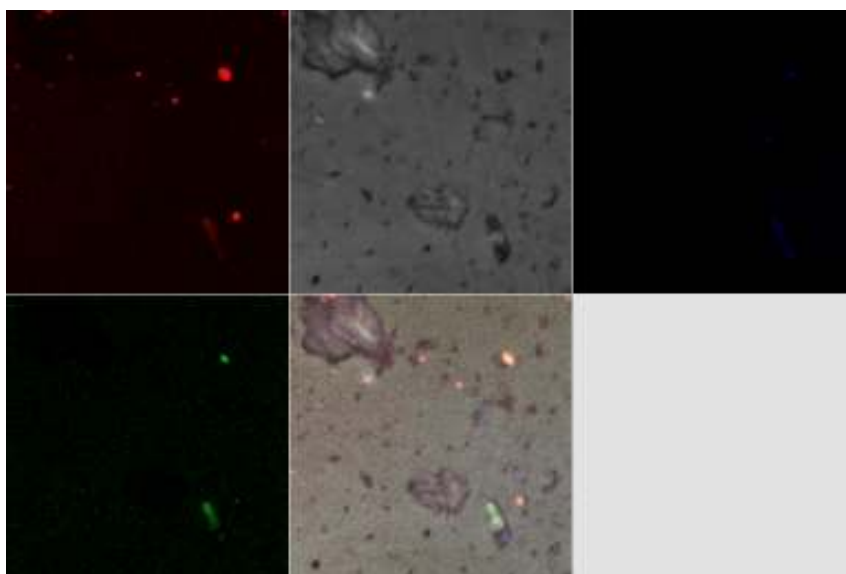
Figure 4.13 Confocal microscopy images of fructose linked SBS at 63 X with excitation wavelength (a) 488 nm (b) 543 nm (c) 405 nm
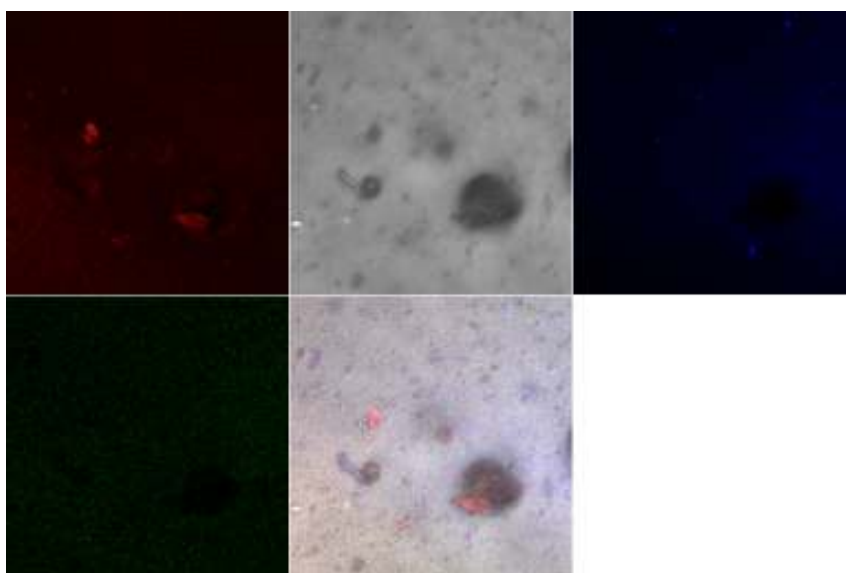
Figure 4. 14 Confocal microscopy images of sucrose linked SBS at 63 X with excitation wavelength (a) 488 nm (b) 543 nm (c) 405 nm
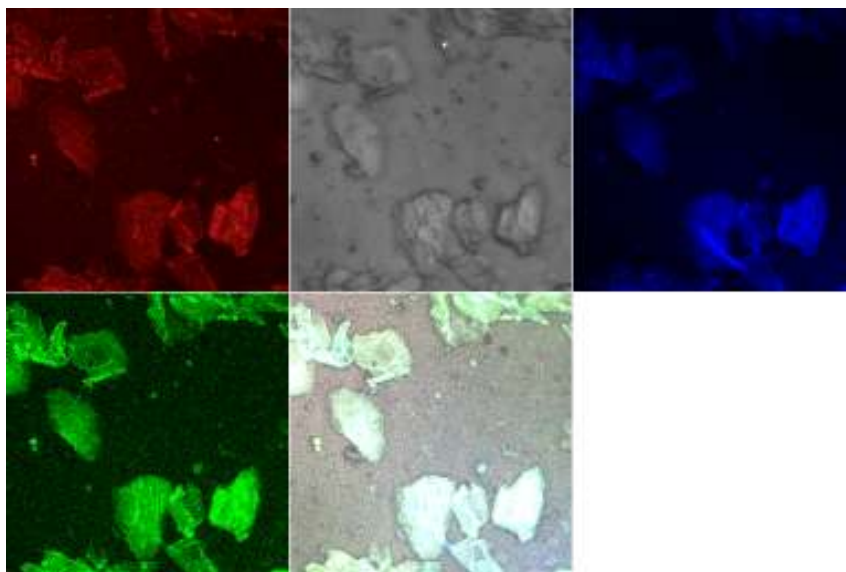
Figure 4.15 Confocal microscopy images of methyl glucoside linked SBS at 63 X with excitation wavelength (a) 488 nm (b) 543 nm (c) 405 nm

Figures 4.13-4.15 shows Fructose, sucrose and Methyl glucoside linked SBS respectively containing pyridinium pendants. These samples are partially functionalized with relatively high residual epoxide content (as discussed in chapter 2). Fructose linked SBS shows low intensity and sucrose linked SBS shows medium fluorescence intensity in the entire three colour region. Methyl glucoside linked SBS shows very high fluorescence intensity and well resolved morphology in all three colours; green, red and blue. The polystyrene domain instead of appearing dark appeared coloured (figure 4.15). This is a departure from the observed trend in other two samples, while all the other sugars have a hydroxyl at the anomeric C, in methyl glucoside we have a methoxy group at the anomeric C. However a detailed study of this aspect was beyond the scope of this study.

Confocal scanning laser fluorescence microscopy analysis of different sugar like glucose, mannose, galactose, maltose, xylose, fructose, sucrose and methyl glucoside linked SBS bearing pyridinium pendants showed fluorescence with varying intensity. The fluorescence was observed in the functionalized butadiene

domains only, while the polystyrene domains showed up as dark spots leading to successful image contrast needed for 3 D imaging of polymer morphology. The noteworthy observations are that:

(i) The image contrast was achieved without attaching any fluorescent tag against the common practice for obtaining images using Confocal scanning laser fluorescence microscopy technique.

(ii) Different sugars showed varying fluorescence intensity in different colour regions.

(iii) Blocking the anomeric carbon showed dramatic increase in fluorescence intensity

These results may be helpful in designing new biocompatible systems, the shelf life of which can be studied more easily than the system which requires tagging with fluorescent probes.

4.3.4 Biocompatibility (cell viability) study of carbohydrate functionalized SBS films

Biocompatibility is a measure of cell viability or cytotoxicity. The cytotoxicity of pyridinium and quaternary ammonium groups containing polymers have been reported by different groups and strongly depend on concentration of cationic charges, the type of alkyl group attached to the quaternized N atom and hydrophilicity of the polymers among other factors (discussed in detail in antimicrobial activity section of this chapter). The phospholipids bilayer comprising the membrane of normal mammalian cells are asymmetrically distributed. The outer layer is composed mainly of zwitterionic phosphatydicholine and sphingomyelin phospholipids, while the inner layer is

composed of negatively charged phosphatydilserine [42]. The toxicity (decreased cell viability) of the cationic groups on the polymer chain is attributed to the disruption of the mammalian cell membrane by its electrostatic attraction to the negative cell surface groups resulting in lysis of the cell leading to cell death.
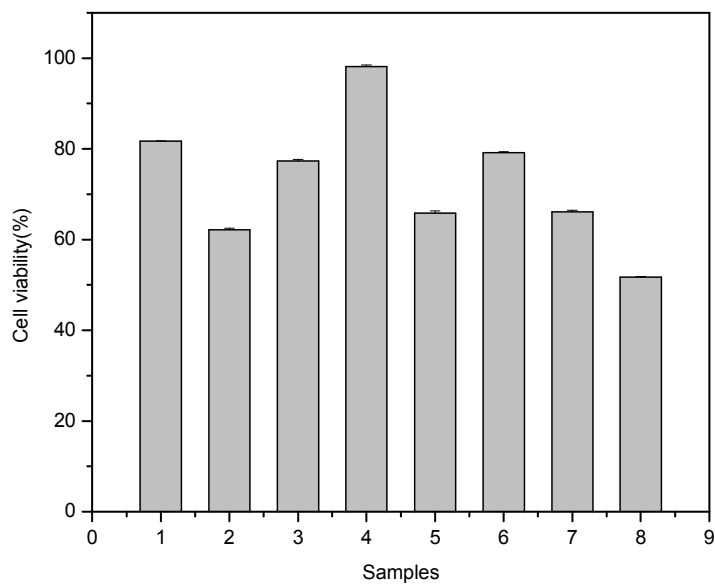
Figure 4.16 Cell viability of human THP-1 monocytes on (1) SBS (2) SBS Epoxide (3) Hydro chlorinated SBS (4) maltose linked SBS (5) galactose linked SBS (6) xylose linked SBS (7) mannose linked SBS (8) glucose linked SBS
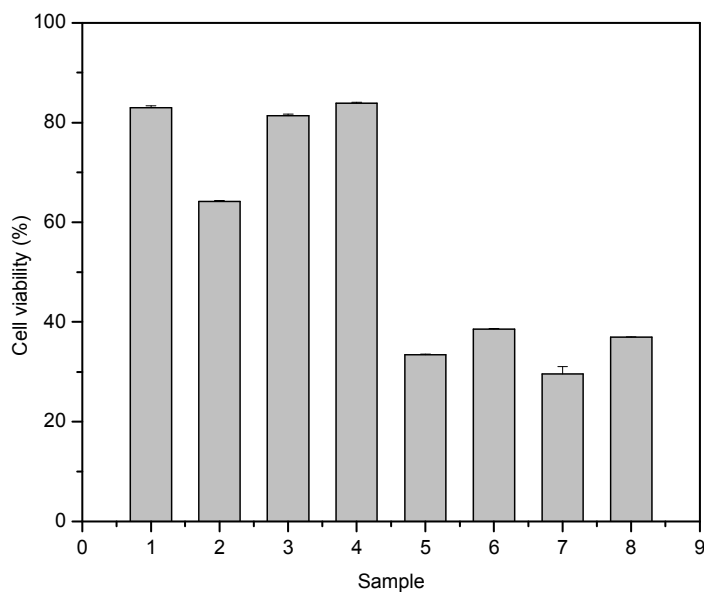
Figure 4.17 Cell viability of human HL-60 monocytes on (1) SBS (2) SBS Epoxide (3) Hydro chlorinated SBS (4) maltose linked SBS (5) galactose linked SBS (6) xylose linked SBS (7) mannose linked SBS (8) glucose linked SBS

Table 4.2 Cell viability data of THP-1 and HL-60 monocyte cells with sugar linked SBS

	Sample	Cell Viability (%)		Sugar[b] content (wt %)	Nitrogen[c] content (at. %)	Residual[a] epoxide%
		THP-1	**HL-60**			
1	SBS	81.652	82.967	0.00	0.00	0.00
2	SBS Epoxide	62.121	64.151	0.00	0.00	100
3	Hydro-chlorinated SBS	77.339	81.398	0.00	0.00	10.8
4	Maltose linked SBS	98.123	83.858	0.37	1.68	7.3
5	Galactose linked SBS	65.876	33.402	0.16	1.53	4.8

6	Xylose linked SBS	79.168	38.575	0.11	ND[d]	0.00
7	Mannose linked SBS	66.127	29.594	0.12	ND[d]	8.00
8	Glucose linked SBS	51.679	36.935	0.09	ND[d]	10.5

[a] calculated from ^{1}H NMR, [b] As determined by phenol-sulphuric acid assay, [c] As determined by XPS, [d] expected to be in the range of 1.5 to 1.7 at. %, ND- not determined

The viability of THP-1 and HL-60 cancer cells on SBS functionalized with different sugars having quaternary nitrogen pendants shown in figure 4.16-4.17 was determined by MTT assay. The MTT is a tetrazolium 3-(4,5-dimethylthiazolyl)-2,5 diphenyltetrazolium bromide) salt that is oxidized by mitochondrial dehydrogenase in living cells to form purple formazan product, damaged or dead cell show no or reduced dehydrogenase activity. The MTT assay is entirely comparative and was carried out using positive control. The absorbance of 490 nm light is directly proportional to the number of viable cells. The results, shown in figure 4.16-4.17 are plotted in units of viability percentage calculated using relation 1.

Cell viability was calculated using the following relationship:

Cell viability % = (OD$_{490}$ sample / OD$_{490}$ control) X 100 ……………..…………1

OD sample= OD of the well treated with different sugar linked SBS having quaternary nitrogen pendants, in the medium

OD control= OD of the wells treated with the medium only without polymer.

The results of this study are shown in Table 4.2 which shows the structure-toxicity effect of functionalized SBS as compared to unmodified SBS on cell viability of THP-1 and HL-60 monocyte cells. SBS shows similar cell viability (81.6 and 82.9%) with both THP-1 and HL-60 cell lines as shown in Table, whereas the viability is significantly reduced in partially epoxidized SBS (62.1 and 64.1%) indicating cytotoxic nature of the epoxidized SBS [43]

The hydro chlorinated SBS have neither sugar and nor quaternary nitrogen/nitrogen containing group and have only covalently linked chlorine and hydroxyl group on the butadiene segment of SBS. Although hydro chlorinated SBS have covalently attached chlorine and residual epoxide it shows cell viability (77.4 and 81.4%) comparable with SBS (81.6 and 82.9 %). This shows that hydro chlorination of SBS does not induce much cytotoxicity. It has limited effect on the cell viability (77.4%) withTHP-1 cell line, which may be due to the residual epoxide. Hydro chlorination has negligible effect on HL-60 cell line which shows almost similar cell viability (81.4%) as unmodified SBS (82.9%). Since all the sugar linked SBS have similar hydro chlorinated components (calculated from ^{1}H NMR integration of sugar linked SBS), they are expected to have limited effect on decreasing cell viability (cytotoxicity) based on the above observations with hydro chlorinated SBS.

Thus, cell viability of SBS functionalized with sugar containing hydro chlorinated and quaternary nitrogen will depend on the anchored sugar weight% and nitrogen contact. Biocompatibility is influenced by the incorporated biocompatible sugar monomers and the nitrogen containing groups. While the anchored sugar will have positive effect on the biocompatibility, the nitrogen containing moiety will have a

negative effect. The overall cell viability (biocompatibility) is determined by the net effect of these two opposing factors.

The order of cell viability among the sugar linked SBS for THP-1 cells was *Maltose linked SBS > Xylose linked SBS > Galactose linked SBS, Mannose linked SBS > Glucose linked SBS.* Maltose linked SBS with 0.37 wt% maltose showed 98.1% cell viability (completely biocompatible) while Glucose linked SBS with 0.09 wt% glucose showed the least cell viability (51.7%). Galactose linked SBS and Mannose linked SBS having sugar content of 0.16 wt% and 0.12 wt% respectively showed similar cell viability (65.8 and 66.1%). Xylose linked SBS with 0.11 wt% xylose showed much higher cell viability (79.1%), this may be due to the absence of residual epoxide which has inhibitory effect on cell proliferation thereby reducing cell viability.

Thus, the cell viability of all the sugar linked SBS except Maltose linked SBS was less than unmodified SBS. This is due to the cell inhibitory effect of quaternary nitrogen pendants present in all the sugar linked SBS, which causes cell death resulting in decreasing value of cell viability. This effect is countered by the anchored sugar which increases the cell viability. A minimum weight percentage of biocompatible sugar monomers are needed to completely neutralize the effect of quaternary nitrogen groups higher amounts of sugar will have an overall positive effect on cell viability as exemplified by maltose linked SBS showing 98.1% cell viability having 0.37 wt% sugar; highest among all the sugar linked SBS samples. Thus, we seem to have on hand a modified synthetic polymer that shows close to 100 % cell viability (biocompatibility), and this system is proposed to be developed further for investigation with more cell lines and with greater extent of maltose content.

The HL-60 cells showed less viability with all the sugar linked SBS as compared to THP-1 cells. Maltose linked SBS showed slightly higher cell viability (83.9%) than SBS (82.9%) and the rest of sugar linked SBS entries 5-8 (Table 4.2) showed significantly reduced cell viability. It seems that HL-60 cell are more prone to cell inhibition with the functionalized SBS as compared to THP-1 cells.

Thus evaluation of biocompatibility of carbohydrate functionalized SBS containing quaternary nitrogen groups gave insight into the structure-toxicity of the elastomeric polymers. It also showed that anchoring of biocompatible monomers is not the only criteria of achieving biocompatibility and the type of functional groups also has significant influence on the biocompatibility of polymeric materials.

4.3.5. Antimicrobial Activity of different sugar linked SBS polymer

Biomedical devices, water storage systems and health care products etc. suffer from high risk of microbial contamination. Biomaterials used in body implant carries the risk of bacterial infection once implanted. The bacteria associated with these infections have often been found to be antibiotic resistant causing life threatening situations for patients undergoing these implants. With the ever increasing use of biomaterials it becomes imperative to develop advanced biomaterials having antimicrobial activities along with biocompatibility and other desired mechanical and physical properties.

Polymeric microbicides have been studied for long years as an attractive alternative to common low molecular weight microbicides mainly because of ease of synthesis on industrial scale, economic viability, stability towards enzymatic degradation [44], non-volatility [45], impermeability to skin [45] and ease of tailoring the functionalization.

Quaternary ammonium and pyridinium based polymers are the most extensively studied antimicrobial polymers [46]. These polymers show antimicrobial action through electrostatic action of the cation to the negatively charged groups on the bacterial cell membrane thereby rupturing and killing it [47]. But these polymers/ ionomers are known to be toxic to mammalian cells due to poor biocompatibility. There have been few studies on synthetic polymeric materials possessing both biocompatibility and antimicrobial activity having no toxicity to mammalian cells.

Since ammonium and pyridinium based polymers are the most widely explored antimicrobial materials, we need to find ways to reduce the cytotoxicity of these polymers. Researchers have tried to circumvent this problem by optimizing hydrophobic-hydrophilic balance by copolymerization of vinyl pyridines with hydrophilic and biocompatible monomers like polyethyleneglycol methyl ether methacrylate (PEGMA) and hydroxyethyl methacrylate (HEMA) [48]. It has been observed by Youngblood et al. that antibacterial activity of quaternized poly(vinyl pyridine) is increased by incorporation of even 1% of HEMA . This was explained by increased hydrophilicity of the material due to the introduction of pendant hydroxyl functionality [49]. Hydroxyl groups promote water interaction with the material bringing bacteria in contact with polymer and spreading it on the surface, thus increasing the antimicrobial activity. In case of highly hydrophobic surface the bacterial interaction with the surface containing antimicrobial moiety is reduced causing decreased antimicrobial activity.

Knowledge of the structure–activity relationship (SAR) allows for the possibility to design and synthesize new cationic amphiphiles with optimized antimicrobial activities for future development. Thus, positive charge, length of alkyl tail on N, hydrophilicity and spatial positioning of positive charge and hydrophobic alkyl tail

[44] are the factors which govern the antimicrobial activity- biocompatibility of a polymer and these needs to be optimized to achieve maximum microbial cell membrane disruption and minimum mammalian cell cytotoxicity. Biocompatibility of microbicidal polymers is one research focus which will help understand the feasibility and limitations of our modified SBS polymers in contact with human body.

Although functionalization of the SBS elastomer has been an interesting and challenging area of research, yet there are only few examples of modification of diene-elastomers. Synthesis of ionomers by ring opening of epoxidized SBS, like sulphonated, phosphated, maleated and quaternary ammonium ionomers has been reported in literature, but to the best of our knowledge there is no reference on carbohydrate functionalization of SBS, nor has evaluation of antimicrobial activities of these ionomers ever been carried out.

Sugars are well known biocompatible hydrophilic molecules and their introduction in polymers is known to introduce biocompatibility [50]. Hence, we hypothesized that functionalization of SBS a hydrophobic synthetic thermoplastic elastomer with sugars will impart biocompatibility, while incorporation of quaternary pyridinium and ammonium moieties will provide the necessary antimicrobial activity to the polymer.

This section of the chapter investigates the influence of sugar and quaternary pyridinium pendants introduced on SBS (synthesis and characterization described in chapter 1) on antimicrobial activities of the functionalized SBS. The antimicrobial activities were determined against bacterial cultures Escherichia coli k-12, Bacillus sp. and yeast cultures Pichia stipitis NCIM 3499, Pichia stipitis NCIM 3497 using a nutrient agar method.

 The results of antimicrobial studies are presented in Table 4.3- 4.6 for the different micro-organisms on different sugar linked SBS containing quaternary nitrogen pendants.

4.3.6 Antimicrobial activity of different sugar linked SBS films containing quaternary nitrogen pendants with E. coli

The effect on the growth of E. coli with different sugar linked SBS films, containing quaternary nitrogen pendants is presented in Table 4.3. It shows the decrease in optical density in sugar linked SBS (reflecting material antibacterial activity) is much less than the starting polymer (SBS) and even the control. It is well established that optical density (OD) is directly proportional to the bacterial cell concentration [51]; hence it decreasing value reflects the bactericidal property of the material.

 Table 4.3 Effect of different sugar linked SBS films containing quaternary nitrogen pendants on the growth of E. coli.

	Sample	OD after 24 h	Inhibition %[a] after 24 h	Sugar[b] content (wt %)	Nitrogen[c] content (at %)
1	SBS	0.8374	2.14	0.00	-
2	SBS Epoxide	0.8172	4.46	0.00	-
3	Glucose linked SBS	0.7718	9.80	0.09	ND[d]
4	Mannose linked SBS	0.7136	16.60	0.12	ND[d]
5	Galactose linked SBS	0.6835	20.12	0.16	1.53
6	Maltose linked SBS	0.6929	19.02	0.37	1.68

7	Xylose linked SBS	0.7168	16.23	0.11	ND[d]
	Control	0.8557			

[a] calculated by the difference between the number of colonies from bacteria with samples and that from bacteria in control, [b]As determined by phenol-sulphuric acid assay, [c] As determined by XPS, [d] expected to be in the range of 1.5 to 1.7 at. %, ND- not determined

It can be seen from above Table 4.3 that all the functionalized SBS samples shows bactericidal property compared to SBS, which is negligible. The bactericidal activity measured after 24 h is in the following order: galactose linked SBS > maltose linked SBS > mannose linked SBS > xylose linked SBS > glucose linked SBS > SBS epoxide > SBS. Thus galactose linked SBS shows the highest activity and glucose linked SBS shows the least activity.

As compared to unmodified SBS the bactericidal activity of galactose and maltose linked SBS is enhanced by 10 fold, mannose and xylose linked SBS by 8 fold and glucose linked SBS by 5 fold. Thus carbohydrate functionalized SBS containing quaternary nitrogen shows significantly higher bactericidal activity.

Introduction of even 0.45 (at. %) of quaternary nitrogen moieties leads to 20% E. coli inhibition in the galactose linked SBS. All the functionalized SBS's, (entries number 3-7) in Table 4.3 shows bacterial growth inhibition ranging from 9.8% to 20%. It is well established that pyridinium and quaternary ammonium groups are responsible for antimicrobial activity in a polymer; hence their incorporation in SBS results in the observed antibacterial activity.

Except glucose linked SBS all the other carbohydrate functionalized SBS shows antimicrobial activity in the same range. Glucose linked SBS has comparatively more residual epoxide (from ^{1}H NMR analysis) which may results in less incorporation of quaternary nitrogen groups leading to comparatively less antimicrobial activity.

4.3.7 Antimicrobial activity of different sugar linked SBS films containing quaternary nitrogen pendants with Bacillus sp.

From Table 4.4 it can be seen that galactose linked SBS (14.28%) shows highest bactericidal property followed by xylose linked SBS (11.85%), while glucose linked SBS shows the least activity. Overall the antibacterial activity of all the functionalized SBS against Bacillus sp. is less as compared to antibacterial activity against E. coli.

Table 4.4 Effect of different sugar linked SBS films containing quaternary nitrogen pendants on the growth of Bacillus sp.

	Sample	OD after 24 h	Inhibition % relative to Control	Sugar[b] content (wt %)	Nitrogen[c] content (at %)
1	SBS	0.8317	1.38	0.00	-
2	SBS Epoxide	0.8268	1.96	0.00	-
3	Glucose linked SBS	0.7964	5.57	0.09	ND[d]
4	Mannose linked SBS	0.7567	10.27	0.12	ND[d]
5	Galactose linked SBS	0.7229	14.28	0.16	1.53
6	Maltose linked SBS	0.7637	9.45	0.37	1.68

7	Xylose linked SBS	0.7434	11.85	0.11	ND[d]
	Control	0.8434			

[a] calculated by the difference between the number of colonies from bacteria with samples and that from bacteria in control, [b]As determined by phenol-sulphuric acid assay, [c] As determined by XPS, [d] expected to be in the range of 1.5 to 1.7 at. %, ND- not determined

4.3.8 Antimicrobial activity of different sugar linked SBS films containing quaternary nitrogen pendants with P. stipitis NCIM 3499

From Table 4.5 it can be seen that galactose linked SBS (13.4%) shows highest inhibition (microbicidal property) followed by mannose linked SBS (12.64%). once again glucose linked SBS shows the least activity (4.9 %). All the other functionalized SBS samples show comparatively less activity.

Table 4.5 Effect of different sugar linked SBS films containing quaternary nitrogen pendants on the growth of P. stipitis NCIM 3499

	Sample	OD after 24 h	Inhibition %[a] after 24 h	Sugar[b] content (wt %)	Nitrogen[c] content (at %)
1	SBS	1.2372	3.14	0.00	-
2	SBS Epoxide	1.2537	1.8	0.00	-
3	Glucose linked SBS	1.2149	4.9	0.09	ND[d]
4	Mannose linked SBS	1.1159	12.64	0.12	ND[d]
5	Galactose linked SBS	1.1063	13.4	0.16	1.53
6	Maltose linked SBS	1.1361	8.7	0.37	1.68
7	Xylose linked SBS	1.1878	7.0	0.11	ND[d]
	Control	1.2774			

4.3.9 Antimicrobial activity of different sugar linked SBS films containing quaternary nitrogen pendants with P. stipitis NCIM 3497

From Table 4.6 it can be seen that maltose linked SBS (24 %) shows highest inhibition (microbicidal property) followed by xylose linked SBS (21.3 %), and mannose linked SBS (20.44 %), while glucose linked SBS shows the least activity (3.82 %). Overall the antimicrobial activity of all the functionalized SBS samples against P. stipitis NCIM 3497 is similar to activity shown by E. coli.

Table 4.6 Effect of different sugar linked SBS films containing quaternary nitrogen pendants on the growth of P. stipitis NCIM 3497

	Sample	OD after 24 h	Inhibition %[a] after 24 h	Sugar[b] content (wt %)	Nitrogen[c] content (at %)
1	SBS	1.1484	3.3	0.00	-
2	SBS Epoxide	1.1636	2.0	0.00	-
3	Glucose linked SBS	1.1419	3.82	0.09	ND[d]
4	Mannose linked SBS	0.9445	20.44	0.12	ND[d]
5	Galactose linked SBS	0.9859	17.0	0.16	1.53
6	Maltose linked SBS	0.9027	24.0	0.37	1.68
7	Xylose linked SBS	0.9344	21.3	0.11	ND[d]
	Control	1.1873			

a calculated by the difference between the number of colonies from bacteria with samples and that from bacteria in control, [b]As determined by phenol-sulphuric

acid assay, [c] As determined by XPS, [d] expected to be in the range of 1.5 to 1.7 at. %, ND- not determined

Figure 4.22 and table 4.7 shows the result for the antimicrobial test for the different carbohydrate functionalized SBS having cationic nitrogen pendants against bacterial and yeast cultures. SBS and partially epoxidized SBS (SBS EP) which does not contain cationic nitrogen nor carbohydrate pendants did not show much antimicrobial activity. However, the growth inhibition of the carbohydrate functionalized SBS having cationic nitrogen pendants was markedly enhanced.

Table 4.7 Summary of growth inhibition after 24h with carbohydrate functionalized SBS having quaternary nitrogen pendants against E. coli, Bacillus sp., Pichia stipitis NCIM 3499 and Pichia stipitis NCIM 3497.

Sample	E. Coli (Inhibition % after 24 h)	Bacillus sp. (Inhibition % after 24 h)	Pichia stipitis NCIM 3499 (Inhibition % after 24 h)	Pichia stipitis NCIM 3497 (Inhibition % after 24 h)
SBS	2.14	1.38	3.14	6.3
SBS Epoxide	4.46	1.96	1.8	
Glucose linked SBS	9.80	5.57	4.9	3.82
Mannose linked SBS	16.60	10.27	12.64	20.44
Galactose linked SBS	20.12	14.28	13.4	17.0
Maltose linked SBS	19.02	9.45	8.7	24.0
Xylose linked SBS	16.23	11.85	7.0	21.3
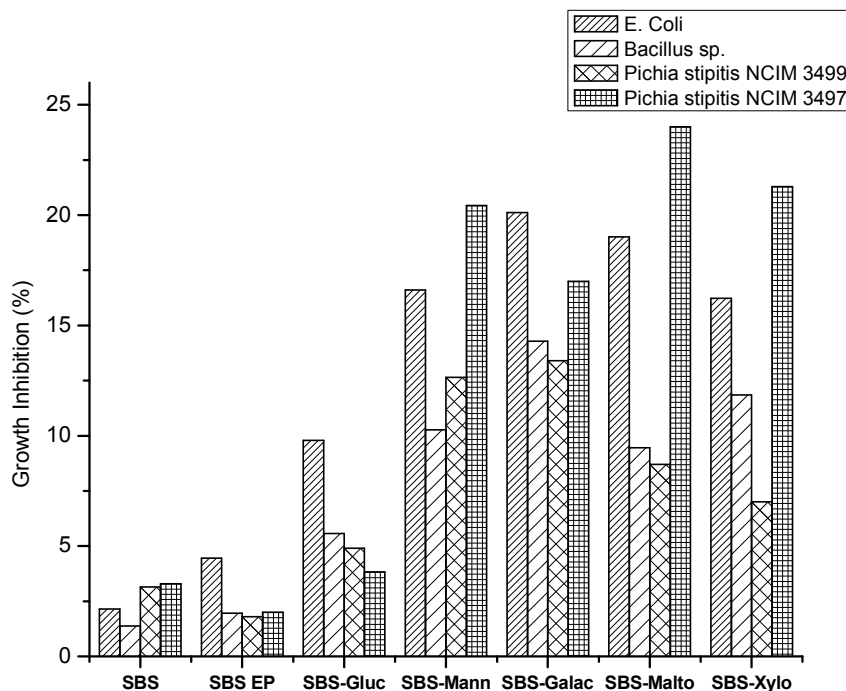
Figure 4.18 Growth inhibition after 24h with carbohydrate functionalized SBS having cationic nitrogen pendants against E. coli, Bacillus sp., Pichia stipitis NCIM 3499 and Pichia stipitis NCIM 3497.

The graphical representation of data as shown in figure 4.18 clearly shows the extent of antimicrobial properties exhibited by different samples.

SBS showed 2.14 % growth inhibition against E. coli and 1.38%, 3.14%, 3.3% against Bacillus sp., Pichia stipitis NCIM 3499 and Pichia stipitis NCIM 3497 respectively. Thus expectedly unmodified SBS can be considered not to have antimicrobial properties.

 The growth inhibition for galactose linked SBS (SBS-Galac) reached 20% and 17% against E. coli and Pichia stipitis NCIM 3497 respectively. Similarly growth inhibition for Maltose linked SBS (SBS-Malto) was 19% and 24 % against E. coli and Pichia stipitis NCIM 3497 respectively, whereas it proved to be less effective in

inhibiting the growth of Bacillus sp. and Pichia stipitis NCIM 3499. Mannose linked SBS (SBS-Manno) and Xylose linked SBS (SBS-Xylo) showed similar growth inhibition against E. coli and Pichia stipitis NCIM 3497. Among all the sugar linked SBS, Glucose linked SBS (SBS-Gluco) showed the least growth inhibition (3.8-9.8%) against all the four micro-organisms.

These result indicate that quaternary nitrogen groups are responsible for the antimicrobial property of the sugar linked SBS. Besides, quaternary nitrogen groups; antimicrobial activity also depends on the hydrophilicity of the polymer which is detailed in the introduction of this section. Introduction of sugar in SBS leads to introduction of pendant hydroxyl functionality. Hydroxyl groups promote water interaction with the polymeric films bringing bacteria in contact with polymer and spreading it on the surface, thus enhancing the antimicrobial activity.

Thus, Even though the concentration of quaternary nitrogen is in the range of 0.4-0.45 at% (calculated from XPS) still the growth inhibition is significant, which could be increased to nearly 100% by increasing the quaternary nitrogen content in the functionalized SBS. Antimicrobial activity primarily depends on quaternary nitrogen content but it also depends on hydrophilicity of the polymer among other factors. Our polymers have both the required functionality and are promising biomaterials for use as antimicrobial polymers.

The current challenge facing the field of polymeric biocides is the reduction of toxicity in antimicrobial polymers. Since sugar monomers increases the biocompatibility and decreases the toxicity to mammalian cells, this sugar effect on antimicrobial activity when studied quantitatively in detail will be helpful in gaining useful insight that could be used to design antimicrobial polymers with minimal cytotoxicity.

4.4. Conclusion

From the above studies discussed in this chapter, we conclude that, the functionalized SBS showed UV activity and enhanced fluorescence of varying intensity depending on the type and amount of linked sugar. Confocal laser scanning microscopy (CLSM) revealed that the fluorescence occurred selectively in butadiene segment of SBS, leading to morphological observations of appearance of surface and inner layers of sugar functionalized SBS. We believe this was perhaps the first study where labelling of a polymeric component with fluorescent dye was not needed to visualize the morphology of a polymeric system by CLSM. The applications of functionalized SBS were determined by in-vitro biocompatibility tests employing HL-60 and THP-1 cell lines. It was found that sugar content had a positive effect on biocompatibility, whereas quaternary nitrogen groups adversely affected the biocompatibilities of the sugar linked SBS samples. Antimicrobial studies of these polymers showed significant microbicidal effect even at low concentration of quaternary nitrogen functionality.

4.5. References:

1. D.J Chauvel-lebret; P. Auroy; M. Bonnaur-Mallet, *Biocompatibility of elastomers chapter 13* **2002**, In: S. Dumitriu, Editor, Polymeric Biomaterials, Marcel Dekker Inc**.,** New York

2. A. S. Kulshrestha, A. Mahapatro, *Polymers for biomedical applications chapter 1* **2008**, ACS; B. D. Ratner, A. S. Hoffman, F. J. Schoen, J. E. Lemon, *Biomaterials Science* **1996**, Eds Academic Press, Orlando

3. S. Ramakrishna, Biomedical applications of polymer composite materials. *Proc. Of the second Asian-Australian Conference on Composite Materials (ACCM-2000) p. 431-436* **2000**, Advanced Institute of Science and Technology, Korea

4. T. C. Ward, J. T. Perry, *J. Biomed. Mater. Res.* **1981**, *15*, 511-525

5. M. Elices, *Structural Biological Materials: Design and Structure- Property Relationships*; 2000, Elsevier Science Ltd., New York

6. R. Guidon, M. King, Y. Marois, P. Ukpabi, X. Ding, Z. Zhang, C. Yang, B. Badour, G. Laroche, L. Martin, *ASAIO* **1997**, 43, 69

7. J. Jiang, A. R. Webb, S. J. Pickerill, G. Hageman, G. A. Ameer, *Biomaterials* **2006**, 27, 1889-1898

8. C. Batich, D. DePalma, *J. Long-Term Effects Med. Implants* **1992**,1, 255

9. R. C. Spencer, *Journal of Hospital Infection* **1999**, 43, S 127

10. J. E. Puskas, Y. Chen, *Biomacromolecules* **2004,** 5, 1141-1154

11. S. Biltresse, M. Attolini, J. Marchand-Brynaert, *Biomaterials* **2005***,* 26, 4576; A. Papra, M. Ayerbe, J. Ramos, J. Forcada*, J. Polym. Sci.* **1999***,* 74, 1699; S. J. Xiao, S. Brunner, M. Wieland, *J. Phys. chem. B* **2001**, 108, 16508

12. J. Klein, *Makromol. Chem., Rapid Commun.* **1989**, 10, 629

13. S. I. Nishimura, T. Furuike, K. Matsuoka, K. Maruyama, K. Nagata, K. Kurita, N. Nishi, S. Tokura, *Macromolecules* **1994**, 27, 4876

14. T. Nakaya, K. Nishio, M. Memita, M. Imoto, *Makromol. Chem. Rapid Commun.* **1993**, *14*, 77

15. P. Galgali, A. J. Varma, U. S. Puntambekar, D. V. Gokhale, *Chemical communications (Cambridge, England)* **2002**, 2884-2885

16. T. Furuike, N. Nishi, S. Tokura, S. I. Nishimura, *Macromolecules* **1995**, 28, 7241

17. S. I. Nishimura, K. Matsuoka, T. Furuike, S. Ishii, K. Kurita, K. M. Nishimura, *Macromolecules* **1991**, 24, 4236

18. D. R. McClay, G. M. Wessel, R. B. Marchase, *Proc. Natl. Acad. Sci* **1981**, 78, 4975

19. L. Bech, T. Meylheuc, B. Lepoittevin, P. Roger, Journal *of Polymer Science Part A: Polymer Chemistry* **2007**, 45, 2172

20.   L. Ying,C. Yin, R. X. Zhuo, K. W. Leong, H. Q. Mao, E. T. Kang, K. G. Neoh *Biomacromolecules* **2003,** 4, 157-165

21.   J. J. Yoon, Y. S. Nan, J. H. Kim, J. G. Park, *Biotechnol. Bioeng.* **2002**, 78, 1-10

22.   K. Merrett, W. Liu, D. Mitra, K. D. Camm, C. R. McLaughlin, Y. Liu, M. A. Watsky, F. Li, M. Griffith, D. E. Fogg, *Biomaterials* **2009**, 30, 5403

23.   G. Ciapetti, E. Cenni, L. Pratelli, A. Pizzoferrato, *Biomaterials* **1993**, 14, 359-364

24. R. M. Shankar, T. K. Roy T. Jana, *Journal of Applied Polymer Science,* **2009**, 114, 732–741

25. T. Li, C. Zhou, M. Jiang, *Polymer Bulletin* **1991**, 25, 211-216

26.   I. E. Dell Erba, R. J. J. Williams, *Polymer Engineering and Science, 351-359, 2006*).

27. D. Wang, T. Imae, *J. Am. chem. Soc.* **2004**,126, 13204-13205

28.   M. A. Petti, T. J. Shepodd, R. E. Barrans, D. A. Dougherty *J. Am. chem. Soc.***1988**, 110, 6825

29. S. Y. Katayama, M. Ariyoshi, K. Ishihara, T. Hirano, H. Jingami, K. Morikawa, *J. Mol. Biol.* **2002**, 316, 711–723

30. B. F. Eichman, E. J. Rourke, J. P. Radicella, T. Ellenberger, *EMBO J.* **2003**, 19, 4898–4909

31. I. Richter, J. Minari, P. Xaxe, J. P. Lowe, T. D. James, K. Sakarai, S. D. Bull, J. S. Fossey, *Chem. Commun.*, 2008, 1082–1084

32. S. Nishiyama, M. Tajima, Y. Yoshida, *Journal of photopolymer science and technology* **2003**, 16,173-180

33. E. M. Kosower, P. E. Klinedinst, *J. Am. chem. Soc.***1956**, 78, 3493

34. E. M. Kosower, *J. Am. chem. Soc.* **1958**, 80, 3253

35. R. A. Mackay, J. R. Landolph, E. J. Poziomek, *J. Am. chem. Soc.* **1971**, 93, 5026

36. D. Haristoy, D. Tsiourvas, *Liquid Crystals* **2004**, 31, 697–703

37. R. K. Raju, A. Ramarai, I. H. Hiller, M. A. Vincent, N. A. Burton*, Phys. Chem. Chem. Phys.* **2009**, 11, 3411

38. E. C. S. Kaposta, D. P. Gamblin, J. Screen, B. Liu, L.C. Snoek, B. G. Davis, J. P. Simons, *Phys. Chem. Chem. Phys.* **2007**, 9, 4444

39. M. Minsky, Memoir on inventing the Confocal microscope, *Scanning* **1988**, 10, 128-138

40. H. Verhoogt, J. V. Dam, A. P. Boer, A. Draaijer, P. M. Houpt, *Polymer* **1993**, 34, 1325-1329

41. M. A. V. Diik, R. V. D. Berg, *Macromolecules* **1995**, 28, 6773

42. A. J. Verleij, R. F. Zwaal, B. Roelofsen, P. Confurius, D. Kastelijn, L. V. Deenen, *Biochim. Biophys. Acta* **1973**, 323, 178-193

43. Gabriela Tavares Bekner Correa; Gabriel Alves Costa Veranio; Licínio Esmaeraldo Silva; Raphael Hirata Junior; Jeffry M. Coil; Miriam F. Zaccaro Scelza; *J. Appl. Oral Sci.* **2009**, 17

44. V. Sambhy, B. R. Peterson, A. Sen, *Angew. Chem Int.* **2008**, 47,1250-1254

45. S. Tan, G. Li, J. Shen, Y. Liu, M. Zong, *J. Appl. Polym. Sci.* **2000**, 77, 1869

46. T. R. Stratton, J. L. Rickus, J. P. Youngblood, *Biomacromolecules* 2009, 10, 2550-55.

47. E. R. Kenawy, S. D. Worley, R. Broughton, *Biomacromolecules* **2007**, 8, 1359-1384

48. B. C. Allison, B. M. Applegate, J. P. Youngblood, *Biomacromolecules* **2007**, 8, 2995-2999

49. P. H. Sellenet, B. Allison, B. M. Applegate, J.P.Youngblood, *Biomacromolecules* **2007,** 8, 19-23

50. B. K. Gorityala, J. Ma, X. Wang, P. Chen, X.W. Liu, ***Chem. Soc. Rev.*** **2010**, 39, 2925 – 2934

51. L. Cen, K. G. Neoh, E. T. Kang, *Langmuir* **2003**, 19, 10295-10303

Appendix 3 Fluorescence emission spectra of different sugar linked

SBS
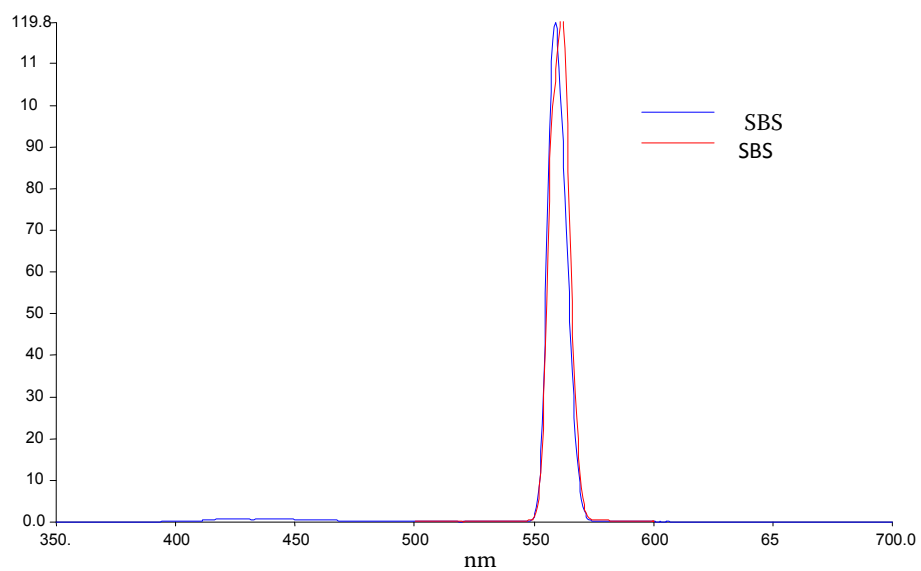
Figure 4.19 Fluorescence emission spectra of SBS and epoxidized SBS
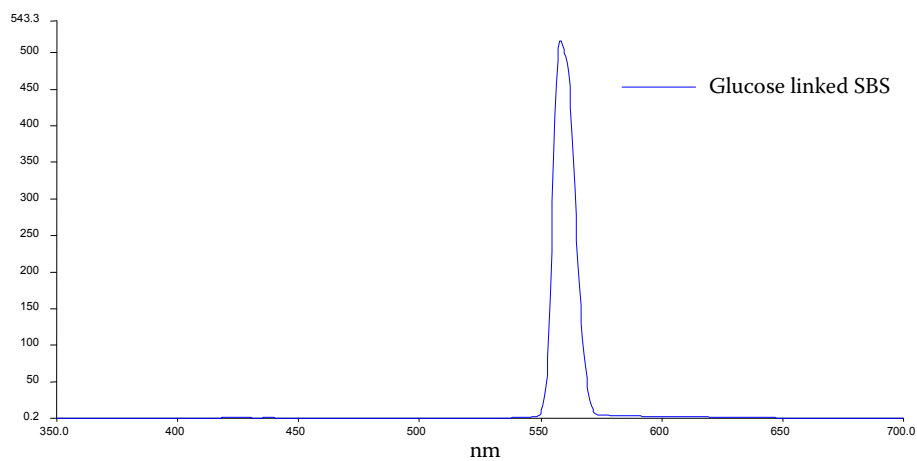
Figure 4.20 Fluorescence emission spectra of glucose linked SBS
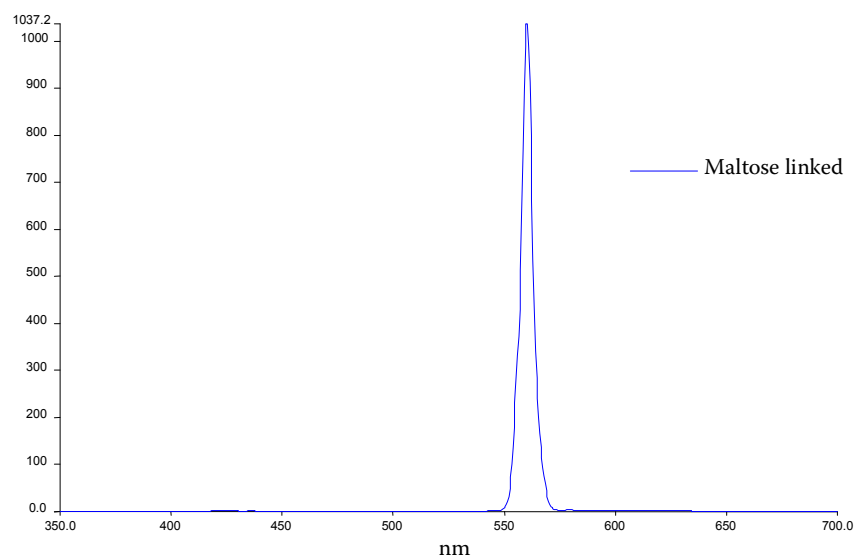
Figure 4.21 Fluorescence emission spectra of Maltose linked SBS
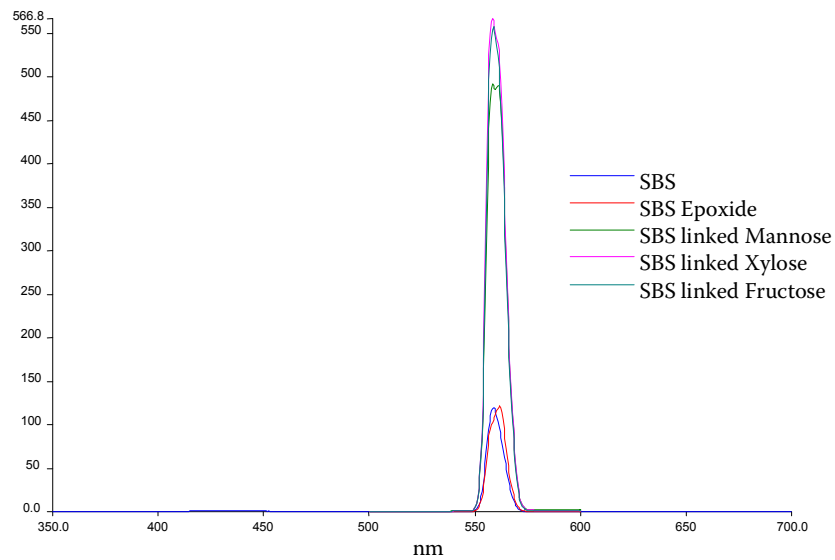
Figure 4.22 Overlapped Fluorescence emission spectra of SBS, epoxidized SBS,

Mannose, xylose and fructose linked SBS
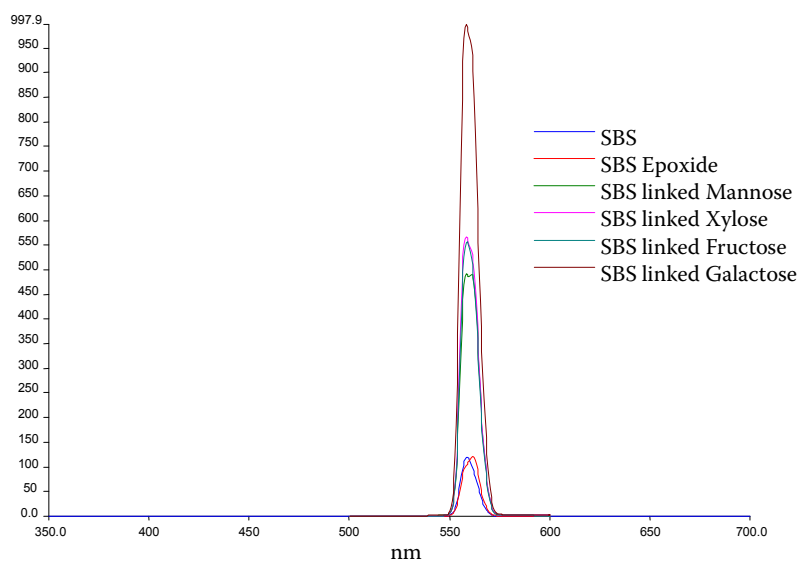
Figure 4.23 Overlapped Fluorescence emission spectra of SBS, epoxidized SBS,

Mannose, xylose, fructose and galactose linked SBS
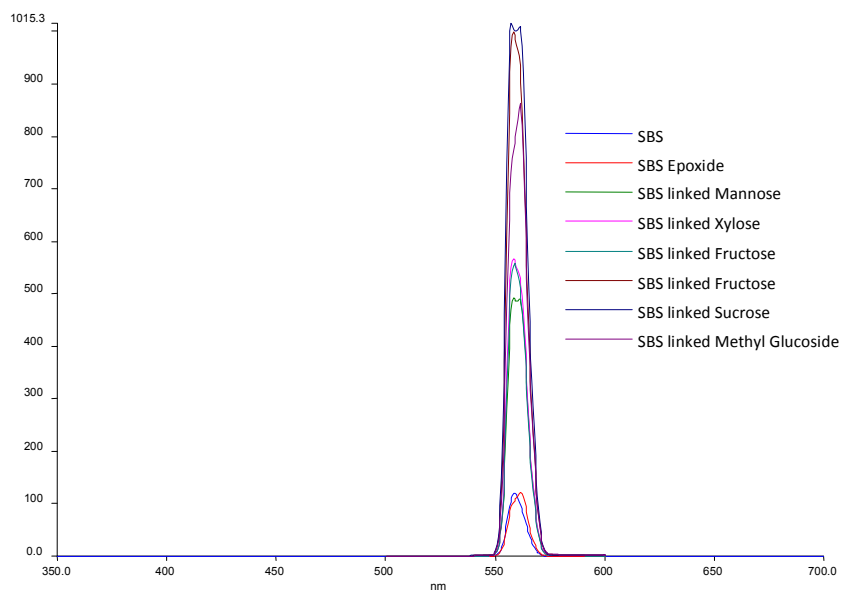
Figure 4.24 Overlapped Fluorescence emission spectra of SBS, epoxidized SBS,

Mannose, xylose, fructose, sucrose and methyl glucoside linked SBS

Chapter 5

Biodegradation and thermal studies of carbohydrate functionalized SBS

5.1. Introduction

Biodegradable polymers have a significant potential in various fields of bioengineering, drug delivery and in vivo sensing [1]. Moreover, these polymers have been a focus of research because of various applications as disposable plastics and in biomaterials area such as scaffolds for regenerating soft tissue in vivo or in vitro. While there exist a significant body of work done on biodegradable plastics [2], there are hardly any reports on introducing biodegradability characteristics onto synthetic elastomers like SBS. Such biodegradable elastomers can have interesting applications in packaging applications. There are three classes of biodegradable elastomers that have been reported in literature: hydrogels [3], elastin-like peptides [4] and polyhydroxyalkonates (PHAs) [5].

According to rubber statistical bulletin, September-October 2006, the world consumption of synthetic rubber (non-biodegradable) alone was 119 million tones, this combined with other non-degradable polymers and elastomers are posing a serious threat to our environment. With a growth rate of 4.6% the consumption of elastomers is bound to increase, aggravating the problem of acute solid waste disposal.

Further, if a biodegradable elastomer also has biocompatibilty, these elastomers can have potential applications in engineering of soft tissues such as blood vessels, heart valves, cartilage, tendon and bladder which exhibit elastic properties. Although some biodegradable elastomers have been developed, most of them require complex and costly synthesis procedures, which translates into higher costs and hinder their commercial exploitation.

The work presented here incorporates methodologies, which takes into account known structure-property relationships needed for obtaining biodegradable elastomers. Our main hypothesis is that incorporation of small amounts of sugars and sugar derivatives by chemically linking them with elastomers will enhance their biodegradation.

As regards thermal properties, published literature shows that there are some reports on thermal studies of synthetic polymers containing sugars. For e.g, sucrose acrylate graft copolymerized on the surface of poly (vinyl chloride) PVC showed decrease in thermal stability as compared to Poly (vinyl chloride) [6]. PVC had an initial decomposition temperature of 248°C, whereas poly(vinyl chloride) grafted with sucrose acrylate had an initial decomposition temperature of 114°C. Copoly (ester amide)s containing L-arabinose units showed single or two-stage degradation pattern depending upon the percentage of the carbohydrate in the polymer, the onset of degradation being 200°C [7]. With higher percentages of carbohydrates in the polymer, i.e. above 20 %, the TGA showed mainly a decomposition pattern with a minor third decomposition stage. The thermal degradation of a copolymer formed by reacting methacryloyl 1,2:3,4-di-O-isopropylidene-α-D-galactopyranose with ethyl acrylate showed a two-stage degradation pattern with the polymer being stable upto 160°C [8].

Most of these studies have been carried out on copolymers containing relatively high amounts of sugars for synthesizing biocompatible polymers. However, by the incorporation of such large quantities of sugar, the intrinsic physical and chemical properties of the polymers are drastically altered. In our case, the objective was to attempt to retain the intrinsic physical and chemical properties of the polymer by incorporating minute quantities of sugars.

5.2. Materials and methods

5.2.1 Thermogravimetric Analysis (TGA and DSC)

The Thermo gravimetric analysis (TGA) was performed on Perkin Elmer TGA-7 in N_2 atmosphere at heating rate of 10 °C min^{-1}. Glass transition temperature (T_g) was measured using DSC Q-10 (TA) in N_2 atmosphere at heating rate of 20 °C min^{-1}

5.2.2 Biodegradation

Polystyrene-block-polybutadiene-block-polystyrene (SBS) (M_w 140,000, 30% polystyrene, 70% polybutadiene) was obtained from Aldrich, USA. All solvents were obtained from SD Fine Chemicals, Pune, India, and were distilled and dried before use. The microorganisms used *Aspergillus niger* NCIM 1025 (ATCC 9642) and *Pseudomonas sp.* NCIM 2220 were obtained from the National Collection of Industrial Microorganisms, National Chemical Laboratory, Pune, India. These cultures were routinely maintained on Potato Dextrose Agar (PDA) slopes.

5.2.2.1 Minimal medium preparation

5.2.2.2 Fungal Culture

The culture was grown in minimal medium (ASTM Nutrient Salts Medium) containing (g/l): KH_2PO_4 0.7; K_2HPO_4 0.7; $MgSO_4.7H_2O$ 0.7; NH_4NO_3 1.0; NaCl 0.005; $FeSO_4.7H_2O$ 0.002.; $ZnSO_4.7H_2O$ 0.002.; $MnSO_4.H_2O$ 0.001. The pH of the medium was adjusted to 6.5 ± 0.2 and sterilized at 121° C for 20 minutes.

5.2.2.3 Bacterial Culture

Cultures were grown in Minimal medium (OECD) containing (g/l): $(NH_4)_2SO_4$, 2.0; K_2HPO_4, 14.0; KH_2PO_4, 6.0; $MgSO_4.7H_2O$, 0.2. The pH of the medium was adjusted to 7.0 prior to sterilization. The medium was sterilized at 121°C for 20 min.

5.2.2.4 Testing of the samples

The test samples were surface sterilized with 70% ethanol overnight and then added separately to the sterilized medium. The cells of the cultures grown in 10 mL Nutrient broth for 24 h at 30 $^{\circ}$C were suspended in 10 ml of saline and this suspension was used as an inoculum. Approximately 1 mL ($\sim10^8$ cells) were inoculated into 50 ml of the minimal medium in 250 ml conical flasks. The flasks were incubated at 28°C with shaking at 180 RPM. The growth was monitored over a period of four weeks. For bacterial culture optical density was measured at regular interval using Systronics 117 spectrophotometer. After 30 days the polymer was separated from the cells. The polymer was further washed many times with water followed by washing with 70% ethanol. It was dried at 50°C and analysed by SEM and the percentage weight losses of the polymers were recorded.

5.2.3 Quantification of sugar content in sugar linked SBS

The sugar content of all the sugar linked SBS was determined by phenol sulphuric acid method as detailed in appendix 4

5.3. Results and Discussion

5.3.1 Thermal analysis of sugar linked SBS

5.3.1.1 Thermogravimetric analysis (TGA)

TG curves of various sugar linked SBS were studied under pure nitrogen atmosphere at heating rate of 10^0 C/min from 50-600 ^{0}C. Table 3 gives the thermal analysis details such as degradation onset temperature (T_{onset}), residue weight %

and maximum degradation temperature (T_{max}) for the thermal degradation of the various sugar linked SBS samples.
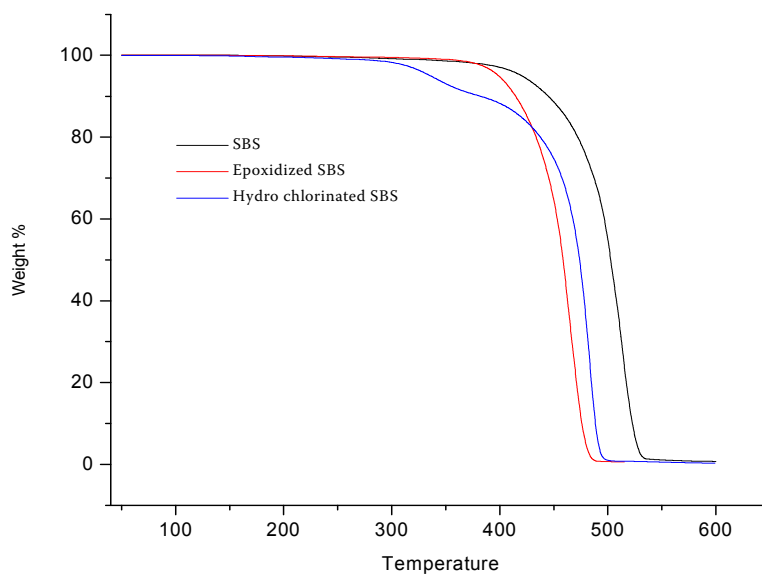
Figure 5.1 Overlapped TGA curves of SBS, epoxidized SBS and hydro chlorinated SBS

Figure 5.1 shows the comparative thermal stabilities of SBS, partially epoxidized SBS and hydro chlorinated SBS.

The onset of degradation for SBS is 400^{0}C after which it starts degrading rapidly. The rate of degradation reaches maximum at 525 ^{0}C and at 600^{0}C it degrades almost completely leaving behind only 0.63 weight% residue. Epoxidized SBS (22 % epoxy groups) has onset degradation temperature of 387^{0}C and degrades rapidly thereafter and rate of degradation is maximum at 479.5^{0}C. It degrades almost completely at 515^{0}C leaving only 0.67 weight % residue. It is interesting to note here that before 430^{0}C hydro-chlorinated SBS is thermally less stable than epoxidized SBS, but after 430^{0}C the thermal stability of hydro-chlorinated SBS increases as compared to partially epoxidized SBS.

 In contrast to SBS and epoxidized SBS, hydro - chlorinated SBS shows a two stage degradation pattern with onset of degradation of first stage at 309 ^{0}C.

Thus modification of SBS by epoxidation and hydro-chlorination seems to decreases the thermal stability of SBS.
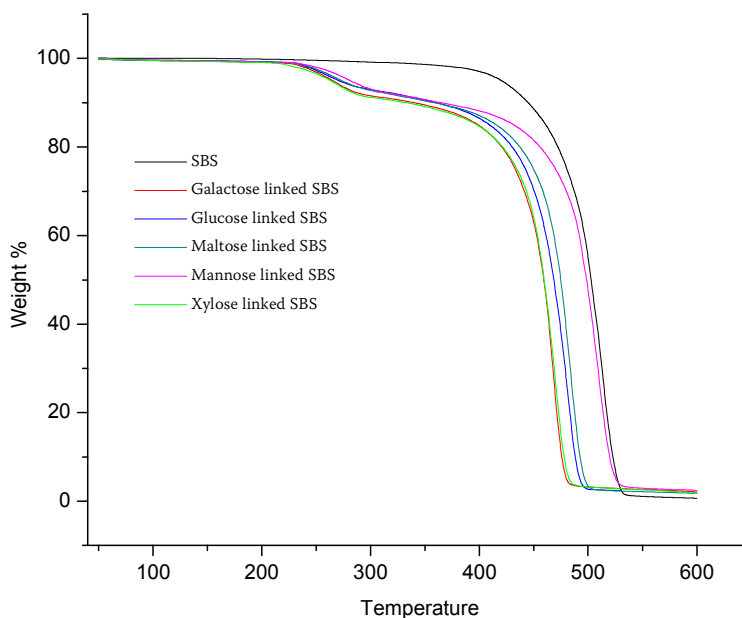
Figure 5.2 Overlapping TGA curves of different sugar linked SBS

Figure 5.2 shows the overlapping TGA curves of sugar linked SBS (samples with near quantitative functionalization; > 90 % epoxy group reacted). It is observed that all the sugars viz. galactose, maltose, glucose, mannose and xylose linked to SBS show two stage degradation patterns.

As we have seen in the preceding section, hydro-chlorinated SBS also shows two stage degradation pattern similar to sugar linked SBS (fig. 5.1 and 5.2). In the sugar linked SBS, following types of pendants are present, namely sugar, hydroxyl group, chlorine group (from hydro-chlorination) and quaternary pyridinium pendants. Hydro-chlorinated SBS has higher onset of degradation (309 ^{0}C), and quaternary

pyridinium also have greater thermal stability [9] owing to their salt nature (even for pure vinyl pyridine initial decomposition occurs at 350 ^{0}C [10]. Thus, both hydrochlorinated and quaternary pyridinium have greater initial onset degradation temperature as compared to sugars. From the figure 5.2 it can be observed that onset of first stage of degradation for different sugar linked SBS varies from 236-249.9 ^{0}C and the maximum degradation temperature ($T_{max.}$) varies from 477- 521.6 ^{0}C. Hence the first stage degradation observed in the sugar linked SBS can be assigned to the attached sugar pendants on SBS.

The second stage of degradation varies depending on the type of sugar linked to SBS and the quaternary nitrogen content. The mannose linked SBS shows thermal stability similar to unmodified SBS, whereas galactose and xylose linked SBS show thermal stability similar to epoxidized SBS, while all other sugar linked SBS show lower thermal stability. The order of thermal stability is; mannose linked SBS > maltose linked SBS > glucose linked SBS > galactose linked SBS, xylose linked SBS. However, the degradation profile for all these polymers is similar and within a narrow range.
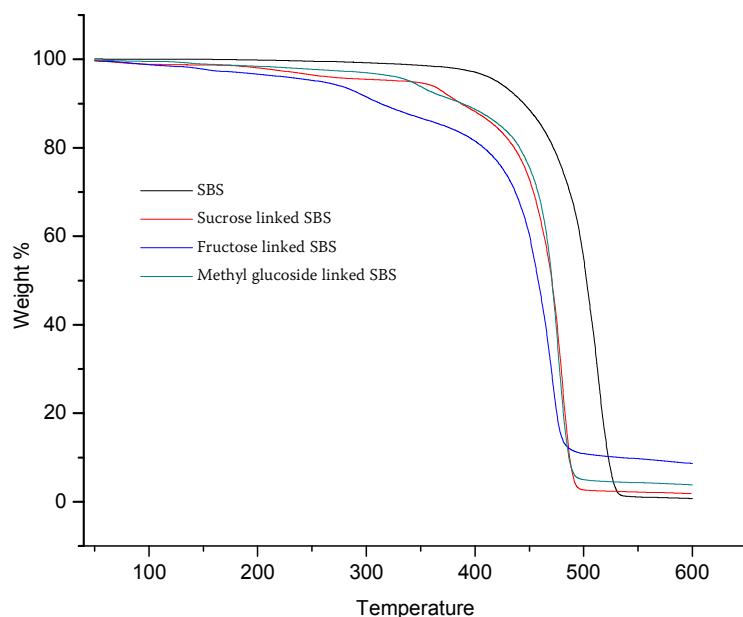
Figure 5.3 Overlapping TGA curves of SBS, sucrose linked SBS, fructose linked SBS and methyl glucoside linked SBS

Figure 5.3 shows Overlapping TGA curves of SBS, sucrose linked SBS, fructose linked SBS and methyl glucoside linked SBS (samples with partial epoxide opening). From the overlapped TGA curves in above figure 5.3, it can be observed that fructose linked SBS shows thermal instability even at 150^0C, while sucrose and methyl glucoside linked SBS shows comparatively more thermal stability. The residue content (8.62%) of fructose linked SBS is significantly higher than both sucrose and methyl glucoside linked SBS samples.

Table 5.1 Thermal analysis of different sugar linked SBS

Sample	T_{onset} ^{0}C		T_5 (°C)	T_{10} (°C)	T_{20} (°C)	T_{90} (°C)	T_{max}(°C)	Residue (wt %)
	1st Stage	2nd Stage						
SBS	478.3		420	445	472	522.5	525	0.63
Epoxidized SBS	438.2		398.7	415.2	433.4	475	479.5	0.67
Hydro chlorinated SBS	309.5	461.3	336	382	437.3	488.4	490.7	0.3
Glucose linked SBS	236	449.5	270	363	430	487.9	490.5	2.5
Galactose linked SBS	239	445.5	265	339	421	475.7	477	2.1
Maltose linked SBS	239.8	453.3	271.4	353.7	437.33	492.3	495.6	1.87
Xylose linked SBS	237	445.6	263	324.9	422.2	477.6	479.5	1.87
Mannose linked SBS	249.9	481.9	279.8	395.5	455	518.7	521.6	2.46
Fructose linked SBS	275	439.6	256	313.2	408	518.8	479.3	8.62
Sucrose linked SBS	359.7	456.2	319.6	386.2	435.6	486.8	489.4	1.85
Methyl glucoside linked SBS	331	458.5	340	390	440.6	486.3	486.7	3.7

Abbreviations: T_5, T_{10}, T_{20}, T_{90} and T_{max}; Temperature at which 5%, 10%, 20%, 90% and maximum weight loss of polymer takes place respectively

The thermal analysis data showing % weight loss at different temperatures along with onset of degradation and maximum degradation temperature is presented in table 5.1. From this data it is clear that functionalization of SBS with sugars, pyridinium chloride and quaternary ammonium chloride groups generally leads to a decrease in thermal stability. However, the low values of initial decomposition temperature (IDT) (200-275°C) compared to SBS indicate that applications for these polymers upto 200 °C are possible. It is envisaged that most applications for such polymers will require maximum temperatures of upto 50 °C, and processing temperatures can be adjusted to be below 200 °C. Previous studies by other workers [6] have shown initial decomposition at much lower temperature (114 °C), which is significantly lower than ours. The present thermal analysis also shows that the decrease in thermal stability is closely related to the type of sugar anchored on SBS.

5.3.1.2 DSC analysis of sugar linked SBS: Glass transition temperature (T_g)

Different sugar linked SBS samples were subjected to differential scanning calorimetry (DSC) analysis in nitrogen atmosphere at a heating rate of 20 °C /min from -90 °C to +250 ^{0}C to determine glass transition temperature. The DSC thermograms of these polymers are shown in Figures and their glass transition temperatures are summarized in table below.

Table 5.2 DSC analysis of different sugar linked SBS

Sample	T_g^{PB} (^{0}C)	T_g^{PS} (^{0}C)
SBS	-92*	60-80*
SBS Epoxide	-71	78
Glucose linked SBS	-57	89
Mannose linked SBS	-60	86
Galactose linked SBS	-60	84
Maltose linked SBS	-60	89
Xylose linked SBS	-57	80
Sucrose linked SBS	-67	80
Methyl glucoside linked SBS	-43	80

* Literature value

T_g^{PB} : Transition temperature of polybutadiene block, T_g^{PS} : Transition temperature of polystyrene block

SBS possess a well-ordered phase-separated morphology consisting of two nearly pure phases and exhibit two glass transition temperatures (T_g), one for butadiene phase (PB) and other for styrene phase (PS). The T_g of PB block is sharp at -90 ^{0}C, but the T_g PS block is broad ranging from 60-80 ^{0}C [11-12]. It can be seen from the table that partially epoxidized SBS showed T_g for polybutadiene block at -71^{0}C which further increases by 11-15^{0}C in the sugar linked SBS samples. All the sugar linked SBS samples show T_g in the range of -57 to -43 ^{0}C.
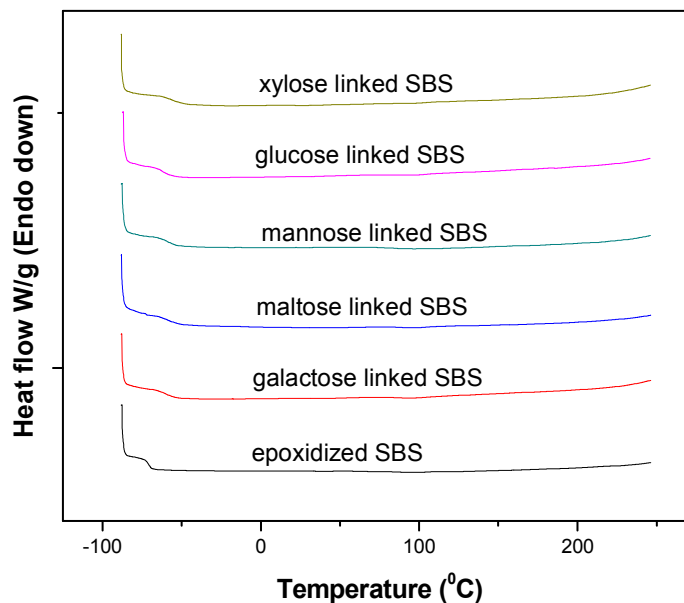
Figure 5.4 DSC curves of different sugar linked SBS compared with epoxidized SBS in N_2 at heating rate 20 °C min^{-1}.

The increase in T_g after epoxidation is due to the increased inter chain interaction of the polar oxirane ring resulting in the increase of cohesive energy thereby shifting the glass transition to higher temperature [13]. With the introduction of quaternary pyridinium chloride ionic moieties along with sugar moieties containing free hydroxyl groups in the sugar linked SBS , hydrogen bonding and inter chain interaction increases further causing further reduction in chain segment mobility than the epoxidized SBS resulting in further increase of glass transition temperatures. Thus, the observed increase in T_g is believed to be due to the combined effect of ion pairs interaction [14] and hydrogen bonding effect operating in sugar linked SBS samples which effectively raises the glass transition temperature. The increase in T_g of sugar linked SBS as compared to epoxidized SBS is quite evident in DSC thermograms of sugar linked SBS shown in figure 5.4 above.
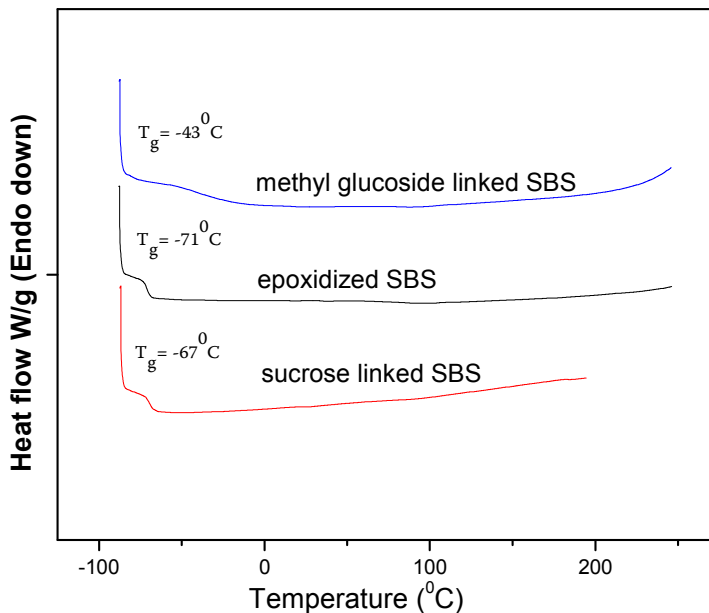
Figure 5.5 DSC curves of sucrose and methyl glucoside linked SBS compared with epoxidized SBS in N_2 at heating rate 20 °C min^{-1}.

Figure 5.5 shows the DSC thermograms of partially epoxidized SBS, sucrose and methyl glucoside linked SBS. Sucrose linked SBS show T_g at -66.9 °C, much lower than other sugar linked SBS samples. This is due to incomplete opening of epoxide ring of the epoxidized SBS resulting in partial functionalization of SBS (as discussed in chapter 2) which results in higher residual epoxide content in the sucrose linked SBS. Due to the partial functionalization the inter chain mobility is not significantly altered as compared to epoxidized SBS resulting in T_g increase of 4 °C only as compared to 11.5 -14.5 °C in other sugar linked samples, which are quantitatively functionalized with minimal residual epoxide content. The methyl glucoside linked SBS shows unusual increase in T_g of 18 °C, which is also corroborated from its TG graph which shows it to be more stable than other sugar liked SBS samples.

Thus, DSC analysis shows that anchoring of sugar and quaternary nitrogen pendants in SBS leads to increase of glass transition temperatures of polybutadiene domains.

5.3.2 Biodegradation studies of sugar linked SBS

We anchored minute quantities of various monomeric sugars like glucose, galactose, mannose, xylose, maltose fructose, sucrose and methyl glucoside with the aim of improving biodegradation of SBS. Instead of using a mixture of several microorganisms, we chose one pure soil bacterial culture (Pseudomonas sp.) and fungal culture (Aspergillus niger) for investigating their individual growth patterns on these new elastomers in comparison to their growth in control solution or onto the unmodified elastomer.

5.3.2.1 Bacterial Biodegradation by Pseudomonas sp.:
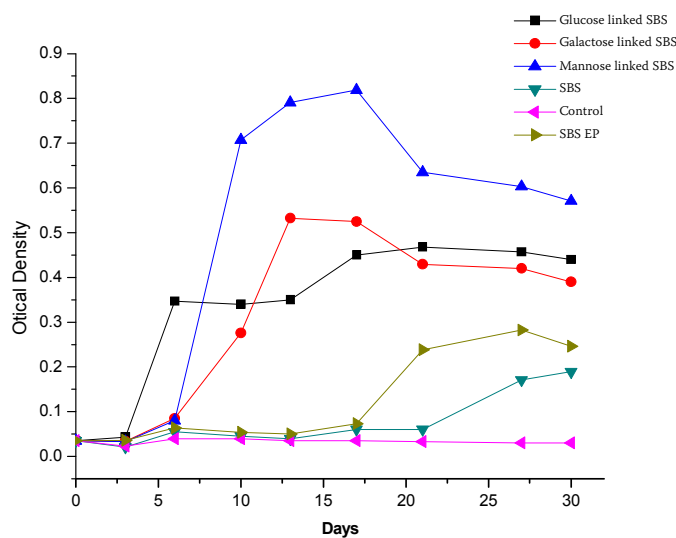
Figure 5.6 Growth pattern of Pseudomonas sp. on different monosaccharides (glucose, mannose, galactose) linked SBS

The bacterial biodegradation behavior of sugar linked SBS by Pseudomonas sp. is presented in Figure 5.6. From the growth pattern of Pseudomonas sp. on different monosaccharide linked SBS. It can be observed that the rates of increase in optical density in sugar linked SBS (reflecting material degradation) is much higher than the starting elastomer (SBS and SBS epoxide) and the control. The galactose linked SBS showed OD maximum in two week, whereas the glucose and mannose liked SBS showed a maximum after two weeks. The mannose derivative showed significant increase in OD as compared to glucose and galactose linked SBS. From the figure 5.6 it is also inferred that mannose linked SBS was more degradable as compared to both glucose and galactose linked SBS using this particular bacterial culture.
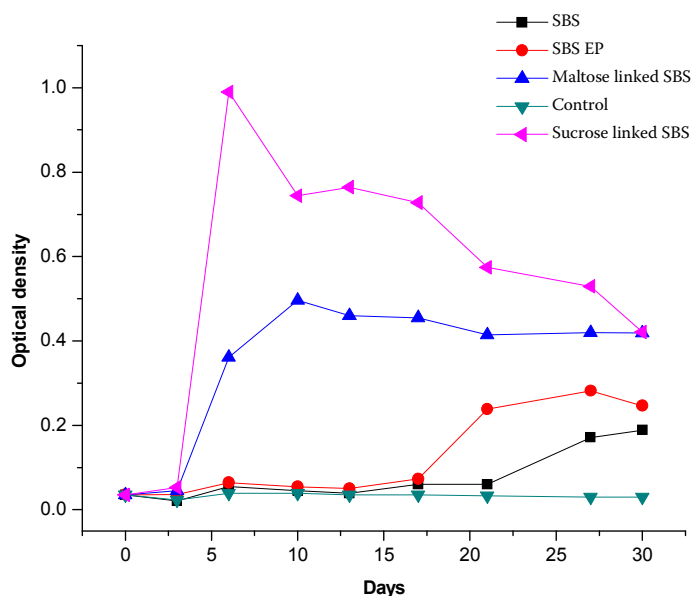
Figure 5.7 Growth pattern of Pseudomonas sp. on disaccharides (maltose, sucrose) linked SBS

Figure 5.7 shows the growth pattern of Pseudomonas sp. on disaccharides (maltose, sucrose) linked SBS. From the figure 5.7 it is observed that the sucrose linked SBS was more degradable as compared to the maltose linked SBS. The

sucrose linked SBS showed OD maximum in one week, whereas the maltose liked SBS showed a maximum after 10 days. The sucrose derivative showed significant increase in OD as compared to galactose linked SBS. Sucrose linked SBS showed the highest OD among all the sugar linked SBS.
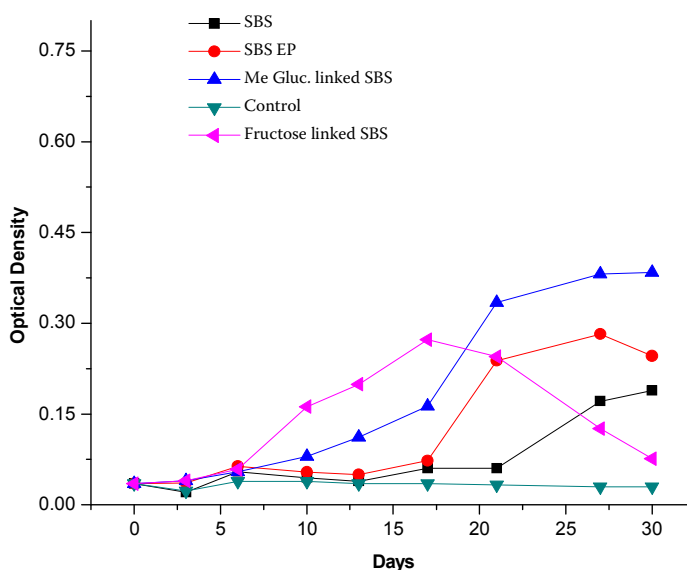
Figure 5.8 Growth pattern of Pseudomonas sp. on α-methyl glucopyranoside and fructose linked SBS

Figure 5.8 shows the growth pattern of Pseudomonas sp. on α-methyl glucopyranoside and fructose linked SBS. From the figure 5.8, it is observed that the fructose linked SBS did not show appreciable difference in OD and hence biodegradation rate as compared to partially epoxidized SBS (SBS EP) and SBS. Fructose linked SBS showed the least OD in among all the sugar linked SBS.
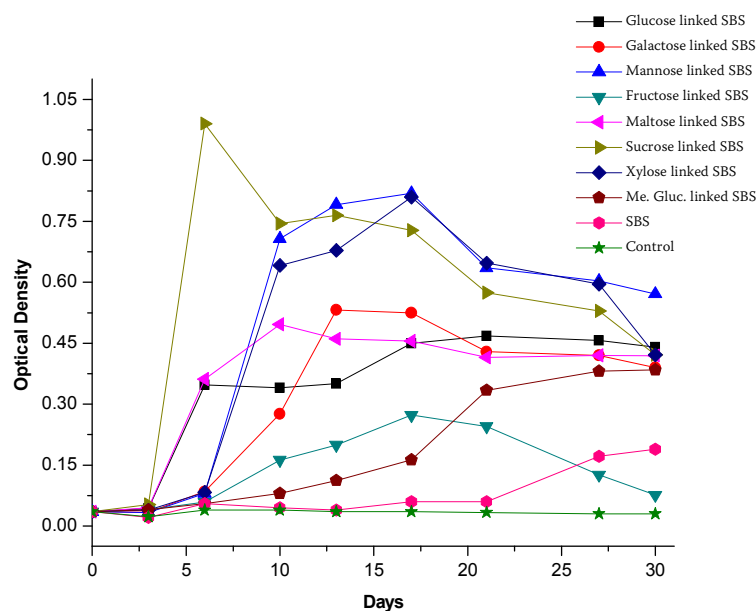
Figure 5.9 Growth pattern of Pseudomonas sp. on different sugars linked SBS

Figure 5.8 shows the growth pattern of Pseudomonas sp. on different sugars linked SBS. From the figure 5.8, it is observed that the rates of increase in optical density (reflecting material degradation) in different sugar linked polymers is much higher than the starting polymer SBS and epoxidized SBS. For Pseudomonas sp. (NCIM 2220), the preference towards biodegradation based on increase in optical density are; sucrose linked SBS > maltose linked SBS > mannose linked SBS > galactose linked SBS > glucose > xylose linked SBS > fructose linked SBS > methyl glucoside linked SBS.

Test organisms used in the present study were standard cultures used for testing samples for their bacterial resistance. The test cultures used in the present study are organisms widely found in the environment. However, use of pure culture system offers the advantage of reproducibility of results, and would aid in designing biodegradation systems for different polymers after their disposal as waste materials. Since Pseudomonas sp. is a common soil bacteria, therefore these results

have implication for disposal of these polymers in soil for obtaining biodegradation.

5.3.2.2 Characterization of bacterial and fungal biodegradation of different sugar linked SBS

The different sugar linked SBS elastomers were characterized by weight loss and SEM analysis of the degraded elastomers. Table 5.3 and 5.4 shows the percent weight loss (indicating biodegradability) of the sugar linked Polystyrene-block-polybutadiene-block-polystyrene (SBS) copolymer with bacterial and fungal culture. It also shows the variation of biodegradability with the type of mono/ disaccharide / pentose sugar attached.

5.3.2.3 Bacterial biodegradation of Sugar linked SBS

Due to adherence of bacterial cells onto the polymer, the weight losses are generally lesser than expected. It is reported that in many such cases, weight loss data are inconclusive due to cell wall accumulation [15].

Table5.3 Weight loss data for bacterial degradation using Pseudomonas sp. over a period of 30 days

Sample	Initial Weight (mg)	Final Weight (mg)	% Weight loss	Sugar content (Weight %)
SBS	250	250	0.0	0.0
SBS Epoxide	250	250	0.0	0.0
Glucose linked SBS	250	248.5	0.6	0.09
Mannose linked SBS	250	247	1.2	0.12
Galactose linked SBS	250	247.2	0.9	0.16
Xylose linked SBS	250	249	0.4	0.11
Maltose linked SBS	250	240.2	3.9	0.37
Sucrose linked SBS	250	239	4.4	0.32

From the above table 5.3, we observe that SBS and partially epoxidized SBS without any sugar linked to it are not degraded by bacterial culture whereas the sugar linked SBS showed significant weight loss ranging from 0.4% to 4.4%. Sucrose linked SBS showed highest weight loss of 4.4 % followed by maltose linked SBS which showed weight loss of 3.9 %. Over 10 times more weight loss than the attached sugar (maximum sugar attached was 0.37 weight %) is observed, suggesting that some polymer chain scission has also taken place along with the loss of sugar during biodegradation.

5.3.2.4 Fungal degradation of Sugar linked SBS

Biodegradation of different sugar linked SBS was also studied with fungal culture Aspergillus niger (NCIM 1025, ATCC 9642) and it was characterized weight loss data. Table shows the weight loss percent of the different sugar linked SBS after biodegradation. It shows that weight loss varies with the type sugar anchored and sugar content of the functionalized SBS. As in the case of bacterial biodegradation here also the weight loss is much more than the attached sugar.

Table 5.4 Weight loss of the sugar- linked polymers degraded by fungal strain

Aspergillus niger

Sample	Initial Weight (mg)	Final Weight (mg)	% Weight loss	Sugar content (Weight %)
SBS	250	250	0.0	0.0
SBS Epoxide	250	250	0.0	0.0
Glucose linked SBS	250	241.8	3.3	0.09
Mannose linked SBS	250	246.7	1.3	0.12
Galactose linked SBS	250	247.3	1.1	0.16
Xylose linked SBS	ND	ND	ND	0.11
Maltose linked SBS	250	234.1	6.3	0.37
Sucrose linked SBS	250	241	3.6	0.32
Me. Glucoside linked SBS	250	246.5	1.4	ND

ND = Not determined

From the above table 5.4 it can be seen that weight loss varies with the type of sugar attached. Thus, SBS and epoxidized SBS having no sugar attached to them was not degraded by the fungal culture.

Maltose linked SBS showed maximum degradation with weight loss of 6.3 %. While sucrose linked SBS showed a weight loss of 3.6 % and glucose linked SBS showed a weight loss of 3.3 %. Galactose linked SBS having comparatively higher sugar content (0.16 weight %) than mannose linked SBS (0.12 weight %) showed weight loss of 1.1 %, lower than its mannose counterpart which showed weight loss of 1.3%. Growth of fungal culture showed specificity for different sugar types

linked to SBS. Thus anchoring of small amount of sugar led to appreciable increase in biodegradation of SBS which otherwise was not biodegradable.

The observed weight loss by fungal culture was many folds higher than the weight of attached sugar, indicating that elastomeric backbone is also being degraded along with sugar. Thus, biodegradation rate can be increased to significant level by tuning the sugar content in the elastomer. These results further supports the strategy developed for synthesis of biodegradable polyolefin in our lab.

5.3.2.5 Scanning electron micrographs (SEM) of the sugar linked SBS after degradation by fungal culture Aspergillus niger (NCIM 10259)

The SEM of sugar linked SBS after biodegradation was recorded to investigate morphology change induced by biodegradation. Some representative samples were chosen in the form of films. After biodegradation the films were thoroughly washed with water to remove the adhering bacteria and fungus and were suspended in 70% ethanol and dried.
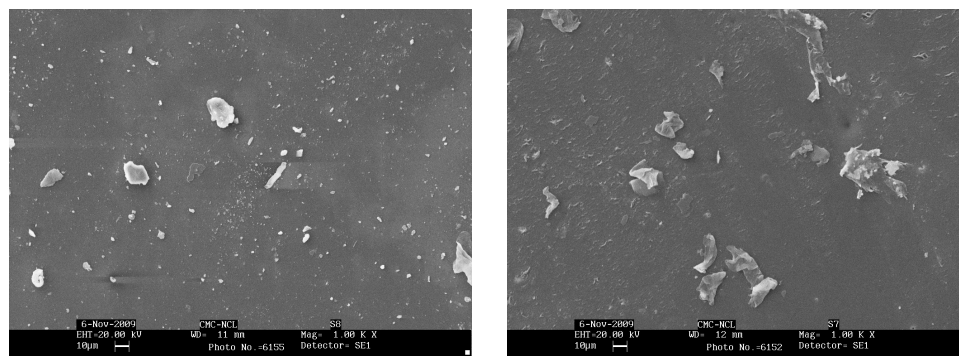
(a)   (b)

 Figure 5.10 SEM of (a) SBS after biodegradation (b) epoxidized SBS after biodegradation

Figure 5.10 shows the morphology of the unmodified SBS and epoxidized SBS after biodegradation. There seems to be practically no change in the morphology of SBS and epoxidized SBS after biodegradation with morphology observed before biodegradation. This is in accordance with the weight loss data where they do not show any weight loss indicating that they are not degraded by Aspergillus niger.

(a)   (b)

(c)   (d)

(e)
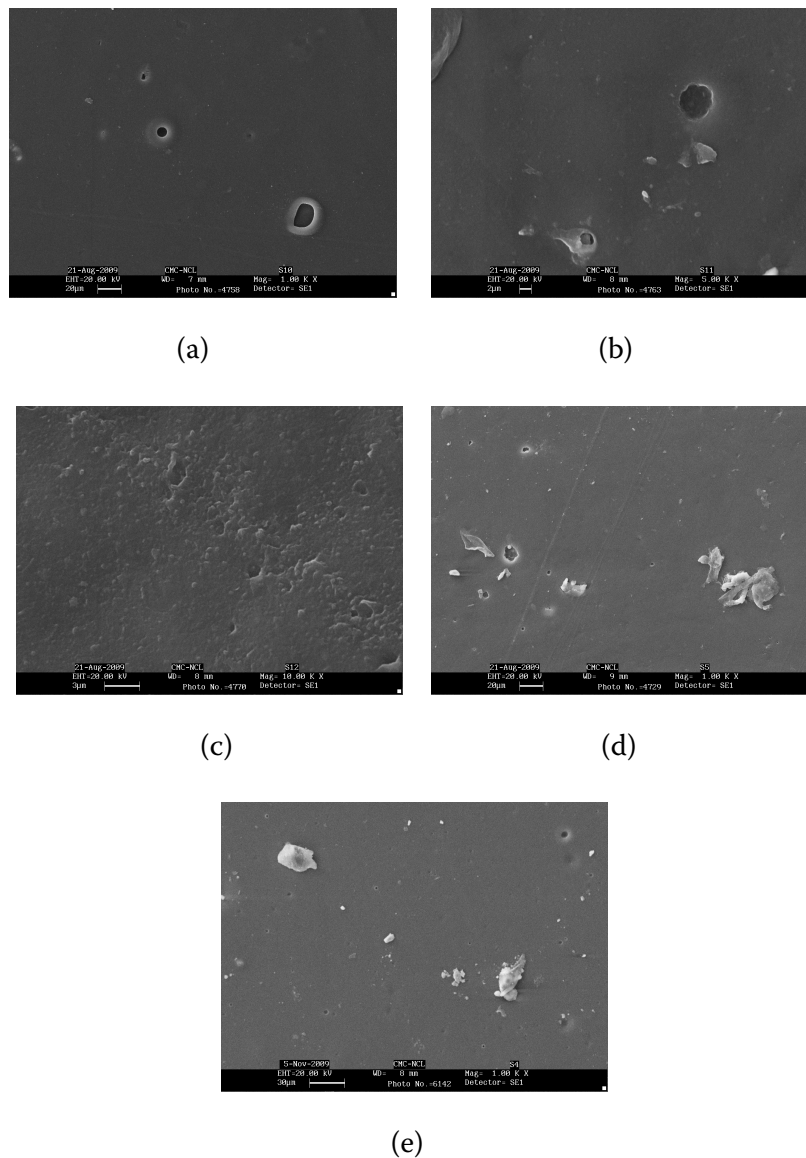
Figure 5.11 SEM pictures after biodegradation of (a) glucose linked SBS (b) mannose linked SBS (c) maltose linked SBS (d) sucrose linked SBS (e) galactose linked SBS

Figure 5.11 show the change in morphology of sugar linked SBS after biodegradation. It is observed that all the sugar linked SBS samples shows formation of cavities on the surface due indicating degradation. Glucose linked SBS shows more cavity formation as compared to mannose linked SBS. The maltose linked SBS also shows similar behaviour and also exhibits increased surface roughness. Galactose linked SBS showed least cavity formation on the surface on account of its less biodegradability.
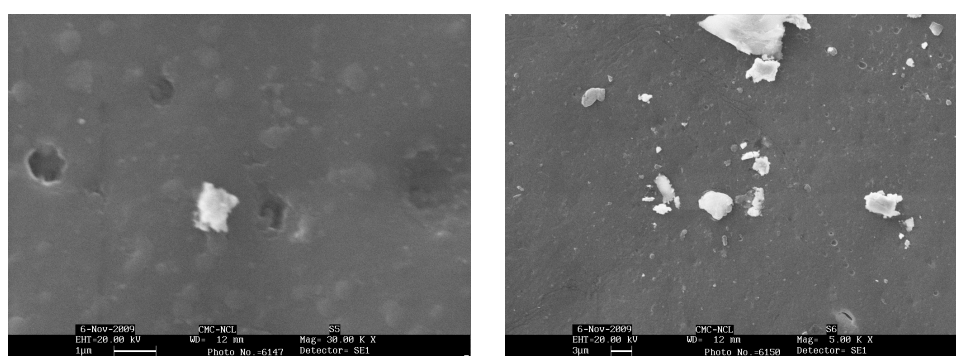
| Sucrose linked SBS bacterial | Mannose linked SBS Bacterial |

Figure 5.12 SEM after biodegradation with Pseudomonas sp. of (a) sucrose linked SBS (b) mannose linked SBS

Similar change in morphology was also observed for the sugar linked SBS degraded by bacterial culture Pseudomonas sp. as shown by representative samples in figure 5.12. Thus, SEM provided a pictorial view of both fungal and bacterial biodegradation, showing cavity formation and increased surface roughness proportional to extent of biodegradation and type of sugar anchored.

The visual growth of the fungus (Aspergillus niger NCIM 1025) is seen from the photograph below in figure 5.13.

Figure 5.13 Photograph showing growth of Aspergillus niger NCIM 1025 on minimal medium (left), SBS (middle) and the glucose linked SBS (right)

5.4. Conclusion

Biodegradation of sugar linked SBS having minute quantities of attached sugar (0.09-0.37 wt %) was studied by bacterial and fungal cultures. The biodegradation was characterized by weight loss and OD data, which showed much higher degradation than the attached sugar, thereby showing potential for biodegradable polymers. These polymers were thermally stable upto 250 ^{0}C as evidenced from thermal analysis. Thus, sugar linked SBS could be processed upto 200 ^{0}C, while other sugar containing polymer reported had significantly lower thermal stability and thus had poor processability.

5.5. References:

1. N. A. Pappas, R. Langer, *Science* **1994**, 263, 1715-1720

2. P. Galgali, A. J. Varma, U. S. Puntambekar, D. V. Gokhale, *Chemical communications (Cambridge, England)* **2002**, 2884-2885

3. K.Y. Lee et al., *Macromolecules* **2000**, 33, 4291-4294

4. J.C. M. Hest, D. A. Tirrel, *Chem. Comm.* **2001**, 1897

5. Y. porier, C. Nawrath, C. Somerville, *Bio/Technology* **1995**, 13, 142-150

6. P. Rios, H. Bertorello, *J. of Appl. Polym. Sci.* **1997**, 64, 1195

7. I. M. Pinilla, M. B. Martinez, J. A. Galbis, *Macromolecules* **2002**, 35, 2985-2992

8. M. J. Carneiro, A. Fernandes, C. M. Figueiredo, A. G. Fortes, A. M. Freitas, *Carbohydrate Polymers* **2001**, 45, 135-138

9. P. Ranganathan, W.K. Fife, M. Zeldin, *Journal of Polymer Science Part A: Polymer Chemistry* **1990**, 28, 2711-2717

10. Y. Liu, F. Meng, S. Zheng, *Macromol. Rapid Commun.* **2005**, 26, 920–925

11. R. M Ikeda, M. L Wallach, R. J. Angelo, *Polym. Preprints Am. Chem. Soc.* **1969**, 10, 1445

12. S. B. Munteanua, C. Vasile., *Journal of Optoelectronics and Advanced Materials* **2005**, 7, 3135 – 3148

13. G. H. Hsiue, J. M. Yang, *Journal of Polymer Science: Part A: Polymer Chemistry* **1990**, 28, 3761-3773

14. Sylvie Gauthier, Denis Duchesne, and Adi Eisenberg, *Macromolecules* **1987**, 20, 753-759

15. B. Lee et al., *Applied and Environmental Microbiology* **1991**, 678-685

5.6. Appendix 4: Quantification of sugar content in sugar linked SBS by phenol sulphuric acid method

Principle and mechanism of the reaction involved for sugar content determination by colorimetric methods (Phenol- Sulfuric acid Method):

Ref: M. Dubois, K. A. Gilles, J. K. Hamilton, P. A. Rebers, F. Smith, *Anal. Chem.* **1956**, 28(3)

This method is based on the following principle:

Concentrated sulfuric acid is used to break the bond between the polymer and the sugar. In case of disaccharides, it also breaks down the disaccharides into monosaccharides. The sugars are then dehydrated to furfural and hydroxymethyl furfural. The furfural compound then further reacts with phenol to produce a furan derivative that has a stable yellow-gold colour. The concentration of carbohydrate is then determined by measuring the absorbance and comparing to a standard curve.

Reaction Mechanism:
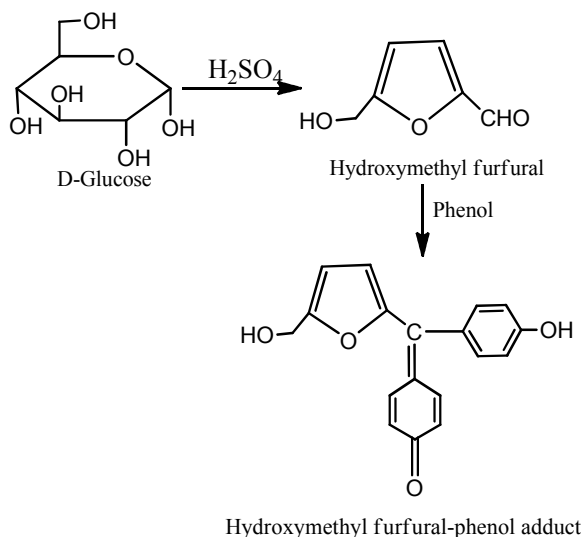
Use of calorimetry for quantification of the sugar content in the different sugar linked SBS: The phenol- sulfuric acid reaction method.

The sugar content of the polymer was found by phenol sulfuric acid assay [16]. Glucose, mannose, galactose, fructose, xylose, maltose, sucrose, and the sugar-linked SBS polymers were dried overnight in vacuum oven at ~60°C. A standard plot for the sugars was plotted using different concentrations (0.01mg/ml to 0.1mg/ml) of the respective sugar in water. The solutions of different concentrations were prepared as follows:

Table 5.5 Preparation of sugar solutions of different concentrations using a stock solution of 0.1 mg/mL (all the test samples were taken in triplicate)

S.No	Solution	Amount of solution 1 added (mL)	Amount of distilled water added (mL)	Final concentration (mg/mL)
1	Solution 1[a]	25	-	0.10
2	Solution 2	20	5	0.08
3	Solution 3	15	10	0.06
4	Solution 4	10	15	0.04
5	Solution 5	5	20	0.02
6	Solution 6	2.5	22.5	0.01
7	Blank Solution	-	25	0

[a] = solution 1 was prepared by dissolving 10 mg of the sugar in 100 mL water

To 2ml of each sugar solution was added 1ml of 5% aqueous phenol followed by a rapid addition of 5ml concentrated sulfuric acid. In a similar way a blank was prepared using distilled water instead of sugar solution. The solutions were placed in a water-bath at 35-40°C for 30 minutes. The absorbency of the sugar solutions was recorded at 490λ (for xylose at 480λ) and a standard plot was plotted. Each of the accurately weighed sugar samples and sugar linked SBS samples in the range of 15 - 25mg was taken in a 50ml beaker to which were added 4ml water and 2ml 5% aqueous phenol solution followed by a rapid addition of 10ml concentrated sulfuric acid. The solutions were placed in a water-bath at 35-40°C for 30 minutes. The solutions were filtered through a sintered disc to remove the undissolved polymeric backbone. The absorbency of these solutions was recorded at 490λ and the unknown concentrations of the sugars were calculated from the standard plot. Using these concentrations the weight percentages of the sugars in the polymers were determined. The range of sugar content in the polymer was found to be between 0.9- 0.37 weight percent.

Table 5.6 Sugar content (weight %) of different sugar linked SBS samples

Sample	Sugar content (wt %)
Glucose linked SBS	0.09
Galactose linked SBS	0.16
Maltose linked SBS	0.37
Xylose linked SBS	0.11
Mannose linked SBS	0.12
Sucrose linked SBS	0.32

Chapter 6

A morphological study of carbohydrate functionalized SBS

6.1 Introduction

Block copolymers occupy a huge area of research because they offer a vast range of possibilities for architecture (self assembly), size and chemical composition. One of the most important classes of synthetic system for creating self assembled structures is amphiphilic block copolymers. In bulk, when the different blocks are chemically immiscible, this results in phase separation leading to formation of ordered domains [1-2]. In solution the interaction between the solvent and different blocks determines well defined morphologies, ranging from micelles and vesicles to continuous network structures. The amphiphilic block copolymers comprising of synthetic and biologically active monomers like sugar, protein and peptides are known as hybrid polymers and they have generated widespread academic and industrial interest because of their potential biomedical applications.

These amphiphilic hybrid polymers can be generated by the copolymerization of hydrophobic and hydrophilic monomers or by chemical modification of hydrophobic polymers with hydrophilic monomers. In the present case the latter approach has been used to functionalize SBS (hydrophobic thermoplastic elastomer) with hydrophilic sugar and ionic moieties to generate amphiphilic SBS.

Herein, we set to explore the morphological study of the synthesized elastomers using different techniques. The morphologies of carbohydrate functionalized SBS were studied using scanning electron microscopy (SEM), atomic force microscopy (AFM), transmission electron microscopy (TEM) and wide angle x-ray diffraction (WAXRD).

6.2 Material and Method

6.2.1 Scanning electron microscopy (SEM)

The surface morphology of SBS and functionalized SBS was investigated using Leica SEM stereoscan 440, Cambridge, UK. The polymeric samples in the form of thin films, before analysis were coated with gold in a sputter coater, in order to achieve conducting surface and were analyzed at an accelerated voltage (potential) of 10 KV.

6.2.2 TEM

The samples were dissolved in chloroform and drop casted on a carbon coated 200 mesh copper grid and observed under a transmission electron microscope (HR-TEM 300 KV Technai-FEI machine) at 200 kV electron beam accelerating voltage. Typically one drop of the solution was dropped on the copper grid, and the extra solution was then allowed to air-dry.

6.2.3 Atomic force microscopy (AFM)

The morphology of sugar linked SBS samples were determined by atomic force microscopy (AFM) on (Veeco, Santa Barbara, CA) apparatus. All the AFM images were obtained by contact mode in ambient air, and the silicon cantilever used was 125 µm in length with a resonance frequency of 325 kHz. Deflection and height images were scanned simultaneously at scan rate of 1Hz. The scan size was 5 x 5 µm.

6.2.4 WAXRD

Wide Angle X-Ray Diffraction (WAXRD) analysis was carried by using powder XRD Xpert-1217 diffractometer. The scanning speed was 4°/ min, with a radiation of CuK- α. The samples were scanned from 2 θ values of 5° to 50°.

6.3 Result and discussion

The morphology of the sugar linked SBS samples were studied using SEM, AFM, TEM and WAXRD to investigate the effect of functionalization of SBS on its morphology and self assembling behaviour.

6.3.1. Scanning electron microscopy (SEM)

The morphology of elastomers has been extensively investigated in literature by scanning electron microscopy (SEM). Thin films of the samples were prepared from chloroform solution for examining their surface morphology by SEM.

(a)

(b)

(c)

(d)
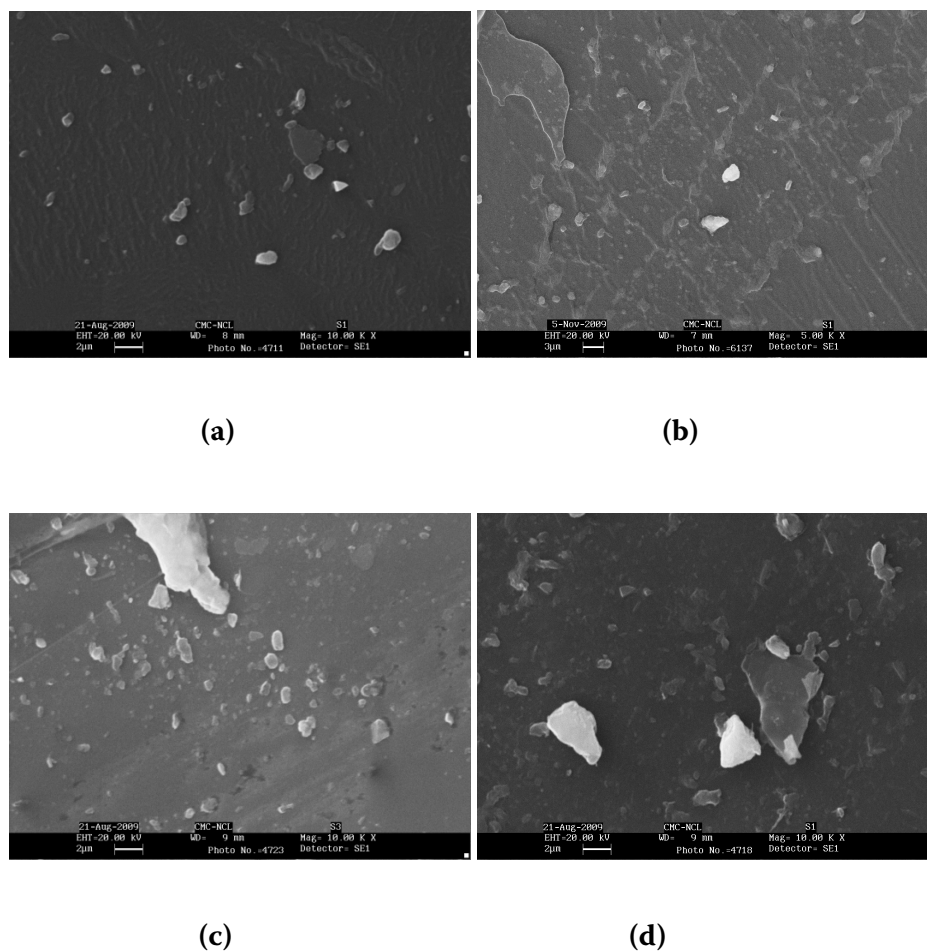
Figure 6.1 SEM micrographs of (a) SBS (b) epoxidized SBS (c) glucose linked SBS (d) mannose linked SBS

Figure 6.1 shows the surface morphology of SBS, epoxidized SBS, glucose linked SBS and mannose linked SBS. SBS is considered a two-phase thermoplastic block copolymer in which spherical polystyrene (PS) domains are dispersed in continuous polybutadiene (PB) phase [3-4]. Similar morphology as reported in literature is observed here for unmodified SBS in above figure [6.1 (a)]. Epoxidation is known to increase compatibility between polystyrene and polybutadiene phase depending on extent of epoxidation [5]. This effect is visible in SEM image of epoxidized SBS [figure 6.1 (b)] where polystyrene domains seems to be less phase

separated as compared to SBS and a smoother surface is observed [figure 6.1 (a)]. With the introduction of hydrophilic sugar moieties and polar ionic groups (pyridinium and ammonium chloride) into a non-polar hydrophobic SBS elastomer, there is an increased tendency between the hydrophilic and hydrophobic segments to form independent phases resulting in a microphase separated structure [6]. The expected self-assembling behaviour into micro phase separated domains of the modified polybutadiene hydrophilic segment could not be observed in the SEM images of sugar linked SBS samples; this is generally observed clearly with TEM. Although self- assembling behaviour is not observed in the SEM's recorded the increased phase separation (crowding of polystyrene domains) as compared to SBS [figure 6.1 (a)] can be observed [figure 6.1 (c) & (d)] of glucose and mannose linked SBS containing pyridinium and quaternary ammonium groups. A similar behaviour is observed for all the sugar linked SBS samples in figure 6.2 (a)-(f).

(a)

(b)

(c)

(d)

(e)

(f)
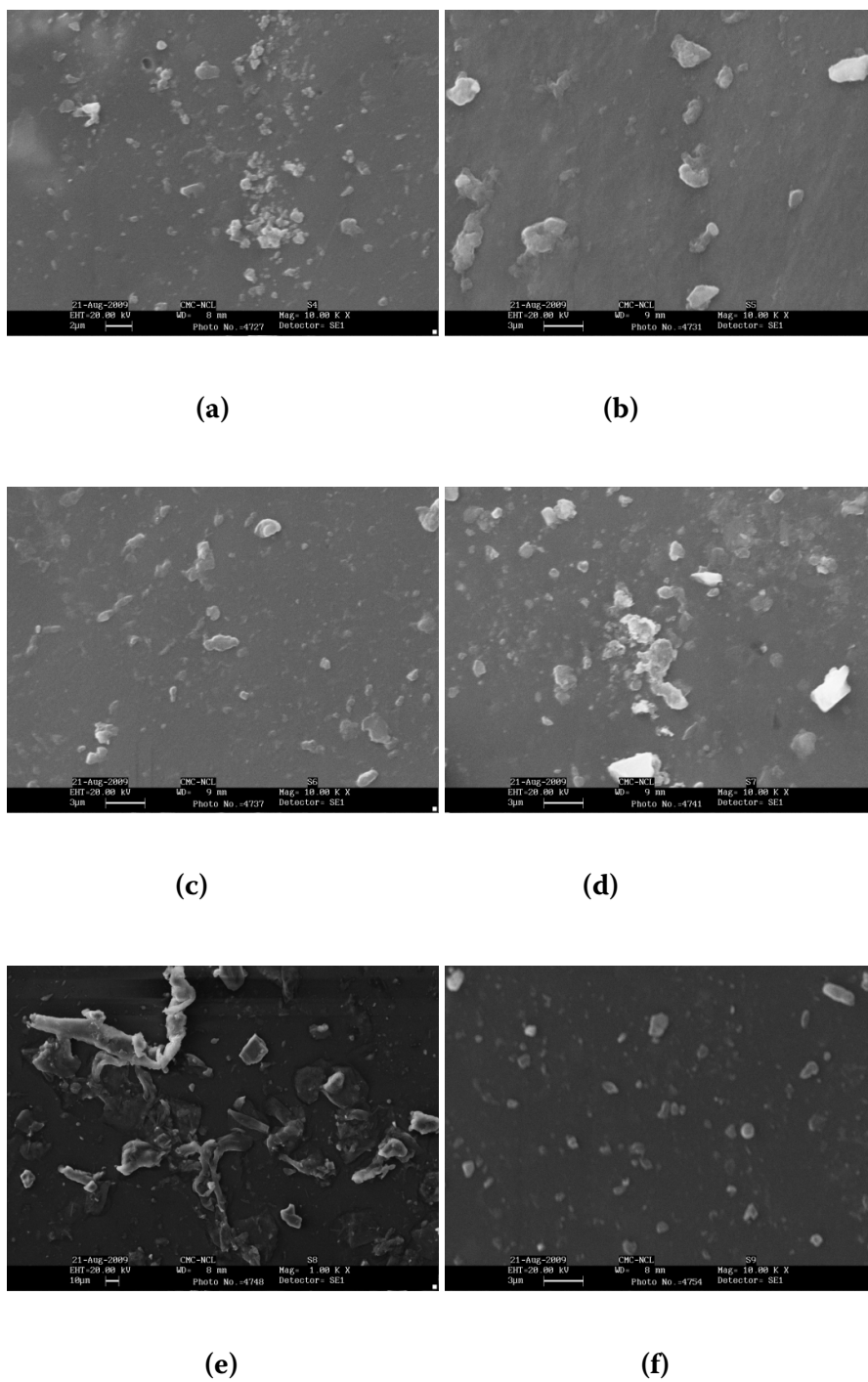
Figure 6.2 SEM micrographs of (a) galactose linked SBS (b) xylose linked SBS

(c) fructose linked SBS (d) sucrose linked SBS (e) methyl glucoside linked SBS

(f) maltose linked SBS

6.3.2. TEM analysis of sugar linked SBS

Transmission electron microscopy (TEM) was used to gain insight into the changes associated with domain structures after functionalization of SBS elastomer with sugar and quaternary ionic groups. Figure 6.3 shows the TEM micrograph of a section of thin film of unmodified SBS. The white spheres in figure 6.3 (a) represent polystyrene domains dispersed in the continuous polybutadiene phase (dark region).
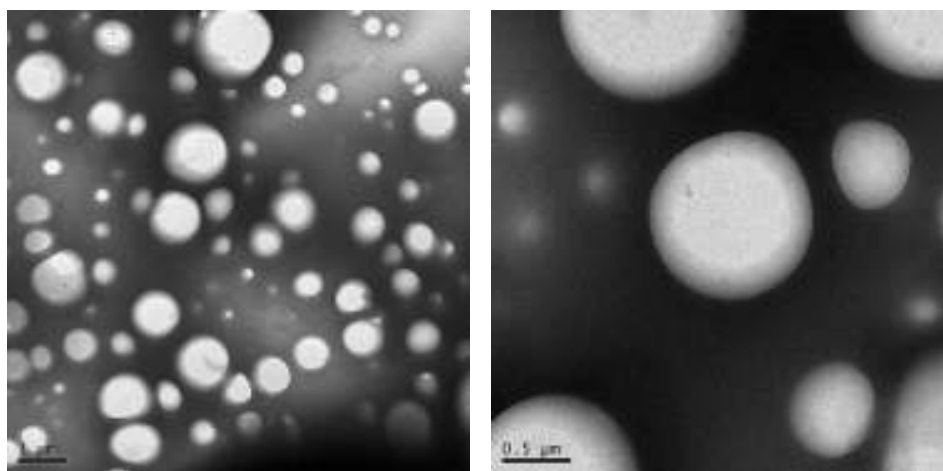
| (a) | (b) |

Figure 6.3 TEM images of unmodified SBS at different magnifications

(a)   (b)
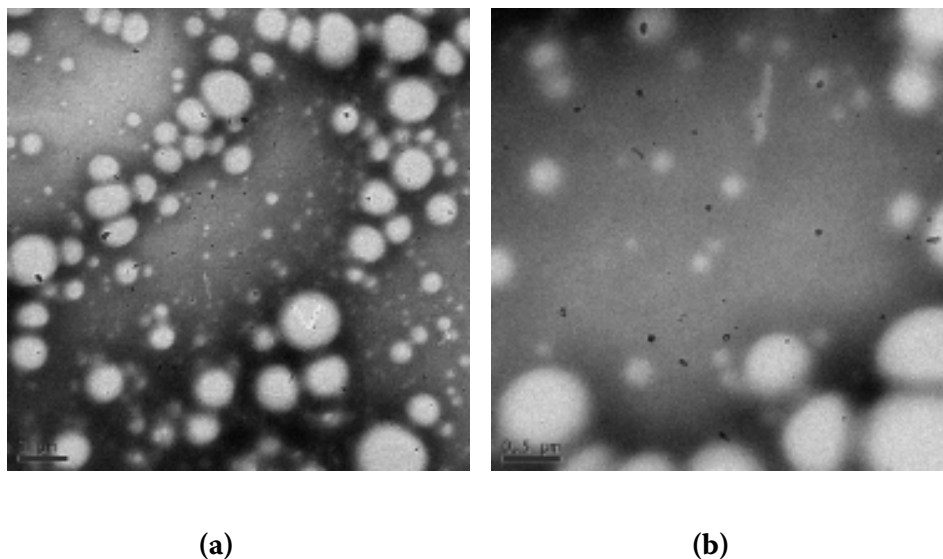
Figure 6.4 TEM images of Galactose linked SBS at different magnification

Figure 6.4 shows the TEM micrographs of the amphiphilic galactose linked SBS containing pyridinium and quaternary ionic groups. It has been widely reported that amphiphilic glycopolymers self assemble into colloidal size aggregates, vesicles and micelles [7] when dissolved in suitable solvents and the morphological architecture depends on the initial copolymer concentration. It can be observed from the figure 6.4 (a) & (b) that after functionalization of SBS some microphase separated black particles are generated selectively in the continuous polybutadiene phase. This is due to the anchoring of sugar [8] and ionic moieties to the polybutadiene segment which tends to self assemble into micelles because of selective solubility of hydrophobic polystyrene - polybutadiene blocks and insolubility of polybutadiene blocks containing hydrophilic pendants. This leads to micelle formation in chloroform solution (organic media) with hydrophilic core having sugar, pyridinium and quaternary ammonium linked polybutadiene and hydrophobic polystyrene outer shell. This hypothesis is supported by L. You et al. report of vesicles formation in glucose grafted 1,2 polybutadiene –block –

polystyrene in both organic and aqueous media, with glucose units forming membrane and polystyrene form the corona of the vesicles in organic media [9]. We have only upto 0.37 weight % sugar content, while You et al. had 17 weight % sugar.

 In the TEM image of galactose linked SBS [Figure 6.5 (c)] aggregation of micelles can be seen. This is probably due to the sugar molecules interactions (strong intermolecular hydrogen bonding) among the micelles. Similar aggregation behaviour of the micelles is also observed in the mannose and maltose linked SBS [figure 6.6 (a) & 6.7 (a)].
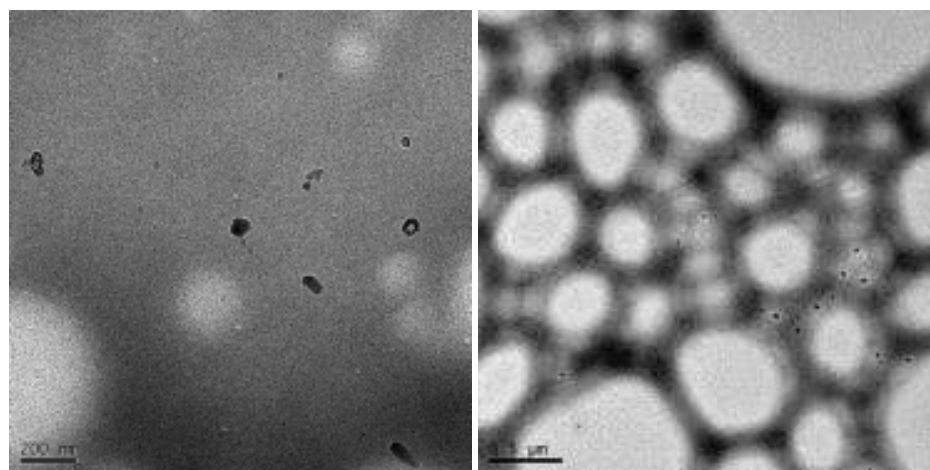
(a)

(b)
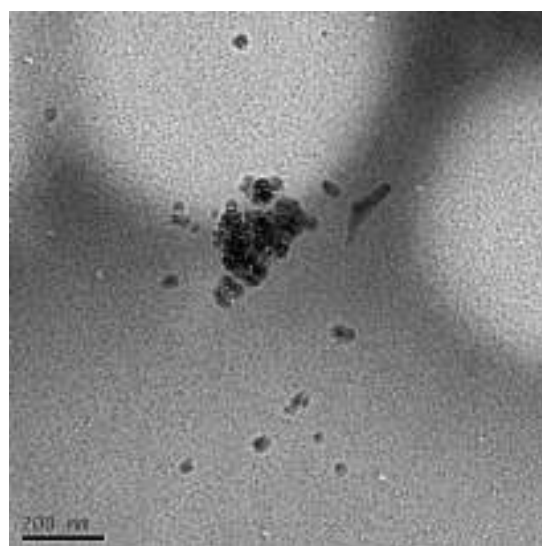
(c)

Figure 6.5 TEM images of (a), (c) galactose linked SBS (b) Glucose linked SBS

<center>(a)   (b)</center>
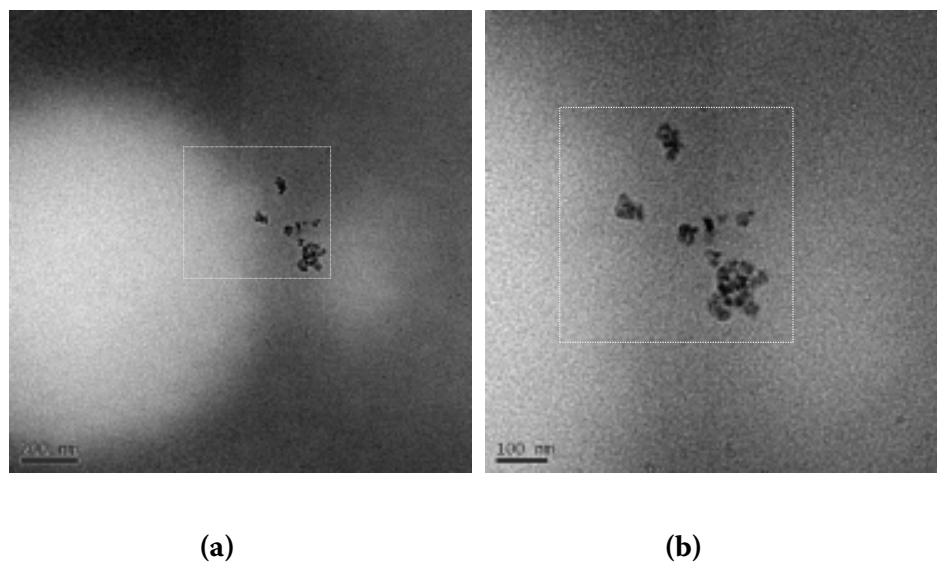
Figure 6.6 TEM images of mannose linked SBS at different magnifications

<center>(a)   (b)</center>
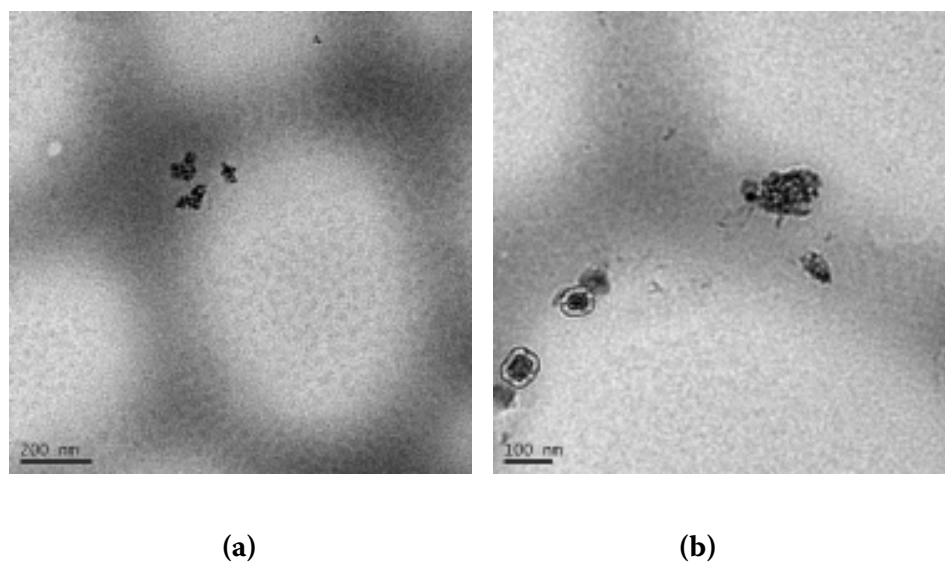
Figure 6.7 TEM images of maltose linked SBS

Figure 6.7 shows the TEM images of maltose linked SBS. Interestingly, along with aggregation of micelles some vesicle like structure is also seen in figure 6.7 (b). Vesicle formation is commonly associated with block copolymers containing carbohydrates either as a pendant or as a co-monomer.

TEM investigation of the sugar linked SBS samples gave good insight into the morphological changes induced in the SBS elastomer due to functionalization.

6.3.3. Atomic force microscopy (AFM) of sugar linked SBS

AFM measurements were performed for characterization of the surfaces of the sugar linked SBS films. Clear differences in surface morphology of the sugar linked SBS samples as compared to unmodified SBS can be seen from figures 6.8-6.16. A relatively homogenous phase separation of polystyrene domains is observed in SBS (figure 6.8).
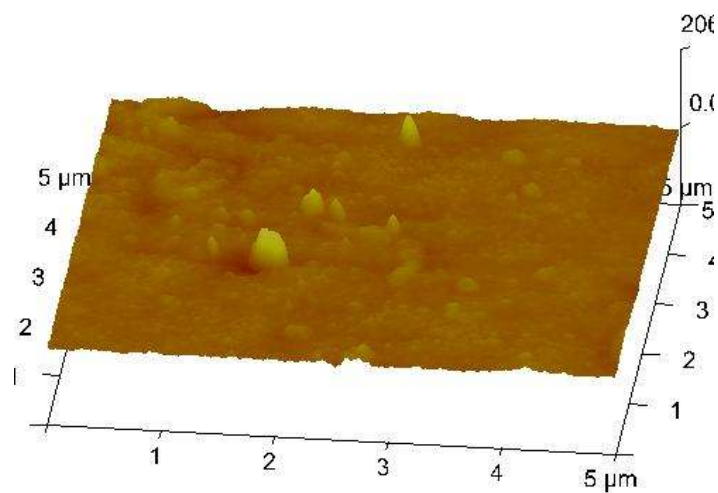
Figure 6.8 AFM image of unmodified SBS
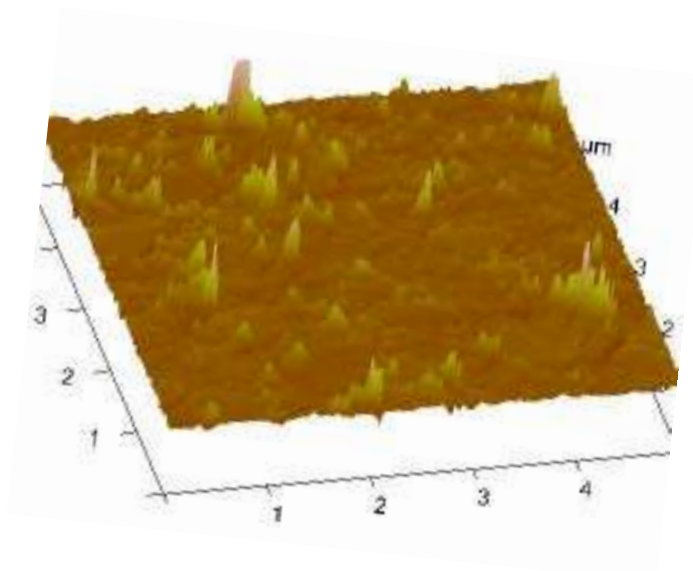
Figure 6.9 AFM image of glucose linked SBS

With functionalization the surface morphology of sugar linked SBS becomes more heterogeneous and surface roughness also increases due to modification, as is evident from the AFM images of the different sugar linked SBS samples (figure 6.9-6.15). Thus, AFM observations are in accordance with those made by SEM.
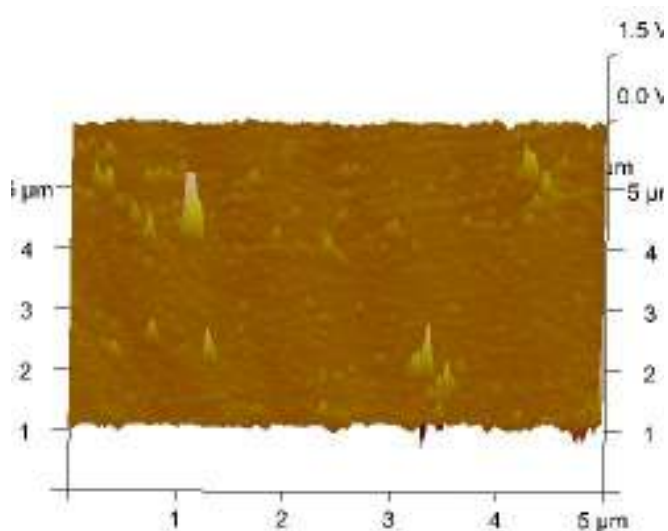
Figure 6.10 AFM image of galactose linked SBS
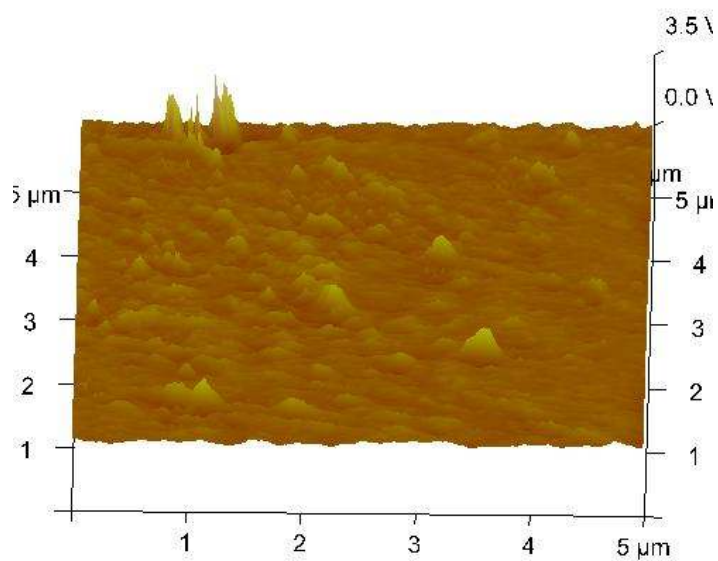
Figure 6.11 AFM image of mannose linked SBS
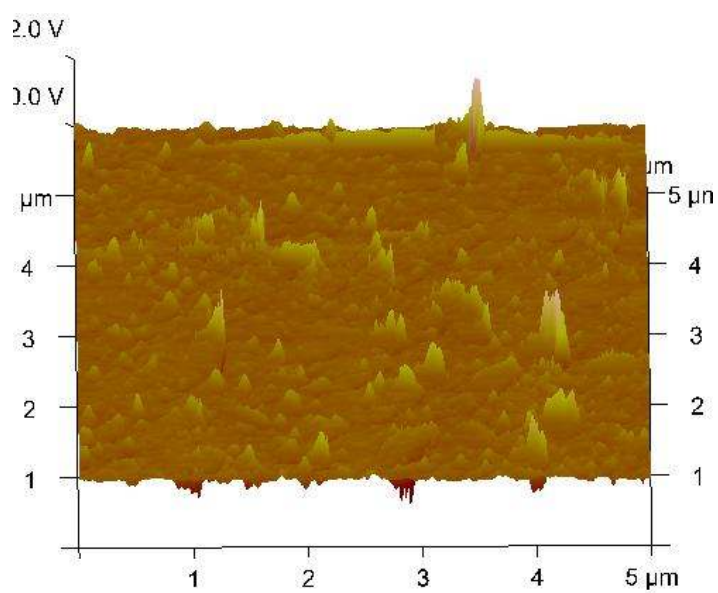
Figure 6.12 AFM image of Maltose linked SBS
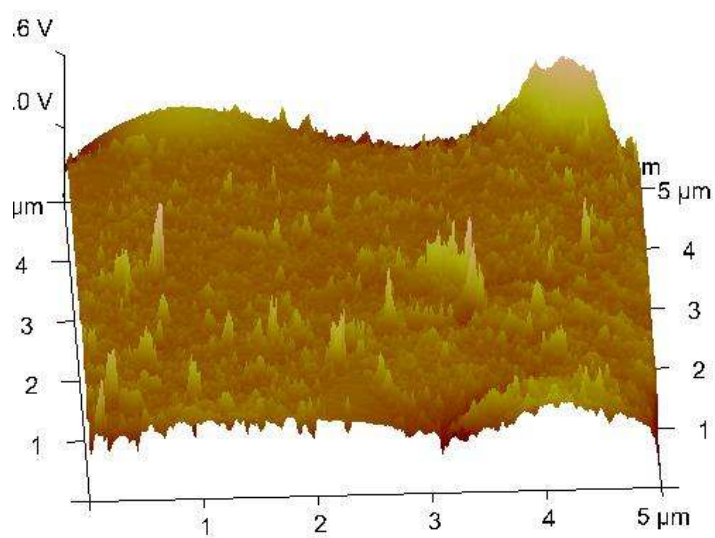
Figure 6.13 AFM image of xylose linked SBS
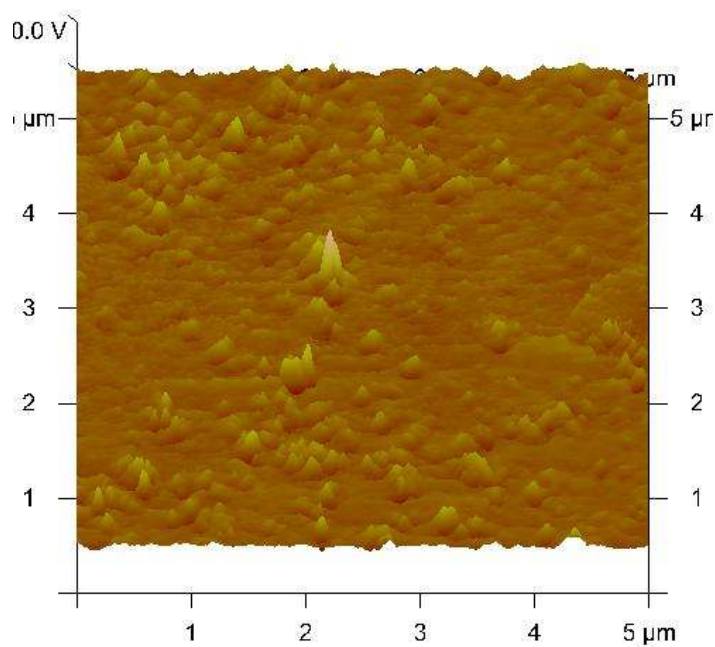
Figure 6.14 AFM image of sucrose linked SBS
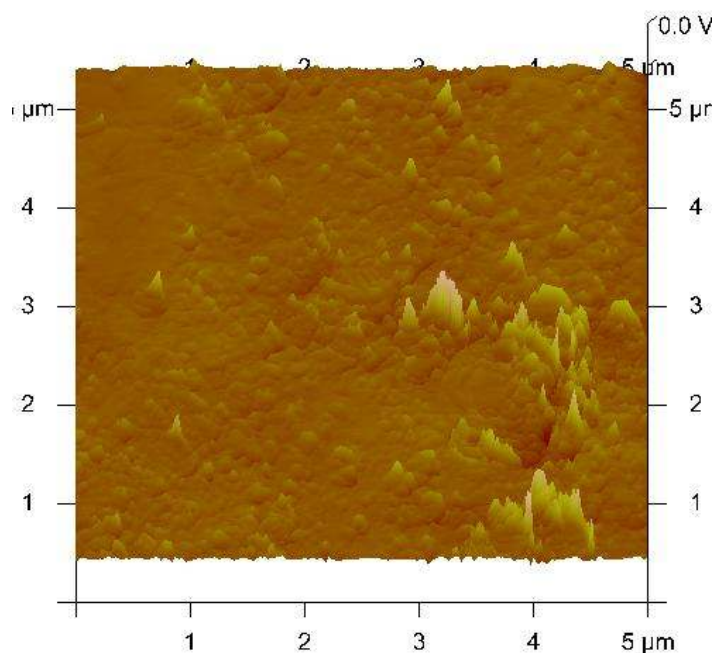
Figure 6.15 AFM image of methyl glucoside linked SBS

6.3.4. WAXRD analysis of sugar linked SBS

SBS is an amorphous [10] thermoplastic elastomer with neither polystyrene nor polybutadiene being crystalline; hence broad peaks corresponding to polybutadiene and polystyrene are observed in the wide-angle X-ray diffraction of unmodified SBS. All the samples were scanned from $2\theta = 5^0$- 50^0 at room temperature.

Figure 6.16 shows the wide-angle X-ray diffraction plots of unmodified SBS and partially (7 & 22 mol %) epoxidized SBS. Three broad peaks are observed in the above WAXRD plots centred at 2θ values of 9.5 ^{0}, 19.7 ^{0} and 28.7 ^{0}. The more intense peak is centered at $2\theta = 19.7$ ^{0} corresponds to amorphous polybutadiene [11-12], while the weaker one is centred at $2\theta = 9.5^0$ corresponds to polystyrene [13]. It can be observed that that the intensity of peak at $2\theta = 19.7$ ^{0} associated with polybutadiene increases with increasing degree of epoxidation. This due to the

introduced oxirane rings in soft polybutadiene blocks which due to its polar nature increase inter-chain interaction leading to more ordered structure.
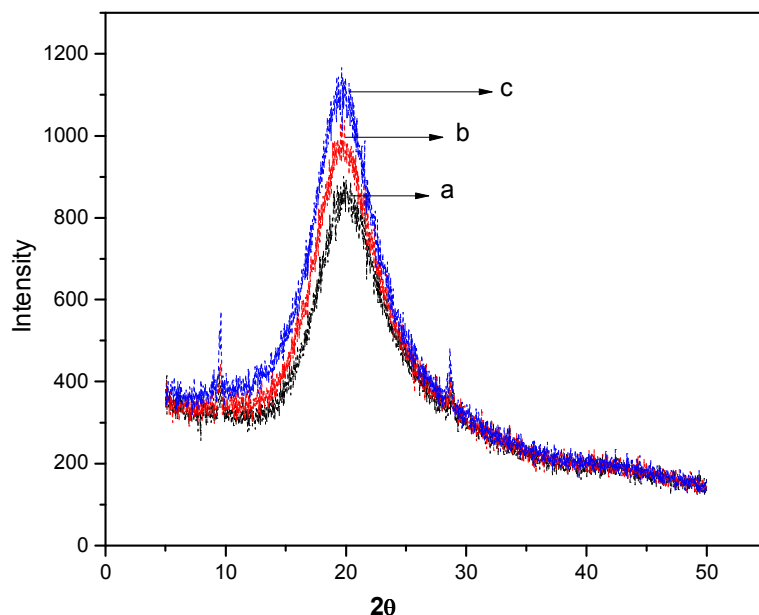
Figure 6.16 WAXRD diffraction plots of (a) SBS (b) 7 mol% epoxidized SBS (c) 22 mol % epoxidized SBS

Figure 6.17 shows the wide-angle X-ray diffraction plots of different sugar linked SBS samples. It can be observed from the above figure that after functionalization of SBS with sugar and quaternary ionic groups there is significant decrease in intensity of peak at $2\theta = 19.7^0$ associated with polybutadiene domain. As a result of anchoring of sugar and quaternary ionic groups there is enhanced hydrogen bonding and ionic interaction which further disrupts the amorphous structure in polybutadiene domain resulting in decreased intensity of peak at $2\theta = 19.7^0$. Moreover, this also proves that indeed sugar and quaternary ionic groups have been covalently attached to the soft polybutadiene domains.

The order of decrease of intensity in sugar linked SBS samples is, maltose linked SBS > mannose linked SBS > galactose linked SBS.

Interestingly, the residual epoxide content of maltose, mannose and galactose linked SBS samples are 7.3, 8 and 4.8 % respectively relative to 22 mol% epoxidized SBS taken as 100 % epoxide content (discussed in chapter 2 & 4), correlating well with the observed order of intensity. We have seen from figure 6.16 that the intensity of polybutadiene peak is sensitive to degree of epoxidation and hence we can presume, had there been no residual epoxide groups, the effect of sugar and pyridinium content would have been even more dramatically seen.
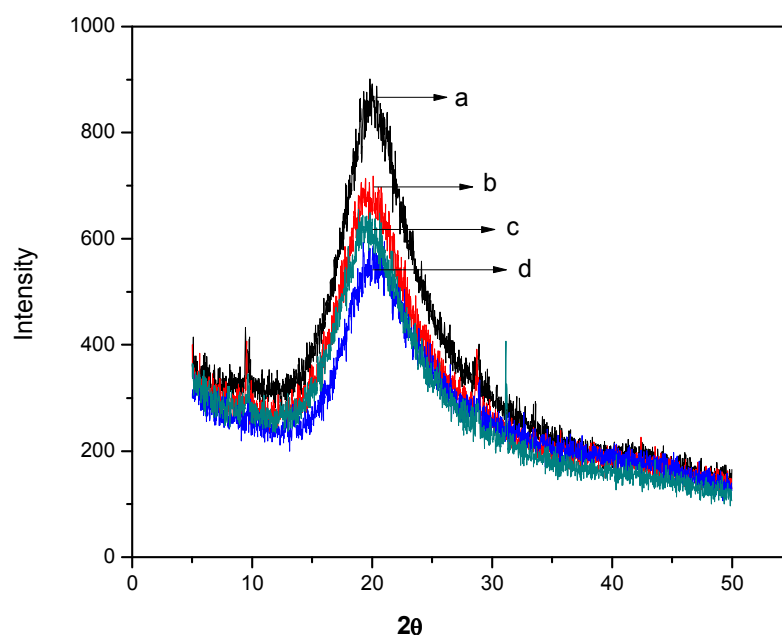
Figure 6.17 WAXRD diffraction plots of (a) SBS (b) maltose linked SBS (c) mannose linked SBS (d) galactose linked SBS

Figure 6.18 shows the wide-angle X-ray diffraction plots of SBS, sucrose and glucose linked SBS. Glucose linked SBS shows decreased intensity at

2 θ = 19.7 ^{0} similar to other sugar linked SBS samples, while Sucrose linked SBS sample show high intensity than even unmodified SBS. This behaviour is in accordance with its high residual epoxide content (70%) on account of its incomplete functionalization (discussed in chapter 2). This observation supports our previous discussion correlating residual epoxide content with the reduction of intensity of polybutadiene peak at 2 θ = 19.7 ^{0}.
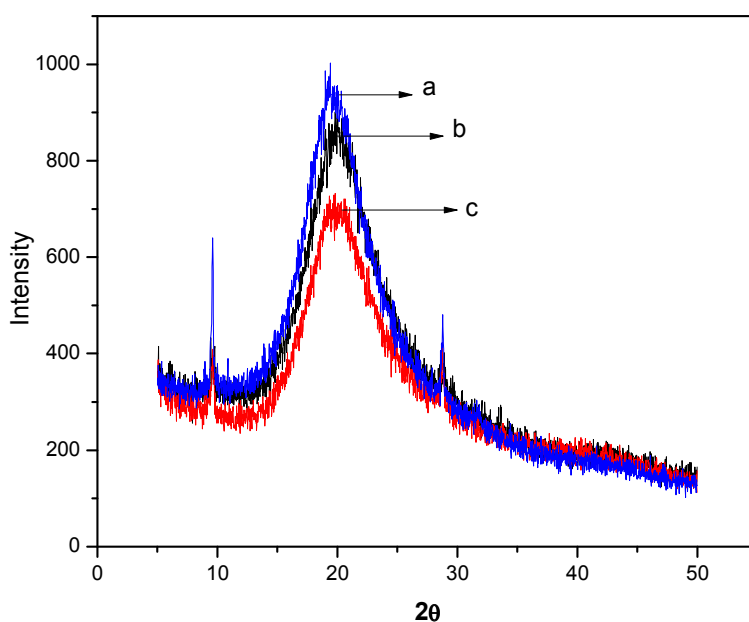
Figure 6.18 WAXRD diffraction plots of (a) sucrose linked SBS (b) SBS (c) glucose linked SBS

6.4. Conclusion:

In conclusion, we can say that the selective functionalization of polybutadiene domains of SBS with sugar and quaternary ionic groups leads to decrease in intensity of the broad peak associated with polybutadiene and the relative intensity of the functionalized SBS is dependent on the residual epoxide content of the sugar

linked SBS elastomers. Moreover, WAXRD technique is helpful in predicting qualitatively the residual epoxide content of the synthesized elastomers besides providing information on morphological changes associated with the functionalization of SBS. SEM, AFM, TEM in conjunction with WAXRD provided the complete morphological picture of the carbohydrates functionalized SBS.

6.5 References:

1. A. V. Ruzette, L. Leibler, *Nat. Mater.* **2005**, 4, 19

2. H. A. Klok, S. Lecommandoux, *Adv. Mater.* **2001**, 13, 1217

3. R. M. Ikeda, M. L. Wallach, R. J. Angelo, *Polym Preprints Am. Chem. Soc.* **1969**, 10, 1445

4. *Journal of Polymer Science: Part B: Polymer Physics* **2005**, 43, 276–279

5. Wlochowicz, C. Slusarczyk, D. Zuchowska, I Malhotra, *Colloid Polym. Sci.* **1990** 268, 618-624

6. Y. Ikeda, Y. Nakamura, K. Kajiwara, S. Kohjiya, *Journal of Polymer Science: Part A: Polymer Chemistry* **1995,** 33, 2657–2665

7. X

8. Y. Ikeda, Y. Nakamura, K. Kajiwara, S. Kohjiya, *Journal of Polymer Science: Part A: Polymer Chemistry* **1995**, 33, 2657–2665

9. L. You, H. Schlaad, *J. Am. Chem. Soc.* **2006**, 128, 13336-13337

10. E. C. Lopez, D. Mclntyre, L.J. Fetters, *Macromolecules* **1973**, 6, 415-423

11. A. F. Halasa, G. D. Wathen, W. L. Hsu, A. Matrana, J. M. Massie, *Journal of Applied Polymer Science* **1991**, 43, 183-190

12. B. X. Fu, A. Lee, T. S. Haddad, *Macromolecules* **2004**, 37, 5211- 5218

13. H. Fong, D. H. Reneker, *Journal of Polymer Science: Part B: Polymer Physics***, 1999**, 37, 3488–3493

Chapter 7

Isolation and characterization of natural polymer Lignin containing residual carbohydrates as a model for synthetic cross linked polystyrene with anchored carbohydrate moieties

7.1. Introduction

In the previous chapters, we synthesized polymers of SBS having aliphatic carbon chains and aromatic blocks, with pendant carbohydrate groups on the aliphatic chains. We can consider these polymers to be mimics of the natural polymer system of lignins isolated from plant biomass. Lignins, when isolated from plant material, have traces of carbohydrate molecules attached to it, giving it structural similarity to the carbohydrate linked SBS synthesized by us (as explained in chapter 2 and 3). Therefore we undertook a study of isolation of lignin from sugar cane bagasse, characterized the material thoroughly, and then studied its biodegradation using lignin degrading enzymes such as laccases.

Lignin is a multifunctional natural polymer that has the potential to be developed into a major industrial raw material for a multitude of applications [1-7]. After cellulose and hemicellulose, lignin is considered to be the most abundant natural polymer present on planet earth. It is estimated that currently planet earth contains 300 billion metric tons of lignin, with an annual biosynthetic rate of production of 20 billion metric tons [8]. Thus, with a perceived shortage of petroleum-based materials as well as a desire to utilize "green materials", the chemistry and technology of lignins is seeing renewed interest.

The chemical structure, molecular weights, molecular weight distribution and degree of crosslinking of lignins depends upon the age of the plant from which it is isolated, the type of plant (hard wood, softwood, grasses, etc). The purity of the isolated lignins depends upon the method of isolation (chemical/biochemical/mechanical), the purification strategy followed, and so on. In order to develop sophisticated applications of lignins, it is most essential to have

highly pure and well-characterized lignin samples. Detailed characterization studies of lignins have been reported in several papers over a period of several decades [9-12]. Yet, the complexity of the structure, the variety of new innovative methods of isolation and purification, and improved instrumentation, leads to new assignments and interpretations of structural features of lignins [13-24], and forms the basis of ever-new research and development efforts.

In particular, lignins are rarely isolated as pure materials, and are always associated with carbohydrate linkages (cellulose, hemicellulose) to varying extents, depending on their isolation procedure. This small carbohydrate content (generally 2-8% by weight in commercial lignins) plays a crucial part in the final reactivity and properties of the polymer. Therefore, in this study, we have carried out a detailed characterization of our laboratory prepared lignin-carbohydrate complexes vis a vis commercial wood lignin , semi commercial organosolv sugarcane bagasse lignin, xylan -free and sulfur-free lignin from bagasse, commercial lignosulfonate from softwood lignin, laboratory prepared liqnosulfonate from sulfur-free bagasse lignins, bagasse lignin-succinic acid adduct, and bagasse lignin succinate-crown ether adduct. Thus in all twelve samples of lignins, lignin-carbohydrate complexes, and other lignin derivatives (three commercial and nine prepared in our laboratory) were investigated and the results are elaborated in this paper. The techniques used for characterization are FTIR, HPLC, thermal analysis, elemental analysis, atomic absorption spectroscopy, and treatment with xylanase enzyme. These diverse lignin samples and diverse experimental techniques have given us a deeper insight into the structures, properties, and the limitations of detection of various features of lignins as a complex molecule. Effects of residual carbohydrate content in lignins, increasing aliphatic chain length, increased crosslinking, effects of small

amount of sulfur content, etc are shown in the changed spectral characteristics and will be valuable in evaluating lignins for new applications research. Our previous work [25] has shown that functionalized polystyrenes, as model systems for lignins, can be made biodegradable by attaching as low as 1% by weight of carbohydrate moieties.

7.2 Experimental

7.2.1 General procedure for preparation of lignin-carbohydrate complexes

Indian sugarcane bagasse was crushed to a fine powder passing through a 100-mesh screen. It was subject to steam pressure ranging from 2 bar to 20 bar for a residence times of 2- 15 minutes, followed by alkali digestion and bleaching sequences. This process yielded lignins containing 3-5 % carbohydrate groups; these could be removed by treatment with a particular strain of xylanase enzyme developed in our laboratory.

7.3 Materials

The following lignin-carbohydrate complexes, carbohydrate-free lignins, and lignin derivatives were either prepared in our laboratory, or procured from alternate sources, as detailed below:

1. Indulin AT (Westvaco, USA) (LS1) is a commercially available wood based lignin-carbohydrate complex. A research sample was kindly provided to us by the company for our research work.

2. Sulfur-free ethanol/water organosolv bagasse lignin-carbohydrate complex (LS2) was prepared in a semi-commercial pilot plant of M/s Pudumjee Pulp and Paper

Mills, Pune, and a sample was kindly provided to us by the company for our research work.

3. Sulfur-free and carbohydrate-free ethanol/water organosolv bagasse lignin (LS3) was prepared by treating (LS2) with xylanase by a proprietary process in our laboratory.

4. Sulfur-free bagasse lignin (LS4) was prepared in our laboratory by a proprietary steam-cum-alkali process followed by precipitation in HCl.

5. Sulfur-free carbohydrate-free bagasse lignin (LS5) was prepared in our laboratory by treating LS4 with xylanase by a proprietary process.

6. Low Sulfur bagasse lignin (LS6) was prepared in our laboratory by a proprietary steam-cum-alkali process followed by precipitation in H_2SO_4.

7. Low Sulfur carbohydrate-free bagasse lignin (LS7) was prepared in our laboratory by treating LS6 with xylanase by a proprietary process.

8. Wood based sodium lignosulfonate (LS8) was obtained commercially from M/s Chembond, Mumbai.

9. Bagasse based sodium lignosulfonate (LS9) was synthesized in our laboratory by a proprietary process using LS4 as a starting material.

10. Bagasse based sodium lignosulfonate (LS10) was synthesized in our laboratory by a proprietary process using LS6 as a starting material.

11. Bagasse lignin-succinic acid adduct (LS11) was prepared by the reaction of LS2 with succinic acid

12. Bagasse lignin-succinic acid-crown ether adduct (LS12) was prepared by the reaction of LS11 with trans-diamino-dibenzo-18-crown ether.

7.4 Characterization

7.4.1 FTIR analysis

A Perkin Elmer Spectrum 1 FTIR was used. The samples were used in the form of KBR discs, which were prepared by grinding 1mg sample/ 100mg pre-dried KBR. The spectra were recorded in the range of 450 cm^{-1} to 4000 cm^{-1}

7.4.2 HPLC analysis

The lignins were subjected to Liquid chromatography in order to compare their compositions. A Dionex HPLC equipped with quaternary gradient pump, injector, multiwavelength programmable UV detector was used for this purpose. The instrument set-up consisted of Aminex-HPX-87H column, an ion exclusion column with mobile phase consisting of 2.75ml 10% H_2SO_4 in 1000 ml double distilled water.

Lignin samples were dissolved in 20mM of NaOH and diluted with 1 mL of the mobile phase, filtered and 20 μL was injected to the column, the detection was carried out at three different wavelength 210 nm, 254 nm and 272 nm.

7.4.3 Thermogravimetric Analysis (TG)

The thermal stability of lignins was studied using Perkin Elmer TGA-7. The TG of various lignins and their derivatives were run up to 700 °C with a heating rate of 10°C/min in nitrogen atmosphere.

7.4.4 Elemental analysis

C,H,N and S were estimated using Carlo Erba CHNS analyzer.

7.4.5 Atomic Absorption Spectroscopy

Determination of the Na content was performed using a Chemito Atomic Absorption Spectrophotometer, Model No-201.

7.5 Results and Discussion

As is evident from the table 7.1 the C and H percentage are in close agreement for LS2, LS4 and LS6. Small percentage of nitrogen also appears for LS6, this could be due to the protein present in bagasse. Soda lignin contains considerable amounts of protein [15], this is evidenced by presence of nitrogen in the elemental analysis. Pan and Sano [26] also found the presence of proteins in alkaline lignins of wheat straw. LS8, LS9 and LS10 show less carbon and hydrogen content due to sulfonation. The Carbon and Hydrogen content in LS11 and LS12 found to be changed could be due to the reaction of lignin and succunic acid in LS11 and further with crown ether in LS12. The presence of sulfur was due to sulfuric acid used in the precipitation of LS6 lignin.

7.5.1. Discussion on assignment of FTIR absorption of lignins

The various FTIR spectra bands origin and their assignments, in the FTIR spectra of different lignin-carbohydrate samples are discussed below.

Table 7.1 Elemental Analysis of various lignin samples

Lignin	% C	% H	% N	% S	Na% By AAS
LS1	59.57	6.29	1.07	2.16	1.042
LS2	62.84	5.37	-	-	0.074
LS3	62.17	5.49	-	-	-
LS4	62.95	5.74	-	-	0.049
LS5	61.87	6.25	0.96	-	-
LS6	62.18	5.72	0.43	1.11	0.416
LS7	61.44	6.34	0.97	-	-
LS 8	45.75	4.49	-	4.94	-
LS 9	44.25	4.54	-	4.20	8.75
LS 10	44.25	4.54	-	4.20	-
LS-11	58.47	4.81	-	-	
LS-12	60.71	5.16	1.54	-	
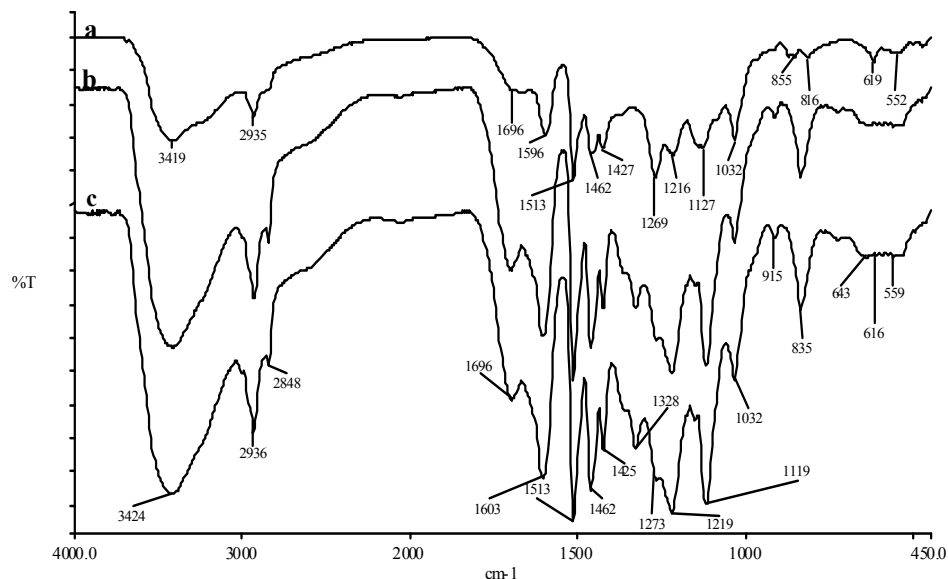
Figure 7.1 FTIR of (a) softwood lignin-carbohydrate complex LS1 (b) bagasse lignin- carbohydrate complex LS4 (c) bagasse lignin-carbohydrate complex LS6

Figure 7.1 shows FTIR spectra of LS1, LS4 and LS6 (i.e, lignin- carbohydrate complexes of softwood and bagasse). The differences between softwood and hardwood lignins have been published by Martinez et. al., 1999 and are in agreement with the above results. Thus, our FTIR studies confirm that Indian sugarcane bagasse lignin isolated by us, and being one of the largest known reservoirs of annually renewable resource (estimated at 200 million tonnes per annum), contains both syringyl and guaiacyl units, similar to hardwood lignins.

LS1 and LS6 contain about 2 % and 1 % sulfur, respectively. This is indicated by the C-S stretching at 619 cm^{-1} (virtually absent in LS2 and LS4) (Fig.7.1). The FTIR spectra of both the LS4 and LS6 lignin are more or less similar in absorption peaks as well as in absorption intensities, except for the minor sulfur content in sulfuric acid precipitated LS6. Therefore precipitation by HCl is a preferred method for iso-

lating lignins. LS4 and LS6 lignin samples were treated with xylanase giv-
ing samples LS5 and LS7 respectively.
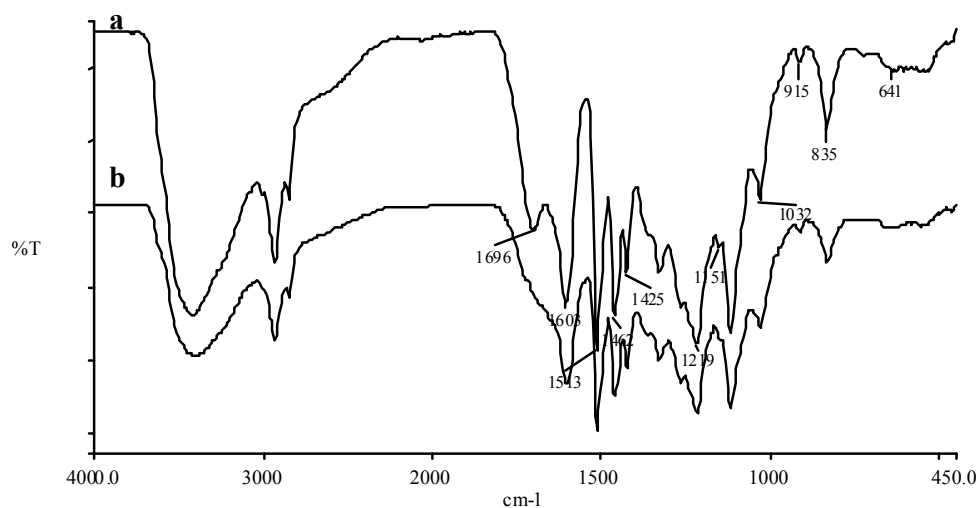
Figure 7.2 FTIR of (a) bagasse lignin-carbohydrate complex LS4 (b) carbohydrate-
free bagasse lignin LS5

The Figure 7.2 shows the band at 1693-1705 cm^{-1}, indicative of C=O stretching,
(due to carbohydrates linked with lignin), has drastically reduced after xylanase
treatment (LS5). This is confirmed by significant reduction in the hydroxyl peak of
LS5. Further evidence of this is seen by the reduction in relative absorbance at
1118cm^{-1}and 1269 cm^{-1} which is an indicative of C=O stretching present in carbo-
hydrates [10]. Similar trends have been observed in case of LS6 and LS7 after the
xylanase treatment. The removals of carbohydrate linkage have also been observed
in HPLC analysis.
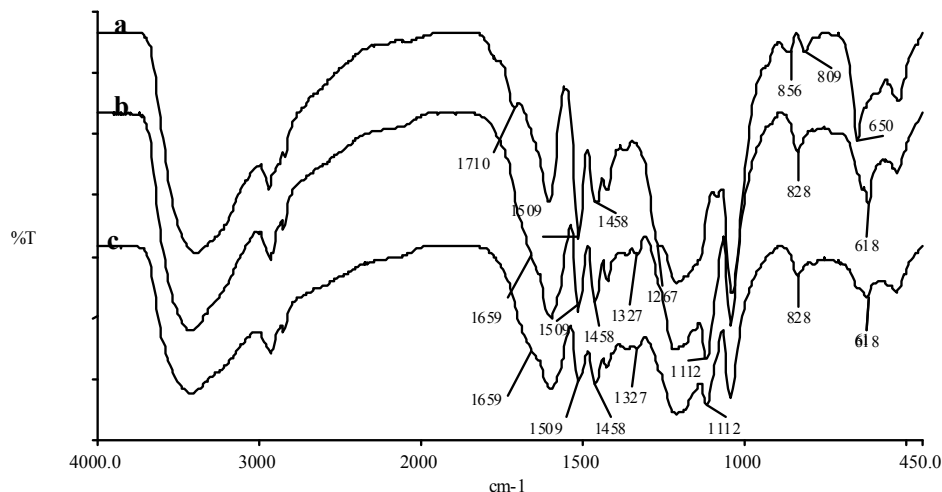
Figure 7.3 FTIR of (a) Commercial softwood lignosulfonate LS8, (b) bagasse lignosulfonate LS9, (c) bagasse lignosulfonate LS10

Figure 7.3 shows the FTIR spectra of lignosulfonates LS8 (softwood based), and LS9 and LS10 (bagasse based). A peak at 1710 cm^{-1} in LS8 (commercial lignosulfonate) could be due to the C=O stretching due to the carbohydrate linkage with lignin. This band is absent in lignosulfonates LS9 and LS10. It appears that carbohydrate groups in LS9 and LS10 prepared by other processes in the laboratory are hydrolyzed under the reaction condition of their preparation (basic aqueous medium, high temperature).

  The band at 655 cm^{-1}, characteristic of lignosulfonate (Nada, Sakhawy &. Kamal, 1998), appears at 650 cm^{-1} for LS8, and at 618-650 cm^{-1} for LS9 and LS10. The presence of sulfur has been confirmed by elemental analysis. This shows that the structure of lignosufonates prepared by the classical sulfite process (LS8) or by sulphonation of isolated lignins (LS9, LS10) are similar, therefore, there is good scope to synthesize lignosulfonates from vast amount of waste lignins.
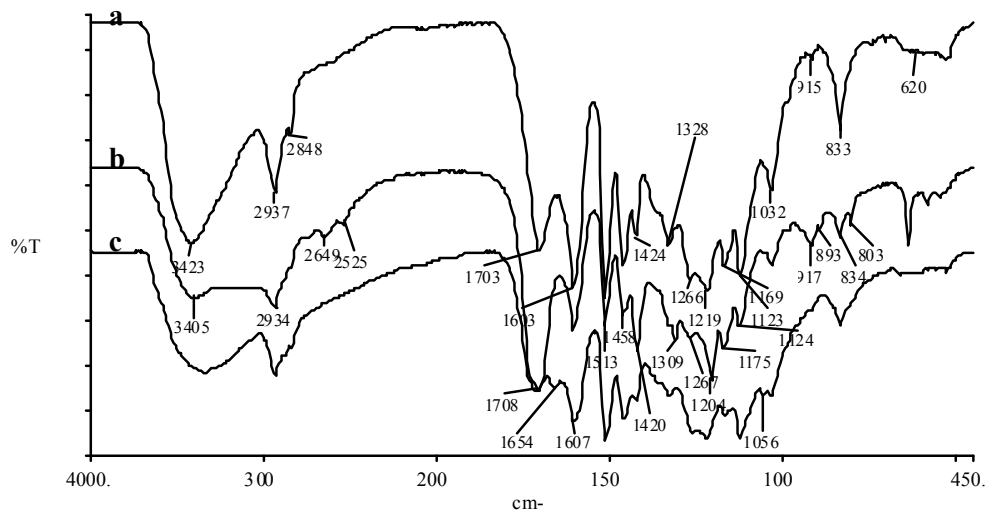
Figure 7.4 FTIR of (a) Organosolv lignin-carbohydrate complex LS2, (b) Bagasse-lignin succinic acid adduct LS11, (c) Bagasse-lignin succinic acid –crown ether adduct LS12

Figure 7.4 shows the FTIR of lignin-carbohydrate complex (LS2) and it's succinic acid and crown ether derivative (LS11, LS12). An amide bond is formed in LS12 (peak at 1654 cm^{-1}). The large amount of carbohydrates in LS2 is seen by the large peak at 3423 cm^{-1}, and it is decreased in LS11 and LS12. In the latter the N-H stretch band merges with this hydroxyl peak. The ester peak in LS11 is clearly seen at 1708 cm^{-1}. However, crosslinking of succinic acid (LS11) by diamino dibenzo 18-crown-6 (LS12) reduces the resolution of the spectra, this is analogous to the lower resolution of Poly (styrene-divinylbenzene) spectrum as compared to polystyrene spectrum (Fig 7.5).
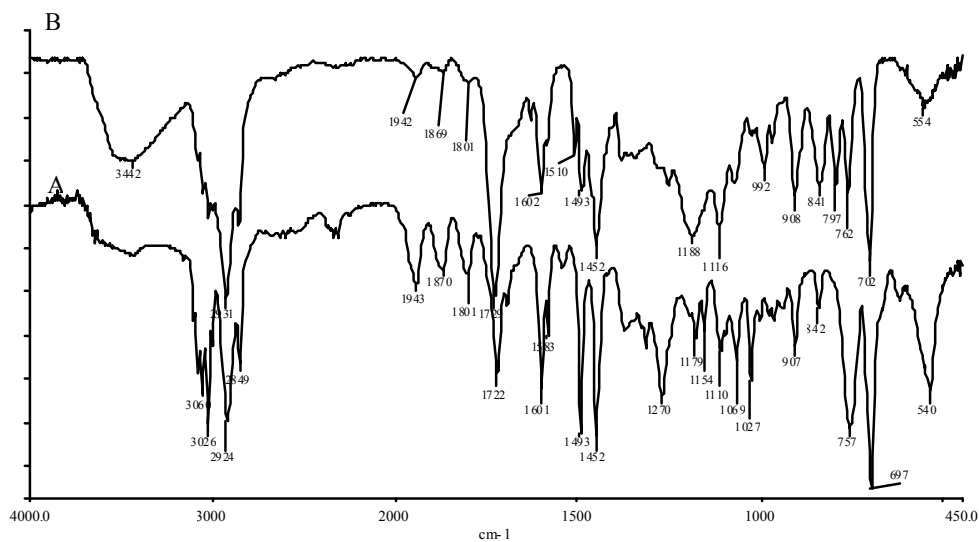
Figure 7.5 FTIR of (a) polystyrene, (b) Styrene-divinylbenzene polymer

Thus, lignins isolated by various methods can be derivatized to interesting new compounds like LS11 and LS12 with vastly different thermal properties (see following section) and characterized by FTIR.

7.5.2. Discussion on thermal analysis

TG curves of various bagasse lignin-carbohydrate complexes as well as carbohydrate-free lignins were obtained under pure nitrogen atmosphere.

Table 7.3 gives the TGA experimental details such as degradation onset temperature (T_{onset}) and maximum degradation temperature (T_{max}) for the thermal degradation of the various lignin samples and degradation wt % from analysis of TGA curves. The thermal curves show first stage of degradation at 100-150^0 C due to the evaporation of residual moisture. The second degradation occurs at 230 to 300^0 C is due to the carbohydrate (hemicellulose) component present in lignin. This therefore represents the upper limits of temperature for processing lignin-carbohydrate complexes. Lignin itself degrades above 300°C and shows maximum degradation at 330-400°C. In nitrogen atmosphere 40-50 % residue was observed up to ~600°C.

No residue is seen for polystyrene and crosslinked polystyrene. Apparently, the many functional groups present in lignins and their derivatives lead to complex crosslinked structures that do not decompose upto 600° C.

Table 7.2 Thermogravimetric Analysis (TGA) data for lignins, xylanase treated lignins and lignin derivatives under nitrogen atmosphere at heating rate of 10^{0} C/min.

Sample	$T_{onset}^{o}C$	$T_{max}^{o}C$	Degradation (Wt %)			
			240	**350**	T_{peak}	**590**
LS1	236	393	7	18	25.1	45.7
LS2	277	389	5.3	20.6	31	55.6
LS3	268	369	4	23	28.3	52.5
LS4	299	390	6.7	20	31	58
LS5	270	368	7.2	26.15	32	57
LS6	289	394	6.2	20	33.6	59
LS7	254	352	4.4	27.5	28	56
LS11	183	218 and 388	16.5	31	11.5 38.1	58
LS12	302	403	4.5	14	25.8	47.2

Softwood based LS1, based on guaiacyl units, probably has more crosslinking sites and appears to get increasingly crosslinked and thermally stable as compared to LS4 and LS6. The THF soluble fraction (LS1A) of softwood based lignin (LS1)

shows less thermal stability than the THF insoluble fraction (LS1B), which is apparently the fraction, which has very high crosslink density (fig7. 6).
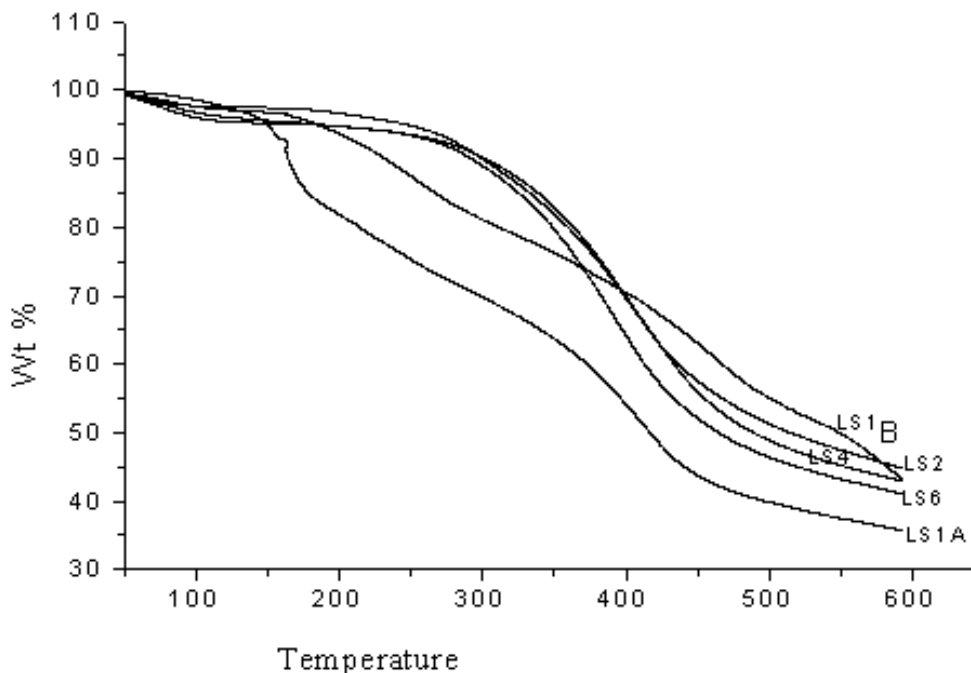
Figure 7.6   Superimposed thermogravimetric (TG) curves of LS1, LS1A, LS2 LS4 &LS6

LS2, LS4, and LS6 were nearly fully soluble in THF (>96%), indicating that these are not strongly crosslinked, which is reflected in their thermogravimetric (TG) curves in figure 7.6. The fact that samples with greater crosslink density degrade more slowly at high temperatures is also proved by the TG curves for polystyrene and crosslinked polystyrene, presented in Figure 7.8. Also, we can conclude that the processes used to isolate lignin to obtain samples LS2, LS4, and LS6 give easily THF soluble lignins than the commercial LS1 made by kraft process, indicating they are more homogenous than LS1.
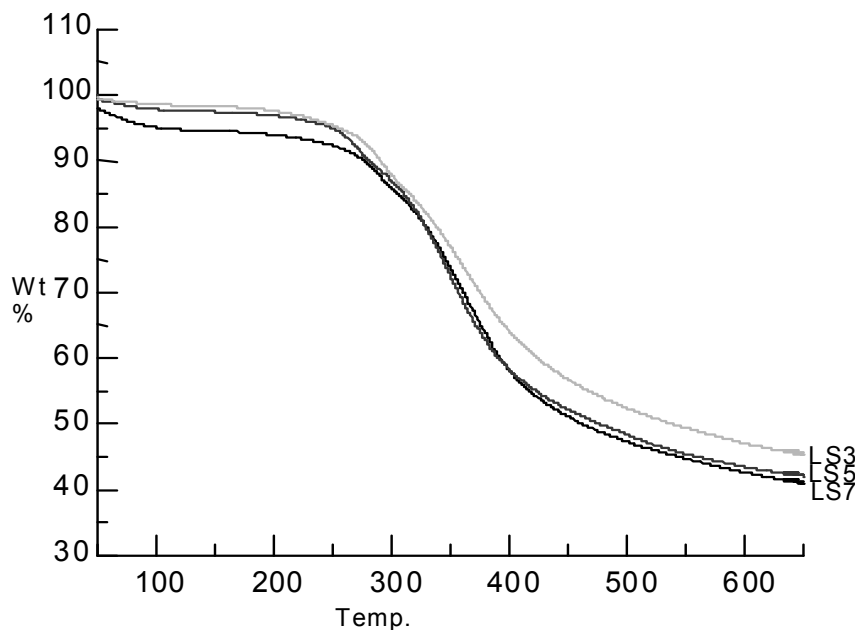
Figure 7.7 Superimposed TG of Xylanase treated lignins LS3, LS5 & LS7

Figure 7.7 shows the TG curves for xylanase treated samples, wherein the xylan content of the lignins is minimal following removal of xylan by xylanase, leading to a carbohydrate-free lignin with more symmetric curves, as would be expected. The initial decomposition temperature and T_{max} of the two lignins (LS4, LS6) were found to be similar even though the isolation process was different; the marginal decrease in onset of degradation of LS6 over LS4 is due to it's small sulfur content. These lignins are more stable than the commercial lignins studied (LS1). T_{onset} and T_{peak} of lignins were reduced after xylanase treatment. The reduction in T_{onset} may be due to chemical separation of carbohydrates from lignin-carbohydrate complex by the xylanase enzyme used for this purification treatment. The reduction in $T_{max.}$ may be also due to enzymatic fragmentation of the lignin molecule itself, which possibly causes structural changes in lignin.
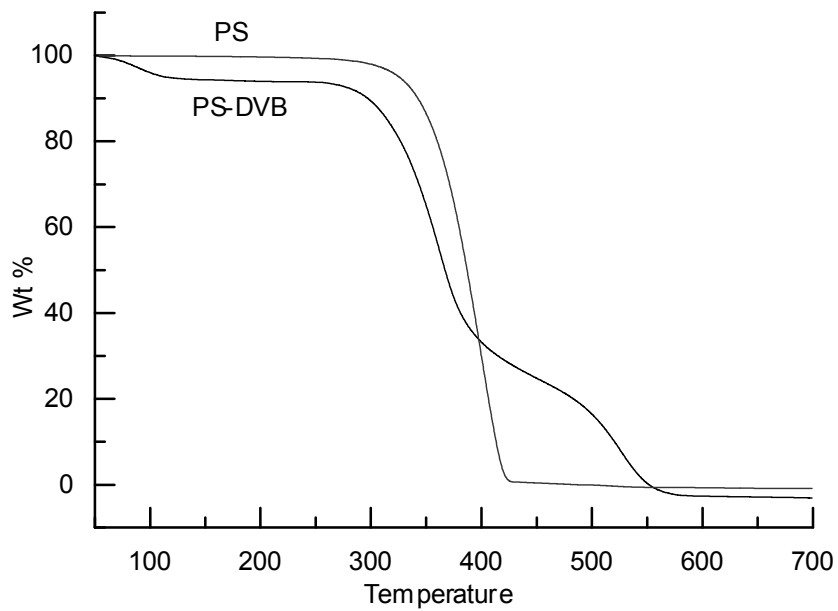
Figure 7.8 TG of standard Polystyrene and Polystyrene-Divinylbenzene (PS
DVB)
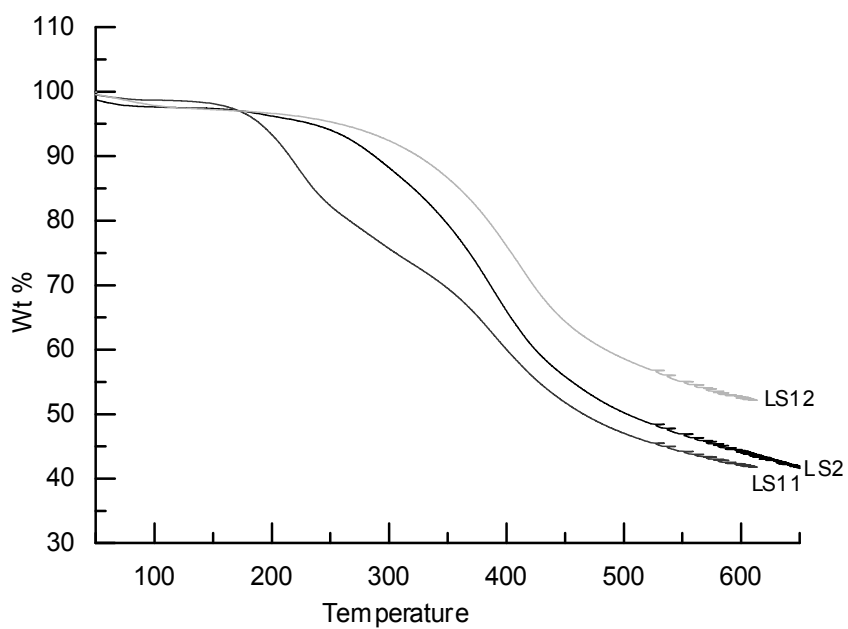
Figure 7.9 Superimposed TG of LS2, LS11 & LS12

The TG of LS11 shows a sharp peak at 218 ^{o}C that could be due to the degradation of aliphatic chain of succinic acid introduced after reaction with lignin. From the TG curve (fig 7.9) it is seen that lignin succinate-crown ether is more stable at higher temperatures (due to crosslinking by stable amide bonds), whereas lignin–succinic acid adduct is unstable (greater aliphatic content). The TG of lignin succinate-crown ether shows more than 100 ^{o}C increase in T_{onset}. and also an increase in the $T_{max,}$ indicating increased crosslinking of the lignin by diamino DB 18-C-6. The degradation at 590°C is also less than the other lignins studied. Thus the thermal analysis of various lignins provides evidence of their homogeneity, carbohydrate content, and extent of crosslinking.

7.5.3 Discussion on HPLC Studies

The lignin samples were analyzed by HPLC for their composition and purity.   The HPLC were scanned at three different UV wavelength 1) 210 nm, 2) 254 nm and 3) 272 nm. Residual carbohydrates in the lignins are likely to be detected at 210 nm, while other chromophores will show up at the higher wavelengths. The results are shown in figures 7.10 and 7.11. It is clear from the HPLC's presented that carbohydrate removal from the lignins by xylanase treatment can be detected by HPLC at the lower wavelength 210 nm (HPLC's of LS4, LS5).
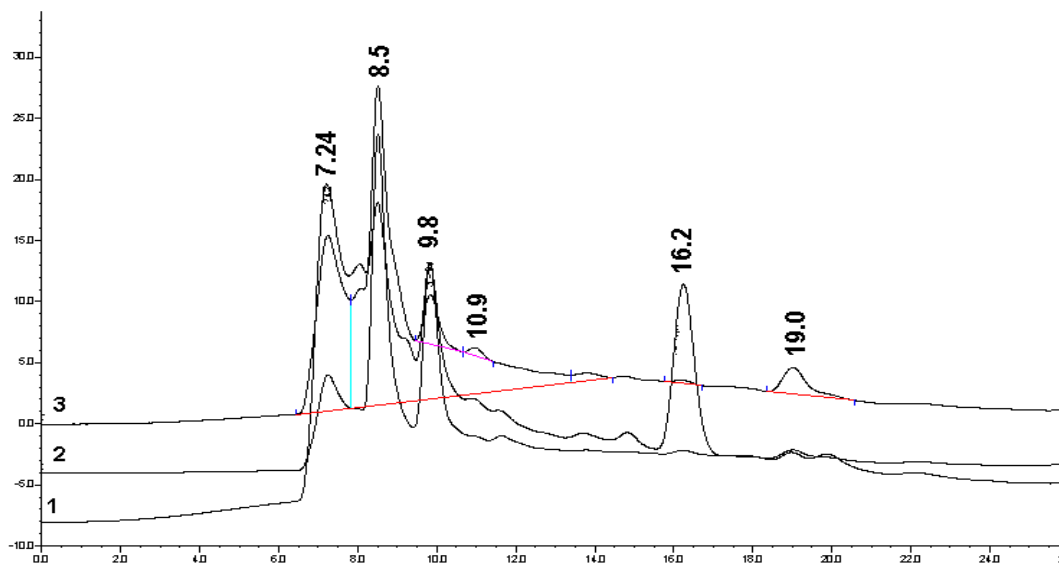
Figure 7.10 HPLC of LS4 at 1) 210nm 2) 254 nm 3) 272nm
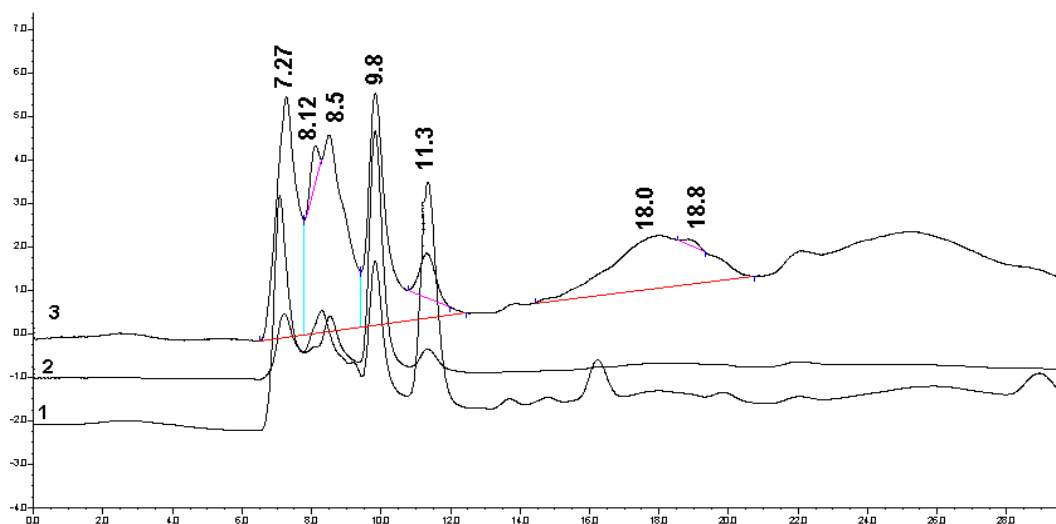
Figure 7.11 HPLC of LS5 at 1) 210nm 2) 254 nm 3) 272nm

Based on the results, we can predict the structures of the lignins and lignin-carbohydrate complexes that can be obtained by varying the source of the biomass (softwood, bagasse, etc.), method of preparation (kraft process or steam process),

and biochemical treatments such as xylanase for removal of residual carbohy-drates. This would help to plan applications for the different lignin preparations. Our previous work (Galgali, Varma, Puntambekar, Gokhale, 2002) has shown that functionalized polystyrenes, as model systems for lignins, can be made biodegradable by attaching as low as 1% by weight of carbohydrate moieties.

The schematic structures are shown in the following diagrams:
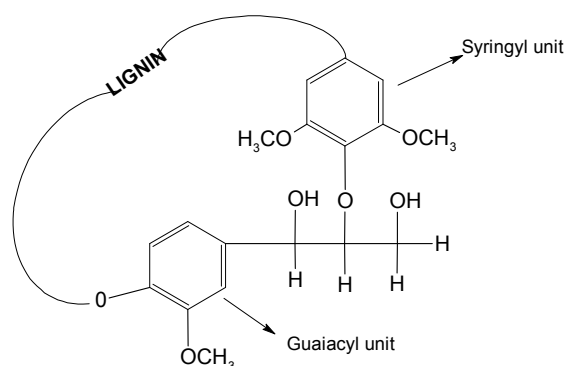
Figure 7.12 Schematic structure of bagasse lignin without carbohydrate and sulfur content (after purification by xylanase enzyme)
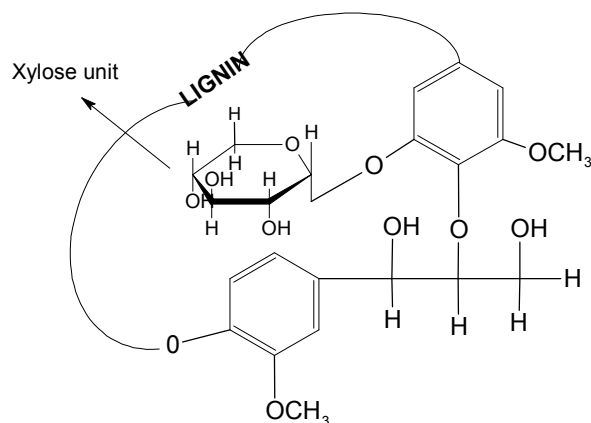
Figure 7.13 Schematic structure of lignin- carbohydrate complex (eg. LS2, LS4, LS6) obtained by steam-explosion or other processes

7.6. Biodegradation of carbohydrate linked lignins by laccase enzyme:

Laccase is one of the few lignin-degrading enzymes that have been extensively studied since 18th century. It is one of the best-understood and widely studied oxidases, in terms of its catalytic mechanism. Most laccases reported so far are extracellular enzymes and differ markedly in their redox potentials, carbohydrate contents, thermal stabilities and substrate specificities. Fungal laccase is responsible for demethylation of lignin and lignin related model compounds, which is thought to be an initial step in lignin biodegradation. Side chain elimination is also responsible for lignin breakdown.

Chemically treated bagasse samples and lignin samples were subjected to laccase enzyme treatment with the aim of studying lignin degradation from the samples. Since cellulose, hemicellulose and lignin are chemically linked together in the biomass, degradation of lignin will eventually lead to release of aromatic and sugar moieties. Hence, we followed the lignin degradation by measuring the phenolics and sugar released during laccase enzyme treatment of various biomass samples.

All the samples were treated with different dosage of laccase enzyme i.e., 20 U/g and 40 U/g and all of them were analysed for weight loss, amount of phenolics released and amount of sugar released.

7.6.1. Phenolics released during laccase treatment
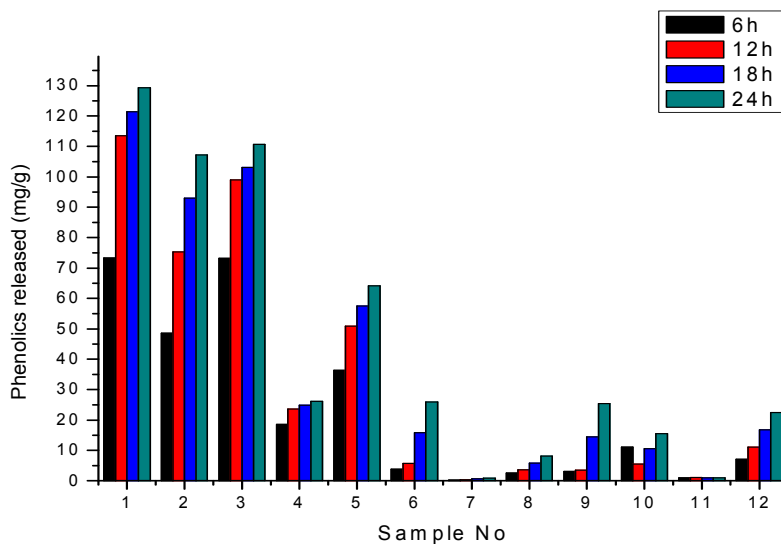
Figure 7.14 Phenolics Released with a treatment 20U/g of laccase enzyme at 6h interval up to 24 h, (1) bagasse lignin isolated by HCl precipitation (2) bagasse lignin isolated by $H_2 SO_4$ precipitation (3) Indulin AT lignin (4) organosolv bagasse lignin (5) pilot plant bagasse lignin (6) untreated bagasse powder (7) bagasse Cellulose (8) 20% NaOH treated bagasse powder (9) sodium chlorite bleached bagasse powder (10) 10% NaOH treated bagasse powder (11) bagasse powder with 3 % $H_2 SO_4$ treated and refluxed in acetone-water (12) steam exploded bagasse with 5% NaOH treatment

Figure: 7.15 Phenolics Released with a treatment 40U/g of laccase enzyme with 6 h interval up to 24 h, (1) bagasse lignin isolated by HCl precipitation (2) bagasse lignin isolated by $H_2 SO_4$ precipitation (3) Indulin AT lignin (4) organosolv bagasse lignin (5) pilot plant bagasse lignin (6) untreated bagasse powder (7) bagasse Cellulose (8) 20% NaOH treated bagasse powder (9) sodium chlorite bleached bagasse powder (10) 10% NaOH treated bagasse powder (11) bagasse powder with 3 % $H_2 SO_4$ treated and refluxed in acetone-water (12) steam exploded bagasse with 5% NaOH treatment

Figure 7.14 and 7.15 gives the phenolics released with a treatment 20 U/g and 40U/g of laccase enzyme at 6h interval from 6 h-24 h.

The phenolics release profile in the lignin samples (samples 1-5) are the highest as expected (both in 20 U/g and 40 U/g treatment), because the laccase enzyme basically cleaves the ether linkages in the lignin, resulting in phenolics release and weight loss.

The trend of weight loss in lignin samples is as follows: 1>3>2>5>4

As can be seen from the above graph bagasse lignin isolated by the HCl precipitation (sample 1) shows more phenolics released compared to the bagasse lignin obtained by $H_2 SO_4$ precipitation (sample 2), while phenolics released from Indulin AT(Sample 3) is in between sample 1 and 2. Organosolv baggase lignin (sample 4) shows the least phenolics release followed by pilot plant bagasse lignin (sample 5).

Thus, Organosolv baggase lignin is the most stable followed by pilot plant lignin and HCl lignin is the least stable. The stability of Indulin At lignin is in between HCl and $H_2 SO_4$ lignin. This also indicates that isolation of lignin by $H_2 SO_4$ is better process as compared to HCl as far as structural stability of the lignin is concerned.

Bagasse cellulose with 0.12 % residual lignin (sample 7) is most stable among all the samples as it is in pure form and nearly devoid of lignin and hemicelluloses, which are attacked by the laccase enzyme. Therefore it releases negligible amount of phenolics.

In case of untreated bagasse powder, lignin structure is not as accessible as in the case of the pure lignin samples so it shows phenolics released next only to lignin samples and even more than the organosolv bagasse lignin.

Among the chemically treated bagasse, sample 8, 9, 10, 11and 12, the phenolics released are in the following order:

9>12>10>8>11

Among the above 5 samples, sample 9 gives the highest value of released phenolics. This may be because sodium chlorite is capable of removing only residual lignin, so most of the lignin is still remaining which is readily available for attack by the lac-

case enzyme. Moreover bleaching acts as a pretreatment making access to the enzyme easy.

In the case of the samples 12, 10 and 8, with increasing concentration of NaOH treatment the lignin contents decreases, thereby decreasing the phenolics released in the subsequent samples.

Sample 11 releases the least amount of phenolics among all the chemically treated bagasse samples. This may be due to H_2SO_4 treatment and refluxing in acetone water removes most of the lignin and hemicellulose.

7.6.2. Sugars released during laccase treatment
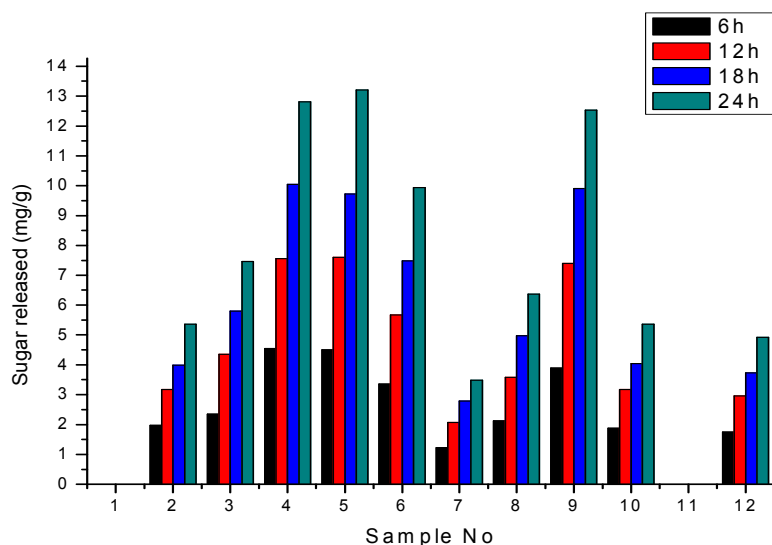
Figure 7.16 Sugars Released with a treatment 20U/g of laccase enzyme at 6h interval up to 24 h, (1) bagasse lignin isolated by HCl precipitation (2) bagasse lignin isolated by H_2SO_4 precipitation (3) Indulin AT lignin (4) organosolv bagasse lignin (5) pilot plant bagasse lignin (6) untreated bagasse powder (7) bagasse Cellulose (8) 20% NaOH treated bagasse powder (9) sodium chlorite bleached bagasse powder (10) 10% NaOH treated bagasse powder (11) bagasse powder with 3 % H_2SO_4 treated and refluxed in acetone-water (12) steam exploded bagasse with 5% NaOH treatment
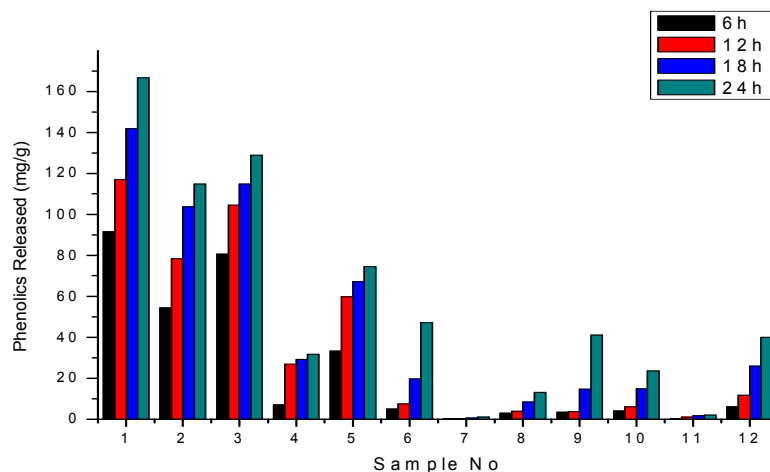
Figure 7.17 Sugars released with a treatment 40U/g of laccase enzyme at 6h interval up to 24 h, (1) bagasse lignin isolated by HCl precipitation (2) bagasse lignin isolated by H_2SO_4 precipitation (3) Indulin AT lignin (4) organosolv bagasse lignin (5) pilot plant bagasse lignin (6) untreated bagasse powder (7) bagasse Cellulose (8) 20% NaOH treated bagasse powder (9) sodium chlorite bleached bagasse powder (10) 10% NaOH treated bagasse powder (11) bagasse powder with 3 % H_2SO_4 treated and refluxed in acetone-water (12) steam exploded bagasse with 5% NaOH treatment.

Figure 7.16 and 7.17 shows the sugar release profile during laccase treatment (20 U/g and 40 U/g) of different samples.

The sugar is released with laccase enzyme treatment because of the cleavage of the bonds between lignin and hemicellulose. So along with the phenolics a corresponding amount of sugars are also released in the reaction medium which is available for estimation.

In case of 20 U/g of laccase treatment there no sugar released in case of bagasse lignin isolated by HCl precipitation (sample 1), but with 40 U/g treatment some sugar gets released. This shows that this sample contains only residual amount of sugar. In case of bagasse lignin isolated by H_2SO_4 precipitation (sample 2) both the treatments (20 U/g and 40U/g) released sugar and was more than sample 1 in all cases. This proves that the lignin isolated from the HCl process was more effective in residual hemicellulose removal than the H_2SO_4 process.

The observed trend of sugar release in all the lignin sample were as follows:

5>4>3>2>1

This trend shows that the pilot plant lignin had the highest amount of residual hemicellulose followed by the organosolv lignin. Indulin AT occupying intermediate position. This also proves that lignin fractionation process of our lab was better than the commercial lignins.

Bagasse Cellulose with 0.12 % residual lignin (sample7) gave values slightly higher than the HCl lignin (sample 1), showing a higher amount of residual hemicellulose but comparatively lesser than all the other samples under study, as expected.

With the untreated bagasse powder (sample 6) the sugars released was on higher side due the reasons as explained in phenolics released section.

Among the chemically treated bagasse, sample 8, 9, 10, 11and 12 the sugar released are in the following order:

9>8>10>12>11 (no sugar released in 11)

Sample 9 shows high sugar released, which may be, because sodium chlorite is capable of removing only residual hemicellulose, so most of the hemicellulose is still remaining which is readily available for attack by the laccase enzyme.

In case of Sample 10 and 12; sample 12 has been subjected to steam explosion as well as alkali treatment, as compared to 10 which has been given only alkali treatment. This reduces the residual hemicellulose in sample 12, which explains the sample 10 showing more sugar released.

No sugar is released in case of sample 11, which may be due to complete removal of hemicellulose by H_2SO_4 treatment and refluxing in acetone water.

Sample 8 gives higher values than sample 10 and 12, which is a deviation from the expected trend.

7.6.3. Total wt loss during laccase treatment
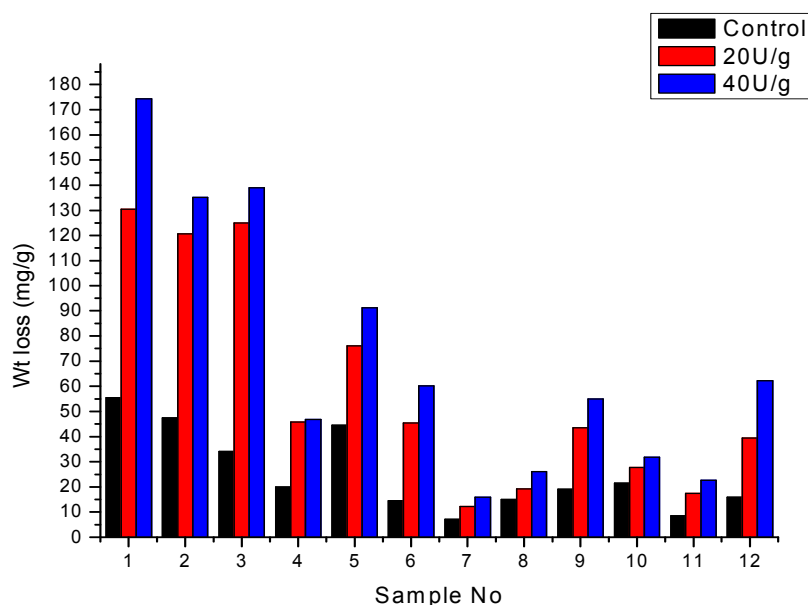
Figure 7.18 Total Wt loss profile under different dose of enzyme after 24 h, (1) bagasse lignin isolated by HCl precipitation (2) bagasse lignin isolated by H_2SO_4 pre-

cipitation (3) Indulin AT lignin (4) organosolv bagasse lignin (5) pilot plant bagasse lignin (6) untreated bagasse powder (7) bagasse Cellulose (8) 20% NaOH treated bagasse powder (9) sodium chlorite bleached bagasse powder (10) 10% NaOH treated bagasse powder (11) bagasse powder with 3 % $H_2 SO_4$ treated and refluxed in acetone-water (12) steam exploded bagasse with 5% NaOH treatment
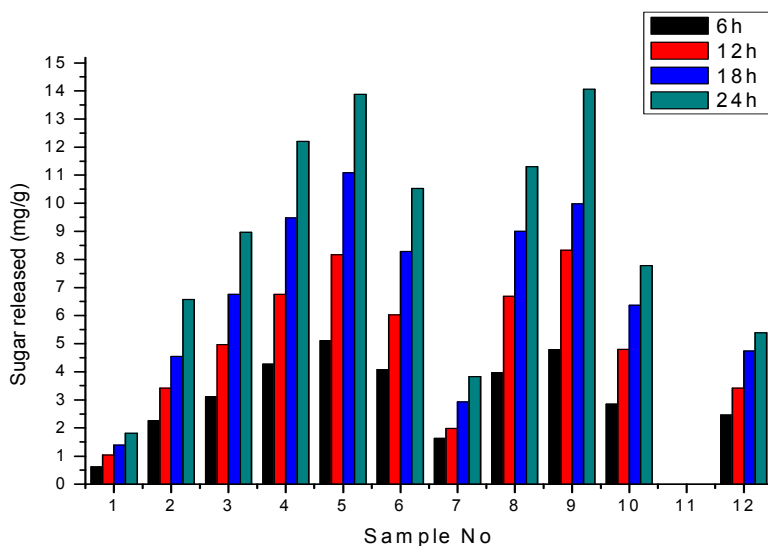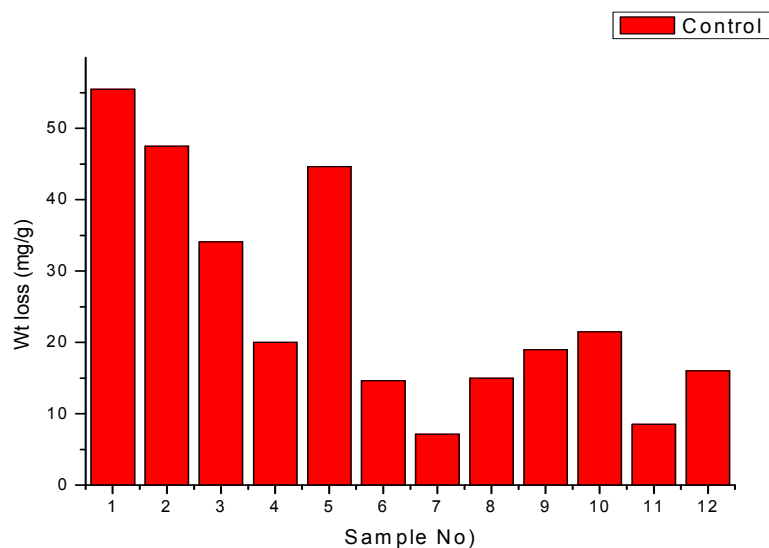

Figure7.19 Wt loss profile under control condition after 24 h, (1) bagasse lignin isolated by HCl precipitation (2) bagasse lignin isolated by $H_2 SO_4$ precipitation (3) Indulin AT lignin (4) organosolv bagasse lignin (5) pilot plant bagasse lignin (6) un-treated bagasse powder (7) bagasse Cellulose (8) 20% NaOH treated bagasse powd-er (9) sodium chlorite bleached bagasse powder (10) 10% NaOH treated bagasse powder (11) bagasse powder with 3 % $H_2 SO_4$ treated and refluxed in acetone-water (12) steam exploded bagasse with 5% NaOH treatment

Figure 7.18 and 7.19 gives the weight loss profile after treatment of the samples with laccase enzyme and under control condition respectively.

Under control condition the weight loss profile is in the following order

1>2>5>3>10>4>9>12>8>6>11>7

Total weight loss = phenolics released + sugars released + undetected components

It seems from the above order of weight loss, that the bagasse lignin isolated by the HCl precipitation (sample 1) shows more weight loss as compared to the bagasse lignin isolated by H_2SO_4 precipitation (sample 2). This shows that HCl treatment causes more disruption and degradation of the lignin structure compared to the H_2 SO_4 treatment used for the isolation of the lignin, leading to their solubilization and thereby more weight loss. Among all the lignin samples from 1-5, organosolv bagasse lignin (sample 4) is most stable under the given conditions followed by In-dulin AT (sample 3). Pilot plant lignin sample 5 has the same stability as that of the lignin isolated from the H_2SO_4 treatment.

Bagasse cellulose (sample 7) is the most stable among all the samples followed by untreated bagasse powder as expected. Cellulose is most stable as it is in pure form and devoid of the soluble fractions like lignin and hemicellulose, which are the main cause for wt loss. In the bagasse powder all the components are in their native state tightly bound with other, so it also gives the least wt loss.

Samples 8-12 are chemically treated bagasse samples with varying amount of hemicellulose and lignin depending on their chemical treatments as detailed in previous two sections, These gives the wt loss accordingly. The wt loss trend under control conditions are as follows:

10>9>12>8>11

Since the total wt loss in the samples after 20U/g and 40 U/g of laccase enzyme treatments are due to combinations of phenolics and sugar released, the trend in

total wt loss is in keeping with the observed trend in phenolics and sugar released trend individually.

Thus, we can say that laccase enzyme treatment can be used as an independent method for the evaluation of lignin and hemicellulose in biomass. It gives good evaluation in the case of pure fractions and chemically treated samples as compared to untreated biomass. This method can be used in conjugation with other existing methods for providing quantitative as well as qualitative insight into the composition of biomass.

7.7. Conclusion

In conclusion, we have shown that a complex molecule like lignin-carbohydrate complex, consisting of a crosslinked hydrophobic aromatic structure linked to hydrophilic carbohydrate moieties (and it's derivatives), is obtainable from different types of divergent sources and chemical isolation procedures. These polymers can have different structural parameters such as presence of lignin-carbohydrate linkages, different guaiacyl/syringyl ratios (wood and non-wood sources of the materials), sulfur linkages (or its absence) due to the isolation process used (such as kraft or soda process), effect of high degree of crosslinking (caused by reactions with diacids), etc., which can be detected by a combined study of FTIR, HPLC at various wavelengths with UV detector, TG, xylanase treatment, solubility and elemental analysis. The complexity of the molecule ensures that one cannot rely on a single spectroscopic method to discern the various facets of the molecule; rather an entire characterization protocol has to be in place to obtain a true picture of the lignin molecule. This detailed characterization is essential while developing diverse applications for this renewable biopolymer, available so abundantly but with li-

mited commercial production. The presence of the carbohydrate linkages can be used for applications requiring greater extents of hydroxyl groups, such as polyurethane polymer systems, epoxy resin prepolymers, and so on. The residual carbohydrate units in lignins, thus not only make the product more economically viable, but also expand the range of its applications. We are doing further work on lignin-carbohydrate complexes by developing them as ingredients of new polymer composites, wherein the carbohydrate moieties will play a key role in anchoring the other components of the polymer system. The presence of the carbohydrate groups is likely to improve the biodegradability of these polymer systems. Our previous work [25] has shown that functionalized polystyrenes, as model systems for lignins can be made biodegradable by attaching as low as 1% by weight of carbohydrate moieties. The carbohydrate moiety, in addition to inducing biodegradability, also serves as reactive site for anchoring other structural parameters to the polymer system. This area of work is gaining increased momentum with the present impetus to utilize renewable resources as well as develop biodegradable polymer materials.

Finally we can say that phenolics released are totally dependent on the final content of the lignin in the sample and the trends are in the expected directions. Thus, pure lignin with trace carbohydrates (samples 1-5) can be degraded with laccases more quantitatively than plain biomass (sample 6). This throws up potential applications for polymeric products based on lignins (containing trace carbohydrates).

7.8 References

1. D. W. Goheen, C. H. Hoyt, *Kirk-Othmer: Encyclopedia of Chemical Technology*, Wily Interscience, New York, **1981**, 14, 294

2. D. W. Goheen, C. H. Hoyt, *Kirk-Othmer: Encyclopedia of Chemical Technology*, Wily Interscience, New York, **1981**, 14, 294

3. C. Wu, F. Leo, W. G. Glasser, *J. Appl. Polym. Sci.*, **1984,** 29, 1111

4. H. Hatakeyama, S. Hirose, T. Hatakeyama, ACS Symposium Series No 397, Eds. W.G. Glasser and S. Sarkanen, Chapter 15, **1989**

5. V. P. Saraf, W. G. Glasser, *J. Appl. Polym. Sci.* **1984,** 29, 1831

6. W.G. Glasser, C.A. Barnett, T.G. Rials, V.P. Saraf, *J. Appl. Polym. Sci.* **1984,** 2, 1815

7. W. G. Glasser, R. H. Leitheiser, *Polym. Bull.* **1984**, 12, 1

8. D. S. Argyropolous, S. B. Menachem, *Biopolymers from renewable resources* Ed. **1998,** D.L. Kaplan, Springer-Verlag, Berlin, p 292

9. K. V. Sarkanen, C. H. Ludwig, *Lignins – Occurrence, formation and structure and reactions,* Wiley-Interscience, New York,. Chapters 5-8, **1971**

10. S. Y.Lin, C. W. Dence, *Methods in Lignin Chemistry*, Springer Verlag, Berlin, Chapters 4-9. **1992**

11. W. G. Glasser, C. A. Barnett, Y. Sano, *J. Appl. Polym. Sci., Appl. Polym. Symp*, **1983,** 37, 441

12. C. Schuerch, *J. Amer. Chem. Soc.* **1952**, 74, 5061

13. S. M. Shevchenko, G. W. Bailey, *J. Mol. Structure (Theochem)*, **1996,** 364, 197

14. J. X. Sun, X. F. Sun, R. C. Sun, P. Fowler, M. S. Baird, *J. Agric. Food Chem.* **2003** 51, 6719

15. R. J. A. Gosselink, A. Abacherli, H. Semke, R. Malherbe, P. Kauper, A. Nadif, J. E. G. van Dam, *Industrial Crops and Products*, **2004,** 19 (3), 271

16. A.J. Varma, *Carbohydr. Polym.* **1984,** 4, 315

17. A. J. Varma, *Polym. Test.*, **1986,** 6, 79

18. D. S. Tsujiyama, A. Miyamori, *Thermochim. Acta*, **2000,** 351, 177

19. B. Xias, F, Sun, R. C. Sun, *Polym. Degrad. Stab.* **2001,** 74, 307

20. A. Majcherczyk, A. Hiittermann, *J. Chromatography, A*, **1997,** 764, 183

21. G.E. Fredheim, S.M. Braaten, B.E. Christensen, *J. Chromatography A* **2002**, 942, 191

22. M. P. Tucker, Q. A. Nguyen, F. P. Eddy, K. L. Kadam, L. M. Gedvilas, J. D. Webb, *Appl. Biochem. Biotechnol.* **2001,** 91-93, 51

23. A.T. Martinez, G. Almendros, F. J. Gonzalez-Vila R. Frund, *Solid State Nuclear Mag. Resonance*, **1999,** 15, 41

24. R. S. Rohella, N. Sahoo, S.C. Paul, S. Choudhary, V. Chakravortty, *Thermochim Acta*, **1996**, 287, 131

25. P. Galgali, A. J.Varma, U. S. Puntambekar D. V. Gokhale, *Chem. Commun.* **2002** 2884

26. X. J. Pan, Y. Sano, *Holzforschung*, **2000**, 54(1), 61

Chapter 8

Conclusion and suggestion for future work

8.1. Summary and conclusions:

The work presented in this thesis was undertaken with the primary objective of developing an understanding of the effect of incorporation of carbohydrates and quaternary nitrogen moieties onto a synthetic elastomer like SBS in terms of enhancement of properties like biocompatibility, biodegradation, fluorescence and antimicrobial properties along with the physical and morphological changes. The present work was directed towards functionalization of Styrene-Butadiene-Styrene (SBS) with minute quantities of carbohydrates (monosacharides, disaccharides and pentose sugars) with simultaneous chlorination, and evaluation of the functionalized SBS for potential biomedical applications.

This was achieved by using two different approaches. In the first, functionalization of SBS with sugars was done by epoxide ring opening by a glycosidation analogous reaction, as a side reaction in this approach, quaternary nitrogen pendants also got attached to the SBS backbone imparting it additional antimicrobial properties. The second approach involved the anchoring of sugars onto SBS using click chemistry. Both these strategies were successfully utilized to anchor minute quantities of sugar molecules without altering the microstructure of SBS. The overall conclusion from the present research work is summarized below:

 A detailed literature search was done on the different methods employed for the modification of polymers with focus on different methods used till date for chemical modification of SBS. Modification of styrene butadiene copolymers, especially with sugars was also presented. The existing and emerging potential applications of modified SBS, including biomedical applications were also described in detail. Methods for synthesizing synthetic glycopolymer were also described, along with limitations of each method. The detailed literature survey

revealed that although there were reports on styrene butadiene glycopolymer synthesis utilizing the 1, 2 linked butadiene units, there was no reports on functionalization of SBS with sugar using 1,4 linked butadiene units. Moreover, these reports were based on incorporation of significantly higher amount of sugar which may alter polymer physical properties. Thus, there was need for further exploration, especially for cases where low degrees of carbohydrate incorporation is desired.

From our study, we found from NMR characterization, that different sugar showed different reactivities towards epoxide opening under the reactions conditions employed. We established the mechanism of these reactions leading to sugar, hydroxyl, chlorine and quaternary nitrogen pendants on SBS backbone by NMR and XPS analysis, which provided convincing information regarding the mechanism of formation of quaternary nitrogen and other pendants on SBS. The other approach that was utilized for achieving our aim was click chemistry, which was accomplished by synthesizing SBS azide from epoxidized SBS and reacting it with propargyl sugars to yield sugar functionalized SBS elastomers.

The functionalized SBS showed UV activity and enhanced fluorescence of varying intensity depending on the linked sugar. Confocal laser scanning microscopy (CLSM) revealed that the fluorescence occurred selectively in butadiene segment of SBS, leading to morphological observations of surface and inner layers of sugar functionalized SBS. We believe this was perhaps the first study where labelling of a polymeric component with fluorescent dye was not needed to visualize the morphology of a polymeric system by CLSM.

The applications of functionalized SBS were determined by in-vitro biocompatibility tests employing HL-60 and THP-1 cell lines. It was found that

sugar content had a positive effect on biocompatibility, whereas quaternary nitrogen groups adversely affected the biocompatibilities of the sugar linked SBS samples. Antimicrobial studies for applications in polymeric microbicides was also explored for the sugar linked SBS, and it was found that the antimicrobial activity depended on a number of factors like, quaternary nitrogen content, hydrophilicity imparted by the sugar molecules and the residual epoxide content. The current challenge faced by antimicrobial polymers is their cytotoxicity towards mammalian cells. Sugar molecules are expected to impart biocompatibility to polymers, hence the evaluation of attached sugar effect on toxicity can be helpful in designing antimicrobial polymers with minimal cytotoxicity.

The different sugar linked SBS samples with low degrees of carbohydrate incorporation, was investigated for biodegradation by bacteria and fungi. The biodegradation was investigated using soil bacteria (Pseudomonas sp.) and fungi (Aspergillus niger). The rates of biodegradation were found to be enhanced by incorporation of even minute quantities of sugars (typically in the range of 0.9-0.37 weight percentage). Weight loss measurements and SEM confirmed the degradation of the polymer. For biodegradation using fungal strains (Aspergillus niger,) only weight loss measurements were used to estimate degradation. The carbohydrate functionalized SBS showed thermal stability upto 250 ^{0} C and it is envisaged that these polymer can be processible below 200 ^{0}C. Moreover, thermal analysis also showed that the thermal stability is closely related with the sugar content of the polymers. DSC analysis showed a well characterized T_g of the butadiene segments for these polymers, and the sugar functionalized SBS showed an increase of 11-15^0 C in T_g values as compared to the epoxidized SBS.

The morphologies of carbohydrate functionalized SBS were studied using SEM, AFM, TEM in conjunction with WAXRD. Phase separated morphology as expected for a block copolymer was observed both in SEM and AFM, both for modified and unmodified SBS. TEM provided a clearer morphological picture, which showed micelle formation and micelles aggregation along with phase separated morphology for the functionalized SBS. The self assembly occurred due to hydrophilic and hydrophobic segments on SBS generated by the presence of sugar, quaternary nitrogen pendants and hydrophobic nature of the SBS polymer. These effects were also reflected in WAXRD measurements where sugar linked SBS having quaternary nitrogen pendants showed relative decrease in the peak associated with polybutadiene.

Finally, we also carried out studies of lignin containing residual sugars, as carbohydrate linked synthetic polystyrene polymer. Lignins from different sources were characterized and their sugar content was determined by xylanase treatment. The effect of sugar content on thermal stability and lignin biodegradation by laccase enzyme was studied and the biodegradation was found to be proportional to lignin and sugar content. Thus, we have showed that nature derived lignin containing residual carbohydrate groups is analogous to carbohydrate linked olefinic copolymers in biodegradation and thermal behavior.

Thus our research work focused on both fundamental and applications aspects of carbohydrate functionalized SBS.

8.2. Suggestion for future work:

- In our study we had simultaneously attached sugar, chlorine and quaternary pendants on SBS, which showed enhanced fluorescence. Reactions with attachment of only sugar molecules should be tried out, to quantify its contribution towards fluorescence. This could open novel applications of these materials as biocompatible fluorescent probes.

- The linking of sugars onto other unsaturated polymer should be tried out, and the effect of such linking on fluorescence and biodegradation of the polymer should be evaluated.

- "Click chemistry approach" using our strategy can be carried out with polymers like chlorosulphonated polyethylene leading to chlorosulphonated polyethylene glycopolymers.

- Our research work has provided fundamental understanding on the effect of biocompatible groups like sugar and antimicrobial groups like quaternary nitrogen on the overall antimicrobial and cytotoxic effects. This strategy and understanding could carry forward for the synthesis of tailored polymeric microbicides.

Publications:

1. Lignin carbohydrate complexes from sugar cane bagasse: Preparation purification and characterizations

   R. Singh, S. Singh, K. D. Trimukhe, K. V. Pandare, K. B. Bastawade, D. V. Gokhale and A. J. Varma, *Carbohydrate Polymers* **2005,** 62, 57–66

2. Enzymatic hydrolysis of delignified bagasse polysaccharides

   M. G. Adsul, J. E. Ghule, **R. Singh**, H. Shaikh, K. B. Bastawde, D. V. Gokhale and A.J.Varma**,** *Carbohydrate polymers* **2005,** *62* , 6-10

   (*Most accessed article placed 13 [th] position among top 25)*

3. Polysaccharides from Bagasse: Applications in Cellulase and Xylanase production

   M. G Adsul, J. E. Ghule, **R. Singh**, H. Shaikh, K. B. Bastawde, D. V. Gokhale., A. J. Varma.   *Carbohydrate Polymers 2004*,57, 67-72

   (*Most accessed, placed 5th position among top 25).*

4. Renewable H_2 from glycerol steam reforming: effect of La_2O_3 and CeO_2 addition to Pt/Al_2O_3 Catalysts

   Tiziano Montini, **Rakesh Singh**, Piyali Das, Barbara Lorenztu, Nicolas Berteo, Pietro Riello, Alvise Benedetti, Giuliano Giambastiani, Claudio Bianchini, Sergey Zinoviev, Stanislav Miertus and Paolo Foransiero, *ChemSusChem* **2010**, 3, 619-628

5. SBS as a versatile scaffold for rapid functionalization with unprotected carbohydrates *(manuscript under preparation)*

   Rakesh Singh, A. J. Varma

6. Carbohydrate functionalized fluorescent thermoplastic elastomer as a novel biocompatible biomaterial having antimicrobial properties *(manuscript under preparation)*

    Rakesh Singh, Sampa Sarkar, Diman Sarkar, A.J. Varma

7. A morphological study of carbohydrate functionalized SBS synthetic elastomer*(manuscript under preparation)*

    Rakesh Singh, A.J. Varma

8. Biodegradation and thermal studies of sugar linked SBS *(manuscript under preparation)*

    Rakesh Singh, M.G Adsul, D.V. Gokhale, A.J. Varma